NASA Contractor Report 177603

Open Airscrew VTOL Concepts

W. Z. Stepniewski and T. Tarczynski

CONTRACT NAS2-12819
September 1992

National Aeronautics and
Space Administration

NASA Contractor Report 177603

Open Airscrew VTOL Concepts

W. Z. Stepniewski and T. Tarczynski

International Technical Associates, Ltd.
1064 Pontiac Road
Second Floor
Drexel Hill, PA 19026-4817

Prepared for
Ames Research Center
CONTRACT NAS2-12819
September 1992

National Aeronautics and
Space Administration

Ames Research Center
Moffett Field, California 94035-1000

TABLE OF CONTENTS

CHAPTER 1

DEVELOPMENT OF BASIC RELATIONSHIPS

1.1 Introduction

Since the entire VTOL field extends, in principle, from pure helicopters to jets or rocket-lifted and propelled aircraft, suitable relationships should be developed that would enable one to compare all of the various concepts and configurations on some common basis. The areas wherein the comparisons should or could be made may be selected as follows:

1. Performance
2. Environmental aspects (chiefly external noise)
3. Cost.

In this particular investigation, a comparison of specific performance items of aircraft representing diverse concepts and configurations constitute the core of the study. Consequently, development of expressions for judging task performance will represent the prime aim of this chapter.

In this respect, one must first determine the task in which the particular performance of the examined concepts and configurations may be judged as superior or inferior with respect to that selected as the baseline. Of the many possible tasks, the broadly interpreted transport mission appears as the most suitable for that purpose.

The prime objective of any vehicle is usually the requirement of moving a number of people or a given amount of cargo over a determined distance. Thus, a relationship showing what fraction of the maximum gross weight at the beginning of the trip; i.e., the relative payload that can be carried over different ranges, could be considered as a universal measurement of the vehicle's ability to perform that prime transport mission requirement.

However, in executing this task, a time limit may appear as a strong constraint. Consequently, cruise speed becomes another important universal measurement of the vehicle's transport capabilty.

But cruise speed is directly associated with the question of 'cost' as represented by the rate of expenditure of energy needed to achieve various levels of the speed of the vehicle. Since all of the aircraft examined in this report use fuels having practically the same caloric values, the fuel consumption per unit of aircraft gross weight and unit of time may be selected as a common measurement of the aircraft's 'energy consumption goodness' in achieving various speed-of-flight levels.

Once the relationship of fuel consumption per unit of gross weight and unit of time vs. speed of flight is established, another important common measure of aircraft performance can be derived: namely, the amount of fuel required per unit of aircraft gross weight and unit of distance flown.

Knowledge of the ratio of aircraft weight empty to its maximum flying gross weight (relative weight empty) permits one to determine the relative payload for zero range (the so-called zero-range payload) and, having the values of the fuel consumption in cruise per unit of gross weight and unit of distance flown, graphs of the previously mentioned relative payload vs. range can be constructed.

Furthermore, the relative ideal productivity (defined as the product of payload and cruise speed divided by weight empty) can now be shown vs. range — thus providing still another means of comparing performance aspects of various examined concepts and configurations. Other common comparative relationships as, for instance, the amount of fuel per unit of payload transported over a given range, can be developed.

Of course, some transportation tasks may be outlined differently; for instance, as a requirement of keeping a number of people or a given payload on station for a specified time. In the case of rotary-wing aircraft, this 'time on station' may include time in, or near, hovering. Here, although the task formulation may be different from that of point-to-point transportation, the basic philosophy of finding a means of comparison that can be applied to various aircraft types remain the same, as can be seen from this chapter.

Once the method of comparing performance is established, the question presents itself as to the selection of a baseline for performing the given task. In this respect, performance of conventional shaft-driven helicopters, the V-22, and other extensively studied tilt-rotor configurations may serve as necessary standards or gauges for comparison.

However, in a still broader field of comparison, one may pose questions regarding the competitiveness of the considered concepts with respect to fixed-wing aircraft — including propeller-driven, turbine-powered, and jet-propelled types. Consequently, some performance characteristics of these aircraft will be generalized and compared with VTOL concepts that have been revitalized by present-day technology.

Finally, in order to give the reader some indication regarding the direction for selecting values of some basic design parameters for VTOL aircraft using wings as a means of lift-generation in forward flight, a few selected relationships showing the influence of speed and altitude of flight, wing loading, wing aspect ratio, and basic cleanness of the aircraft on its lift-to-drag ratio will be discussed.

It is believed that using the above-outlined philosophy of comparison giving some idea regarding the selection of the optimal design parametric values, a definite, although broad-brush painted picture regarding the possibilities of the old, but revitalized, concepts to perform basic transport tasks will emerge. This, in turn, should provide a rational basis for determining the amount of time and effort that should be spent in various research and development areas.

1.2 Presentation of Comparison Inputs

1.2.1 Weights

Weight aspects are interpreted and presented as fractions of the maximum flying gross weight (W) of the aircraft. Consequently, the following definitions will be used:

Relative weight empty

$$\overline{W}_e = W_e/W \tag{1.1}$$

where W_e is the weight empty.

Relative useful load

$$\overline{W}_{ul} = (W - W_e)/W = 1 - \overline{W}_e. \tag{1.2}$$

Relative payload in general

$$\overline{W}_{pl} = W_{pl}/W \tag{1.3}$$

where W_{pl} is the payload.

Relative zero range, or zero time payload

$$\overline{W}_{0_{pl}} = (W - W_e - W_{crew} - W_{tf})/W$$

or

$$\overline{W}_{0_{pl}} = 1 - \overline{W}_e - \overline{W}_{crew_{tf}} \tag{1.4}$$

where $\overline{W}_{crew_{tf}}$ is the joint relative weight of the crew and trapped fluids.

1.2.2 Fuel Consumption

In range (R) considerations, the fuel consumption per pound of aircraft gross weight and nautical mile $(FC_w)_R$ can be computed when the fuel flow in lb per hr (FF) at a given speed of flight (V, in kn), and aircraft gross weight (W) are known:

$$(FC_w)_R = FF/WV. \tag{1.5}$$

Similarly, fuel consumption per pound of gross weight and one hour flight duration $(FC_w)_t$ (be it hover or forward translation) can be expressed as follows:

$$(FC_w)_t = FF/W. \tag{1.6}$$

where $\overset{\circ}{FF}$, as before, is the total aircraft fuel flow in pounds per hour during the specified regime of flight (from hover to V_{max}).

1.2.3 Payload vs. Range

A general expression for the determination of the payload that can be carried by any aircraft or vehicle in general over a range (R) can be developed from a basic differential equation giving the elementary variation in the gross weight of the vehicle (dW) over an elementary distance traveled (dR). Knowing the gross-weight and distance-related fuel consumption $(FC_w)_R$ expressing fuel utilization (say, in pounds) per unit of gross weight (also in pounds) of the vehicle's gross weight and unit of distance (in nautical miles) traveled, dW becomes

$$dW = -W(FC_w)_R dR. \tag{1.7}$$

The total weight of fuel required to fly a distance R can be exactly computed once the intended flight path is established; and speed, altitude, ambient conditions, and $(FC_w)_R = f(W, V, \rho, T)$ are known (where ρ is the air density and T is the ambient temperature).

However, in a comparative study such as this where relative merits regarding load-carrying capabilities are mutually compared, a simple relationship for the relative payload vs. range can be developed by assuming that the fuel consumption per pound of gross weight and one nautical mile remains constant throughout the entire flight.

Under these circumstances, integration of Eq. (1.7) would give the amount of fuel required for range R:

$$(W_{fu})_R = \left\{1 - \exp\left[-(FC_w)_R R\right]\right\} W \tag{1.8}$$

and the relative quantity of fuel $(\overline{W}_{fu})_R$ is obtained by dividing both sides of Eq. (1.8) by the maximum flying gross weight W:

$$(\overline{W}_{fu})_R = 1 - \exp[-(FC_w)_R R]. \tag{1.9}$$

Remembering that $\overline{W}_{0_{pl}}$ defines the relative zero range payload, an expression especially useful for our comparative study for the relative payload vs. range is obtained:

$$\overline{W}_{pl_R} = \overline{W}_{0_{pl}} - 1 + \exp[-(FC_w)_R R]. \tag{1.10}$$

In the above equation, $(FC_w)_R$ is in lb/lb,n.mi, while R is the range in n.mi.

An expression for the relative payload vs. time (t) on station – whether in hover or in forward flight – can easily be obtained in a way similar to the development of Eq. (1.10):

$$\overline{W}_{pl_t} = \overline{W}_{0_{pl}} - 1 + \exp[-(FC_t)t] \tag{1.11}$$

where $(FC_w)_t$ (also assumed to be invariant) is the amount of fuel consumed per pound of the aircraft gross weight and one hour, and t is the time on station in hours.

Looking at Eqs. (1.10) and (1.11), one may clearly see that the relative payload vs. range or time relationships are dependent on two parameters: the zero-range (time) relative payload levels (first term in those equations) and the fuel consumption values; per pound of gross weight and nautical mile in Eq. (1.10), and pound of gross weight and one hour of flight in Eq. (1.11).

The $\overline{W}_{O_{pl}}$ term in Eqs. (1.10) and (1.11) abviously reflects the structural efficiency of the design, since it is directly related to the relative weight empty (Eq. 1.4)).

The second term in Eq. (1.10) is governed by the $(FC_w)_R$ values which reflect aero-thermodynamic efficiency of the aircraft as a whole with respect to the distance flown. Similarly, in Eq. (1.11), the $(FC_w)_t$ term represents a measure of the aero-thermodynamic efficiency of the aircraft with respect to the time of flight. For helicopter-type rotorcraft, the relative payload vs. time is of special interest for the hover regime of flight.

Figure 1 was prepared to illustrate the interplay between structural weight and aero-thermodynamic efficiency aspects for two zero-range relative payload values, 0.4 and 0.6, assuming that $(FC_w)_R$ = 0.00031 lb/lb,n.mi for helicopters, 0.00023 for tilt-rotors, and 0.00016 for turboprops.

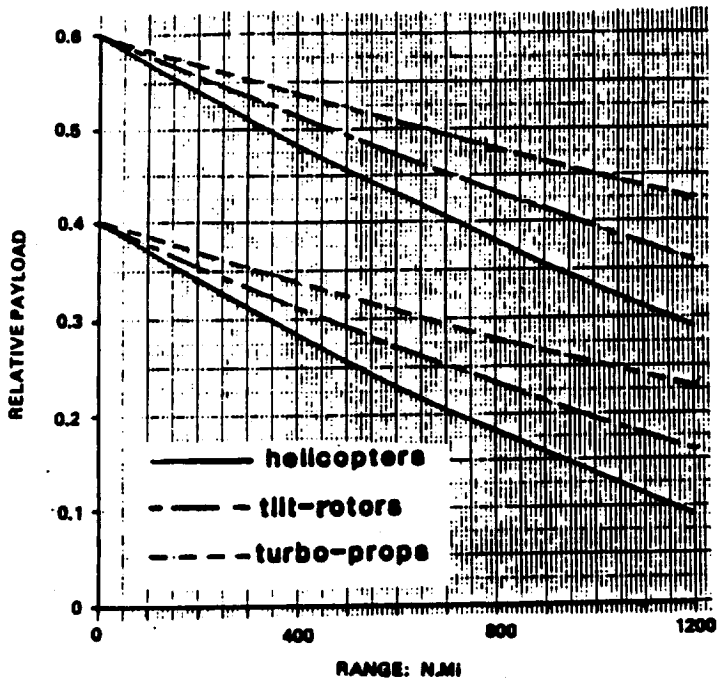

Figure 1.1 Relative payload variation vs. range for helicopters, tilt-rotors, and turboprops

A look at this figure will indicate that for aircraft characterized by inherently high $(FC_w)_R$ values (i.e., steep slopes at the $\overline{W}_{pl} = f(R)$ curves), high $\overline{W}_{O_{pl}}$ — in other words, low $\overline{W}_e$ values — give them the possibility of being competitive with respect to more fuel-efficient counterparts as far as transportation of a given payload up to the same range values are concerned.

1.2.4 Fuel Consumption Aspects

Total fuel flow (FF) in lb/hr represents the rate at which an aircraft consumes fuel under specified regimes of flight, as represented by gross weight, speed, and ambient conditions. This, obviously, means that the fuel flow of all powerplants should be summed up for aircraft having mixed types of powerplants acting simultaneously in a particular regime of flight.

The gross weight-related rate of fuel consumption $(FC_w)_t$ in lb/lb,hr becomes:

$$(FC_w)_t = FF/W \tag{1.12}$$

where the gross weight W is in pounds.

Fuel consumption per pound of gross weight and nautical mile of distance flown is obtained by dividing Eq. (1.12) by the speed of flight in knots:

$$(FC_w)_R = FF/WV. \tag{1.13}$$

For all types and configurations of aircraft examined in this report, a comparison of $(FC_w)_R$ values is important, since their levels dictate the slope in the relative payload vs. range relationship. Consequently, the influence of some important design parametric values on fuel consumption per pound of gross weight and nautical miles flown will be briefly reviewed later in this chapter.

For all VTOL aircraft, the time and gross-weight-related fuel consumption may be of some interest in all regimes of flight. But, for helicopters, where hovering requirements often constitute one of the most important parts of their mission definitions, a comparison of $(FC_w)_t$ values in hover becomes essential in determining the competitive position of the examined configurations with respect to those of the baseline. In order to make such comparisons for rotor tip-driven vs. shaft-driven types, special sections in Chapter 2 will be devoted to $(FC_w)_t$ computations.

Fuel consumption per pound of payload at various ranges $(FC_{pl})_R$ may be considered as another useful gage for comparing various types of aircraft and configurations with respect to their effectiveness as transport vehicles.

Under the simplifying assumption that $(FC_w)_R$ = const, the amount of fuel required by an aircraft to travel distance R is given by Eq. (1.8), and the payload that can be carried over that distance can be obtained by multiplying Eq. (1.10) by W. Dividing Eq. (1.8) by the modified Eq. (1.10), one obtains

$$(FC_{pl})_R = \left\{1 - \exp[-(FC_w)_R R]\right\} \Big/ \left\{\overline{W}_{0_{pl}} - 1 + \exp[-(FC_w)_R R]\right\}. \tag{1.14}$$

Looking at Eq. (1.14), one will again note an interplay between the $\overline{W}_{0_{pl}}$ and $(FC_w)_R$ parameters. Types and configurations characterized by high $(FC_w)_R$ values may still remain competitive up to some range levels with the more fuel-efficient types if their zero-range relative payloads remain sufficiently higher (i.e., relative weights empty are lower) than those of their competitors. This point is illustrated in Figure 1.2.

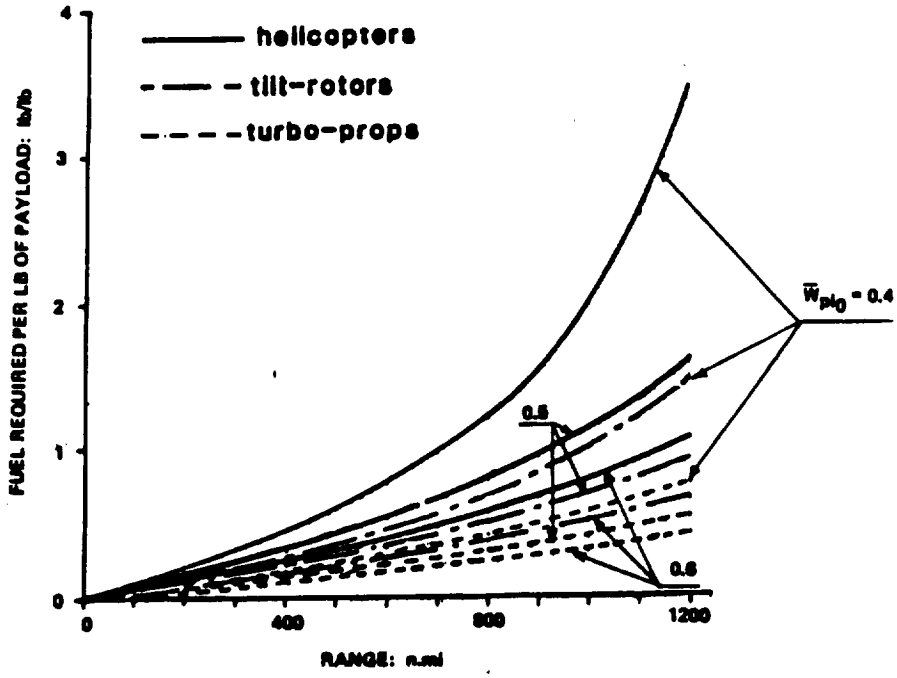

Figure 1.2 Fuel required per pound of payload vs. range

1.2.5 Relative Productivity

Relative productivity may be considered as still another universal gauge for measuring transport effectiveness of aircraft representing different types and configurations.

Actual relative productivity ($\overline{PR}$), as related to transporting a payload corresponding to range, (W_{pl_R}), is usually defined as follows:

$$\overline{PR} = V_{wk} W_{pl_R} / W_e \tag{1.15}$$

where V_{wk} is the so-called work speed which, in repetitive operations, is computed on the basis of distance traveled and total time elapse between two consecutive operations (Ref. 1).

However, the ideal relative productivity is based on the aircraft or, in general, the cruise speed of the vehicle:

$$\overline{PR}_{id} = V_{cr} W_{pl_R} / W_e. \tag{1.16}$$

In both of the above equations, the numerators express the quantity of lb-n.mi, ton-n.mi, or passenger miles that can be moved per hour which, obviously, can be considered as a measure of the actual (Eq. (1.15)) or ideal (Eq. 1.16)) transport effectiveness of an aircraft, or vehicle in general. Assuming that the cost is proportional to weight-empty, Eqs. (1.15) and (1.16) may be considered as a means of evaluating the economic effectiveness of a vehicle.

It is obvious that the so-established criteria would make sense for the types of vehicles when costs per pound of the structure are similar. Although the idea of relative productivity may not prove suitable for comparing, say, aircraft and cargo ships,within one family such as helicopters or even transport aircraft in general, it may provide some measure of cost effectiveness.

Dividing W_{pl_R} and W_e in Eq. (1.16) by W and then substituting Eq. (1.10) for $\overline{W}_{pl_R}$, Eq. (1.16) can be rewritten as

$$\overline{PR}_{id} = \left\{ \overline{W}_{0_{pl}} - 1 + \exp[-(FC_w)_R R] \right\} V_{cr}/\overline{W}_e \tag{1.17}$$

or, assuming for simplicity that $\overline{W}_{0_{pl}} = 1 - \overline{W}_e$, the following approximate expression can be obtained:

$$\overline{PR}_{id_{appr}} = \left\{ 1/\overline{W}_e \exp[(FC_w)_R R] \right\} - 1. \tag{1.18}$$

Looking at the above equation, one can see that here again, the cost-affectiveness of a vehicle is the result of an interplay between performance (V_{cr}), relative fuel economy $(FC_w)_R$, and relative structural weight ($\overline{W}_e$). As far as the last influence is concerned, Figure 1.3 may prove quite instructive.

In this figure, the approximate ideal relative productivity of the three types of aircraft is plotted vs. relative weight empty for four ranges (0, 400, 800, and 1200 n.mi). In addition, the following rather conservative assumptions were made regarding relative fuel consumption and cruise speed values: $(FC_w)_R$ = 0.00031 lb-n.mi and V_{cr} = 130 kn for helicopters, $(FC_w)_R$ = 0.00023 and V_{cr} = 200 kn for tilt rotors, and $(FC_w)_R$ = 0.00016 and V_{cr} = 240 kn for turboprops.

This figure also reconfirms the importance of low $\overline{W}_e$ levels for all three types of aircraft as far as maintaining high productivity is concerned.

It may be exprected that within similar gross-weight classes, the relative ideal productivity of fixed-wing aircraft in general, including turboprop transports, will be higher than that of helicopters and present tilt-rotors. With respect to the latter, advanced turboprops should have potentially lower relative weights empty, lower fuel consumption per pound of gross weight and one nautical mile (cleaner aerodynamics and higher wing aspect ratios) and, possibly, somewhat higher cruise speeds. However, in those operations where vertical takeoffs and landings are required, this productivity advantage will be of little value to conventional turboprops. Thus, helicopters and tilt-rotors remain, at present, as the only true baseline references for the VTOL operation field.

1.3 Discussion of Parameters Influencing Performance

1.3.1 General

It was clearly indicated in Section 1.2 that as far as broadly interpreted transport missions of carrying some payloads over various ranges are concerned, the most important

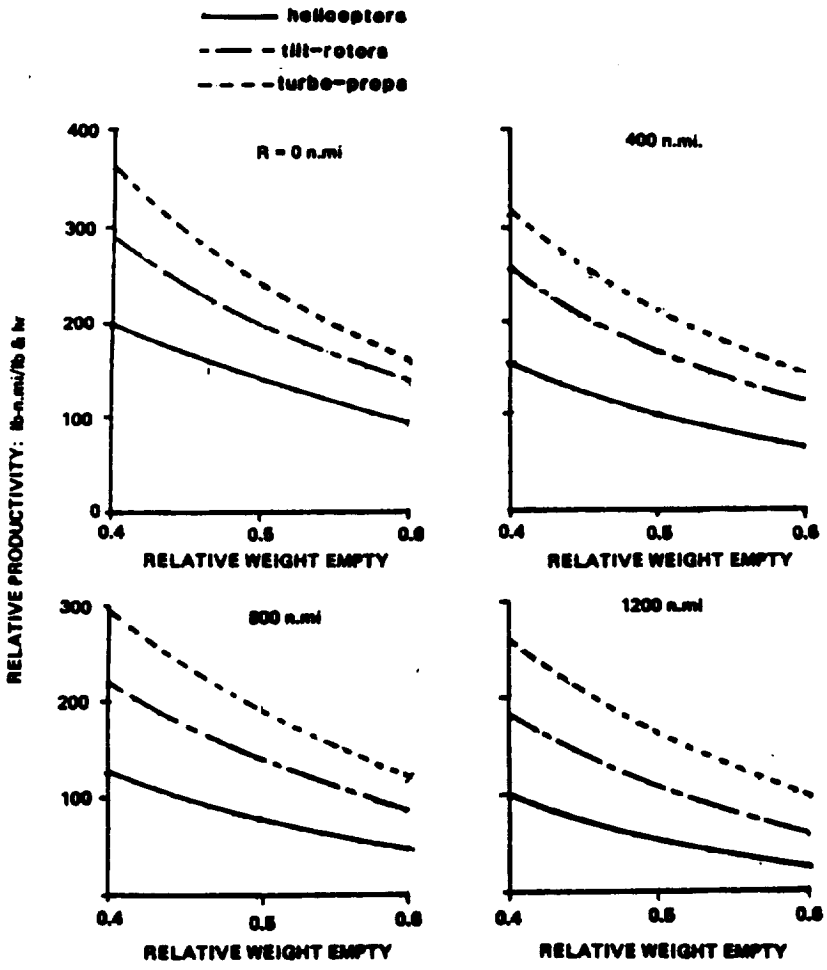

Figure 1.3 Examples of approximate ideal relative productivity vs. relative weight empty

factors affecting 'goodness' of an aircraft to perform such tasks are (1) relative zero-range payload or, in other words, relative weight empty, (2) fuel consumption per pound of the aircraft gross weight and one nautical mile flown at a given cruise speed, and (3) absolute cruise speed value.

In the case of missions built around the requirement of keeping a given payload on station for a specified time, the two most important factors are (1) zero time relative payload (obviously synonymous with zero-range payload), and (2) fuel consumption per pound of gross weight and unit (say, 1 hour) of flight time. In helicopters performing crane operations, levels of fuel consumption per unit of weight and unit of time becomes especially important for hovering and near-hovering regimes of flight.

With respect to the relative zero-range (time) values, it is obvious that the higher they are and thus, the lower the relative weight empty, the better. An extensive discussion of factors affecting relative weight-empty levels is beyond the framework of this study. However,

a reader interested in this subject can get some information regarding temporal and gross-weight related weight-empty trends, and the influence of structural materials on $\overline{W}_e$ levels from Ref. 2.

As previously mentioned, the most important aspects of time and gross-weight related fuel consumption in hover will be discussed in Chapter 2. Consequently, only the case of fuel consumption per pound of gross weight and one nautical mile will be briefly discussed here, and some of the important parameters influencing $(FC_W)_R$ will be indicated.

1.3.2 Atmospheric Conditions

Atmospheric environment of flight is the result of an interplay between pressure altitude and ambient temperature. Both of these factors affect air density values, while temperature may be considered (with a very high degree of accuracy) as the sole variable influencing the speed of sound and thus, Mach number levels.

The influence of a combination of ambient temperature with pressure altitude is especially important for VTOL operations. Performance of most vertical thrust generators is affected by the air density and, in some cases, Mach number values. Power outputs and, to some extent, powerplant sfc may also vary with ambient temperature and pressure changes. Figure 1.4 is shown to illustrate the dependence of the relative air density, $\overline{\rho} = \rho/\rho_0$, (where ρ_0 is the air density at SL, Std), on pressure altitude and air temperature.

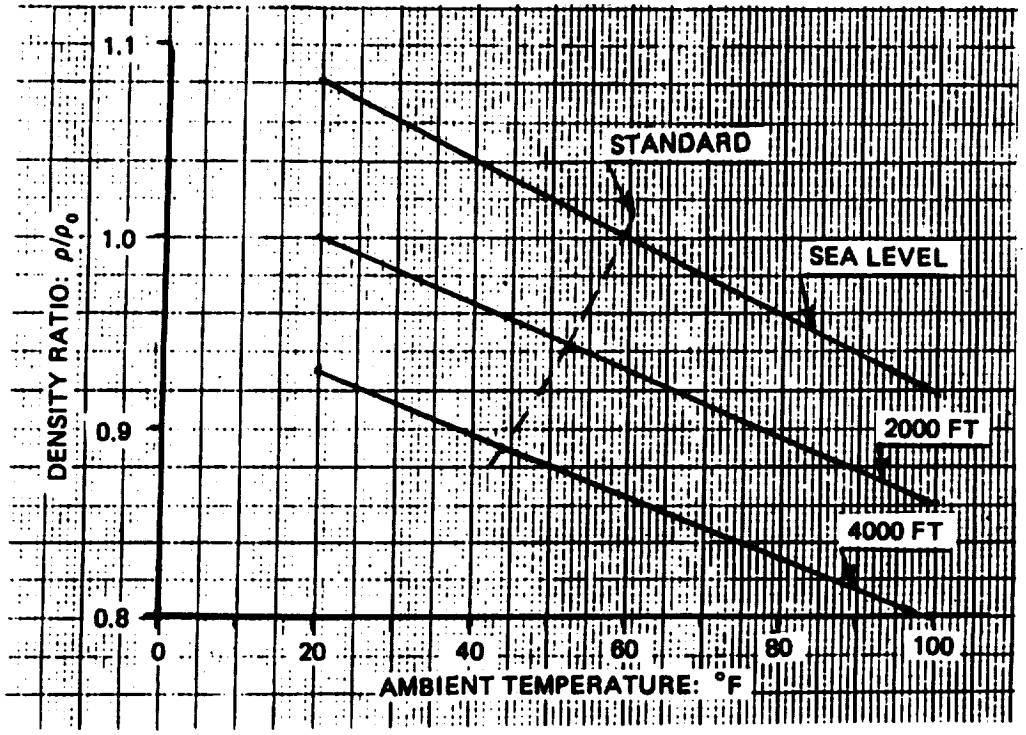

Figure 1.4 Variation of relative air density with ambient temperature at three selected pressure altitudes

Drag rise on the advancing blade of rotorcraft and of the whole fixed-wing aircraft when attaining elevated subsonic speeds with respect to air are related, not to the speed per se, but to the corresponding Mach number levels. In this respect, especially from an operational point of view, it becomes important to know the air velocities at various altitudes corresponding to a given Mach number value. Figure 1.5 is shown here to illustrate that point for the STD atmosphere case. Looking at this figure, one can see that, for instance, M = 0.8 would be reached at 529 knots at SL, 492 knots at 20,000 ft, but already at 459 knots at 40,000 ft.

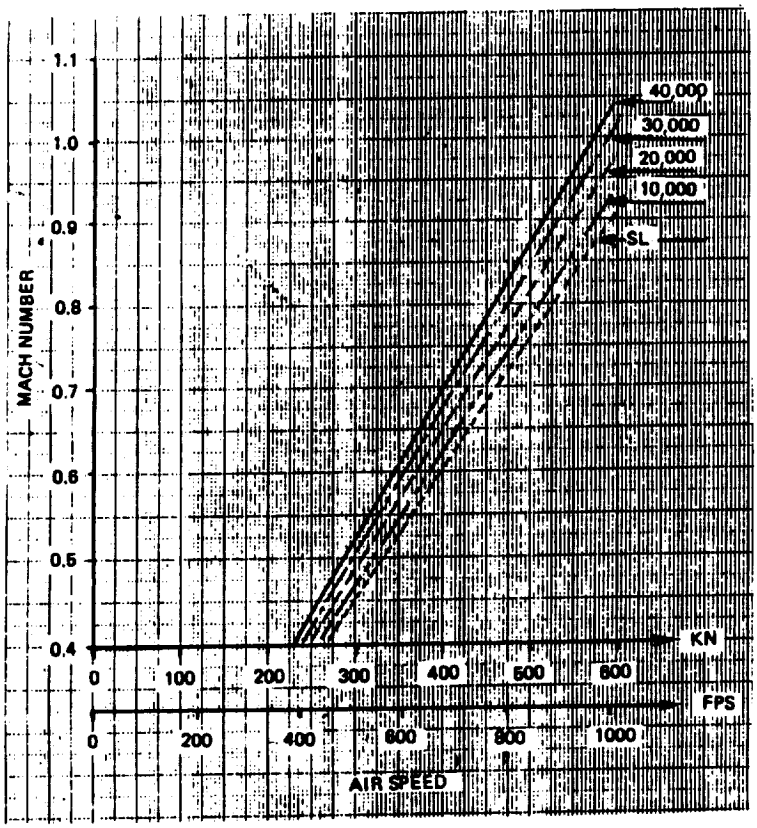

Figure 1.5 Mach numbers vs. various standard altitudes

1.3.3 Parameters Influencing Fuel Consumption

It was indicated in Section 1.2 (Eq. 1.5)) that in determining $(FC_w)_R$ values, the total rate of fuel consumption (FF, in lb/hr) should be established first. This, obviously, means that in such rotorcraft types as compounds where forward propulsion may be provided by various types of powerplants different from those driving the lifting rotors, separate accounting of the rate of fuel consumption should be made for all of the powerplant units, and then summed up. Because of the possibility that the resulting total fuel flow could

vary greatly depending on the distribution of the 'work' effort between the various powerplants, it is difficult to establish some general relationships which would indicate the influence of various other factors and design parameters on FF and hence, $(FC_w)_R$ or $(FC_w)_t$ values. Consequently, fuel efficiency of aircraft with mixed types of engines (working at the same time) should be judged individually for each aircraft configuration once an optimal work distribution between different types of powerplants for a given regime of flight has been established.

By contrast, for aircraft types where engine(s) of a single species sustain the aircraft in flight, it is easier to develop relationships which would indicate the role of various factors and design parameters on (FC_w) levels.

1.3.4 Parameters Influencing OGE Hover Performance

For shaft-driven rotorcraft, the total SHP required in hover OGE can be expressed as follows:

$$SHP_h = k_v^{3/2} W \sqrt{w/2\rho_0\bar{\rho}}/550FM\eta_{ov} \tag{1.19}$$

where k_v is the vertical download factor (ratio of thrust required to gross weight), w is the disc loading in psf, ρ_0 = 0.002378 slugs/cu.ft, $\bar{\rho}$ is the relative air density, FM is the rotor figure of merit, and η_{ov} is the ratio of rotor power required to the corresponding shaft power.

The rate of hourly fuel consumption in lb/hr of the aircraft as a whole will be

$$FF_h = SHP_h sfc \tag{1.20}$$

where sfc is the engine specific fuel consumption (lb/hr,hr) corresponding to the powerplant rating required in hover under given ambient conditions.

The fuel consumption per pound of rotorcraft gross weight and hour (see Eqs (1.19) and (1.20)) becomes:

$$(FC_w)_{th} = 0.0264k_v^{3/2}\sqrt{w/\bar{\rho}}sfc/FM\eta_{ov}. \tag{1.21}$$

Eq. (1.21) clearly indicates that the following parameters (listed in order of their usual degree of importance) are (1) lifting rotor disc loading, (2) engine sfc, (3) rotor figure of merit, (4) ratio of rotor power to shaft power, and (5) download factor.

In rotorcraft using blade-driven lifting rotors, there is such a variety of thermodynamic and mechanical schemes that it becomes difficult to single out some definitive factors and parameters that would be common to all encountered design approaches. However, even in this situation, it is possible to indicate a factor which would be of special importance to all blade-tip-driven rotorcraft. Such a common factor may be the thrust specific fuel consumption (tsfc) in lb/lb,hr of units driving the blades.

Such a thrust specific fuel consumption in hover can be defined as

$$tsfc_t = FF/T_t \tag{1.22}$$

where FF is, as always, the rate of fuel consumption by the aircraft as a whole, and T_t is the total tip thrust needed to drive the rotor.

Since, in blade-driven schemes, the lifting rotor is the only source of power, Eq. (1.19) can be used to express the rotor power required.

Consequently, the total tip thrust required can be obtained by dividing Eq. (1.19), with the 550 number omitted, by the tip speed V_t (in fps):

$$T_t = k_v^{3/2} W\sqrt{w/2\rho_0\bar{\rho}}/FM\eta_{ov}V_t \tag{1.23}$$

and the specific fuel consumption per pound of GW and hr can be obtained by dividing Eq. (1.23) by W and multiplying by $tsfc_t$:

$$(FC_w)_{t_t} = 14.5k_v^{3/2}\sqrt{w/\bar{\rho}}\,tsfc_t/V_tFM\eta_{ov}. \tag{1.24}$$

The significance of such parameters as disc loading, figure of merit, and download factors will be the same as in Eq. (1.21). But the η_{ov} value will be closer to 1.0 since, in tip-driven schemes, there is no power loss for the lifting rotor torque compensation (as in the single-rotor configuration), and mechanical transmission efficiency does not enter the picture. The sfc is replaced by $tsfc_t$, and tip speed appears as a new parameter.

Figure 1.6 was prepared to give the reader some idea as to how some of those factors may influence the $(FF_w)_{t_h}$ levels in shaft and tip-driven schemes. This figure shows $(FF_w)_{t_h}$ vs. w. For the shaft-driven configuration, this was done for the two assumed sfc values of 0.4 and 0.6 lb/hr,hp, which includes most of the specific fuel consumptions currently encountered in practice. For tip-driven types the $tsfc_t$ values extend from those typical for the low bypass ratio turbofans (BPR $\leq$ 2.0) to those of ram-jets. In addition, the following assumptions were made for all types of helicopters: V_t = 700 fps, M_t = 0.63, $\bar{\rho}$ = 1.0, k_v = 1.0, and FM = 0.72, while η_{ov} = 0.87 was assumed for shaft-driven types, and 0.95 for tip-driven types, respectively. For jet-type helicopters, the following values of $tsfc_t$ at M_t = 0.63 were taken from Figure 3.3 of Ref. 3: low bypass ratio turbofans, 0.68, and pure jets 1.0 lb/hr,lb. For ducted air with tip burning (1000°K) and ram-jets types, $tsfc_t$ = 2.4 and 7.1 lb/hr,lb, respectively, were estimated from Ref. 4, p. 107.

When looking at Figure 1.6, one should remember that this is a rough representation of the trends in fuel consumption per pound of gross weight and one hour of flight for the shaft-driven and various tip-driven helicopter concepts. A more detailed study of this aspect will be conducted in Chapter 2. Nevertheless, from this figure alone, one would note that for the same disc-loading levels, there exists a very large difference in $(FC_w)_t$ values for helicopters representing various concepts of driving the lifting rotor(s).

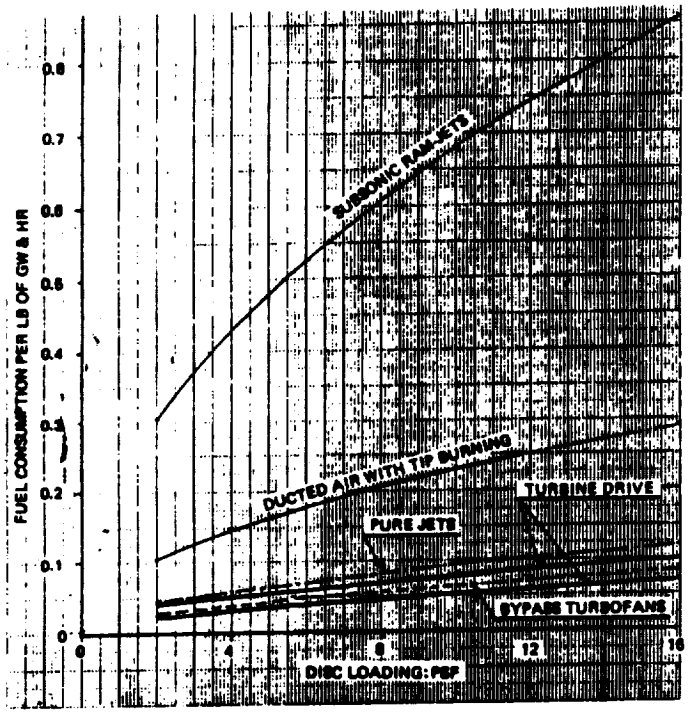

Figure 1.6 A comparison of trends in fuel consumption per pound of gross weight and 1 hr in hover OGE, SL STD, for shaft and tip-driven helicopters

For instance, for subsonic ram-jet helicopters, the fuel consumption per unit of gross weight and unit of time appears to be about ten times higher than for their shaft-driven counterparts at the same disc loading. In spite of such odds, serious, nonamateurish attempts were made to develop operational ram-jet-driven helicopters, showing that the designers hoped to compensate for the fuel consumption handicaps through such advantages as the extreme simplicity of the aircraft — leading, in turn, to very low relative weight-empty values and potentially low unit prices. Thus, this extreme case may be cited as an example of the previously mentioned importance of the interplay between the relative weight empty and fuel consumption per unit of gross weight and time in achieving a desired performance in hover.

As a postscript, it may be added that in the case of ram-jet helicopters, the extreme noise making these aircraft operationally unacceptable was probably the main reason for abandoning any further attempts toward improvement.

1.3.5 Parameters Influencing Horizontal Flight Performance

For rotorcraft where shaft-type engines provide all power required in horizontal flight (SHP_{req}), an idea of the gross weight to the equivalent drag ratio (W/D_e) was introduced as a common gauge for measuring the aerodynamic efficiency of the aircraft. It may be recalled that this quantity at any speed of flight in knots (V) is defined as follows:

$$W/D_e = WV/325\,SHP \tag{1.25}$$

where the gross weight is in pounds.

Knowing the gross weight to the equivalent drag ratio values as a function of the speed in horizontal flight, the total rate of the hourly fuel consumption by the aircraft becomes:

$$FF = (W/D_e)^{-1} W\,sfc\,V(1.69/550) \tag{1.26}$$

and fuel consumption per pound of aircraft gross weight and one nautical mile flown is obtained by dividing Eq. (1.26) by W and V:

$$(FC_w)_R = 0.00307(W/D_e)^{-1} sfc \tag{1.27}$$

where sfc is the engine specific fuel consumption at the power setting and ambient conditions corresponding to horizontal flight at speed V (in knots).

For propeller-driven fixed-wing aircraft, the SHP required in horizontal flight can be expressed as

$$SHP_{req} = (W/D)^{-1} WV/325\eta_{pr} \tag{1.28}$$

where $W/D = L/D$ is the actual lift-to-drag ratio of the aircraft, and η_{pr} is the propeller propulsive efficiency.

The $(W/D)\eta_{pr}$ product may be called the gross-weight (lift), to the equivalent drag ratio:

$$(L/D)\eta_{pr} \equiv (W/D)\eta_{pr} \equiv W/D_e. \tag{1.29}$$

Equations for the total rate of fuel flow and fuel consumption per pound of gross weight and one nautical mile flown become identical with Eqs. (1.26) and (1.27), respectively. Now, the weight to the equivalent drag ratio, as defined by Eq. (1.25), becomes an important tool for direct comparison of the fuel efficiency of various shaft-driven concepts and configurations. This is especially convenient, since sfc may, in principle, be the same for like rated power class engines, regardless of the type of aircraft on which they are installed. Consequently, knowledge of the $(W/D_e) = f(V)$ relationship may be all that is needed to judge at a glance the effectiveness of energy utilization of a given shaft-driven type of aircraft as a whole.

For jet-propelled aircraft, the rate of fuel consumption by an aircraft flying horizontally and assuming that weight-to-drag ratios are identical to the lift-to-drag ratios, will be

$$FF = (W/D)^{-1} W\,tsfc \tag{1.30}$$

where *tsfc* is the engine thrust specific consumption in lb/lb,hr. Knowing the relationship between *tsfc* and speed (Mach number) of flight at given ambient conditions, the fuel consumption per pound of aircraft gross weight and nautical mile flown can be computed from the following expression derived from Eq. (1.30):

$$(FC_w)_{R_j} = (W/D)^{-1} tsfc/V. \tag{1.31}$$

Looking at Eqs. (1.27), (1.29), and (1.31), one would note that in fixed-wing configurations, the (W/D) levels represent one of the most important factors regarding energy utilization aspects of aircraft in transport tasks. Consequently, it may be useful to recall the design parameters and ambient conditions that play a major role in maximization of the W/D or, in other words, minimization of the D/W values.

The total drag of an aircraft deriving its lift ($L = W$) from the wing in horizontal flight is

$$D = q[(f + S_w C_{D_o})\lambda_{compr} + (C_L^2/\pi AR_e)S_w]. \tag{1.32}$$

In this equation, q is the dynamic pressure of flight (for V in knots, $q = 0.0034\bar{\rho}V^2$), f is the equivalent flat plate area (in sq.ft) of the aircraft, less wings, S_w is the reference wing area, C_{D_o} is the profile drag coefficient of the wing, λ_{compr} is the drag rise factor due to compressibility effects (assumed for simplicity as being the same as for the parasite and wing drags), AR_e is the effective wing aspect ratio, and C_L is the wing lift coefficient.

Remembering that in horizontal flight, $C_L = w_w/q$, where w_w is the wing loading, and dividing Eq. (1.32) by W, the following expression for the drag-to-gross-weight ratio is obtained:

$$(D/W) = q[(1/w_f) + (C_{D_o}/w_w)]\lambda_{compr} + (w_w/\pi AR_e q). \tag{1.33}$$

Making $\partial(D/W)/\partial q = 0$, the q value at which D/W becomes a minimum; i.e., W/D a maximum, is obtained:

$$q_{opt} = \sqrt{w_w/\pi AR_e[(1/w_f) + (C_{D_o}/w_w)]\lambda_{compr}}. \tag{1.34}$$

Multiplying the numerator and denominator in Eq. (1.34) by the wing loading, Eq. (1.34) becomes

$$q_{opt} = w_w/\sqrt{\pi AR_e[(w_w/w_f) + C_{D_o}]\lambda_{compr}}. \tag{1.34a}$$

But $w_w/w_f \equiv (W/S_w)/(W/f) = f/S_w \equiv C_{D_{par}}$, where $C_{D_{par}}$ is the parasite drag coefficient of the aircraft less wings. $C_{D_{par}} + C_{D_o}$ can, in turn be called the total noninduced aircraft drag coefficient ($C_{D_{nind}}$) and Eq. (1.34a) can simply be written as

$$q_{opt} = w_w/\sqrt{\pi AR_e C_{D_{nind}}\lambda_{compr}}. \tag{1.34b}$$

By the same token, the optimal value of the wing loading corresponding to the given q of flight, wing aspect ratio, and degree of aerodynamic cleanness of the aircraft as expressed by the $C_{D_{nind}}$ level, can be obtained by solving Eq. (1.34b) for w_w:

$$w_{w_{opt}} = q\sqrt{\pi AR_e C_{D_{nind}} \lambda_{compr}} \tag{1.35}$$

Substituting Eq. (1.34b) into Eq. (1.33), a useful expression for the interpretation of the influence of some important design parameters on the optimal gross weight lift-to-drag ratio is obtained.

$$(W/D)_{max} = \tfrac{1}{2}\sqrt{\pi AR_e/[(w_w/w_f) + C_{D_o}]\lambda_{compr}} \tag{1.36}$$

or, remembering that $(w_w/w_f) + C_{D_o} = C_{D_{nind}}$, Eq. (1.36) may be rewritten in a coefficient form:

$$(W/D)_{max} = \tfrac{1}{2}\sqrt{\pi AR_e/C_{D_{nind}}\lambda_{compr}} \tag{1.37}$$

The above developed relationships are illustrated by a few figures which should enable the reader to see at a glance how various design parameters influence optimal gross-weight (lift) to drag ratio levels.

Figure 1.7 was prepared to show the interplay between wing aspect ratio, wing loading, and overall aerodynamic cleanness of the aircraft in determining the $(W/D)_{opt}$ levels.

The lower part of the graph shows the influence of wing loading (vertical scale) and cleanness of the airframe (indicated by the equivalent flat plate area loading values). For instance, assuming that wing loading is 100 fps and the anticipated w_f = 2000 psf, the airframe parasite drag coefficient is seen as equal to 0.05. To this, the expected profile drag coefficient of the wing (0.008 in the example shown in Figure 1.7) is graphically added. Should it be anticipated that the flight Mach numbers would be high enough to significantly increase the previously obtained total noninduced drag coefficient level, then a proper correction (λ_{compr}) should be applied (here, λ_{compr} = 1.0 is assumed). As shown in the upper part of this figure, the combined influence of the $C_{D_{nind}}$ and AR values on the W/D levels can be examined. It can also be seen that in our example of $C_{D_{nind}}$ = 0.068, the optimal weight (lift) to drag ratio would be about 7.4 for AR = 4, but would increase to $(W/D)_{max} \approx 11.6$, should the aspect ratio be equal to 10.

One question that could be asked when formulating a basic concept of a VTOL aircraft which cruises in the fixed-wing configuration is what the wing loading should be in order to ascertain that at the intended flight speed and altitude, the aircraft would operate at or near its W/D (L/D) optimum. Eq. (1.35) answers this question analytically. However, a graphical interpretation of that equation may be better suited for understanding the role of various design parameters (Figure 1.8).

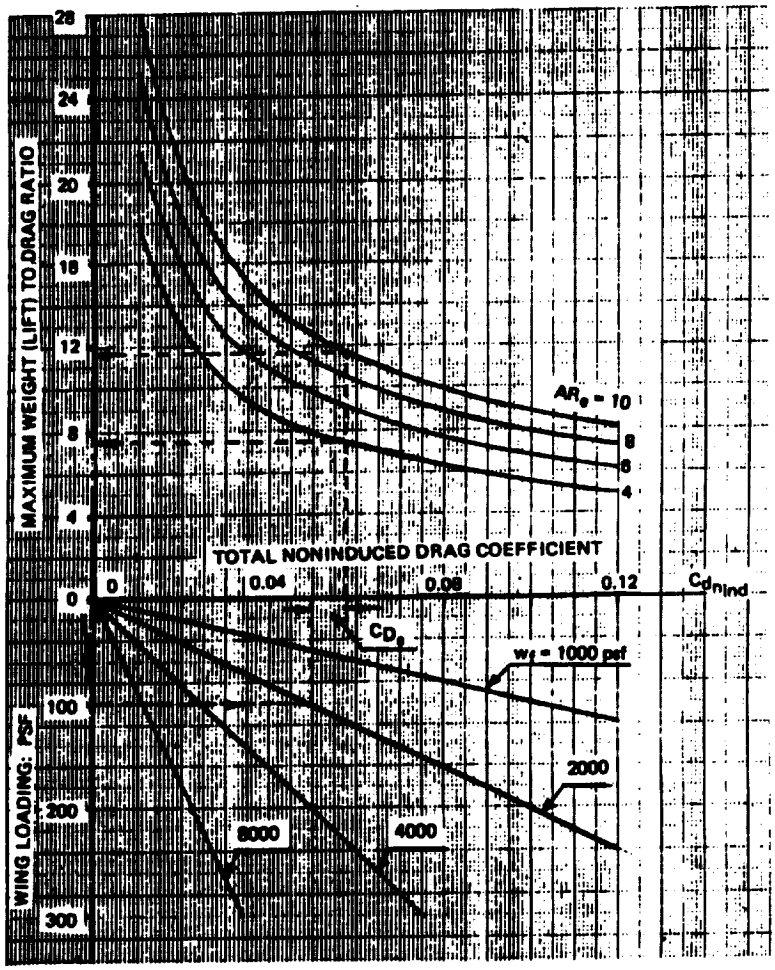

Figure 1.7 Illustration of the influence of wing loading, airframe aerodynamic cleanness (w_f levels), profile drag, and wing aspect ratio on the $(W/D) \equiv (L/D)$ optimal values

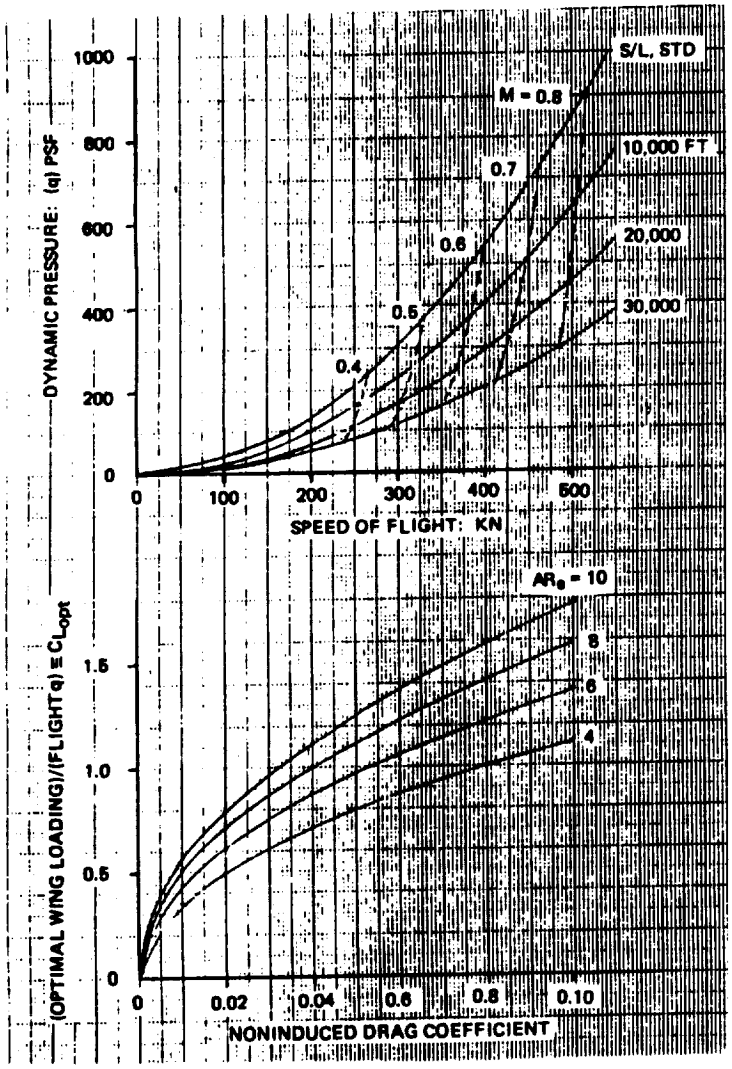

Figure 1.8 Approximate determination of optimal wing loading for given speed and altitude of flight

From the upper graph of this figure, the approximate values of dynamic pressure and Mach number corresponding to the intended speed and altitude of flight can be read. Knowledge of the flight M level should give a clue whether compressibility corrections should be applied and thus, provide the level of the noninduced drag coefficient of the aircraft as a whole that can be expected. Having this latter figure, and knowing the anticipated geometric and effective wing aspect ratio (AR_e), the approximate ratio of optimal wing loading to the flight q corresponding to the intended speed and altitude of flight can readily be read from the lower graph shown in Figure 1.8.

It should be recalled at this point that the wing loading to the flight dynamic pressure ratio is equal to the aircraft lift coefficient (C_L): $C_L = w_w/q$.

Consequently, looking at the so-obtained optimal w_w/q ratios, one would be able to judge whether the corresponding ideal $C_{L_{opt}}$ values would still be within the envelope of the lift-coefficient values possible for the aircraft. It might be necessary, in some cases, to select a wing loading lower than its theoretically optimal value.

1.3.6 Regions of Fuel Consumption per Lb of GW and N.Mi.

In conclusion of these general considerations of energy utilization aspects in forward flight by an aircraft as a whole, Figure 1.9 is presented. Here, regions of the possible optimal $(FC_w)_R$ values vs. corresponding cruise speeds are outlined for the following aircraft of the 10,000 to 100,000 gross-weight class representing the current state of the art: helicopters, tilt-rotors, turboprops, and turbofans.

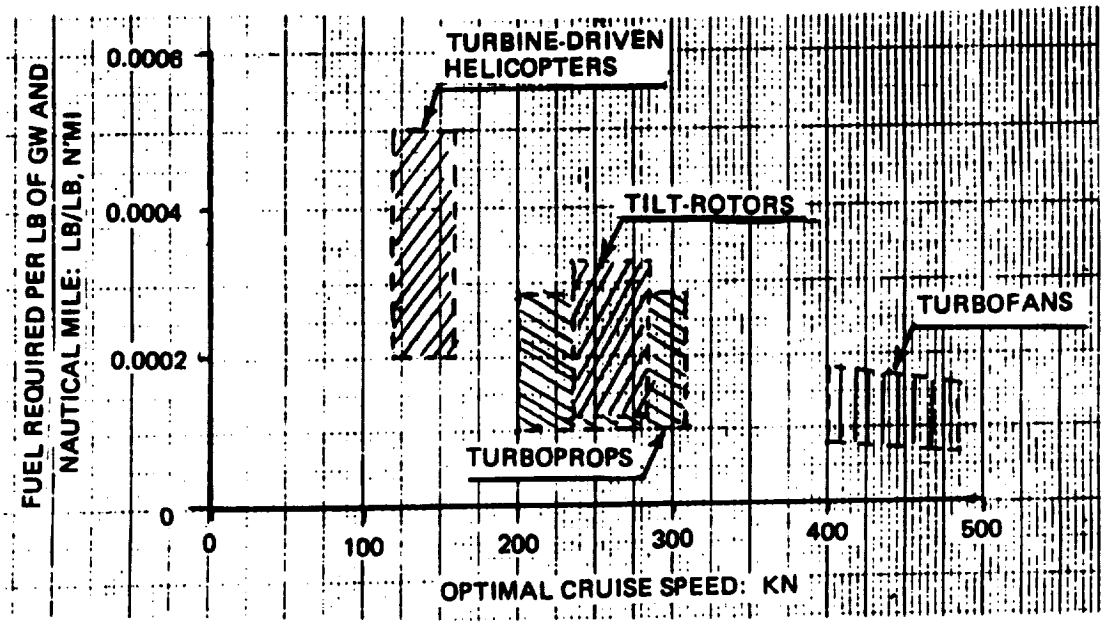

Figure 1.9 Regions of possible optimal $(FC_w)_R$ values vs. corresponding cruise speeds for some contemporary aircraft

The $(FC_w)_R$ regions shown in this figure were established by taking, as the abscissas of the corner points, the lowest and highest cruise speeds encountered for a given type of aircraft as shown in Table 1.1. Then, the highest and lowest probable values of the ordinates for the corner point were computed from Eqs (1.27) and (1.31) by taking the worst and best combinations of the $(L/D_e)_{max}$ and sfc for the shaft-driven aircraft, and L/D_{max} and tsfc for turbofan aircraft.

TABLE 1.1

RANGES OF ASSUMED PARAMETRIC VALUES[3,5,6,7]

	PARAMETRIC VALUES	AIRCRAFT TYPE			
		HELICOPTERS	TILT-ROTORS	TURBOPROPS	TURBOFANS
	Highest V_{cr}, Kn	160	280	310	480
	Lowest V_{cr}, Kn	120	230	200	400
BEST	$(L/D_e)_{max}$ or L/D_{max}*	6.0	11.0	12.0	16.0
BEST	sfc, lb/hp,hr	0.40	0.40	0.40	–
BEST	tsfc, lb/lb,hr	–	–	–	0.5**
WORST	$(L/D_e)_{max}$ or L/D_{max}*	4.0	6.0	7.0	12.0
WORST	sfc, lb/hr,hr	0.65	0.65	0.65	–
WORST	tsfc, lb/lb,hr	–	–	–	0.9

Notes: *Turbofans
**High BPR

If one would mark the points on Figure 1.9 corresponding to the $(FC_w)_R$ values at specified best cruise speeds for presently operational aircraft, one would note that most of the points would be located in the lower half of the shown regions. However, some points may be even above the shaded area.

Of particular interest, are the bottom lines of the $(FC_w)_R$ regions, as they would indicate already existing potentials regarding achieving low $(FC_w)_R$ levels at cruise speeds representative of various types of aircraft. Consequently, they may serve as the baseline in evaluating future concepts and configurations.

As to the particulars of the optimal $(FC_w)_R$ boundaries, it may be expected that classical turboprops would have some advantage over the presently configured tilt-rotors, as tilt-rotors have inherently low aspect ratios.

With respect to the bottom line of the turbofans, one may object that it may be somewhat unconservative, since it represents a combination of the highest, presently encountered, $(L/D)_{max}$ values and lowest current *tsfc* levels as represented by the high BPR type engines. This, of course, would require large nacelles, or fuselage bulges, thus leading, in principle, to lower $(L/D)_{max}$ levels than those obtainable for aircraft equipped with low, or no, BPR engines requiring more slender nacelles, or smaller protrusions for housing the powerplants. However, should unducted fans (UDF) be used, then a combination of maximum L/D values and a low *tsfc* (even lower than the 0.6 lb/lb,hr assumed in Table 1.1) would become possible.

In summary, Figure 1.9 may be considered as a fair representation of trends in $(FC_w)_R$ levels and cruise speeds for various aircraft in the $10{,}000 < W < 100{,}000$-lb gross-weight class, while their bottom lines may be taken as optimal boundaries representing the current state of the art.

CHAPTER 2

TIP DRIVEN HELICOPTER CONCEPTS

2.1 Introduction (Historic Perspective)

The basic idea of putting a rigid body into rotary motion by discharging a jet of fluid from nozzles located at the periphery of the body goes back to the first century A.D. At that time, Hero (also called Heron) of Alexandria developed what was probably then considered a toy, consisting of a steam-driven rotor (Figure 2.1(a)).

In more modern times, there were many attempts to apply the principle of jet propulsion to rotors of various rotorcraft by discharging either hot or cold gases, largely from discrete nozzles located at the blade tips. There were also projects aimed at discharging part of the gas through slots extending along the blade span (but still mostly in the tip region), thus combining propulsion with some aspects of circulation control.

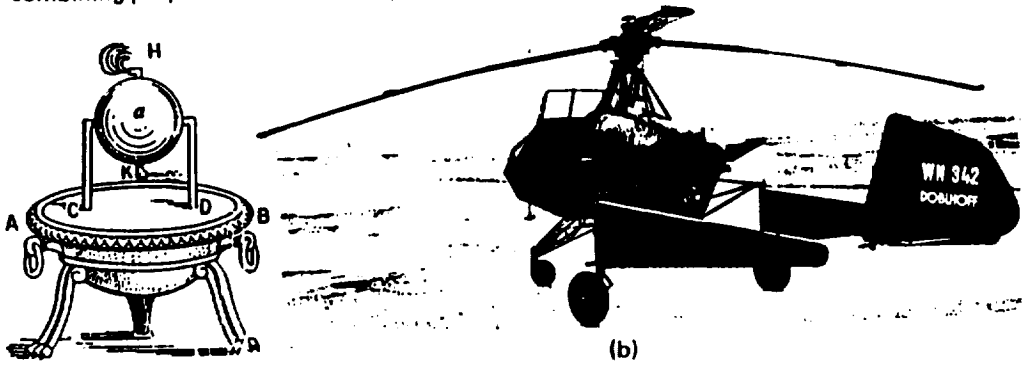

(a) Hero's aeolipile: A B, steam boiler; C D, supports; a, revolving globe; H K, nozzles.

Figure 2.1 State of the art design progress from the steam-driven globe of Hero (1st Century AD) to the jet-driven WN-342 of von Doblhoff (early 1945)

As for 'reduction to practice' of the concept of the jet-driven rotor, von Doblhoff's helicopters developed during the 1943-45 time period were probably the first rotorcraft of that type to achieve flight-test status. His fourth model, the WN-342 in early 1945 (Figure 2.1(b)), used rotor jet drive for takeoffs and landings and, in forward flight, worked as a propeller-driven autogiro. During the post-war period, von Doblhoff continued to further develop the idea of combining the jet-driven rotor with the autogiro principle by working on the McDonnell XV-1 compound helicopter.

As to other pioneering efforts of adapting jet propulsion to helicopters, the development of an aircraft by the Jet Helicopters Company in Montreal, Canada should be cited. In this case, the B-36, a single-seater of approximately 3000 lb GW was designed and built along the concepts and patents of W. Brzozowski during the 1944-46 time period and was eventually ground tested around the 1950s but, to the best knowledge of these investigators, it was never flown (Figure 2.2).

Figure 2.2 B-36 helicopter of Jet helicopter Company, Canada

In both of the above described configurations, air was brought to a higher than atmospheric pressure level by a compressor located in the airframe. However, in Doblhoff's approach, compressed air was mixed with gasoline and then ducted to the blade tips where it was ignited by means of spark plugs. In the B-26 case, compressed air was ducted to the blade tips, where fuel was supplied to the burners.

Shortly after World War II, especially in the 1950s and 1960s, many schemes similar to those of von Doblhoff and Brzozowski, as well as other variants of tip-driven rotors, were either actually constructed or, at least, seriously studied. All of the so-developed helicopters can be roughly divided into two basic types:

(1) Rotorcraft with airframe-mounted compressed air or gas generators, where gases are ducted through the blades for either direct discharge through tip nozzles or, in the case of compressed air, the flow of gases is further energized by fuel combustion in special – usually tip-mounted – burners, and

(2) Configurations where complete powerplants are blade mounted; in most cases, at the tip.

Helicopters belonging to the first type can, in turn, be divided into the following sub-types:

(a) Cold Jets. Here, air is brought to a high pressure by a compressor located in the airframe and then ducted through the blade and discharged through blade-tip nozzles. The Sud-Aviation Djinn of the 1950s can be cited as the most successful representative of that category (Figure 2.3) while, at present, a helicopter design based on this same principle is being carried out by Voljet of New Jersey under the leadership of Liberatore (Figure 2.4).

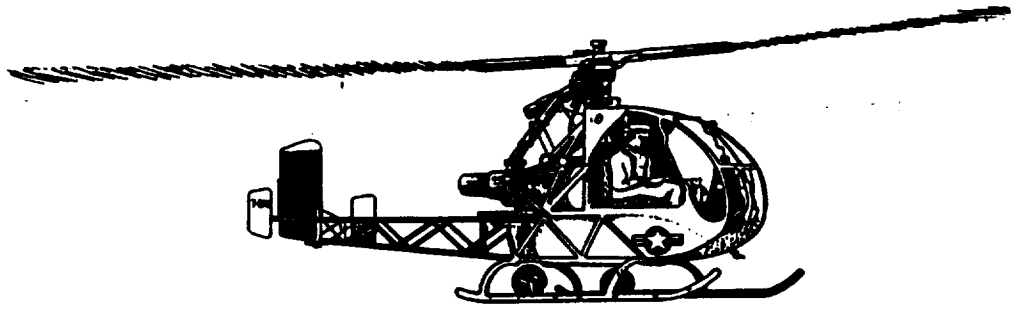

Figure 2.3 The S.O. 1221 Djinn compressed-air-driven helicopter

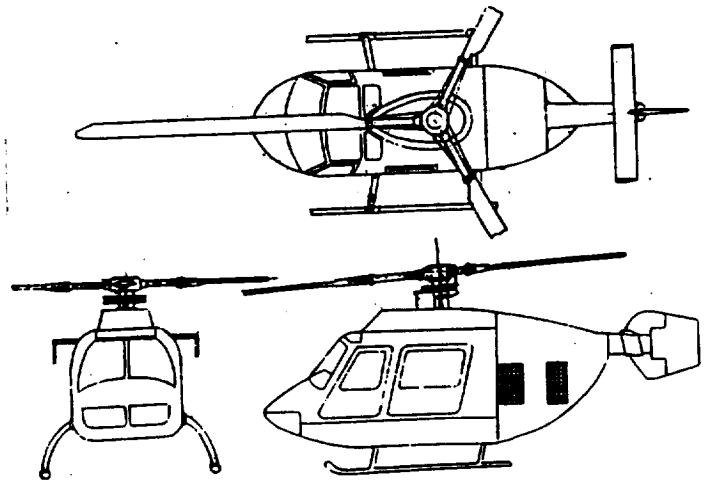

Figure 2.4 The Voljet Model 280 compressed-air-driven helicopter

(b) Tip Burning. Tip-burning types represent variants of von Doblhoff's and Brzozowski's original approaches, wherein energy contained in the compressed air flowing through the blade ducts is further augmented by fuel burning in the tip region. Two compound helicopters, the McDonnell XV-1 (Figure 2.5) and the Fairey Rotodyne (Figure 2.6) can be cited as the most prominent representatives of this type of reaction rotor drive.

Figure 2.5 McDonnell XV-1 experimental compound helicopter

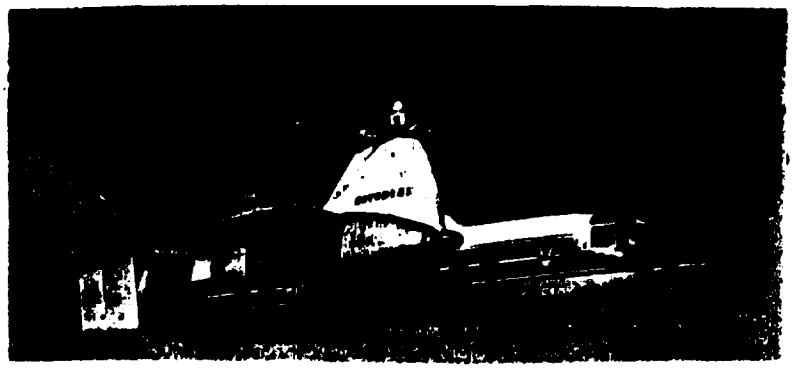

Figure 2.6 Fairy Rotodyne compound passenger transport system

The most objectional characteristics of this system of rotor propulsion were noise and high fuel consumption.

(c) Hot or Warm Cycle. In this scheme, a mixture of compressed air and engine exhaust gases (Figure 2.7) is produced by a generator; again, located in the airframe and then ducted to blade-tip nozzles, where it is discharged at basically subsonic speeds and temperatures as low as 230°C.

Considerable research and design work on the so-called 'warm' system was conducted by the MBB company (then Bölkow) under the leadership of Heidelberg in the late 50s and early 60s. These efforts were directed toward development of a heavy-lift transport helicopter, the BO-X model (Figure 2.8).

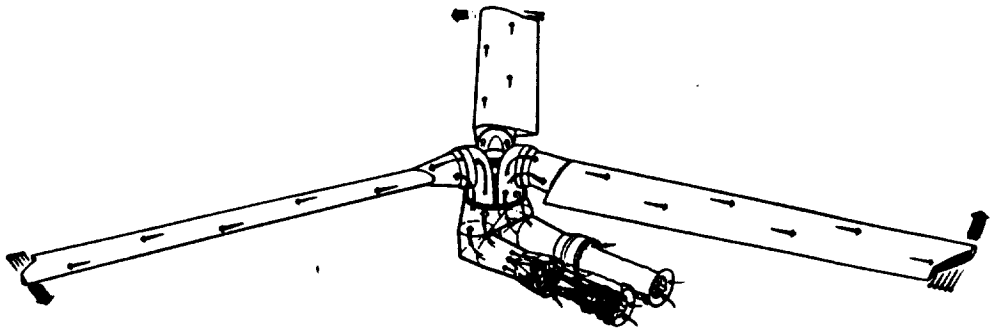

Figure 2.7 Scheme of warm pressure jet-driven system (Ref. 8)

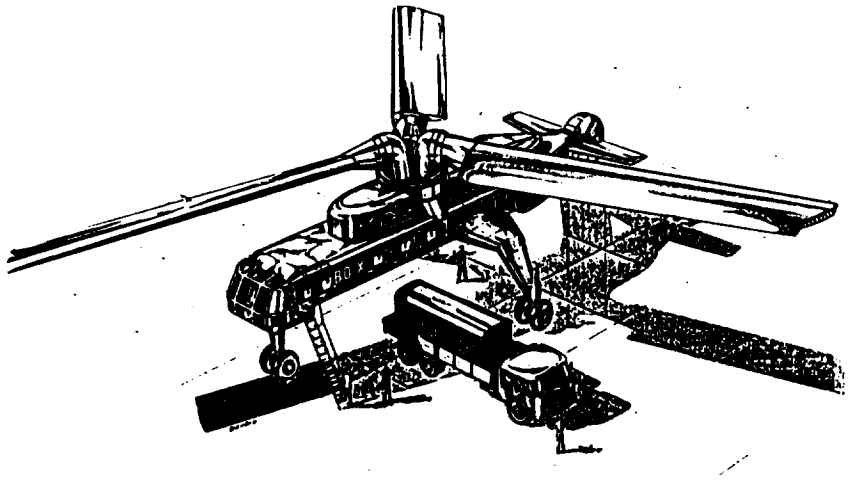

Figure 2.8 Artist's impression of the BO-X heavy-lift helicopter

The BO-X project was aimed at a machine capable of meeting and exceeding the U.S. heavy-lift helicopter specification of lifting payloads of approximately 20 tons (actually 26.5 tons for the BO-X) at 6000 ft, 95°F ambient conditions.

In order to establish a solid technical background for design efforts, Bölkow Company, in the early sixties, constructed a large (31-m dia) rotor using the Heidelberg system. This rotor was capable of developing thrusts of over 30 tons, and had been extensively tested on a special rotor test stand powered by a G.E. dual-flow turbine, producing a maximum 18,000 gas hp (Figure 2.9).

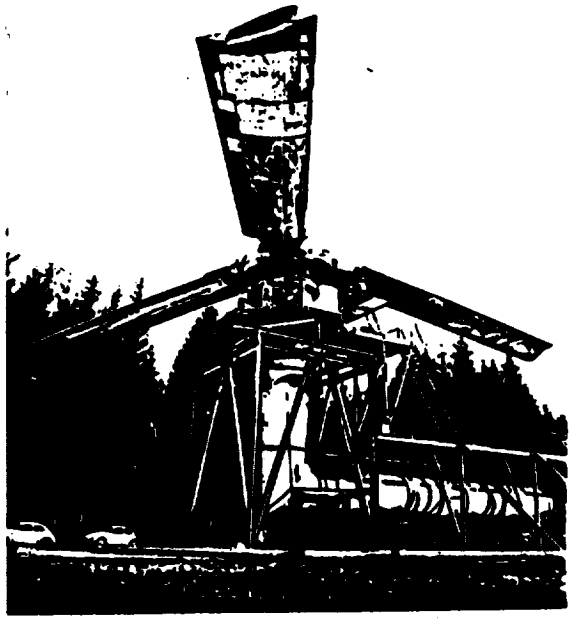

Figure 2.9 Test facility for the full-scale, tip-driven rotor using a low-pressure reaction propulsion system

It should be noted that the key to the feasibility of the final BO-X design based on the so-called 'Heidelberg warm, low-pressure gas system' was the use of dual flow (bypass = 1) turbofans such as the Pratt Whitney JT8D engines installed on Boeing 727 planes (Ref. 8).

In this country, research on the hot/warm pressure-jet systems and design studies regarding possible applications of that approach for heavy-lift helicopters were carried out primarily by Hughes. One scheme of their system, known as the hot pressure-jet system (discussed in detail by Nichols in Ref. 9), is shown in Figure 2.10.

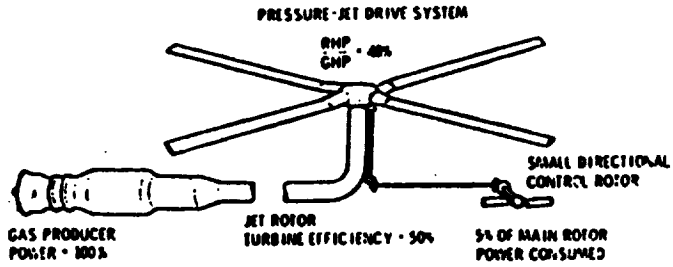

Figure 2.10 Scheme of Hughes hot pressure-jet system [9]

One can see from this figure that the principle is practically the same as that of Heidelberg (Figure 2.7). The difference consisted of a trend toward higher pressures and temperatures in the Hughes designs than those in the Bölkow systems.

It should be noted that similar to studies by Bölkow, studies by Hughes in the 1960s also indicated that their system can, in principle, be competitive with shaft-driven configurations in the heavy-lift helicopter class. An 0.7-scale model aircraft of the full-scale Hughes XV-9A machine based on the hot-cycle approach was test flown (Figure 2.11).

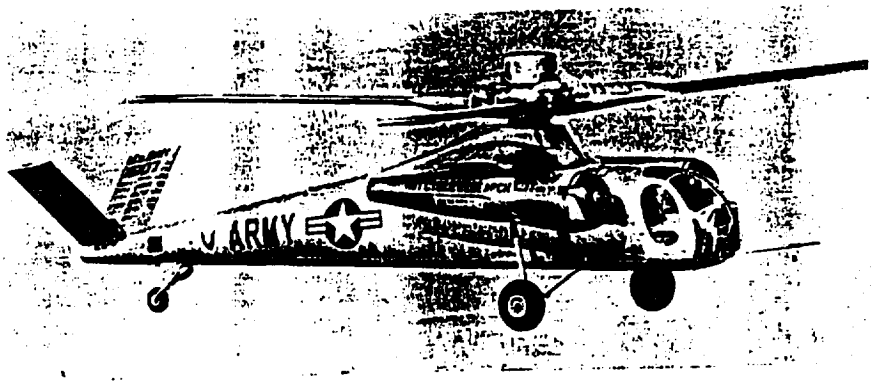

Figure 2.11 Hughes XV-9A helicopter based on the hot pressure-jet drive system

In the late seventies and early eighties, Hughes Company and the David Taylor Naval Ship Research and Development Center conducted studies of a warm cycle approach similar to the Bolkow concept, but included an investigation of incorporating circulation control. A very-heavy-lift helicopter (VHLH) was designed along those lines (Figure 2.12, Ref. 10).

This helicopter, having a gross weight of about 270,000 lb powered by four low-bypass-ratio Pratt & Whitney F-100 or G.E. F-101 engines, was designed to carry the 60-ton XM-1 Main Battle tank for a distance of 100 nautical miles in a ship-to-shore assault mission. An interesting feature of the design was incorporation of blade circulation control, thus permitting one to eliminate root pitch control and opening the possibility for use of higher harmonic inputs to reduce vibrations associated with the two-bladed rotor configuration.

Helicopters belonging to the tip-mounted powerplant groups can, in turn, be divided into the following sub-types:

1. Ram jets are probably the simplest conceptual solution for tip-driven rotors, as ram-jet engines have no moving parts, and thus are capable of sustaining the high g-fields encountered at the blade tips. The Hiller HJ-1 Hornet (Figure 2.13), and

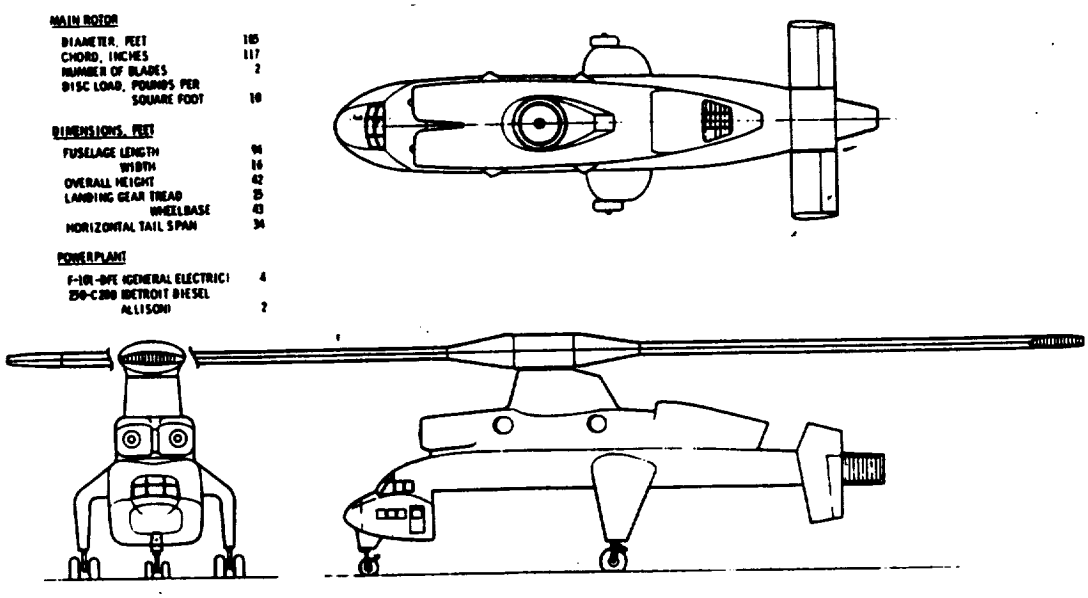

Figure 2.12 VHLH General Arrangement

the Dutch Kolibrie (Figure 2.14) may be cited as representatives of this type which were produced in small quantities. Noise and extremely high fuel consumption were the most objectionable characteristics of these rotorcraft.

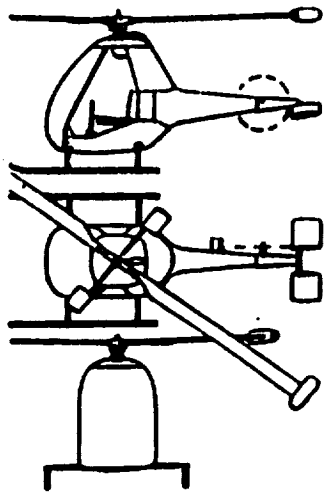

Figure 2.13 The Hiller HJ-1 Hornet ram-jet-driven helicopter

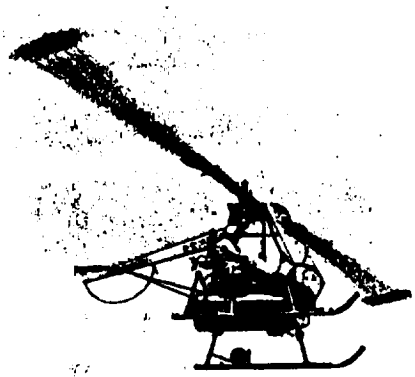

Figure 2.14 Production model of the NHI H-3 Kolibrie ram-jet-powered helicopter

2. Blade tip-mounted turbojets, wherein complete turbojets are mounted at the blade tips. Originally, studies in Great Britain indicated a potential feasibility of this approach for heavy and very heavy helicopters (Figure 2.15 (Ref. 11)). In this country, anticipated promises of tip-mounted turbojets prompted tests conducted by Hiller in the early 1960s, wherein the feasibility of the concept was investigated by whirling the Williams jet engine at a centrifugal acceleration of about 200+ g's. Extensive design studies were also performed by Hiller and Piasecki in the mid-sixties (see Appendix).

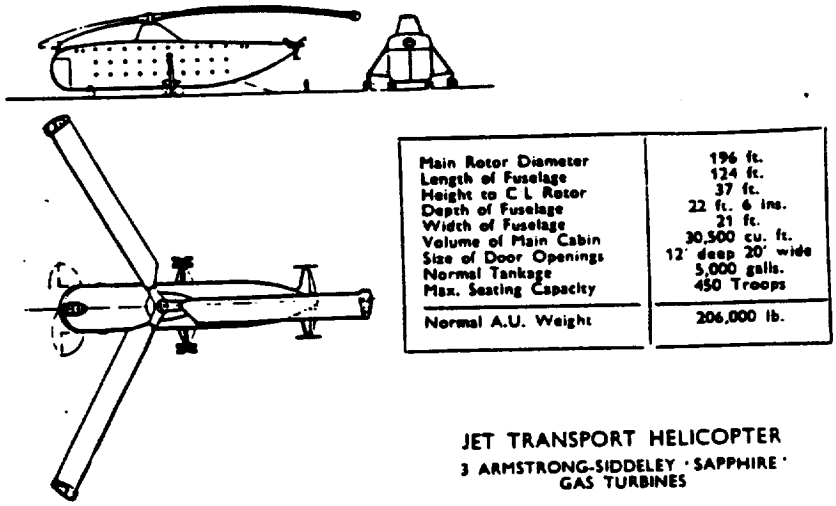

Figure 2.15 "Giant," the original early 1950's concept of turbojet-driven rotors applied to heavy-lift helicopters[11]

However, no actual helicopter having tip-mounted turbojets was ever built. Professor H. Velkoff (Ohio State University) indicated to these investigators that the high cost of developing, or even adapting, existing powerplants to high-g

operational conditions was probably the chief reason for the lack of actual development along those lines. Also, high noise levels and somewhat higher fuel consumption than for shaft-driven types also probably contributed to the lack of actual development of the blade tip-mounted turbojet concepts.

3. Blade tip-mounted unducted fans. From the point of view of effective fuel energy utilization, all of the tip-driven rotor concepts discussed so far have a common flaw. Because the exit velocity from the thrust-producing blade-tip nozzles is much higher (sonic, or close to sonic at elevated temperatures) than the rotor tip speed, the propulsive Froude efficiency is quite low. Furthermore, in the fuselage mounted gas generator concepts, ducting losses encountered by gases flowing from the generator to the blade tips additionally contribute to the reduction of overall fuel efficiency. Consequently, thrusters installed at the blade tips, or slightly inboard, that would operate at a high propulsive efficiency and suffer no duct losses appears as a desirable step toward more efficient fuel utilization. In this respect, airscrew-type thrusters appear as an attractive possibility. The idea of using propellers as a means of driving a lifting rotor is not new, as witnessed by the Isacco helicopter in 1929 (Figure 2.16). However, at tip-speed values commonly now in use in helicopter design ($V_t \approx 700$ fps

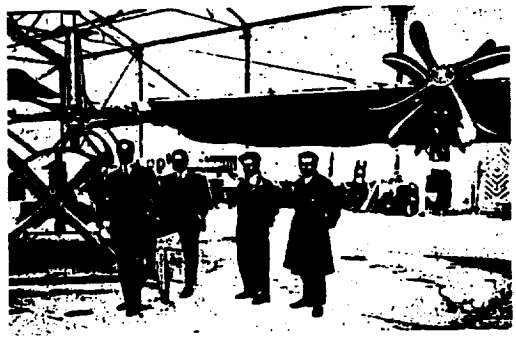

Figure 2.16 Isacco's 1929 helicopter

and higher), the propulsive efficiency of conventional propellers begins to deteriorate. By contrast, the installed efficiency of unducted fans (UDF) is superior to that of both conventional propellers and jets (Figure 2.17, Ref. 12). Consequently, work currently being performed on the development of unducted fans (UDF) for high subsonic fixed-wing aircraft should encourage one to take a fresh look at the general type of tip-mounted complete powerplants – this time, using unducted fans. Because of the high propulsive efficiency of the UDF, one may

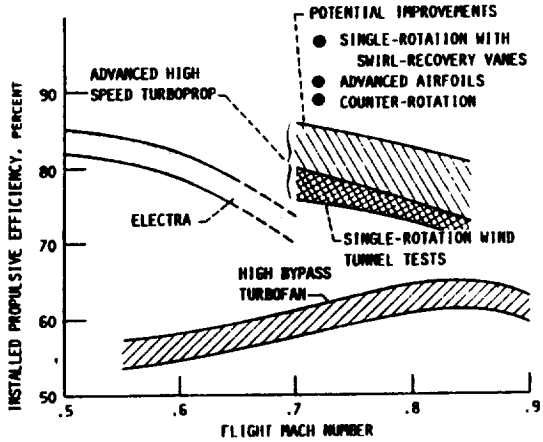

Figure 2.17 Installed propulsive efficiency trends of advanced transports compared with equivalent technology turbofans[12]

expect that specific fuel consumption referred to the rotorcraft gross weight $(FC_w)_t$ can be brought to shaft-driven helicopters levels. Specific fuel consumption related to zero-range payload $(FC_{0pl})_t$ should be considerably better than for the shaft-driven counterparts because of anticipated lower relative weight empty $(\overline{W}_e)$ values resulting from the elimination of the mechanical drive system. With respect to single-rotor configurations, additional gains in the weight-empty values and overall efficiency can be expected because of the elimination of the torque-compensating tail rotors.

In order to get a better feeling, both for potential gains in $(FC_w)_t$ and $(FC_{0pl})_t$ as well as the general feasibility of the concept, two hypothetical single-rotor crane helicopters of 400,000 and 200,000 lb gross weight are studied here in a somewhat cursory way (see Appendix A). It is believed, however, that in spite of its limited scope, this study should provide sufficient data to answer some basic questions regarding the competitive position of the unducted-fan concept with respect to shaft-driven types, and to indicate the direction for more detailed studies and research.

In conclusion of this historic perspective review, a brief list of representative tip-driven helicopters (both past and those under current development), along with some important characteristics assembled from Refs. 7, 8, 10, 11, 13, 14, 15 and 16 is presented in Table 2.1.

At this point, it should be recalled that the principal incentive for studying and developing the tip-rotor-driven helicopter has been, and still is, to eliminate the mechanical transmission and avoid the necessity for torque compensating devices in single-rotor configurations. Both solutions would hopefully lead to more favorable relative weight-empty and simpler designs.

TABLE 2.1A
PRINCIPAL CHARACTERISTICS OF REPRESENTATIVE TIP-DRIVEN-ROTOR HELICOPTERS USING AIRFRAME-MOUNTED AIRGAS GENERATORS

	COLD CYCLE			WARM/HOT CYCLE			
PRINCIPAL CHARACTERISTICS	DJINN	VOLJET 280	VOLJET 281 (STUDY)	BOLKOW BO-X	HUGHES XV-9A	GEORGIA TECH (STUDY)	HUGHES/DAVID TAYLOR (STUDY)
APPROX. DESIGN YEAR	1953	1987	1982	1960-64	1960	1988	~1980
GROSS WEIGHT, LB	1,763	4,850	233,000 NORM 291,000 MAX	99,225 N 147,735 M	15300 25,500 MAX	76,970	268,000
WEIGHT EMPTY, LB	838	2,170	104,752	44,100	8,700	30,788	91,300
RELATIVE WEIGHT EMPTY %	47	45	47.1 NORM 37.7 MAX	43.8 NORM 30.0 MAX	57 NORM 34 MAX	40	34
ROTOR RADIUS, FT	18.04	19	103	58.56	27.5	48.7	92.5
ROTOR ARTICULATION	GIMBAL	GIMBAL	GIMBAL	FLAPPING	FLAPPING HINGE		FLAPPING
NUMBER OF BLADES	2	3	6	3	3		2
ROTOR SOLIDITY, %	2.7	5.4	0.106	13.9	0.134		6.7
BLADE t/c %	18	18		~20			15
DISC LOADING PSF.	1.72	4.28	7.0 NORM 8.73 MAX	9.2 NORM 13.7 MAX	6.44 10.74	10.3	10
TIP SPEED, FPS	510 HOVER 661 T.O. 755 JUMP T.O.	600	550				700
JET VELOCITY, FPS	~1150	1180	1180				
POWER PLANT(S)	TURBOMECA PALOUST IV 240 AIR HP	PWL PT6C-60 1150 HP	8 x ALLISON x T -701 PLUS 8 LOAD COMPRES		2 X GE YT64 GAS GENERAT.	32020 POWER REQ.	4 x P&W F-100 OR 4 x GE F401
INSTALLED POWER LOAD, LB/HP	7.34	4.22				[2.33]	
NOISE LEVEL	108 DB@50FT 102 DB @ 100 FT						
REMARKS							

TABLE 2.1B
PRINCIPAL CHARACTERISTICS OF REPRESENTATIVE TIP-DRIVEN-ROTOR HELICOPTERS USING TIP-MOUNTED POWER PLANTS

	FUSELAGE-MOUNTED COMPRESSORS; TIP BURNERS			RAMJETS		TURBOJETS	UNDUCTED FANS
PRINCIPAL CHARACTERISTICS	6.0 1110 ARIEL II	MCDONNELL XV-1	FAIRY ROTODYNE	HILLER HORNET	KOLBRIE	FITZWILLIAMS HYPOTHETICAL "GIANT"	HYPOTHETICAL 400,000 LB
APPROXIMATE DESIGN YEAR	1948-49	1951-55	1957	1950	1955	~ 1950	1989
GROSS WEIGHT, LB	2,376	5,380	39,000	1,080	1,323	60000 (MAX) 53000 (NORM)	400,000
WEIGHT EMPTY, LB	1,595	4762 (WITH UNKNOWN WT OF INSTRS.)	23,000	231	440	20,700	167,000
RELATIVE WEIGHT EMPTY %	67.0	[88.5]	59.0	21.0	33.3	34.5 (MAX)	41.8
ROTOR RADIUS, FT	17.7	15.5	45	11.5	16.5	52	100
ROTOR ARTICULATION		GIMBAL	FLAPPING				GIMBAL
NUMBER OF BLADES	3	3	4	2	2	3	3 TO 6
ROTOR SOLIDITY, %	4	9	6.37			~10.5	11
BLADE t/c, %							24/12
DISC LOADING PSF.	2.4	7.13	6.14	2.6	1.55	7.07 (MAX)	12.5
TIP SPEED, FPS		665	720			550	700
JET VELOCITY, FPS						~1500	~760
POWER PLANT(S)	220	R-975-19 550 HP	NAPIER ELAND N.E.7 2x3250			6 ARMSTRONG TURBOJETS 1000 LB THR	TOTAL INST. HP 83045
INSTALLED POWER LOAD, LB/HP	10.8	9.80	6				4.82
FUEL CONSUMPTION PER LB OF G.W. & HR (HOVER)		0.32*	0.24/0.25	[0.29]	[0.23]	[~0.1]	[~0.06]
NOISE LEVEL		130 DB AT 30 FT	[112 DB AT 200 FT]				
REMARKS		*TESTS, REF 17					

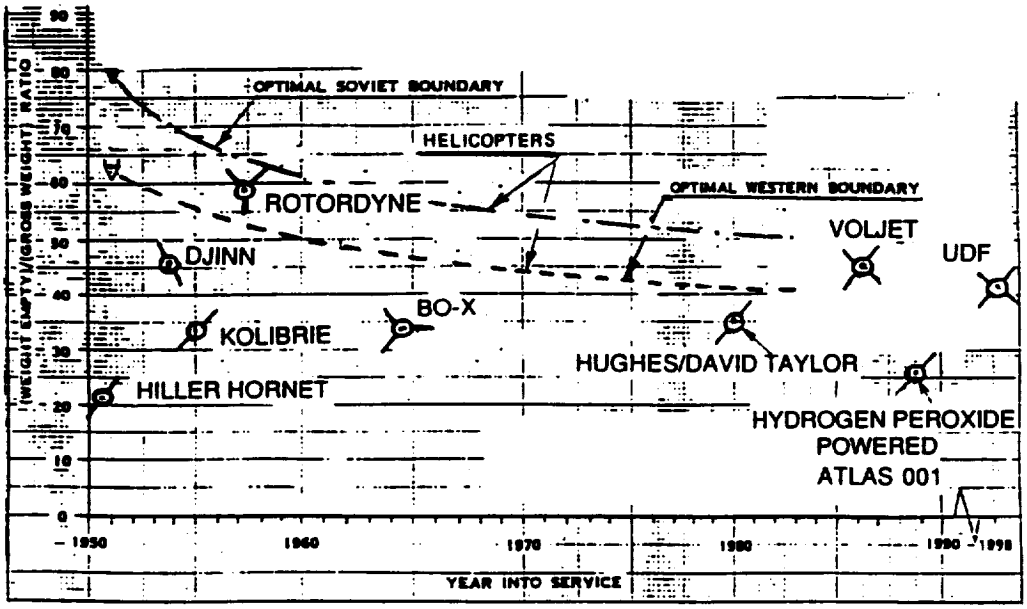

Figure 2.18 Comparison of relative empty weights of tip-driven vs. shaft-driven helicopters

Figure 2.18 was prepared in order to give the reader some insight as to the weight-empty trends of tip-driven helicopters vs. their shaft-driven counterparts. Looking at this figure and Table 2.1 will indicate that, indeed, great reductions in relative weight-empty have been achieved. It can also be stated that tip rotor-driven helicopters may, in principle, represent a definite potential for simplification of design. This point is well illustrated in Figure 2.19 where a comparison is shown between the drive system of the BO-X and a single rotor shaft-driven helicopter (Ref. 8). However, there are two characteristics constituting an Achilles heel in most jet-driven concepts: (1) high FC_{w_t} except for the UDF concept (Figure 2.20), and (2) in many cases, an absolutely unacceptable noise level – especially in tip-burning and ramjet types.

Because of the importance of specific fuel consumption aspects – both with respect to GW and zero-range (i.e., zero-time) payload, an investigation on this subject is discussed in the following segment of this chapter. It is believed that in this way, one of the important factors determining the competitive position of tip-driven concepts in comparison with their shaft-driven counterparts will be examined in some detail. Because of budgetary and time limitations, forward flight aspects, as well as other important factors such as noise and cost will be touched upon in a purely qualitative way only.

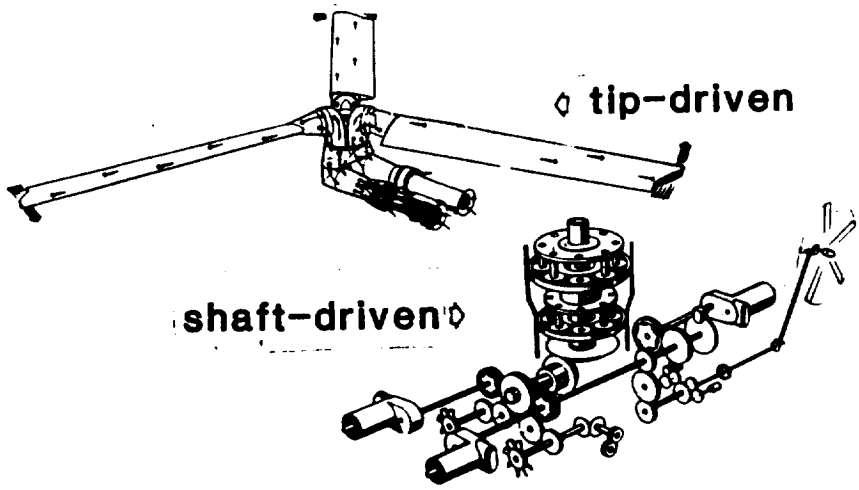

Figure 2.19 Comparison of drive systems of the BO-X vs. a conventional single-rotor helicopter (Ref. 8)

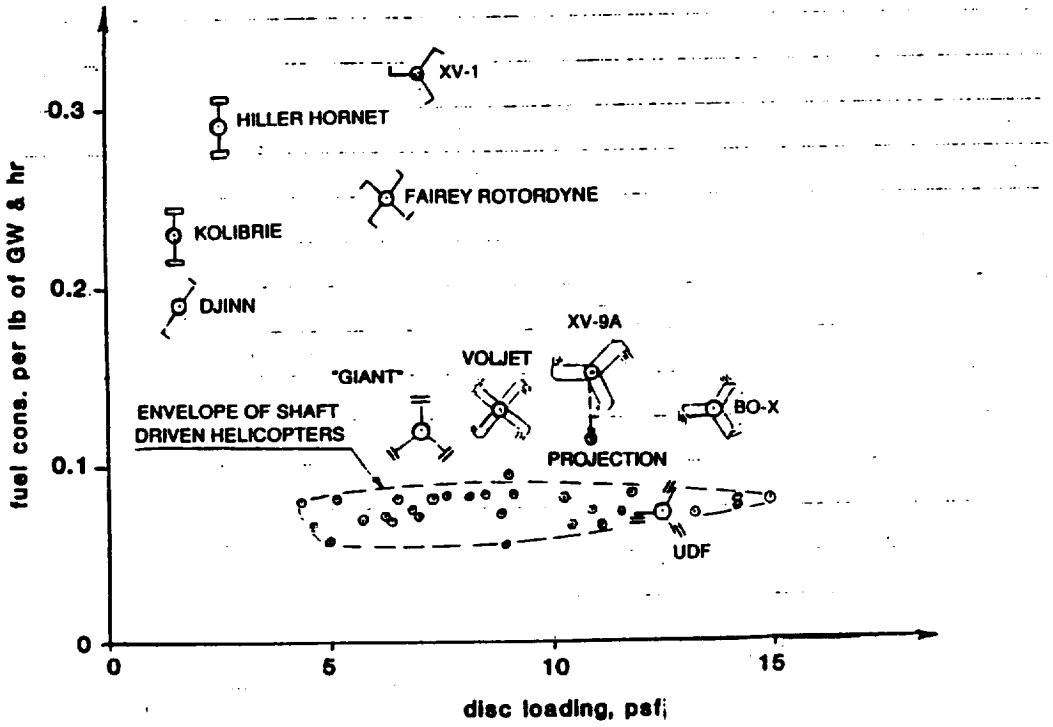

Figure 2.20 Gross weight specific fuel consumption in hover of tip-driven helicopters vs. shaft-driven helicopters (test data & detail estimates, Refs. 5, 7, 8, 11, 13, and 17)

The $(FC_w)_t$ and $(FC_{o_{pl}})_t$ in hover for cold and hot cycles (including a brief discussion of tip burners) are examined first. Then the same specific fuel consumption is examined for blade-mounted powerplant types. Special attention is paid to helicopters having tip-mounted unducted fans as potentially showing the greatest promise with respect to fuel consumption aspects. This is done by conducting cursory design studies of the very heavy crane-type helicopters of the 400,000 and 200,000-lb gross-weight class.

Overall concluding remarks regarding tip-driven helicopters are presented and recommendations given at the end of this chapter.

2.2 Fuel Consumption Aspects in Hover

2.2.1 General

In determining specific fuel consumption, either by pound of rotorcraft gross weight $(FC_w)_t$ in lb/lb-hr, or by its zero-range or zero-time payload $(FC_{o_{pl}})_t$ in lb/lb-hr, the first step would consist of accounting for total fuel consumed in a unit of time (hr) in a particular regime of flight when the aircraft gross weight is W.

For the case of fuselage-installed generators of gases driving the rotor (compressed air, or a mixture of compressed air and powerplant exhaust), the hourly consumption by all engines during running time in a particular regime of flight represents the only fuel expenditure to be considered.

Schemes involving blade-tip burners would require accounting for hourly fuel flow to the burners in addition to that going to the powerplant(s) driving the compressor(s).

For concepts based on blade-installed rotor-driven powerplants, the fuel delivered to the powerplants usually constitutes the sole fuel consumption of the aircraft.

The above-described approach should be applicable to almost all hovering operations. However, in those special cases when, in forward flight, auxiliary thrusters are in operation, the hourly fuel consumption by the thrusters should also be taken into account.

2.2.2 Ducted Air Schemes

Ducted air schemes — also called cold jets — represent the simplest configuration of jet-driven rotorcraft with powerplants mounted in the airframe. It can be seen from Figure 21 (reproduced from Ref. 15) that by using engine exhaust gases for yaw control, practically all of the shaft power delivered by the powerplant (except for a very small amount needed for driving accessories) goes for generation of compressed air which, when eventually discharged through the blade-tip nozzles, drives the rotor.

Assuming that the rotor horsepower (RHP) required in hover OGE under assumed ambient conditions has been determined (computed), the shaft horsepower (SHP) needed for the RHP value can be expressed as follows:

$$SHP = RHP/\eta_{comp}\,\eta_{duct}\eta_{noz}\,\eta_{pr} \tag{2.1}$$

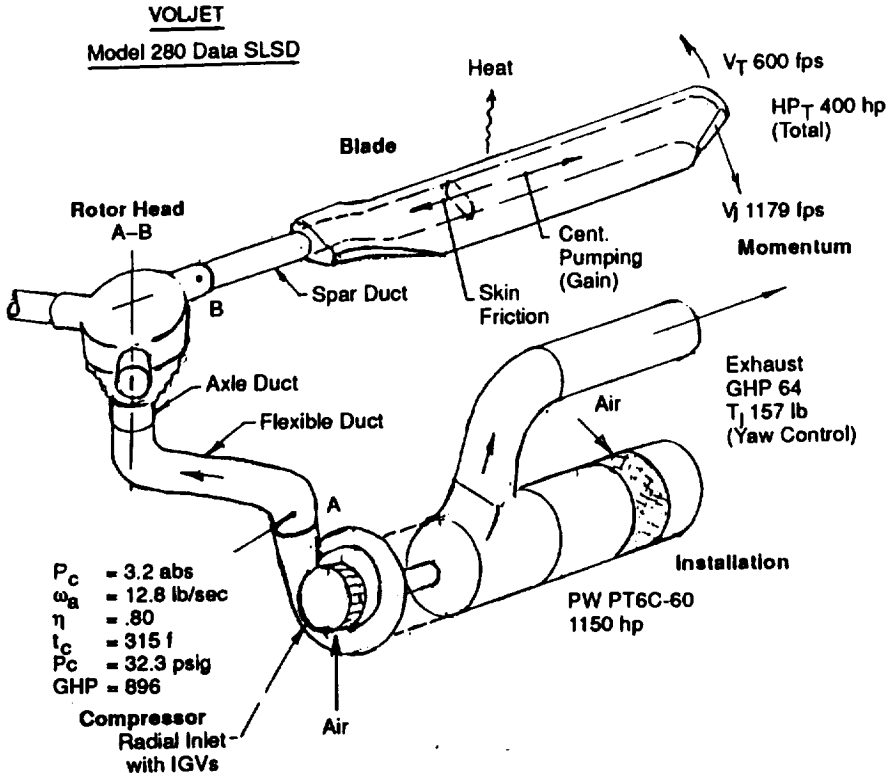

Figure 2.21 Scheme of the cold-jet compressed-air flow system

where η_{comp} is the compressor efficiency, η_{duct} is a coefficient reflecting energy losses encountered due to ducting of the compressed air from the compressor exit to the nozzle(s), η_{noz} is the nozzle efficiency, and η_{pr} is the propulsive efficiency of the tip thruster.

It is easy to deduce from Eq. (2.1) that FC_w will be

$$FC_w = (RHP/W)\text{sfc}/\eta_{comp}\eta_{duct}\eta_{noz}\eta_{pr} \tag{2.2}$$

where sfc represents specific fuel consumption of the powerplant.

$FC_{0_{pl}}$ can, in turn, be written as

$$FC_{0_{pl}} = (RHP/W)\text{sfc}/\eta_{comp}\eta_{duct}\eta_{noz}\eta_{pr}\overline{W}_{0_{pl}} \tag{2.3}$$

where $\overline{W}_{0_{pl}}$ is the relative zero-range and zero-time payload.

Since the sfc of the powerplant is usually determined by the engine manufacturer, it may be considered as invariant as far as design optimization of the cold-jet rotorcraft is concerned. Consequently, the designer's efforts to obtain the lowest possible FC_w values would concentrate on maximization of the η product which, in analogy to the shaft-driven rotorcraft, may be called the overall efficiency of the cold-jet system,

$$\eta_{ov_{cj}} = \eta_{comp}\eta_{duct}\eta_{noz}\eta_{pr}. \tag{2.4}$$

This $\eta_{ov_{cj}}$ maximization should be done while keeping the (RHP/W) values as low as practical. Of the η's appearing in Eq. (2.4), η_{comp} may be considered as "semi-invariant" – simply representing the best obtainable values for the current state of the art ($\eta_{comp} = 0.88$ for axial, and $\eta_{comp} = 0.86$ for centrifugal types). η_{noz} may also be considered as semi-invariant, as its value is usually $\eta_{noz} \approx 0.9$. Thus, the largest variations could be expected in η_{duct} and η_{pr}.

A high η_{duct} would favor low velocity of the flow through the duct. However, this trend may run into strong constraints of excessive structural weight and aerodynamically disadvantageous, excessively thick airfoils, etc., should the duct sections be kept as large as desired.

Since it is usually impractical to include a divergent part into the thrusting nozzle, the exit velocity would be close to the sonic one corresponding to temperature of the exhaust gases. The propulsive efficiency of the thruster in hover can be expressed as

$$\eta_{pr} = 2V_t/(V_t + V_j), \tag{2.5}$$

where V_j is the jet exit velocity, and V_t is the rotor tip speed.

One can see from Eq. (2.5) that since, usually, $V_j > 1117.0$ fps, the high propulsive efficiency would favor the tip speed being as high as possible which, in turn, may run into constraints of excessive profile drag and too low rotor solidity (which, on its part, would adversely affect the desirability of a large duct cross-section in the blades).

It should also be remembered that η values, selected to minimize FF_w, may have a detrimental effect on structural weight and hence, on the $\overline{W}_{o_{pl}}$ level.

A compromise balance between these potentially conflicting requirements may be made in light of defined operational requirements. Thus, a further discussion of this subject would be beyond the limits of the present study. Here, however, it would be of interest to determine how, in general, the $(FC_w)_t$ and $(FC_{o_{pl}})_t$ of the cold-jet rotorcraft would compare with the corresponding figures for shaft-driven conventional helicopters.

Assuming that the (RHP/W) and sfc values of the powerplants are the same for cold-jet and corresponding shaft-driven helicopters,

$$(RHP/W)_{cj} = (RHP/W)_{sh} \text{ and } sfc_{cj} = sfc_{sh}, \tag{2.6}$$

the ratio of $(FC_w)_t$ and $(FC_{o_{pl}})_t$ for both types can be expressed as follows:

$$(FC_w)_{t_{cj}}/(FC_w)_{t_{sh}} = \eta_{ov_{sh}}/\eta_{ov_{cj}} \tag{2.7}$$

and

$$(FC_{o_{pl}})_{t_{cj}}/(FC_{o_{pl}})_{t_{sh}} = (\eta_{ov_{sh}}/\eta_{ov_{cj}})(\overline{W}_{o_{pl_{sh}}}/\overline{W}_{o_{plc_j}}) \tag{2.8}$$

where $\eta_{ov_{sh}}$ represents the ratio of RHP to SHP for shaft-driven helicopters. It is shown in Ref. 5 that, in hover, the typical $\eta_{ov_{sh}} \approx 0.87$.

As to the ratios of RHP to the SHP of cold-jet helicopters, calculations for the Voljet (Ref. 15) indicate that the highest total of $\eta_{ov_{cj}} = 0.365$. This would result in $(FC_w)_{t_{cj}}/(FC_w)_{t_{sh}} = 2.38$. Actual flight test results for the Djinn (Ref. 13 and Table 2.1) give 0.19 lb/lb,hr, while for shaft driven turbine helicopters of that time frame having similar disc loadings, the $(FC_w)_t$ should not be higher than about 0.07 lb/lb,hr. Thus, the $(FC_w)_{t_{cj}}/(FC_w)_{t_{sh}}$ ratio would amount to about 2.7. A comparison of the above figure with that for the Voljet seems to indicate that progress in $\eta_{ov_{cj}}$ values was achieved between the Djinn and Voljet times (late 40s vs early 80s).

Assuming that in future designs, a η_{ov} as high as $\eta_{ov_{cj}} = 0.47$ can be achieved, the gross-weight related specific fuel consumption of cold-jet helicopters would still be about 1.85 times as high as for their shaft-driven counterparts.

With respect to specific fuel consumption related to zero range (or time) payload, one should note that the cold-jet type is well suited for small non-transport helicopters, where the weight of the crew may constitute a large fraction of the useful load and thus, strongly affect the $\overline{W}_{o_{pl}}$ levels. Consequently, selection of useful load $(\overline{W}_{ul})$ rather than $\overline{W}_{o_{pl}}$ as a base of reference appears as more meaningful for assessing this aspect of energy consumption per unit of load and unit of time.

Since the relative useful load

$$\overline{W}_{ul} = 1 - \overline{W}_e, \tag{2.9}$$

the specific fuel consumption per pound of useful load in hover $(FC_{ul})_t$ can be obtained by dividing the right side of Eq. (2.2) by Eq. (2.9). Thus, the ratio of $(FC_{ul})_{t_{cj}}$ for the cold-jet configuration to that of shaft-driven types becomes

$$(FC_{ul})_{t_{cj}}/(FC_{ul})_{t_{sh}} = (\eta_{ov_{sh}}/\eta_{ov_{cj}})[(1 - \overline{W}_{e_{sh}})/(1 - \overline{W}_{e_{cj}})]. \tag{2.10}$$

The relative weight-empty of the Djinn cold-jet helicopter amounted to $\overline{W}_e = 47\%$, which was about 12% lower than values represented by the optimal boundary for the shaft-driven helicopters of that time (early 50s; see Figure 2.18, and Figures 1.1 and 1.2 of Ref. 2.

For contemporary machines as represented by Voljet studies, relative weights empty as low as $\overline{W}_e = 37.7\%$ are anticipated (Ref. 16, also see Table 2.1). Using $\overline{W}_e = 36.0\%$ as probably representing the possible minimum, and $\eta_{ov_{cj}} = 0.47$ as the probable upper limit, and assuming $\eta_{ov_{sh}} = 0.87$ and $\overline{W}_{e_{sh}} = 0.42$ for shaft-driven helicopters, Eq. (2.10) would give the following: $(FC_{ul})_{t_{cj}}/(FC_{ul})_{t_{sh}} \approx 1.7$.

The above-performed study of fuel consumption aspects in hover clearly indicates that as far as gross weight, payload or useful load-related specific fuel consumption is concerned, figures for the cold jets can be expected to be at least 85% higher for $(FF_w)_t$ and about 70% higher for $(FF_{wl})_t$ than for their shaft-driven counterparts. It should be remembered, however, that under some operational conditions (both civilian and military), the higher 'price' in fuel consumption may be acceptable as compensation for the relative mechanical simplicity of the configuration and higher zero-range (time) useful and payload values.

2.2.3 Ducted Hot and Warm Gas Schemes

Ducted hot-gas schemes, also called hot-jet schemes, present a more difficult structural problem than cold jets because of the ducting of hot gases (temperatures over 1000 °F) through the blades. In addition, engine exhaust products can not be used for yaw control. Thus, a small tail rotor would usually be required. However, with respect to the most efficient use of fuel energy, there should be some advantages.

In order to evaluate these advantages, the $(FC_w)_{t_{hj}}/(FC_w)_{t_{sh}}$ and $(FC_{opl})_{t_{hj}}/(FC_{opl})_{t_{sh}}$ ratios in hover will be examined as in the preceding case of the cold jets.

The present analysis will follow the approach outlined by Nicols (Ref. 9), and the basic components of the drive system are as shown in Figure 2.22.

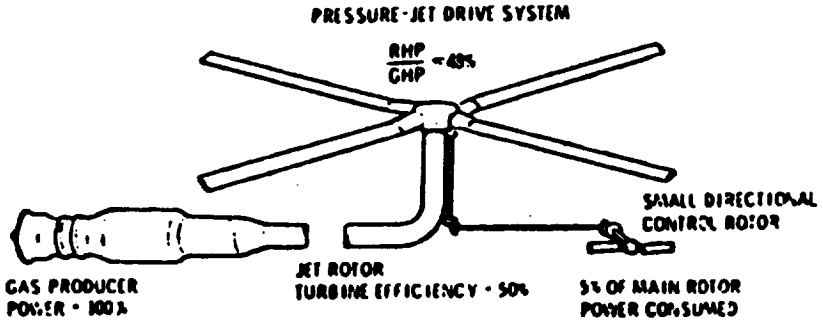

Figure 2.22 Scheme of the hot-pressure jet-drive system

In the approach taken in Ref. 9, the power available at various stations of the drive system is expressed as a fraction (percentage) of the power generated in the gas producer.

A similar approach is taken for shaft-driven configurations. In both cases, the final goal consists of determining what fraction or percentage of the power generated by the gas producer (GP) becomes available as rotor power (RP). Knowing the $(RP/GP)_{hj}$ ratios for the hot jet, as well as $(RP/GP)_{sh}$ values for the shaft-driven configuration, the $(FC_w)_{hj}/(FC_w)_{sh}$ ratios can be determined.

This is done as in the preceding case by assuming that at an equal gross weight and identical ambient conditions, $RP_{hj} = RP_{sh}$. It is further assumed that the specific fuel consumption of the gas producer supplying hot gases to the rotor is the same as when the same gases are used to drive the power turbine of the shaft-type engine. Under this assumption, the ratio of FC_w for the hot-jet to that of the shaft-driven configuration becomes:

$$(FC_w)_{hj}/(FC_w)_{sh} = (RP/GP)_{sh}/(RP/GP)_{hj} \tag{2.11}$$

In Ref. 9, the hot-jet-driven rotor is treated as a turbine, just as the free turbine of the shaft engine. In this reference, it is stated that for typical values of pressure losses and tip-speed ratios, warm-cycle powerplant turbine efficiencies of 50% maximum are to be expected in comparison with the 83% maximum obtained by the free turbine of a shaft engine.

Consequently, assuming a 5% RP loss for yaw control and operation of accessories, the rotor power to the gas generator power ratio for the hot jet may be expected to attain a value of

$$(RP/GP)_{hj} = 0.5 \times 0.95 = 0.475.$$

For shaft-driven concepts, assuming $\eta_{ov} = 0.87$ (as in the preceding case) the corresponding ratio will be

$$(RP/GP)_{sh} = 0.83 \times 0.87 = 0.722.$$

Substituting the above (RP/GP) values into Eq. (2.11), one would obtain

$$(FC_w)_{hj}/(FC_w)_{sh} = 1.52.$$

Thus, for hot-jet concepts, it can be seen that the gross-weight specific fuel consumption should be about 50% higher than for their shaft-driven counterparts.

With respect to zero-range (time) payload specific fuel consumption, it should be noted that in a study of a tip-jet-driven heavy-lift helicopter incorporating circulation control (Ref. 10), a relative weight-empty as low as $\overline{W}_e = 0.34$ is expected, and for the warm-cycle Bolkow design, $\overline{W}_e = 0.32$ (Ref. 8). In a study of design concepts for an advanced cargo rotorcraft (Ref. 18), $\overline{W}_e = 0.40$ was estimated. Assuming an average of the above three figures; i.e., $\overline{W}_e = 0.35$, a $\overline{W}_{pl_0} \approx 0.645$ for an aircraft of the 150,000-lb gross-weight class can be anticipated, while for a shaft-driven helicopter of the same gross-weight class, the relative zero-range (time) payload of $\overline{W}_{pl_0} \approx 0.575$ corresponding to $\overline{W}_e = 0.42$ may be expected. This would lead to $(FC_{o_{pl}})_{hj}/(FC_{o_{pl}})_{sh} = 1.40$, which is better than the corresponding 1.7 value for cold jets.

For the so-called warm cycle such as the Bolkow BO-X and Hughes/David Taylor VHLH, no separate analysis of the $FC_w)_{wc}/(FC_w)_{sh}$ and $(FC_{o_{pl}})_{wc}/(FC_{o_{pl}})_{sh}$ ratios was

made. However, it is believed that these ratios would not be much different from those determined for the hot cycle. The figures of $(FC_w)_{h_{wc}}$ = 0.12 lb/lb,hr shown in Table 2.1 for the BO-X when compared to $(FC_w)_{h_{sh}}$ = 0.076 obtained as an average for the 100,000-lb gross weight class, gives $(FC_w)_{h_{wc}}/(FC_w)_{h_{sh}}$ = 1.58. Although this figure is somewhat higher than the 1.52 ratio computed for the hot cycle, one should expect that, in practice, the warm cycle should be slightly more efficient. This would be due to (1) a slightly better propulsive efficiency (lower jet exit velocity), and (2) lower ducting losses may be possible since, because of the lower temperature of the flowing gases and, consequently, no need for special insulation, more of the blade cross-sectional area could be used as a gas duct.

2.2.4 General Remarks re Blade Tip-mounted Powerplants

In blade tip-mounted powerplants, all engine components required for generating thrust (needed for sustaining rotation of the rotor) form a complete unit, while only fuel is supplied from the outside. Therefore, knowledge of such engine characteristics as thrust and *tsfc* when moving at the rotor tip speed (V_t) under assumed ambient conditions (pressure altitude and temperature) represent all the inputs needed for cursory estimates of fuel consumption for rotorcraft using this type of powerplant. For concepts based on the UDF, such as the hypothetical heavy-lift helicopters, where the shaft turbines and unducted fan assemblies are mounted near the blade tips, the necessary information would include engine sfc and fan propulsive efficiency at a given power setting when moving through air of given ambient characteristics at a speed equal to the V_t. All of these aspects are briefly discussed in the following sections.

2.2.5 Jet-Type Powerplants

See Figure 2.15 for the overall configuration of tip-mounted-jet helicopters. The rotor horsepower required (RHP_{req}) in hover (say OGE) by a rotorcraft at a given gross weight and air density corresponding to the assumed ambient conditions can be computed using conventional performance prediction methods. Consequently, the total thrust needed at all blade tips ($T_{t_{tot}}$) will be

$$T_{t_{tot}} = 550RHP/V_t. \tag{2.12}$$

Assuming that b is the number of blade, the tip thrust required per blade would be

$$T_{t_b} = T_{t_{tot}}/b. \tag{2.13}$$

Because of vertical climb and maneuvering requirements, the installed thrust will usually be somewhat higher than the required hovering T_{t_b} value. This means that, in hover, the engine will operate at a somewhat lower thrust level than the nominal engine rating.

Knowing tsfc at the partial thrust setting when the engine is moving through the air (of given temperature and pressure) at a speed V_t, the specific fuel consumption per pound of the rotorcraft gross weight in lb/lb/hr, can be expressed as follows:

$$(FC_w)_h = T_{t_{tot}} tsfc/W. \tag{2.14}$$

Substituting Eq. (2.12) for $T_{t_{tot}}$, Eq. (2.14) can be rewritten as follows:

$$(FC_w)_h = 550(RHP/W)tsfc/V_t. \tag{2.15}$$

A glance at the above would indicate that in order to minimize the $(FC_w)_h$ values at a given level of rotor power required per pound of gross weight, the tsfc should be as low, and the rotor tip speed as high, as possible.

Remembering that payload for zero range can be written as $W_{o_{pl}} = W\overline{W}_{o_{pl}}$, an expression for the specific fuel consumption per pound of zero-range (time) payload can easily be obtained.

$$(FC_{o_{pl}})_h = 550(RHP/W)tsfc/V_t \overline{W}_{o_{pl}}. \tag{2.16}$$

With respect to the above equation, all remarks previously made in conjunction with Eq. (2.15) are still valid, to which a truism may be added that the relative payload for zero range (time) $(\overline{W}_{o_{pl}})$ should be as high as possible.

Ratios of the gross-weight and payload specific fuel consumption of the tip-mounted jet types to those of shaft-driven concepts can easily be derived from Eqs. (2.15) and (2.16) as

$$(FC_{o_{pl}})_{h_j}/(FC_w)_{h_{sh}} = 550\, tsfc\, \eta_{ov}/sfc_{sh}\, V_t \tag{2.17}$$

and

$$(FC_{o_{pl}})_{h_j}/(FC_{o_{pl}})_{h_{sh}} = 550\, tsfc\, \eta_{ov}\, (\overline{W}_{o_{pl_{sh}}}/\overline{W}_{o_{pl_j}})/sfc_{sh}\, V_t, \tag{2.18}$$

respectively.

In order to simplify the fuel consumption comparison indicated by Eqs. (2.17) and (2.18), the following assumptions are made:

Tip speed	V_t = 700 fps
$(RHP/SHP)_{sh}$	η_{os} = 0.87
sfc (shaft driven)	sfc_{sh} = 0.4 lb/hr & hp

Now, Eq. (2.17) can be rewritten as a sole function of the tsfc of the tip-mounted jet engines:

$$(FC_w)_{h_j}/(FC_w)_{h_{sh}} = 1.71\, tsfc. \quad (2.19)$$

A glance at Eq. (2.19) would indicate that for $tsfc < 0.58$ lb/lb,hr, the tip-mounted jet-engine concept would become more fuel efficient (with respect to gross weight) than shaft-driven helicopters having powerplants capable of *sfc* as low as 0.40 lb/lb,hr.

Trends in the *tsfc* vs M for various types of jet engines having $2.6 \leq BPR \leq 9.8$ are shown in Figure 2.23 (Fig. 40 of Ref. 19). This figure indicates that, as may be expected, *tsfc* becomes lower as the bypass ratio (BPR) increases. As to the order of magnitude of *tsfc*, which may be expected at $M = 0.63$ — approximately corresponding to $V_t = 700$ fps — one can see that for DCFF; i.e., directly coupled front fan, jet engines having BPR = 2.7, *tsfc* = 0.74 lb/lb,hr.

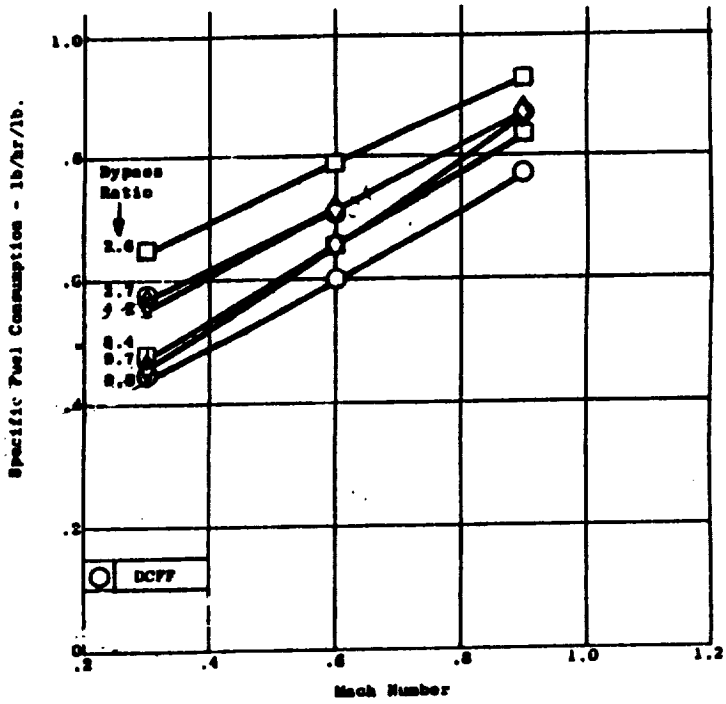

Figure 2.23 Thrust specific fuel consumption vs. Mach number (turbine inlet temperature = 2480°R)

For instance this means that a rotorcraft driven by a tip-mounted DCFF turbojet having BPR = 2.7 would have a $(FC_w)_j$ about 26% higher than its shaft-driven counterpart having powerplants exhibiting *sfc* = 0.4 lb/lb,hr.

Dividing the right side of Eq. (2.19) by the relative zero-range (time) payloads, an expression for $FC_{o_{pl}}$ ratios is obtained

$$(FC_{o_{pl}})_j/(FC_{o_{pl}})_{sh} = 1.71 \text{ tsfc } (\overline{W}_{o_{pl}})_{sh}/(\overline{W}_{o_{pl}})_j. \quad (2.20)$$

From early studies of the blade tip-mounted jet-engine configuration (Ref. 11), a value of $\overline{W}_{o_{pl}} = 0.62$ is obtained as an average for the 60,000 and 220,000-lb class helicopters. Using present technology, a $\overline{W}_{o_{pl_j}} \approx 0.65$ can probably be obtained, while for shaft-driven configurations, $\overline{W}_{o_{pl_{sh}}} \approx 0.52$. Using these numbers, Eq. (2.20) can be rewritten as follows:

$$(FC_{o_{pl}})_j/(FC_{o_{pl}})_{sh} = 1.37 \text{ tsfc}. \quad (2.20a)$$

One can see from the above expression that for tsfc < 0.73 lb/lb & hr, the tip-jet helicopters would have lower $FC_{o_{pl}}$ levels than their shaft-driven counterparts. Since tsfc $\approx$ 0.73 lb/lb,hr approximately corresponds to the tip Mach number of M = 0.63, (Figure 2.15), it appears that with respect to the zero-range (time) payload specific fuel consumption, helicopters based on tip-mounted jet engines may prove to be competitive with shaft-driven types.

2.2.6 Blade Tip-mounted Unducted Fans

The basic concept of blade tip-mounted unducted fans (UDF) is similar to that of the blade tip-mounted jet engines (Figure 2.24).

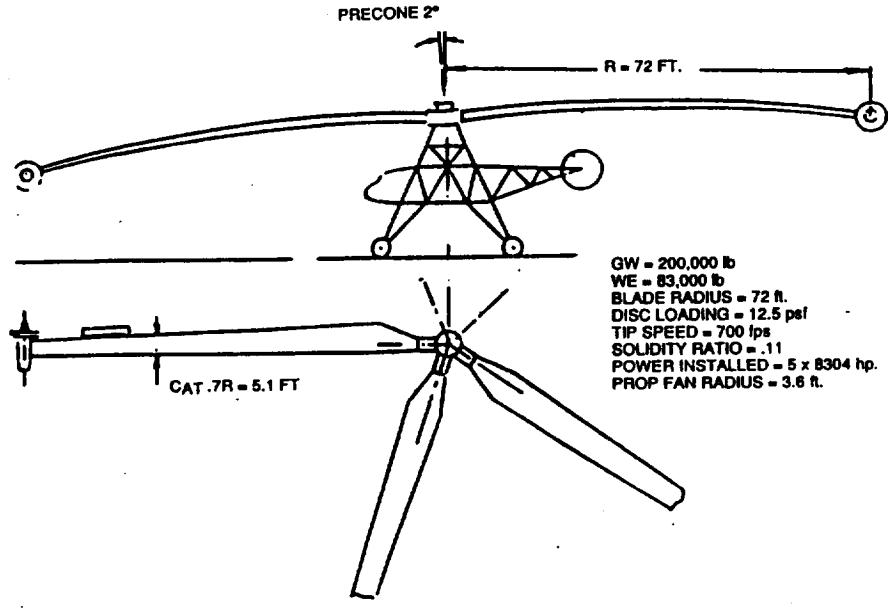

Figure 2.24 Sketch of a hypothetical helicopter based on a tip-mounted unducted-fan concept

Assuming that the rotor horsepower required in hover (RHP) has been calculated, and that the propulsive efficiency (η_{pr}) of the tip-mounted unducted powerplant unit is known, and neglecting losses associated with yaw control and operation of accessories, the total shaft horsepower needed in hover becomes $SHP_{req} \approx RHP/\eta_{pr}$.

Knowing the SHP_{req} and the corresponding sfc values of the turbine, the $(FC_w)_{ufh}$ in hover can be written as follows:

$$(FC_w)_{ufh} = (RHP/W)sfc_{uf}/\eta_{pr} \tag{2.21}$$

and

$$(FC_{o_{pl}})_{ufh} = (RHP/W)sfc_{uf}/\eta_{pr}(\bar{W}_{o_{pl}})_{uf} \tag{2.22}$$

where sfc_{uf} is the specific fuel consumption of the turbine driving the UDF.

Assuming that a comparison is made for the same values of (RHP/W) and $sfc_{uf} = sfc_{sh}$, the desired ratios of FC_w and $FC_{o_{pl}}$ for the UDF-type powerplants and conventional shaft-driven concepts can be expressed, similar to preceding cases, as

$$(FC_w)_{ufh}/(FC_w)_{shh} = \eta_{ov}/\eta_{pr} \tag{2.23}$$

and

$$(FC_{o_{pl}})_{ufh}/(FC_{o_{pl}})_{ufh} = (\eta_{ov}/\eta_{pr})\,[(\bar{W}_{o_{pl}})_{sh}/(\bar{W}_{o_{pl}})_{uf}]\,. \tag{2.24}$$

With respect to the UDF propulsive efficiency, one can see from Figure 2.17 that for contrarotating fans, $\eta_{pr} \approx 0.87$ can be expected at M = 0.63.

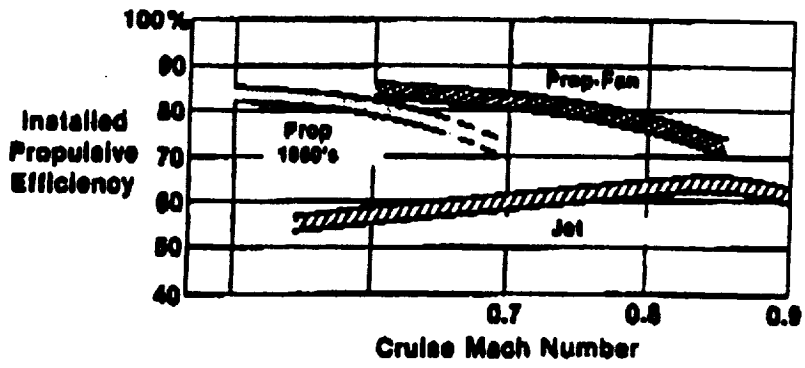

Figure 2.25 NASA, Lewis data re propulsive efficiency of UDF (prop-fan) vs. Mach number (upper line for contrarotating fans)

Since, for shaft-driven configurations, $\eta_{ov} \approx 0.87$, Eq. (2.23) would indicate that for helicopters based on the UDF concept, a gross-weight related specific fuel consumption equal to that of shaft-driven counterparts can be expected.

The UDF zero-range (time) payload specific fuel consumption would definitely be better than for the shaft-driven configurations because much higher $\overline{W}_{o_{pl}}$ values – similar to those of tip-mounted jets – can be expected.

2.2.7 Discussion of Fuel Consumption Aspects in Hover

FC_w and $FC_{o_{pl}}$ in hover was investigated in some detail for the following tip-driven helicopter types: (a) cold jets, (b) hot jets, (c) tip-mounted jet engines, and (d) tip-mounted unducted fans. Other types listed in Table 2.1 were excluded, as it appears to these investigators that there is little chance in the foreseeable future that these systems may be incorporated into practical operational aircraft. The chief reason for their probable exclusion would be unacceptable noise levels of the ram-jet, pulse-jet, and tip-burning schemes. Noise level may also represent one more obstacle on the road toward developing an acceptable operational helicopter based on tip-mounted jet engines. However, there is a remote possibility that the noise level of jet-engine type helicopters could be reduced to an acceptable level and, for this reason, this configuration was retained in the comparative study of fuel consumption aspects.

TABLE 2.2

SOME IMPORTANT FUEL-CONSUMPTION CHARACTERISTICS IN HOVER

PROPULSION TYPE CHARACTERISTICS	(1) (FCw)h/ (FCw)shh	(2) (FCopl)h/ (FCopl)shh	(3) $\overline{W}$opl	(4) 0.066 × (1) = (FCw)h
COLD JET*	1.8	1.7	0.63	0.119
HOT JET	1.52	1.40	0.62	0.100
TIP-MOUNTED JET ENGINES	1.26	1.11	0.65	0.083
TIP-MOUNTED UDF	1.00	0.97	0.59**	0.066
SHAFT-DRIVEN	1.00	1.00	0.57	0.066

*HEAVY LIFT

**CONSERVATIVE

Ratios of the FC_w values of the above investigated tip-driven concepts to those of the shaft-driven type are listed in the first column of Table 2.2. In the second column, relative zero-range (time) payload values are given.

Some important characteristics relating to fuel consumption in hover of the compared configurations is depicted in this table. However, in order to get a still clearer picture of these aspects, a graph showing payload vs. time in hover for the five propulsion types shown in Table 2.2 was prepared, computing $\bar{W}_{pl} = f(t)$ from the following equation (see Chapter 1, Section 2.2).

$$\bar{W}_{pl} = \bar{W}_{pl_o} - (1 - e^{-(FC_w)_h t}) \tag{2.25}$$

where FC_w (assumed constant) is in lb/lb,hr, and hover time t is in hours.

Assuming, for shaft-driven helicopters of the 100,000-lb and higher gross-weight class, that $(FC_w)_{sh_h} = 0.066$ lb/lb,hr (optimal value from Table 6.4, Ref. 5), the corresponding values of $(FC_w)_h$ for tip-driven types shown in Column 4, Table 2.2 were computed by multiplying 0.066 by the ratios listed in Column 1 of this table. Then, using the $\bar{W}_{pl_o}$ values listed in Column 3, the relationships expressed by Eq. (2.25) were computed and plotted in Figure 2.26.

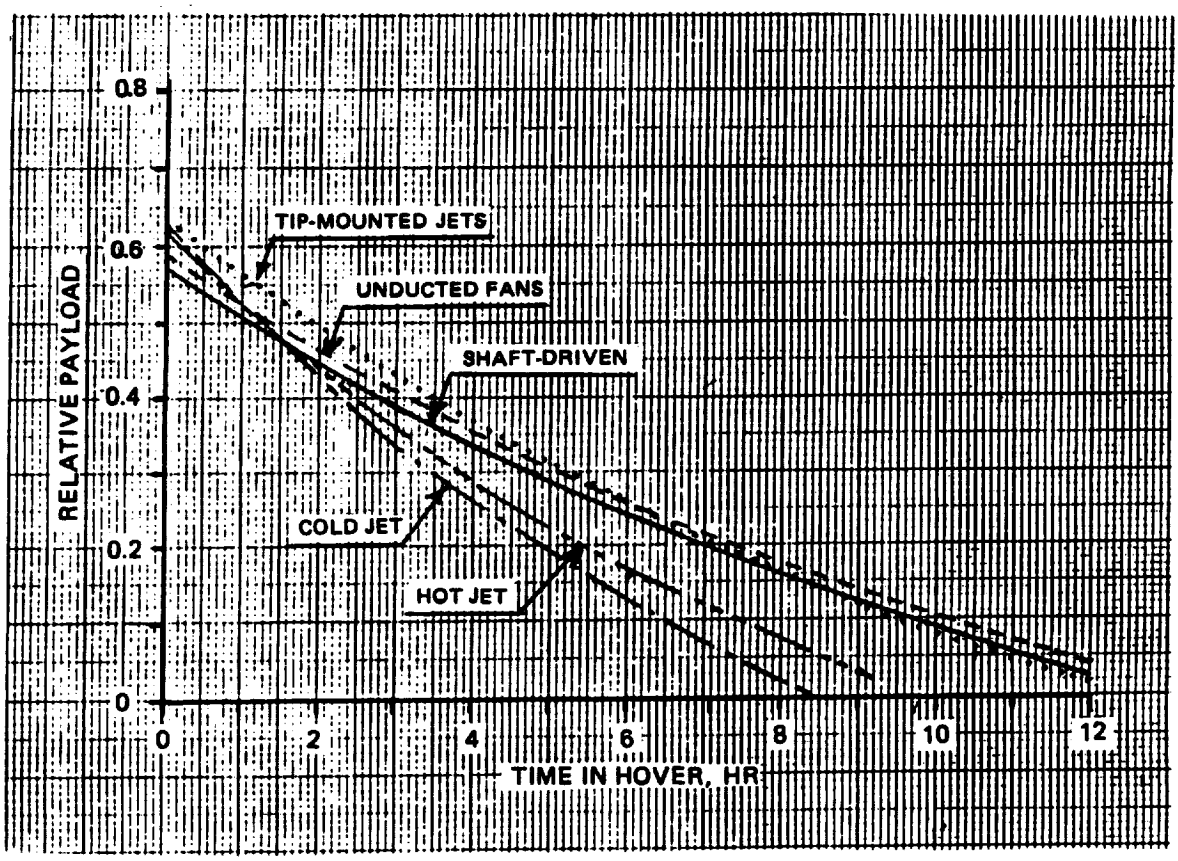

Figure 2.26 Relative payload vs. time in hover

By examining this figure and Table 2.2, the following observations regarding fuel consumption of tip-driven helicopters in hover can be made: All of the four considered tip-driven configurations show that in spite of the higher specific fuel consumption per units of gross weight and time, they are capable of carrying higher relative payloads for some period of time than shaft-driven types. The period of potentially higher relative payloads extends to 1.5 hours for the cold jet, and is slightly higher for the hot jet. However, for tip-mounted jet engines, this period extends to approximately 8.5 hours. Tip-mounted UDF configurations are slightly superior to their shaft-driven counterparts with respect to $\overline{W}_{pl}$-carrying capability throughout the whole time span. It should be noted, however, that the $\overline{W}_{pl} = f(t)$ for the tip-mounted jet engine type may be somewhat optimistic, as the relative weight-empty data were based solely on the studies of Fitzwilliams made during the early fifties (Ref. 11), with no further investigation by other sources. In contrast to tip-mounted jet engines, the relative weight-empty of the UDF type is probably conservative, since it was established (see Appendix) for 6- and 5-bladed rotors of the 400,000 and 200,000 lb gross-weight helicopters, respectively, where blade-tip droop requirements probably increased the load-carrying blade cross-section areas beyond those needed to provide adequate strength.

Consequently, the payload-carrying ability in hover shown for UDF-type helicopters is probably conservative, and thus considerably better fuel consumption characteristics with respect to zero-range (time) payload can be expected for this type than for their shaft-driven counterparts. However, in order to answer this question with more certainty than presented here, design studies of the UDF configuration would be required.

2.3 Load-Carrying Aspects In Forward Flight

Because of the limited scope of this study (budget and time), a comparison of the load-carrying abilities of tip-driven vs. shaft-driven helicopters in forward flight will consist of a cursory investigation of relative payload vs. distance-flown aspects only. The required relationship is expressed by the following formula (developed in Chapter 1, Section 2), which is similar to Eq. (2.25).

$$\overline{W}_{pl_R} = \overline{W}_{pl_o} - (1 - e^{-(FC_w)_R R}) \tag{2.26}$$

where $(FC_w)_R$ is the fuel consumption per pound of rotorcraft GW and one nautical mile flown, and R is the distance (range) flown, in nautical miles.

In order to compute the $\overline{W}_{pl_R} = f(R)$ relationship from Eq. (2.26), it is assumed that the $(FC_w)_R$ of each type represents the minimal fuel consumption per unit of weight and unit of distance flown. It is further assumed that for shaft-driven configurations $(FC_w)_{sh_R} =$ 0.00045 lb/lb,n.mi, which corresponds to the optimal boundary for Western helicopters of the $W >$ 100,000-lb GW class (Figure 7.18, Ref. 5). For the compared tip-driven types,

it is assumed that their $(FC_w)_R$ values remain in the same ratio to that of the shaft-driven ones as they were in hover. In other words, they will be computed by multiplying 0.00045 by the FC_w ratios from Column 1 of Table 2.2. The so-obtained FC_{w_R} values are shown in Table 2.3, where the $\overline{W}_{pl_o}$ values are repeated from Column 3 of Table 2.2.

TABLE 2.3

SOME IMPORTANT FUEL-CONSUMPTION CHARACTERISTICS IN FORWARD FLIGHT

PROPULSION TYRE	$\overline{W}$opl	0.00045x(1), T 2.2 lb/lb, n.mi
COLD JET*	0.63	0.00081
HOT JET	0.62	0.00068
TIP-MOUNTED JET ENGINES	0.65	0.00057
TIP-MOUNTED UDF	0.59**	0.00045
SHAFT-DRIVEN	0.57	0.00045

*HEAVY LIFT **CONSERVATIVE

Using the figures given in Table 2.3, the relative payload vs. range (in n.mi) relationships were computed from Eq. (2.26) and are shown in Figure 2.27.

Looking at this figure, one can see that at short distances (up to approximately 200 n.mi.) the four tip-driven helicopters examined here should have higher load-carrying capabilities than their shaft-driven counterparts. In this respect, the tip-mounted jet-engine configuration appears quite attractive. However, as in the case of hover, a word of caution must be added, since the high $\overline{W}_{pl_o}$ values which contributed to the favorable $\overline{W}_{pl}$ vs. range relationship are based on a single source of information (Ref. 11). It should also be emphasized that, as in the case of hover, the payload vs. range characteristics of the UDF helicopters would probably be better than shown in in Figure 2.27.

In summary, one can see that as in the case of hover, tip-driven configurations could have performance characteristics that would make them competitive, under some operational conditions, with shaft-driven types as far as load-carrying vs. distance abilities are concerned.

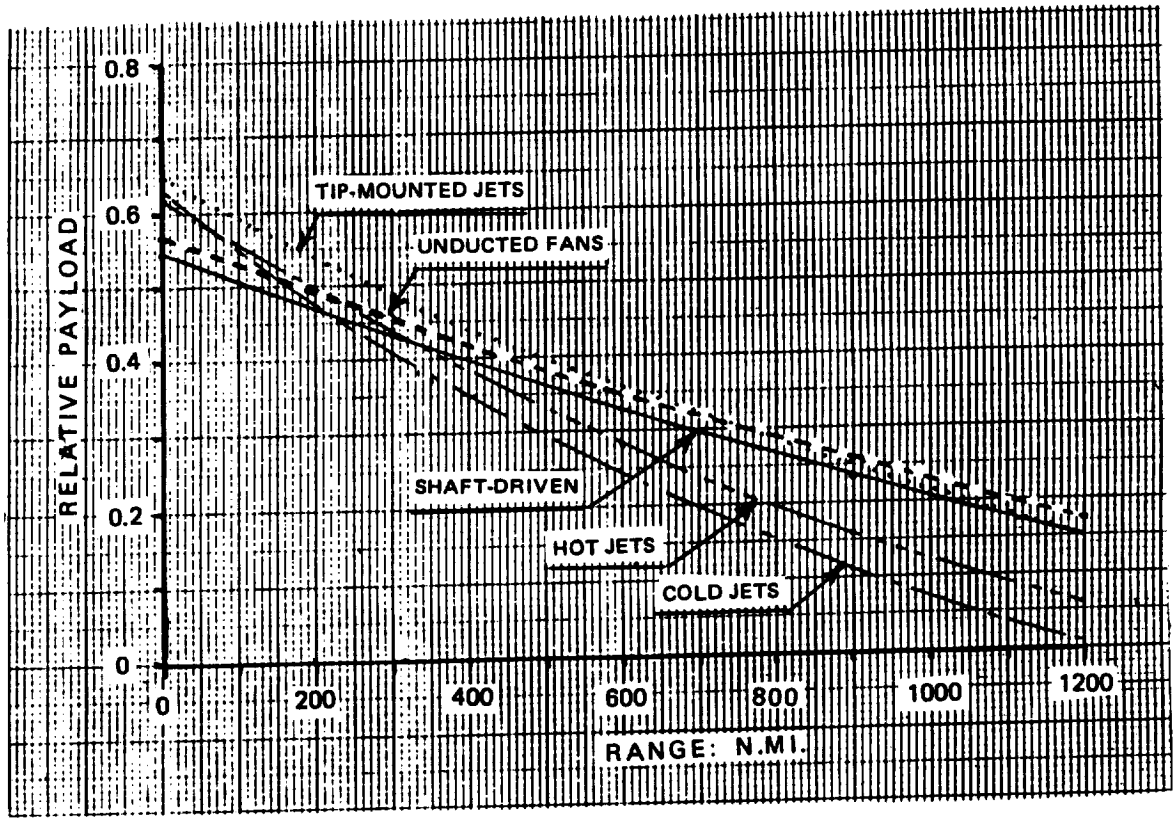

Figure 2.27 Relative payload vs. range

2.4 Concluding Remarks and Recommendations

2.4.1 Concluding Remarks

The main feature of tip-driven rotor concepts is simplification of the design through elimination of the mechanical drive system and main-rotor torque compensation devices in single-rotor helicopter configurations. This aspect appears as attractive in the light of present technology as it did to early designers of jet-driven helicopters. Furthermore this attractiveness appears, in principle, to be equally as strong for large and very large transport and crane helicopters as for smaller configurations.

However, in spite of successfully solving the mechanical-drive system problems for machines of over 100,000-lb gross weight, as examplified by the single-rotor Mil-26 and the tandem Boeing XCH-62A configurations, one may expect that for very heavy helicopters having gross weights of over 200,000 lb, mechanical transmissions would become more and more complex. In addition, an increase in the relative weight of the mechanical drive would contribute toward an increase of the relative weight empty.

Consequently, the tip-drive approach appears to be the more logical approach in the design of VHL helicopters. At present, two solutions to tip driving VHL helicopter rotors appear feasible: one, based on fuselage-mounted energy converters where the energized cold, warm, or even hot, gases are ducted through the blades to the tip nozzles; or two, having energy converters (pure jets, turbofans, or unducted fans) located at the blade tips.

The first of these approaches has an advantage in that the energy converters are not located in high "g" fields as in the tip-mounted cases. Thus, powerplants may be selected from available jet engines without incurring considerable redesign and special certifications. However, at present, unless some practical method of increasing the mass flow at the nozzle is devised, exhaust velocities of blade-propelling gases must be high. This obviously leads to a low propulsive efficiency and generates potential noise problems. Overall efficiency is further lowered because of ducting losses. On the other hand, the possibility of combining the cold, warm, or hot jet principle with some form of circulation control, as in the David Taylor–Hughes approach, for actual control of the helicopter, or higher harmonic inputs to suppress vibrations, represents a definite 'plus' for this concept.

As for blade-tip mounted powerplants, the previously mentioned operation in the high "g" field and other problems such as one-engine inoperative conditions and striking objects with the blade tips are only some of a long list of problems. However, from the point of view of energy consumption per pound of gross weight or payload and hour of flight, or nautical mile flown, all configurations with blade-tip mounted powerplants appear more efficient than those with fuselage-located energy converters. Furthermore, of all blade-tip mounted powerplant configurations, those based on unducted fans emerge as the most energy efficient. This, obviously, is the result of the high propulsive efficiency of contrarotation, which is a must for the blade-mounted UDF.

The high "g" operational environment unfortunately poses a serious problem for the UDF's, as well as for other blade-tip mounted powerplants. However, should it become possible to transfer large amounts of energy through the blades with small losses, then the location of prime energy converters in the fuselage would alleviate at least some of the problems. If, for instance, superconductivity at ambient temperatures ever becomes an industrial reality, then large and very large transport crane helicopters using tip- or near-tip-mounted unducted contrarotating fans could become very energy efficient configurations — both with respect to unit of gross weight and even more important, unit of payload.

With respect to cost, it may be assumed that the purchase price of the cold and warm-cycle tip-driven helicopters of a given operational gross weight should be lower than that of their shaft-driven counterparts. This would be due to the greater simplicity of design and better relative weight-empty values of the tip-driven types. By contrast, the fuel cost per pound of payload and hour of flight as well as nautical mile flown will be higher for the tip-driven types. Consequently, no clear-cut advantage of one type over another can be indicated as far as direct operating cost is concerned. This question could be answered on a case-to-case basis only.

In tip-mounted powerplant types such as low BPR turbofans and UDF's, fuel costs per pound of payload and hour of flight as well as nautical mile flown may be equal or lower

than those for shaft-driven helicopters of the same gross-weight class. However, the purchase cost of tip-driven helicopters of equal gross weights may be lower, or even much higher, than that of its shaft-driven counterpart, depending on how the development and/or adaptation cost of powerplants suitable for high "g" field operations will be absorbed. Any indications regarding the DOC of the compared helicopters will, obviously, depend on the answer to the above question.

The present level of knowledge regarding noise aspects of all tip-driven helicopters appears quite low. There are, of course, some experimental data regarding jet-driven helicopters of the past. But the information is scattered and, to the best knowledge of these investigators, there is no well organized material related to the noise problems of these types of rotorcraft and no indications as to design philosophy which would lead to lowering the external noise level.

2.4.2 Recommendations

Because of its potential for military and civilian applications, the whole field of helicopters incorporating tip-driven rotors should not be neglected. However, for budgetary reasons, probably only a small-scale effort can be afforded at this time. Consequently, present and near future efforts should be focused on the following areas.

1. Broad review of the external noise aspects of cold, warm, and hot cycle, as well as various blade-tip mounted powerplants. Indication of the possible avenues of reducing the noise level and estimates of associated performance and weight penalties.

2. Periodic reviews of the requirements for heavy and very heavy transport or crane helicopters and design studies including various tip-driven concepts.

3. Conduct broad preliminary design or concept and operational aspects studies of the heavy and very heavy transport or crane helicopters based on the UDF principle.

4. Designate an individual, or individuals, within the US Army R&TA and NASA organizations who would be responsible for establishing and monitoring research efforts related to rotor tip-driven helicopters.

Note: Some of the above indicated recommendations can probably be realized through cooperation with the Centers of Excellence at Georgia Tech, Renssalaer Polytechnic Inst., and Maryland University.

CHAPTER 3

COMPOUND HELICOPTERS

3.1 Introduction (Definitions and Historic Perspective)

3.1.1 Definition and Purpose

The definition of 'compound helicopter,' or simply compound, is usually applied to rotorcraft of the basic helicopter type where, in cruise and high-speed flights, propulsive thrust is provided either entirely or, to a large extent (say 75%), by special propelling devices instead of rotors[20]. These propelling devices may consist of open or shrouded propellers, turbofans, pure jets, or even rockets, although the latter appears unlikely at this time. In many configurations, fixed-wing type surfaces usually provide lift in forward flight, thus unloading the main rotor(s). However, some lift is always retained on the rotor(s), not only as a source of control, but also as a contribution to the flapping stability of the blades.

As to the purpose of compounding, the original incentive for aircraft of this type was chiefly motivated by the desire to shift the retreating blade stall barrier to higher flight-speed levels through unloading of the rotor by the lift generated by a wing or wings. The auxiliary horizontal thrust provided by a propeller(s) or other devices would further contribute to improved high-speed capabilities through (a) additional alleviation of the stall barrier through a lower rotor thrust inclination, and (b) reduction of the rotor profile drag resulting from a reduction in the angle of attack of the lifting rotor disc.

In addition, compounding would permit the designers to operate the lifting rotor(s) in forward flight at a higher advance ratio than those normally accepted for helicopters or, due to the auxiliary thruster, to accomplish this in autorotation which, in turn, could lead to better lift-to-equivalent-drag ratios.

Finally, because of the auxiliary thrusters, not only the rotor disc, but also the fuselage during high speeds of flight can be kept at a low-drag attitude with respect to the flight path. This, in turn may contribute to higher weight-to-equivalent-drag ratios for compounds than would be possible for pure helicopters at the same flight speeds.

With respect to finding some justification for the compound in the time-frame of the late eighties and early nineties, discussions and meetings were held with the following individuals: Dr. R. Carlson of the US Army ARTL, Messrs. D. Meyers and F. Piasecki of Piasecki Aircraft, and Dr. H. Velkoff of Ohio State University. Their personal opinions re both civilian and military aircraft are summarized below.

Civilian. F. Piasecki and D. Meyers believe that in the civilian market, compounds can, in principle, find a niche in operations where vertical takeoff and landing requirements—especially as applied to downwash velocity and external noise level— should be similar to those of conventional helicopters, while cruise and vibration levels would be better.

However, it should be noted that in addition to the opinion of the representatives of Piasecki Aircraft, it is a truism that acceptance of the compound in the civilian market could happen only under the condition that cost aspects, including the price of the aircraft and DOC, would be reasonable when compared with that of helicopters and new rotorcraft concepts such as tilt-rotors.

Military. With respect to military applications, the following points were emphasized by all of the persons interviewed. In nap-of-the-earth or low-altitude flights in general, rotorcraft having lifting rotors in basically horizontal positions during high-speed maneuvers would have a definite operational advantage over those having vertical rotor discs. This is especially true for aircraft equipped with large diameter lift generators (for example, conventional tilt-rotors). Horizontally located rotors would have a better chance of avoiding contact with tree branches and lower vegetation such as bushes and tall grass. This operational aspect would also favor application of torque-compensating and propulsive devices of enclosed (e.g., NOTAR and Fenestron), or shrouded types such as Piasecki's ring-tail.

Another requirement of nap-of-the-earth and low-altitude flights is quick response maneuvers; i.e., the capability of pulling high g's in both vertical ($g > 3.0$) and horizontal ($g > 0.25$) directions. This requirement can be satisfied better by compounds than by pure helicopters. With respect to improving the high vertical g capabilities, the addition of a wing or wings appear as the simplest solution for maneuvering at higher flight speeds (above the power bucket). However, one should note that to some extent, the same goal may be achieved through 'overblading' of the lifting rotor; i.e., by providing a higher rotor solidity than required for a good figure-of-merit value in hover. However, wings would represent an additional advantage with respect to agility requirements, as ailerons could contribute to a quicker initial response and a higher rate of roll than those obtainable through helicopter-type controls. As to horizontal acceleration and deceleration requirements, installation of a thruster of sufficiently high capacity would probably represent the most desirable solution. This would be due to the possibility of executing horizontal acceleration or deceleration without the necessity of tilting the fuselage, as might be required in the case of the pure helicopter. Tilting the fuselage may be detrimental to the accuracy of firepower from various weapons.

In addition to the above opinions offered by the experts consulted, it should also be noted that thrusters based on such concepts as Piasecki's Ring-Tail and possible future evolution of the NOTAR would represent devices wherein the main rotor torque compensation and horizontal propulsion features are combined in a single unit.

In summary, it appears that compounding offers some potential operational and performance improvements over pure helicopters, which may be of interest to civilian, but especially to military applications. However, one should keep in mind that various penalties in performance (chiefly, hover and vertical climb), structural weight, and overall complexity may be considered as the 'cost' of compounding.

It is believed that the material presented in this chapter will help the readers to formulate their own opinions regarding the benefits versus penalties of compounding.

3.1.2 Historical Perspective

Basic ideas of compounding can be traced to the de la Cierva Autogiros from the twenties and thirties, since they relied on horizontal thrusters (propellers) as a source of

propulsion, while some of the machines were equipped with a wing, producing lift in combination with the rotor. However, the first practical case of incorporating compounding principles into a helicopter-type rotorcraft was probably represented by the Fairey Gyrodyne, developed under the leadership of J.A.J. Bennett in the late forties (Figure 3.1).

Figure 3.1 The Fairey Gyrodyne

As shown in the above figure, this single-rotor machine was characterized by the absence of a tail rotor. A tracking prop located at the tip of the starboard wing compensated for main-rotor torque. The aircraft was powered by a 525 hp Alvis Leonides nine-cylinder, fan-cooled, engine. The tip-path plane of the rotor was maintained nearly level in cruise. This was achieved by arranging the torque compensating propeller so that it provided the required thrust for forward flight, while balancing the residual torque from the limited power applied to the rotor (Ref. 7).

The Gyrodyne proved to be faster than contemporary pure helicopters by establishing an official speed record of 124.3 mph on June 28, 1948. Its relative empty weight amounted to 0.72, which was only slightly higher than for the helicopters of that time.

Jet Gyrodyne. The original Gyrodyne was modified in 1953 (first flight in January 1954) into the so-called Jet Gyrodyne (Figure 3.2) in order to investigate various design features to be incorporated into the Fairey Rotodyne.

The original, shaft-driven, three-bladed, 52-ft diameter rotor was replaced by a two-bladed, tip driven, 60-ft diameter rotor. Compressed air was pumped through blade ducts to tip burners, where fuel was injected. Instead of a single tractor propeller torque compensator, two pusher propellers were installed.

Figure 3.2 The Fairey Jet Gyrodyne

The powerplant system consisted of an Alvis Leonidas engine (similar to the original Gyrodyne engine) driving two propellers. However, it could be set to drive two Rolls-Royce Merlin air compressors in parallel through a friction clutch. These compressors supplied air to the blade-tip units.

The compressors were engaged for takeoff, and the rotor was driven by tip jets, while the propellers were set to give zero thrust. The aircraft was then flown in forward flight as a helicopter, while the propeller pitch was increased to maintain zero thrust. The compressors were declutched at cruise altitude, and the engine power was directed to the propellers, while the rotor was tilted back into autorotation. The above-described transition was first achieved in March 1955 (Ref. 7).

Fairey Rotodyne. The main features of the Fairey Rotodyne (Figure 3.3) developed under the leadership of G.S. Hislop are described and discussed in Refs. 21 and 22, and may be summarized as follows.

Development of the Rotodyne was aimed toward the creation of a rotorcraft capable of carrying 40+ passengers, or cargo, at cruise speeds higher than those of contemporary helicopters. Further goals were: (a) elimination of the tail rotor with its complexity in transmission and control, and (b) simplification of the power drive to the rotor[21]. This, hopefully, would lead to achieving an operating economy competitive with fixed-wing aircraft over stage distances of around 200/250 miles.

Two prototypes of the Rotodyne were built, and the first flight took place in November 1957. The aircraft was powered by two Napier Eland turboprop engines of 3150 hp each, which either supplied air to the rotor-tip combustion units (Figure 3.4) or each driving a four-bladed, 13-ft diameter propeller.

For takeoffs and landings as well as during initial forward flight, the aircraft operated as a tip jet-driven helicopter. In cruise, the aircraft operated as an autogiro with all forward thrust provided by the propellers, while a large portion (unlike the autogyro) of the gross weight was carried by the wing.

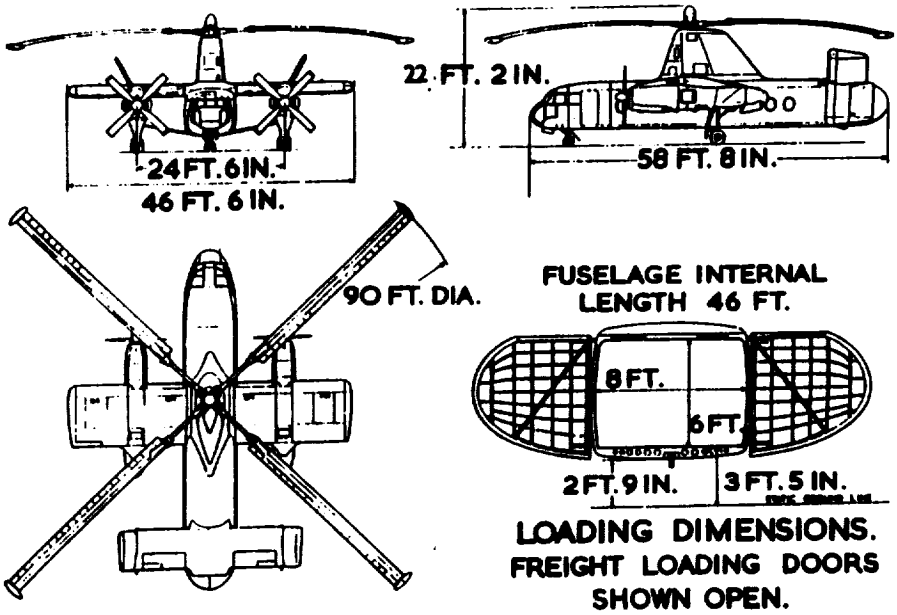

Figure 3.3 The Fairey Rotodyne

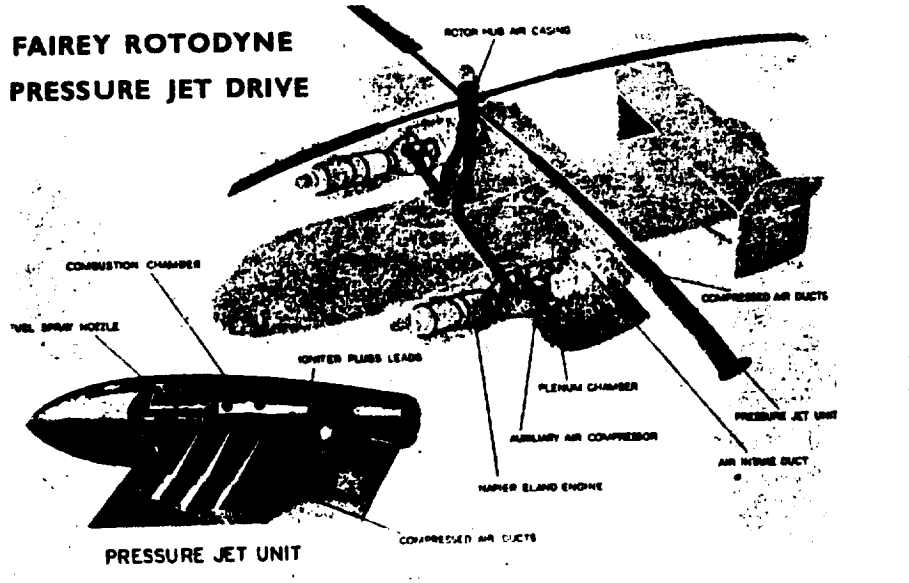

Figure 3.4 Diagram of air duct and tip-jet system[21]

The Rotodyne was very quiet and smooth in the autogiro stage. However, in the helicopter regime of flight when the tip burners were functioning, the noise level was so high that it excluded the possibility of operating close to populated areas. Attempts were made to alleviate this situation through application of various silencers (Figure 3.5). However, the most effective silencers contributed a considerable blade drag in autorotational stages of rotor operation.

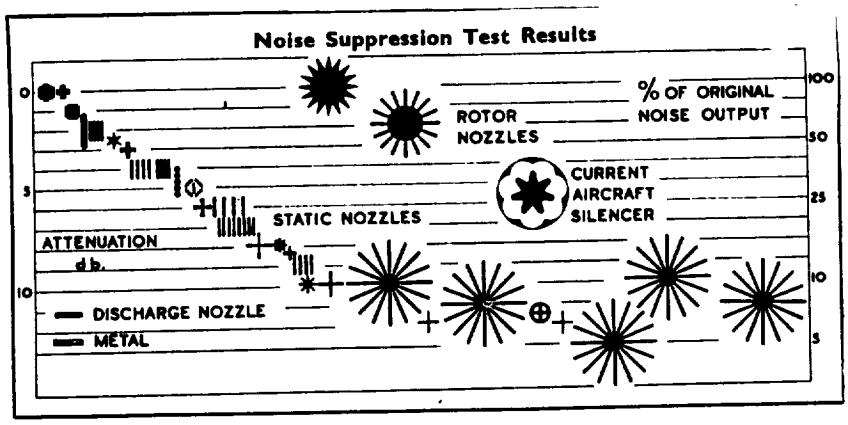

Figure 3.5 Attenuation with various silencers[21]

Westland Rotodyne. Further development of the Rotodyne was undertaken by Westland. The load-carrying capacity of the intended Westland Rotodyne would have been increased to 70 passengers or 18,000-lb of cargo. Powerplants were to consist of two Rolls-Royce Tyne turboprop engines with a maximum rating of 4240 shp. The proposed rotor diameter would have increased from the 90 ft of the Fairey prototype to 109 ft, while the corresponding gross weight would increase from 39,000 to 58,500 lb, thus retaining almost the same disc loading of 6.14 psf as the original version.

Several dozen provisional orders were received for the enlarged version of the aircraft. However, the orders were never executed, and an actual aircraft was never built. This turn of events was caused by a combination of several factors, the most probable being (a) fear of, and, in some cases, certainty of unacceptable noise levels during takeoffs and landings making it unlikely that the aircraft would be licensed to operate at heliports located close to populated areas, and (b) there was some indication that actual performance levels would not be as good as originally anticipated. But these investigators were unable to verify this point.

McDonnell XV-1. The XV-1 (Figure 3.6), officially first flown in July 1954[23], was developed under the leadership of F. von Doblehoff and K.H. Hohenemser, the latter being chiefly responsible for aerodynamic and dynamic aspects of the design[24].

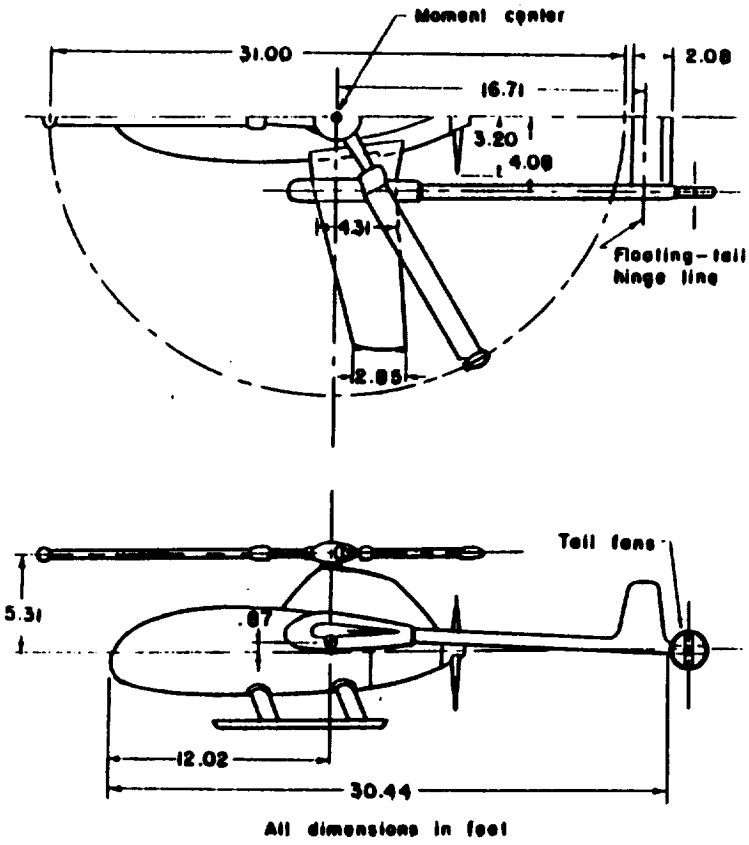

Figure 3.6 Two-view drawing of the XV-1 compound

Along with the Jet Gyrodine and Rotodyne, the XV-1 is an example of a compound where basic elements of compounding (i.e., provision of independent forward thrusters and rotor unloading) were combined with a rotor that was tip-driven for takeoff and landing maneuvers as well as low-speed flight. However, in cruise, the rotor autorotated at about half of its hover rpm, supplying 15 percent of the total lift, while conventional fixed wings produced the remaining 85 percent. A Continental R975 550 hp reciprocating engine powered a pair of radial compressors during helicopter flight and a fixed-pitch pusher propeller in airplane flight. Air from the compressors was ducted through hub and blades to supply the pressure jet units.

The blades were attached to a gimbal-mounted floating hub by use of two bundles of stainless steel straps per blade arranged in a horizontal plane so that each blade may freely flap. Pitch was changed by bending these straps collectively or differentially.

Directional control in hover was produced through the use of two hydraulically driven fixed-pitch fans, which were controlled by rudder pedals. At high speed, directional control was obtained by conventional rudders.

Lateral control at slow speed was produced by lateral rotor tilt and, in high-speed flight, by ailerons. Both ailerons and lateral rotor controls were permanently connected to the stick.

Longitudinal control in low-speed flight was produced by longitudinal rotor tilt, whereas a floating tab-controlled stabilizer was used in high-speed flight.

Sud Ouest 1310 Farfadet. The S.O. 1310 Farfadet (Figure 3.7[7]) was first flown as a helicopter in May 1953, and achieved first conversion in July 1953. This rotorcraft is still another example of the combination of the application of tip-driven rotors to compounds.

Figure 3.7 The S.O. 1310 Farfadet with nose-mounted turboprop and jet-driven rotor

As in the preceding cases, this rotorcraft was operated as a jet-driven helicopter during takeoffs, landings, and low-speed flights. A 360-hp Turbomeca Arius II turbo-compressor, located in the fuselage aft of the cabin, supplied compressed air to the blade tips, where small combustion chambers were located. During forward flight, the rotor turned in autorotation producing a small amount of lift, while the fixed wing provided the primary aircraft support. Forward thrust was generated by a variable-pitch propeller driven by a 360-hp Turbomeca Artouste II turboprop engine. Thus, the power to the Farfadet was provided by two independent gas-turbine units: the Aeriel III for helicopter regimes of flight and the Artouste II for cruise. The Farfadet was never put into production.

VFW-Fokker H3 Sprinter. The idea of incorporating a jet-driven rotor into the compound helicopter was still alive in the late sixties and early seventies, as witnessed by the development of the VFW-Fokker H3 Sprinter (Figure 3.8).

However, in contrast to the preceding cases of this design, no fuel burning at the blade tips was present. Instead, for vertical takeoff, landing, and hover, a turbo-compressor provided compressed air to tip-drive the three-bladed rotor. The H3 in these modes functioned as a conventional helicopter. For transition to forward flight, the power was transferred progressively to shrouded propellers on each side of the fuselage and the rotor began autorotating

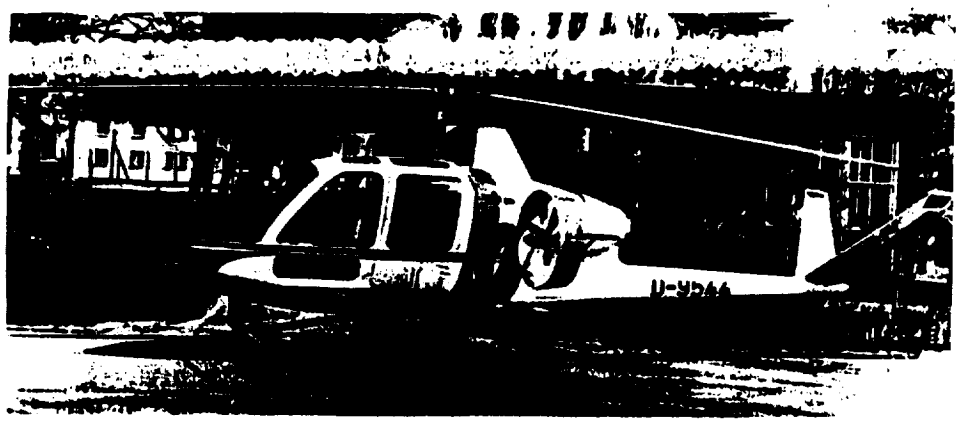

Figure 3.8 Prototype of the VFW-Fokker H3 Sprinter three-seat cabin rotorcraft

once the aircraft was in horizontal flight. The method of propulsion eliminates the need for conventional transmission and drive-shaft systems, hydraulic systems, clutches, and torque compensation (i.e., tail rotor). Full rotor autorotation is maintained in the event of engine failure.

Among the advantages claimed for the design are its simplicity, both to fly and to maintain; and improvements in safety, cost-effectiveness, and noise reduction compared with conventional aircraft.

It should also be noted that the anticipated relative weight empty of 0.51 was quite good for a compound. But the cruise speed of 135 knots, basically on the same level as that of pure helicopters of that time and of the same weight and power class, was not spectacular.

As to the more important details of this design, one would find that the rotor had three fully articulated, constant-chord blades having NACA 23015 sections. The rotor rpm range was from 280 to 480. The powerplant consisted of one Allison 250-C20 turboshaft engine with a maximum constant rating of 346 hp (400 hp for takeoff), which either supplied compressed air to drive the rotor, or drove (through mechanical transmission) two seven-bladed shrouded propellers mounted on stub fairings on the sides of the fuselage.

Remarks re Compounds with Jet-Driven Rotors. Of the six compounds reviewed up to this point, five of them, namely, the Jet Gyrodyne, Rotodyne, XV-1, Farfadet, and Sprinter, represent the same basic design philosophy of combining a single jet-driven lifting rotor with an airscrew type forward propulsor. Wings carrying a substantial lift (up to 85 percent of gross weight) were used on all of the above aircraft, with the exception of the Sprinter. Also, with the exception of the Sprinter, the rotor jet propulsion consisted of blade-tip burners. The cold-jet principle was applied to the Sprinter. Nevertheless, in all cases, jet propulsion of the rotors was used for takeoffs, landings, and low-speed flights only, while in high-speed regimes of flight, the aircraft were flown basically as autogyros; i.e., with rotors in autorotation.

The chief justification for the above-outlined design philosophy was the desire to eliminate the need for main rotor torque compensating devices as well as the whole mechanical rotor drive system and thus, to simplify the whole configuration. Furthermore, designers of these compounds believed that a rotor in autorotation would generate lower vibratory inputs in cruise than its mechanically driven counterpart. In addition, a rotor already in autorotation would contribute to safety aspects in case of power failure.

In spite of the many attractive characteristics, none of the jet-rotor compound types reviewed so far were put into production. For the tip-burning configuration, the operationally unacceptable noise level was probably chiefly responsible for its failure. For the cold-jet type (Sprinter), the high noise level was not the problem. However, according to Janes, 1972, "The method of propulsion intended originally proved unsuitable for aircraft of this size; thus current flight testing is being concentrated on system development. Flight testing of a second H3 prototype, which has a more powerful engine and an improved compressor, began in early 1972 and was progressing satisfactorily at the time of this writing." Nevertheless, neither the H3 nor its larger derivative, the H4, was put into production.

Compounds with Mechanically Driven Rotors in All Regimes of Flight. The rotorcraft reviewed below represent a different approach to the compounding concept. All have mechanically-driven rotors in all regimes of flight (except, of course, in the case of a complete engine failure). These configurations are chiefly represented by single-rotor types, but some side-by-side designs are also discussed (one actual, and one hypothetical).

To facilitate an investigation into possible future trends in compounding, advantage is taken of a Soviet study by Tishchenko et al (Ref. 25) of 52-ton gross-weight compounds having up to 450 km/hr (243 kn) cruise-speed capabilities. These rotorcraft are designated as 'hypothetical'.

Piasecki 16H-1 Pathfinder. The Piasecki 16H-1 Pathfinder (Figure 3.9), first flown in February 1962, was the second single-rotor compound in the world with a mechanically-driven rotor. The original Gyrodyne was the first, but its rotor autorotated in high-speed flight, while in the Piasecki design, some fraction of the engine power was directly transmitted to the lifting rotor.

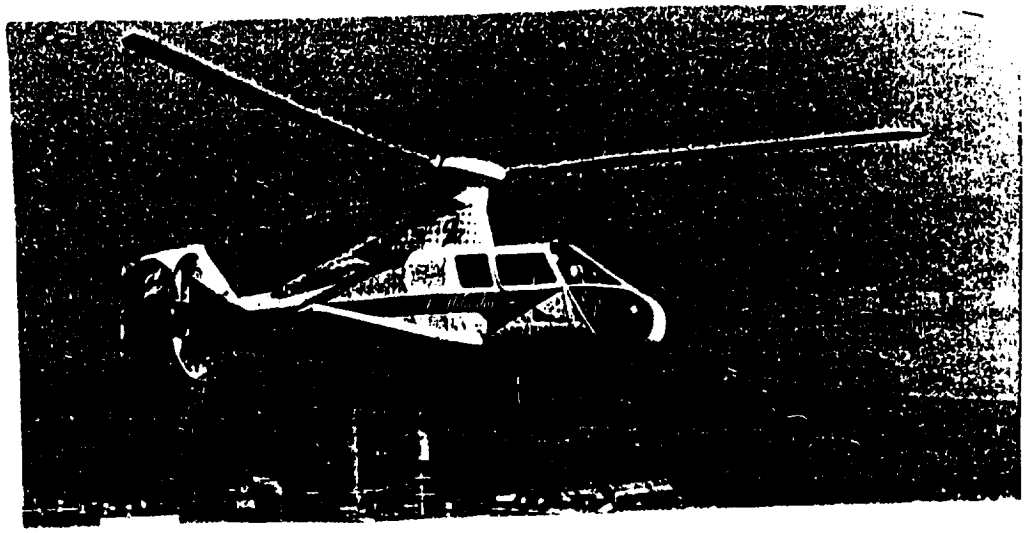

Figure 3.9 Piasecki 16H-1 Pathfinder

Because of the mechanical drive concept, the Pathfinder design team (headed by F.N. Piasecki, D. Meyers, and Z. Ciolkosz) had to face the problem of providing a main rotor torque-compensating device in addition to the forward propulsor. The basic idea of dealing with this problem was somewhat similar to that of the Gyrodyne: one major component would serve both purposes. However, the practical incorporation of this basic idea was different in the two cases. Instead of an offset propeller as in the Gyrodyne, the Pathfinder was designed with a so-called ring-tail consisting of a shrouded propeller mounted along the aircraft's longitudinal axis, and a set of controllable vanes capable of side-deflecting the propeller slipstream through almost 90 degrees. This solution provided the necessary main-rotor torque compensation in hover and slow-speed flight maneuvers. In high-speed flight, the ring tail served as the main propulsor of the aircraft since the lifting rotor, unloaded by means of a wing, provided only a fraction of the necessary horizontal thrust.

Powered by a 400-hp, PT6 shaft-turbine engine, the 16H-1 logged a total of 185 flight hours, during which speeds of up to 170 mph were attained.

> "The 16H-1 evoked interest throughout the military, but their armament and armor needs tripled the gross weight. Convinced that this was the best path for a new attack helicopter, the Army initiated a competition for the 'Advanced Aerial Fire Support System' (AAFSS), and for supporting technology programs, one of which was the 16H-A." (Ref. 26).

Piasecki 16H-1A Pathfinder. The Piasecki 16H-1A Pathfinder (Figure 3.10) represented a modification of the original 16H-1 model. The new rotorcraft was developed under an Army contract which specified a required high-speed capability of over 200 mph. Consequently, a GE T-58 turbine rated at 1050 shp, new drive system, new propeller to absorb the increased power, and a 44-ft diameter rotor (H-21) were added, and the fuselage was lengthened to accommodate eight people.

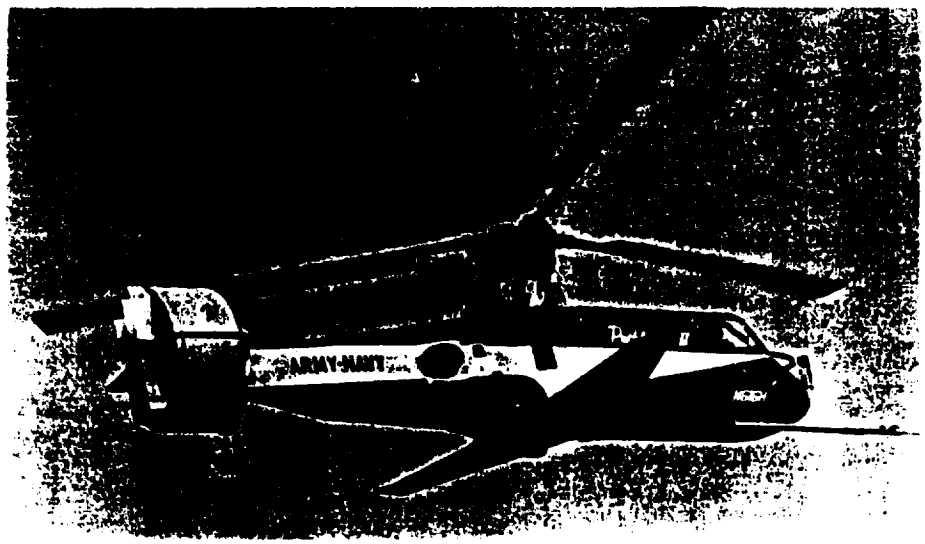

Figure 3.10 Piasecki 16H-1A Pathfinder

A three-bladed Hartzell propeller hub was modified so that it would be directly controlled through the 16H servo control system.

The 16H-1A made its initial flight in November 1965, and logged more than 150 hours under a joint Army/Navy test program, including flight at forward speeds of up to 225 mph. It was highly maneuverable in forward flight, flew sideways up to 35 mph, was flown backwards at 32 mph, and numerous autorotative tests were made[26].

The 'ring-tail' antitorque, forward propulsion, and integrated control subassembly provided many advantages in compounding the helicopter. The 16H-1 was normally flown in forward flight with the main rotor pitch reduced, the aircraft level, and the cyclic pitch stick slightly forward. In case of engine failure, this gives the pilot an opportunity to enter into autorotation while decreasing the rotor pitch. It is not time-critical, as in the case of a conventional helicopter which requires conversion from power pitch to autorotative pitch in less than two seconds, In the Pathfinder-type configurations, the propeller absorbs the energy of the air flowing by and drives it back into the rotor, thereby assisting in maintaining rotor rpm while the pilot arranges the collective pitch of the rotor and pitch of the propeller.

The success of the compound helicopter flight-test program sparked a large Army competition for a full-scale development and production program for 375 aircraft. The winner was the 'Cheyenne' helicopter, which will be discussed later.

Piasecki 16H-3. The Piasecki 16H-3 (Figure 3.11) represents a project for a commercial or military compound developed along the lines of the Pathfinder.

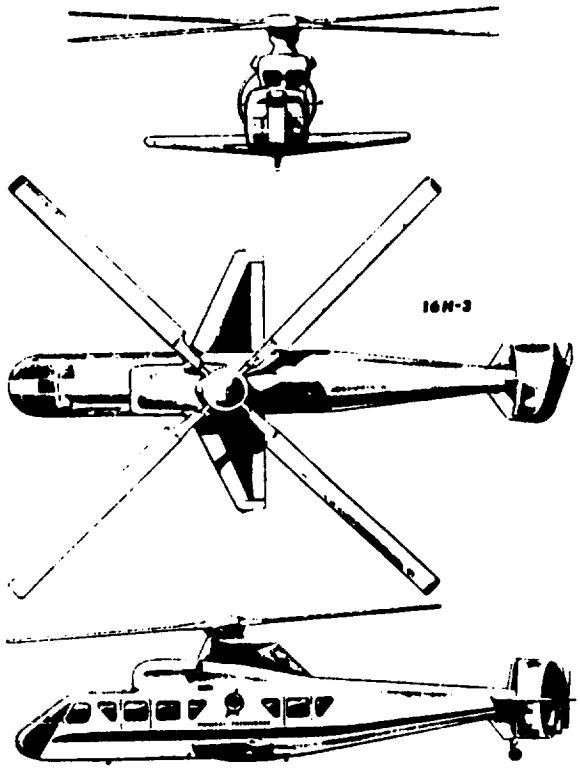

Figure 3.11 Projected Piasecki 16H-2 compound

Its maximum gross weight for vertical takeoff was established at 10,400 lb, in comparison to that of 8000 lb for the 16H-1A. Although the rotor diameter of the new model was expected to be the same (44 ft) as that of its predecessor, the number of blades was increased from 3 to 4. The power installed was also higher, as two PT6-830 turboshaft engines rated at a maximum continuous power of 750 hp each were installed. The above modifications should assure a maximum cruise speed of 170 kn at 5000 ft, and a maximum flying speed of 200+ knots.

In concluding this review of the Piasecki compounds, it should be noted that wind-tunnel tests of the improved version of the full-scale ring tail are scheduled for 1992.

Lockheed AH-56A Cheyenne. The Lockheed AH-56A Cheyenne (Fig. 3.12) was developed as a result of a US Army competition for an Advanced Aerial Fire Support System (AAFSS). The initial order was for 10 prototypes, all of which were delivered by July 1968. However, prior to their delivery, a production order for 375 AH-56A compounds had been issued but, because of main-rotor instabilities, the Army cancelled the production order. Lockheed continued work on the Cheyenne until the early seventies, when all activities in this area were stopped.

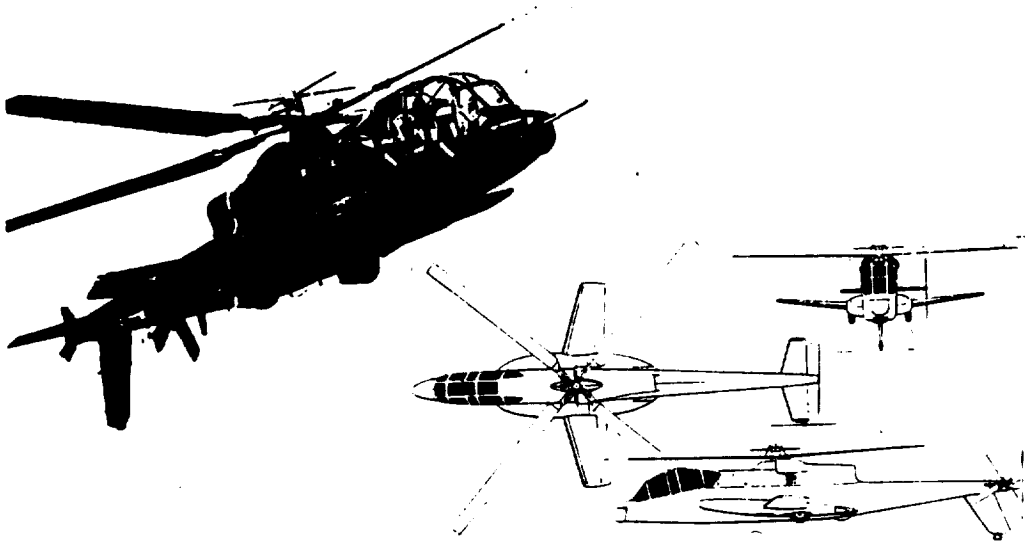

Figure 3.12 Lockheed AH-56A Cheyenne

The AH-56A was a two-seated compound helicopter with a small low-set fixed wing and a retractable wheel landing gear. The powerplant consisted of one 3925 SHP General Electric 764-GE-16 shaft-turbine, driving a four-bladed rigid main rotor, a four-bladed tail rotor mounted at the tip of the port horizontal tail surface, and a 10-ft diameter pusher propeller at the extreme tail.

The small low-set cantilever wing contained preset tab deflectors, but no ailerons or flaps. The wing provided almost complete unloading of the main rotor in high-speed flight.

It should be noted that the quoted figures regarding speed capabilities at the design takeoff weight of 16,945 lb were as follows: at SLS, V_{max} = 220 kn, $V_{cr_{max}}$ = 210 kn, and at 10,000 ft, $V_{cr_{max}}$ = 205 knots.

Lockheed XH-51A. The design of the Cheyenne was, to a large extent, based on experience acquired in the development and flight testing of the Lockheed Model 186, military designated XH-51 research compound (Fig. 3.13).

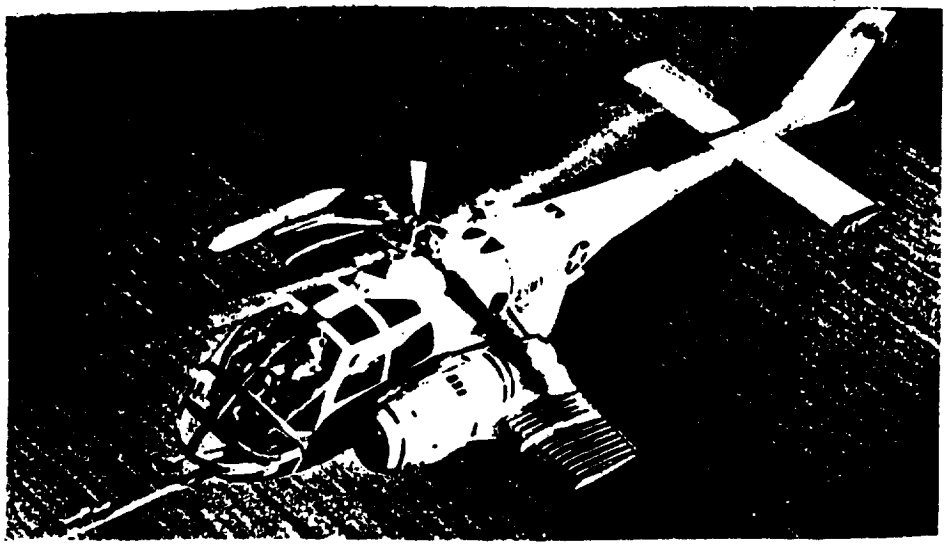

Figure 3.13 Lockheed Model 186, military XH-51A compound

The compound version shown above was developed from the research helicopter designated as XH-51A, which used the then so-called rigid rotor. The aircraft was characterized by a low drag, as its equivalent plate area totaled 8.8 sq.ft[7]. This amounted to an equivalent flat-plate area loading of 512.5 psf, which should be considered good for a helicopter having a maximum gross weight of 4100 lb (for comparison, see Fig. 7.5, Ref. 5). A mechanical stabilizing gyro was located in series between the blades and the pilot's controls. The powerplant consisted of one 500 shp Pratt & Whitney(UAC) T74(PT6B) shaft-turbine engine.

The compound version (Fig. 3.13) was obtained by modifying the original XH-51 helicopter. This was done by installing a 2600-lb (1180 kg) st Pratt & Whitney J60-P-2 turbojet engine mounted on the port side of the cabin, and a cantilever mid-set wing, spanning 16 ft, 11 in. Its normal takeoff weight was 4500 lb. The first flight, without using the turbojet, was made in September 1964. During subsequent flight testing in June 1967, it attained a speed of 263 kn (302.6 mph, 487 km/hr), the fastest speed recorded for any rotorcraft at that time[7].

Bell Model 533. The original Model 533 was a YUH-1B Iroquois helicopter which Bell modified under U.S. Army contract for service as a high-performance research vehicle to evaluate various rotor systems and methods of drag reduction.

The jet compound was developed in 1963 by the addition of a small swept wing and two Continental J69-T-29 turbojets, rated at 1700 lb (771 kg) st, mounted in pods on each side of the fuselage (Fig. 3.14).

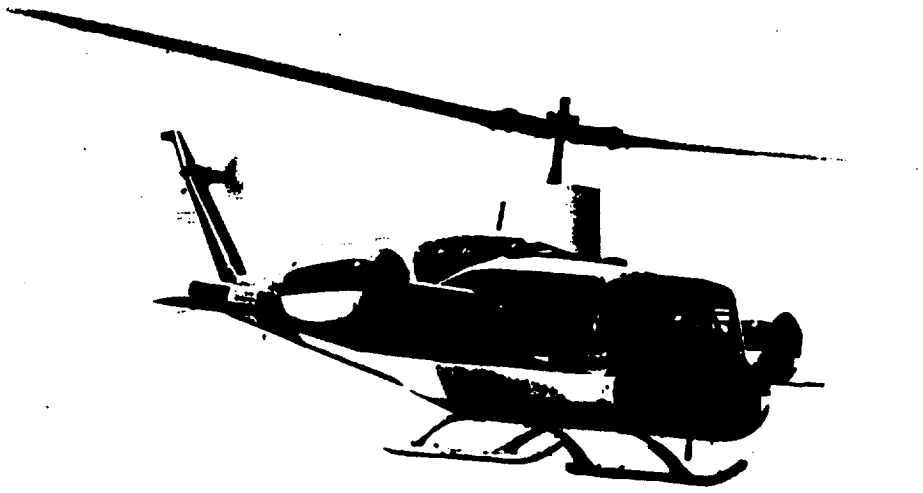

Figure 3.14 Compound version of Bell Model 533

In October 1964, the Model 533 became the first rotorcraft to exceed a speed of 200 kt, by attaining 236 mph (380 km/hr) during a test flight.

In April 1965, it became the first to reach 250 mph in level flight. During the same test flight, it attained 254 mph (409 km/hr) in a slight dive and demonstrated its maneuverability by performing 28 turns and 60-degree banks at speeds of around 200 mph. A Mach number of 0.985 was achieved at the tips of the advancing blade of the two-blade rotor, which has special tapered tips. Takeoff weight of the aircraft was 8600 lb.

Early in 1968, the Model 533 was again modified to take more powerful auxiliary turbojets, this time, two wing-tip-mounted Pratt & Whitney JT12A-3's, each rated at 3300 lb st, for further testing in the 250-kn speed range. It was announced in May 1969 that the Model 533 had attained a speed of 274 knots. The two-blade main rotor was then followed by a four-blade flex-beam rotor system[7].

Other Western Compounds. It should be noted that in addition to the above reviewed compounds, practically every major Western helicopter company either built, designed or, at least, studied some form of the compound concept.

Some of these aircraft simply represented modifications of standard configurations by the addition of turbojet engines and, in most cases, a wing.

For instance, the UH-2 Kaman compound (Fig. 3.15) was created by installing a G.E. J85 turbojet engine and a wing. In 1964, the so-modified aircraft achieved a speed of 216 mph[20] (188 kn).

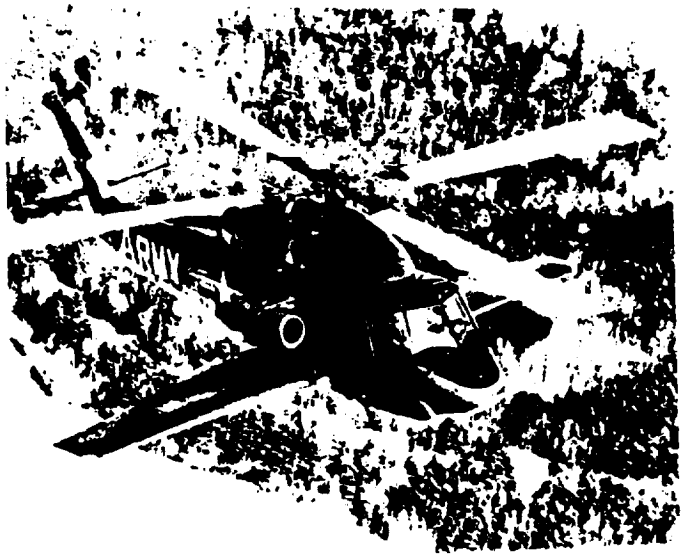

Figure 3.15 Kaman UH-2 compound helicopter —1964

It is indicated in Ref. 20 that a Sikorsky S-61F with two Pratt and Whitney J60 engines in addition to the normal twin T58 powerplant, reached 241 mph (210.2 kn) in July 1965.

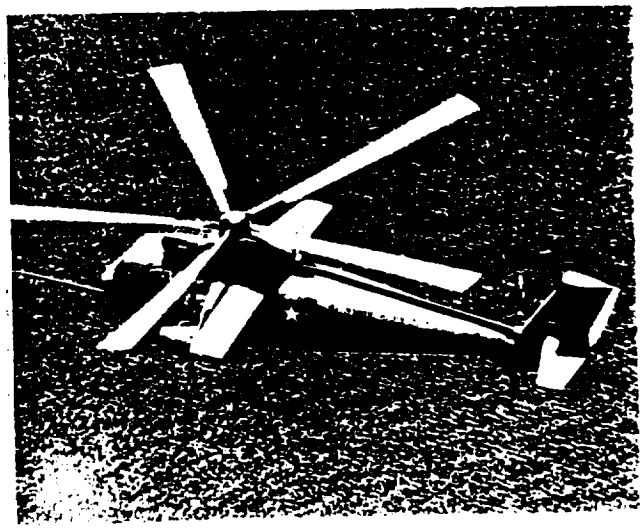

Figure 3.16 Sikorsky S-61F compound helicopter — 1965

Advancing Blade Concept (ABC). Of helicopter configurations that appear especially suitable for compounding through installation of a horizontal thruster, the Sikorsky ABC (Advancing Blade Concept) comes to one's mind. In this configuration, lift in the high-speed regime of flight is created almost entirely on the advancing blades of the rigid coaxial rotor system. The retreating blades are unloaded, thus eliminating the blade stall problem. Consequently, there is no need for auxiliary wings to unload the rotor and/or to assure a high degree of roll control at high speeds and low density altitudes, as the rotors remain highly responsive even under these conditions.

By contrast, it appears that compounding through installation of auxiliary thrusters would be quite advantageous as, with respect to the flight path, it would permit one to retain the most desirable inclination of the rotor discs independently of the flight speed.

In this way, an aircraft can be obtained that unlike all other VTOL concepts, would go from vertical takeoff, through high-speed regimes of flight, and back to vertical landing with no change in the basic configuration (Figure 3.17).

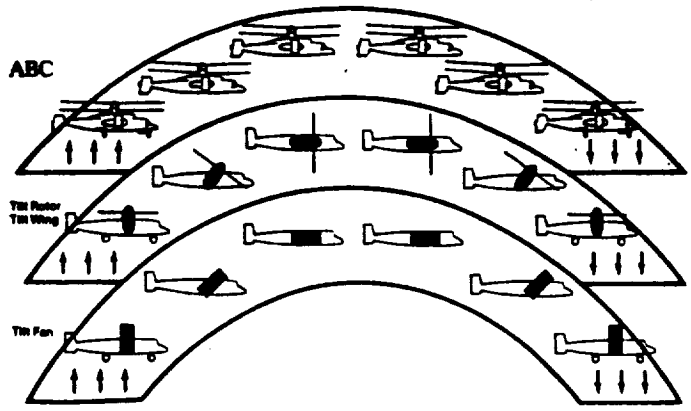

Figure 3.17 ABC high-speed aircraft does not require reconfiguration from hover to cruise, back to hover, and landing

It appears that horizontal propulsors based on shaft driven concepts; i.e., propellers and ducted and unducted fans, should be the most suitable types, as a single powerplant system would serve as a source of energy in all regimes of flight.

Of all possible shaft-driven horizontal propulsors, ducted fans located either at the sides of the fuselage or in the tail section, appear to be the most desirable configuration as far as operational safety requirements are concerned. A two-ducted fan system is shown for example in Figure 3.18.

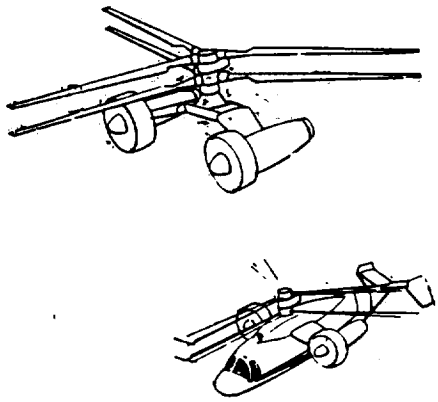

Figure 3.18 Example of ABC dynamic system based on two ducted fans

Development of the ABC concept began in 1972 when Sikorsky announced that the company was designing and building a research aircraft, designated S-69, to flight test the Advancing Blade Concept rotor system, under a US Army contract. Subsequently, the value of the contract was increased to cover detail design changes and the construction of two demonstrator aircraft under the Army designation XH-59A. The first aircraft made its first flight on 26 July 1973 (Ref. 7, yr 79-81).

Following completion of flight tests in the pure helicopter configuration in March 1977, two Pratt & Whitney J60 turbojet engines were added for auxiliary forward thrust in a high-speed configuration (Figure 3.19).

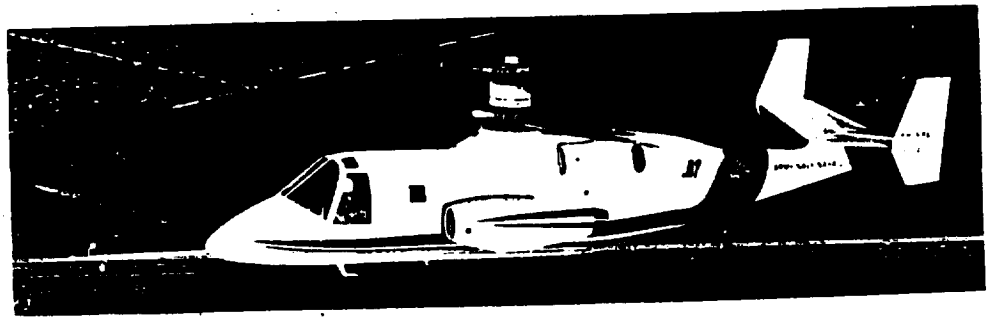

Figure 3.19 Sikorsky S-69 (XH-59A) prototype for evaluation of the ABC rotor system

On 21 April 1980, the S-69 attained a speed of 238 knots (441 km/hr: 274 mph) in level flight. Its maximum design speed is 300 knots (555 km/h: 345 mph) at a 2g load factor[7].

Numerous design studies were performed at Sikorsky regarding the possibilities of the ABC application to aircraft designed for various missions ranging from light helicopters (LHX) to civilian transports. Mission requirements influenced, in turn, the design of the ABC rotor[27]. It appeared, however, that in any case, lift to equivalent drag ratio of the ABC rotor, although better than for conventional helicopters, would still be much lower than for fixed wings—even of moderate aspect ratio of, say, 6. Figure 3.20[27] based on flight test results of the XH-59A illustrates this point.

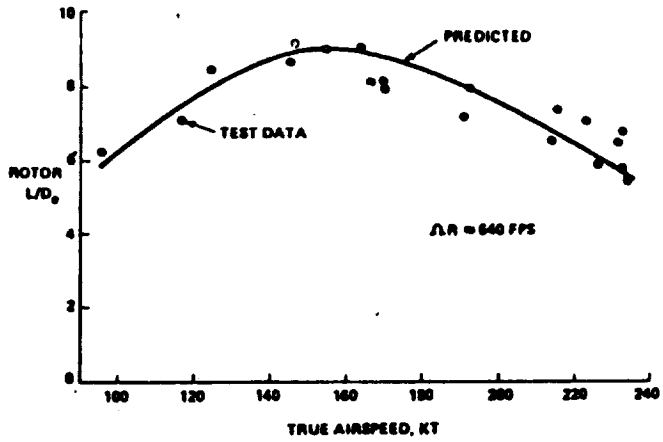

Figure 3.20 Lift to equivalent drag ratio of the ABC rotor vs. speed of flight

The relative weight of the ABC rotor group would probably be higher than for other compound helicopters, but one should remember that there will be other weight savings, because there is no need for auxiliary wings and a main-rotor torque compensating system. For instance, the relative weight of the XH-59A rotor group amounted to 17.6%. However, it should be noted that it was designed using conventional materials and fabrication methods from the early seventies period. A considerable relative weight reduction of the ABC rotor system can be expected through the application of lighter weight high-strength structural materials.

In spite of promising possibilities, technical interest and actual design and experimental efforts devoted to the ABC system appears to be at a low level as of this writing.

Rotor Systems Research Aircraft (RSRA). In conclusion of this glance at the history of Western compounds, it should be emphasized that in this country there is a very versatile research tool for investigating various aspects of compounding; namely, the Sikorsky RSRA (Rotor Systems Research Aircraft) shown in Figure 3.21.

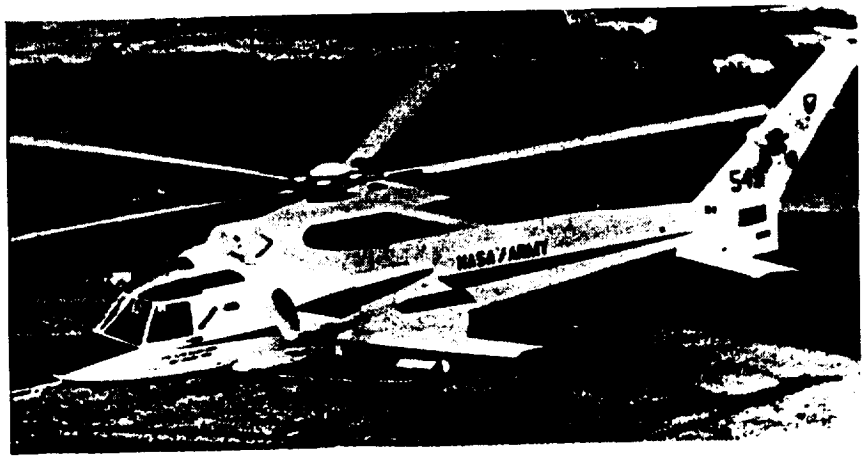

Figure 3.21 The Sikorsky RSRA in flight

The load-measuring system of this aircraft permits one to measure, in flight, the loads experienced by all the major components of a compound (Figure 3.22).

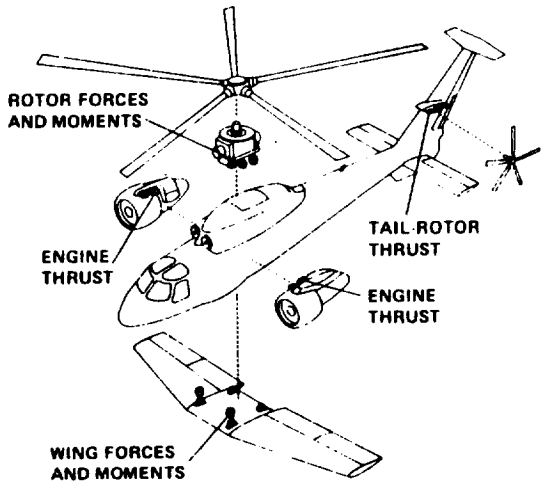

Figure 3.22 Load-measurement systems of RSRA[28]

Remarks re Soviet Compounds. To the best of these investigators' knowledge, no Soviet compound has ever been put into production. Probably, there were experimental rotorcraft of this type in the USSR, but no published data can be found in written literature. However, one Soviet experimental compound; namely, the Kamov Ka-22, became better known in the West because of establishing a rotorcraft speed record of 221.4 mph

(192.3 knots) in October 1961. Furthermore, some insight into the approach of the Soviet designers to helicopter compounding philosophy can be gained from a study by Tishchenko, et al[25] of that configuration in application to a 52-ton gross-weight transport. Consequently, the Ka-22 and the Tishchenko compounds (Ref. 25), which will be called hypothetical aircraft, are briefly reviewed in the following sections.

Kamov Ka-22. The Kamov Ka-22 compound helicopter (Figure 3.23) was conceived as a large transport, probably capable of accommodating up to 100 passengers[7].

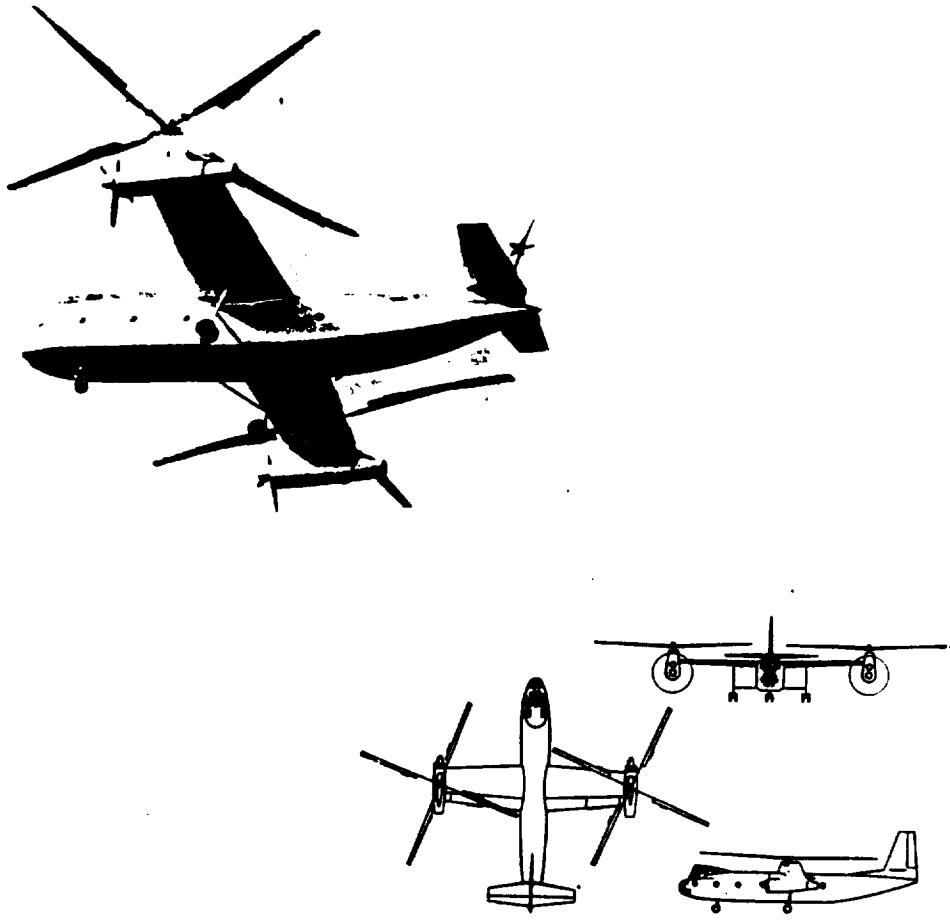

Figure 3.23 Kamov Ka-22 compound transport

The Kamov Ka-22 was powered by two turbine engines of 5622 hp each, which drove four-bladed lifting rotors for takeoffs, landings, and low-speed maneuvers. In cruise, all of the engine power was probably absorbed by the propellers, while the rotors autorotated as in an autogiro. The chief designer, N. Kamov, indicated in 1966 that interest.

in that configuration was still active in the USSR. However, it appears that this interest was never translated into further development of the Ka-22 derivatives.

Hypothetical Soviet Compounds of Tishchenko. Apparently, a broad study was performed by the Tishchenko design team before selecting a final configuration for a large 52-ton gross-weight rotorcraft transport. Eventually, the study led to the development of the Mil Mi-26 helicopter. However, other configurations were investigated, including side-by-side (Fig. 3.24) and single-rotor (Figure 3.25) compounds[25].

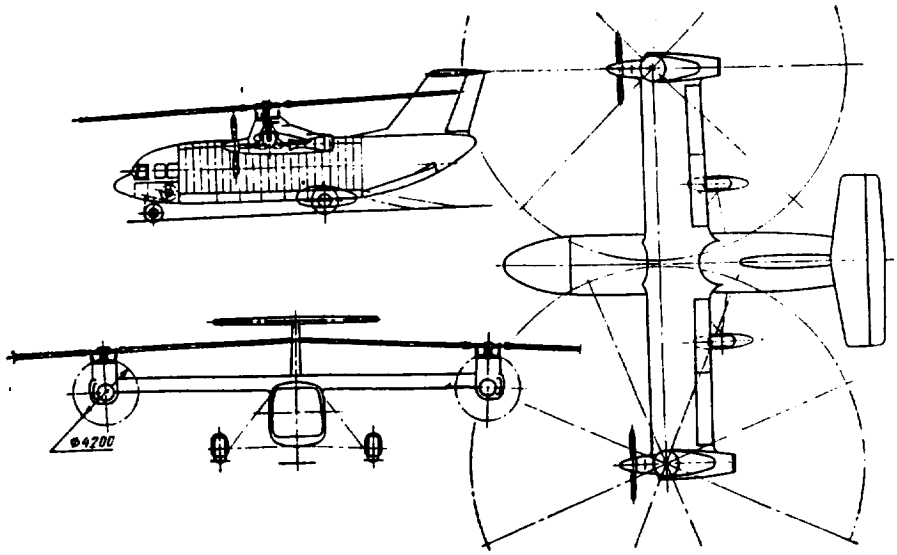

Figure 3.24 Tishchenko's hypothetical 52-ton gross-weight side-by-side compound.

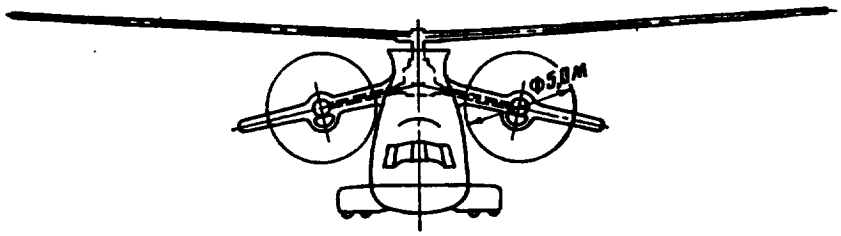

Figure 3.25 Tishchenko's hypothetical 52-ton gross-weight single-rotor compound

These aircraft, which will be called hypothetical compounds, were supposed to have a gross weight of 52 metric tons, while cruise speeds were postulated as equal to 350, 400, and 450 km/hr; i.e., 189, 216, and 243 knots. Their competitive position with respect to conventional and winged helicopters of various configurations was evaluated. On the basis of data contained in Ref. 25, a graph showing relative payload ($\overline{W}_{pl} = W_{pl}/W$) vs. distance flown were made (Figure 3.26). This was done for all six of the hypothetical compounds.

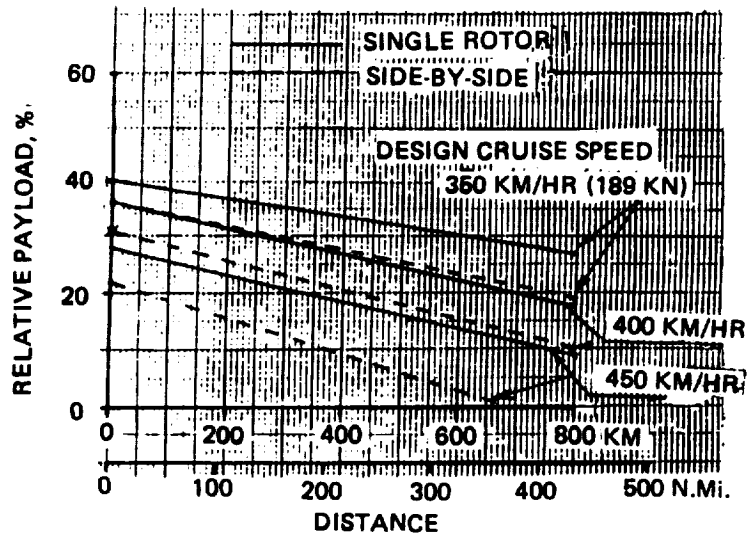

Figure 3.26 Relative payload vs. distance flown for Soviet hypothetical single-rotor and side-by-side compound configurations

A glance at Figure 3.26 would indicate that the single-rotor compound is definitely superior to the side-by-side configuration as far as load-carrying capabilities at all three design cruise speeds are concerned. It can also be seen that for both types, the payload decreases as the design cruise speed goes up.

In order to see whether the higher cruise speed would compensate for the loss of payload-carrying capacity, Figure 3.27, showing the absolute ideal productivity, was prepared: $\Pi = W_{pl} \times V_{cr}$, where W_{pl} is in metric tons and V_{cr} is in knots.

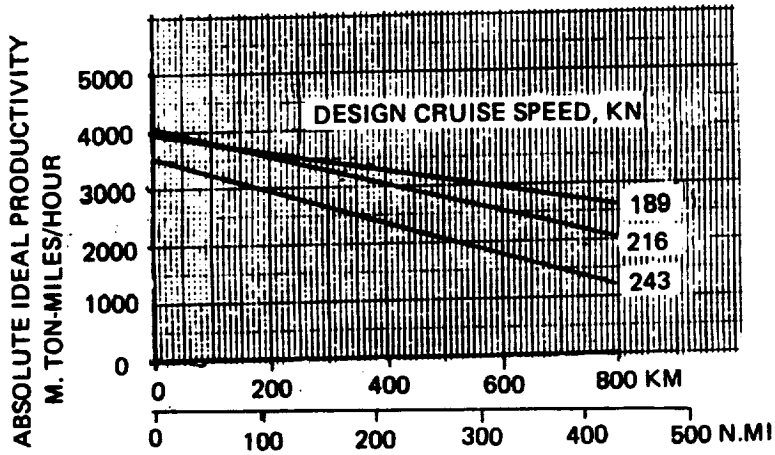

Figure 3.27 Absolute ideal productivity vs range of single-rotor hypothetical compounds designed for various cruise speeds

Figure 3.28 was prepared to give the reader a still better insight regarding the influence of design cruise speed on productivity. Here, absolute ideal productivity for three selected ranges (0, 200, and 400 n.mi) is plotted vs design cruise speed.

An examination of Figures 3.27 and 3.28 would suggest that for single-rotor transport compounds, the design speed within the 200-230-knot range would probably represent a sound performance requirement. It can be seen that for operational ranges of up to 200 n.mi, which would probably be of prime interest for compound applications, the loss in productivity with increasing design cruise speed is small (up to some 220 knots). On the other hand, 200-220-knot cruise speeds would give the compound an advantage of about 50 to 70 knots over pure helicopters. This differential could, in principle, contribute to the creation of a competitive edge over pure helicopters in short-haul transportation.

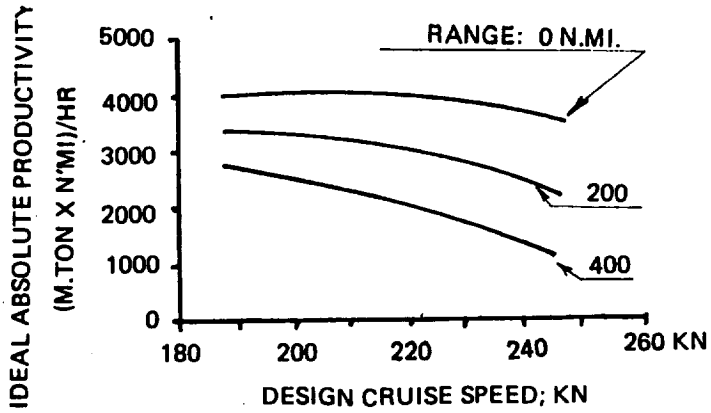

Figure 3.28 Ideal absolute productivity vs. design cruise speed

3.2 Discussion of Historical Trends

General. All compounds being reviewed in this chapter are divided into two gross-weight classes; one representing maximum flying gross weights up to 30,000 lbs, and another with gross weights higher than 30,000 lbs. Some of the important characteristics of the considered compounds are summarized in Tables 3.1A and 3.1B, and trends exhibited by some of those characteristics are illustrated by the appropriate graphs and discussed in some detail in the following sections.

Disc Loading. Disc loadings of the compounds listed in Tables 3.1A and 3.1B are plotted vs. maximum flying gross weight in Fig. 3.29.

A glance at this figure would indicate that disc loadings of the majority of past compounds are within the 5 to 7 psf bracket. However, exceptions are the Fairey Gyrodyne at 2.26 psf, which is well below, and the AH-56A at 11.03 psf, which is above those values. It is interesting to note that disc loadings of the Soviet hypothetical single-rotor compounds are all higher than that of the AH-56A and decrease with the increasing design cruise speed levels: 13.9 psf for V_{cr} = 189 kn, and drops down to 11.8 psf for the 243-kn cruise compound. Looking at Figures 3.29 and 7.1 of Ref. 5 where disc loadings of typical Western and Soviet helicopters are also presented vs. gross weight, one would find that disc loadings of compounds are, in general, similar to those of pure helicopters of the same gross weight class.

TABLE 3-1A

COMPOUND HELICOPTERS UP TO 30,000 LB GROSS-WEIGHT CLASS

	MODEL & YEAR	FAIREY GYRODYNE 1948	FARFADET 1953	McDONNELL XV-1 1954	FAIREY JET GYRODYNE 1954	PIASECKI 16H-1 1962	PIASECKI 16H-1A PATHFINDER 1965	PIASECKI 16H-3	LOCKHEED AH-56A CHEYENNE 1967	VFW-FOKKER H3 SPRINTER 1970
	CONFIGURATION	SR, SD, MW*	SR, TD, LW	SR, TD, HW	SR, TD, MW**	SR, SD, LW	SR, SD, LW	SR, SD, LW	SR, SD, LW	SR, TD
PRIMARY CHARACTERISTICS	ROTOR RADIUS, Ft	26.0	16.54	15.5	30.0	20.5	22.0	22.12	25.2	14.27
	ROTOR(S) DISC AREA, Ft	2,122.6	1057.8	754.4	2,826	1,319.6	1,519.8	1,536.4	1,994	639.91
	TOTAL WING AREA, Ft^2	61.81		99.6		84.24	84.24	84.24	130	
	EXPOSED WING AREA, Ft^2	37.95		73.0		56.62	56.62	56.62	82.8	
	WING SPAN, Ft	17.8	20.67	26.0		20.0	20.0	20.0	26.7	
	$\frac{\text{TOTAL WING AREA}}{\text{ROTOR DISC AREA}}$	0.03		0.13		0.055	0.055	0.055	0.065	
	$\frac{\text{EXPOSED WING AREA}}{\text{ROTOR DISC AREA}}$	0.0179		0.097		0.037	0.037	0.037	0.041	
	$\frac{\text{WING SPAN}}{\text{ROTOR RADIUS}}$	0.68	1.11	1.68		0.975	0.909	0.904	1.06	
	POWERPLANT, HP	525	360*	550		400	1,250	1500	3,435	400
	PROPULSOR(S) and DIAMETER, Ft	ONE PROP 7.0		6.4		5.5	5.5	5.5	ONE PROP*** 10.0	(2 PROPS) 2.9
	GROSS WT, LB	4,800		5,222	7,000	4,200	8,000	10,400	22,000	2,134
	WEIGHT EMPTY, LB	3,450		4,000		2,811	4,550	5,956	11,725	1,091
	RELATIVE WE	0.72		0.77		0.62	0.57	0.57	0.53	0.51
	DISC LOADING, PSF	2.26		6.9		3.18	5.26	6.77	11.03	3.33
	INSTALLED POWER LOADING, LB/HP	9.14		9.5		10.5	7.62	6.93	6.4	5.33
	V_{max}, KN	107.9				147.6	195.4		212.0	
	V_{cruise}, KN	95.5				130.0	178.0	169.3	195.0	135.0

*Prop at Right Wing Tip
**2-Pusher Props
***Intermeshing with Antitorque Prop

CONVERSION: Kg X 2.205 = LB
m X 3.281 = FT
m^2 X 10.76 = FT^2
m/h X 0.8684 = KN
Km/h X 0.5396 = KN

LIST OF SYMBOLS: SR, Single Rotor; SBS, Side-by-Side; LW, Low Wing; MW, Mid Wing; HW, High Wing; SD Shaft Driven; TD, Tip Driven

TABLE 3-1B

COMPOUND HELICOPTERS OVER 30,000-LB GROSS WEIGHT CLASS

	MODEL & YEAR	FAIREY ROTODYNE 1957	KAMOV VINTOKRYL 1961	WESTLAND ROTODYNE [1962]	TISHCHENKO HYPOTHETICAL					
					SINGLE ROTOR; V_{cruise}, KN			SIDE–BY–SIDE, V_{cruise}, KN		
					189	216	243	189	216	243
	CONFIGURATION	SR, HW, TD	SBS, HW, SD	SR, HW, TD	SR, HW, SD	SR, HW, SD	SR, HW, SD	SBS, HW, SD	SBS, HW, SD	SBS, HW, SD
PRIMARY CHARACTERISTICS	ROTOR RADIUS, Ft	45.0	34.4	54.5	51.2	52.3	55.6	37.9	38.7	41.2
	ROTOR(S) DISC AREA, Ft	6,350	7,431.5	9,326.6	8,231.3	8,588.8	9,706.9	9,020.6	9,405.5	10,659.9
	TOTAL WING AREA, Ft^2	475	1,576.6	580.0	361.5	484.2	574.6	1,063.7	1,084.7	1,160.4
	EXPOSED WING AREA, Ft^2	385.9	1,309.0	471.2	[289.2]	386.5	[459.7]	901.3	922.3	998
	WING SPAN, Ft	46.5	89.3	51.4	[32.5]	54.3	55.8	81.2	82.8	87.8
	$\frac{\text{TOTAL WING AREA}}{\text{ROTOR DISC AREA}}$	0.075	0.21	0.062	0.044	0.056	0.059	0.118	0.115	0.109
	$\frac{\text{EXPOSED WING AREA}}{\text{ROTOR DISC AREA}}$	0.061	0.176	0.0506	[0.035]	0.045	[0.047]	0.10	0.98	0.094
	$\frac{\text{WING SPAN}}{\text{ROTOR RADIUS}}$	1.03	2.59	0.93		1.04	[1.0]	2.14	2.14	2.15
	POWERPLANT, HP	2 X 3000	2 X 5622	2 X 5250	16,350	27,360	33,920	25,120	31,820	43,750
	PROPULSOR(S) and DIAMETER, Ft	2 PROPS 13	2 PROPS 16.8	2 PROPS 14.5	2 PROPS 9.84	2 PROPS 16.4	2 PROPS 16.9	10.0	13.8	13.8
	GROSS WT, LB	39,000		58,500	114,700	114,700	114,700	114,700	114,700	114,700
	WEIGHT EMPTY, LB	23,000		40,150	68,090	72,555	82,092	72,368	79,903	88,795
	RELATIVE WE	0.59		0.69	0.59	0.63	0.71	0.63	0.68	0.77
	DISC LOADING, PSF	6.14		6.27	13.9	13.3	11.8	12.7	12.2	10.76
	INSTALLED POWER LOADING, LB/HP	6.5		5.6	7.0	4.2	3.4	4.6	3.6	2.6
	V_{max}, KN	165.8	190							
	V_{cruise}, KN	147.6		199.0	189.0	216.0	243.0	189.0	216.0	243.0

[ ] Approximate Value

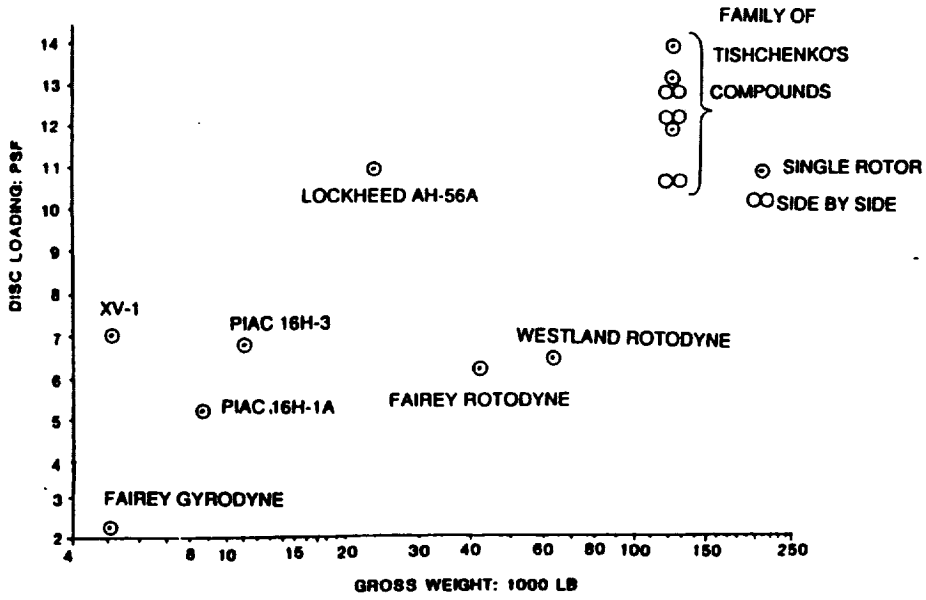

Figure 3.29 Disc loading vs. maximum flying gross weights of compounds

Power Loading & Specific Power. Trends in the installed power loading presented in Fig. 3.30 are based on the shaft power of the powerplants, and do not include power generated by the tip-burning of fuel in cases of jet-driven rotors. This approach is justified by the fact that rotor jet propulsion (when present) was used exclusively for takeoff, landing, and low-speed maneuvers. During high-speed flights, shaft power was the only source of propulsion. Consequently, the trend represented by Fig. 3.30 should basically reflect power needs resulting from high-speed requirements.

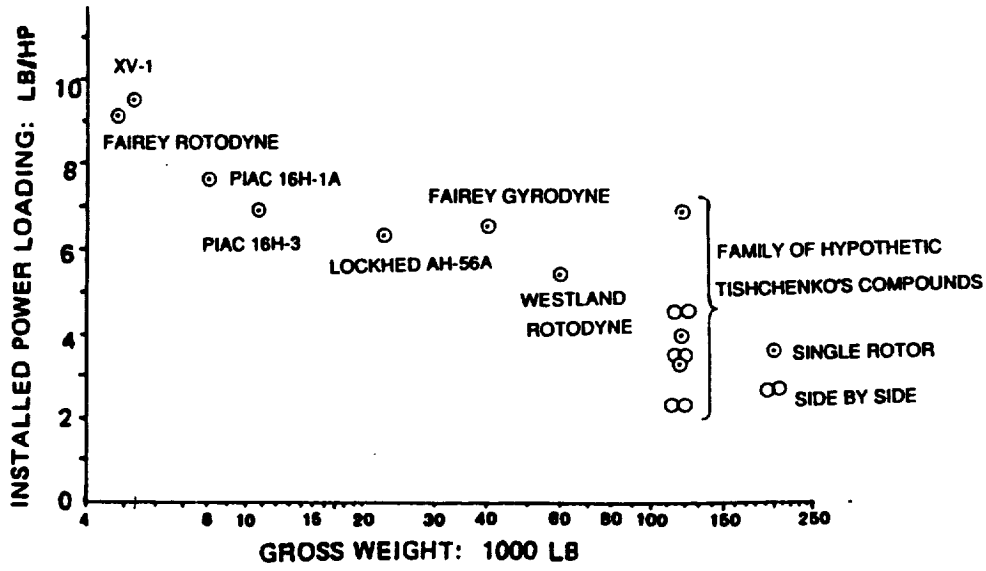

Figure 3.30 Trends in installed power loadings

Figure 3.31 was prepared in order to still better illustrate this relationship. Here, the installed specific power; i.e., installed power per pound of maximum flying gross weight, is plotted vs. cruise speed.

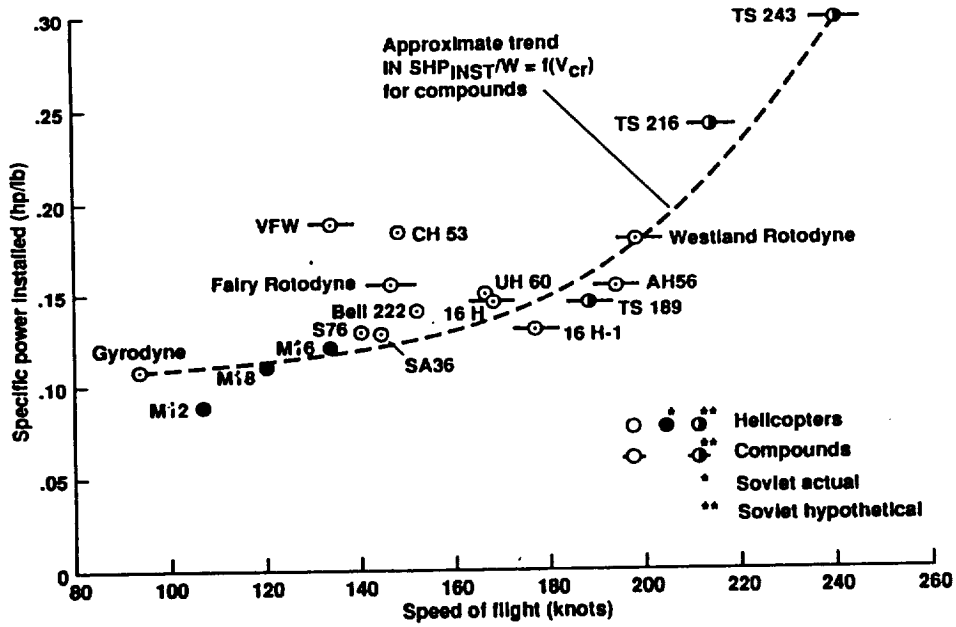

Figure 3.31 Installed shaft horsepower loading vs. cruise speed

Approximate relationships between installed specific power and cruise speed are depicted in this figure. A number of points showing $(SHP_{ins}/W) = f(V_{cr})$ were added for contemporary single-rotor pure helicopters to show how they compare with the compounds. Examining the location of the helicopter points with respect to the compound trend curve, one would note that the installed power loadings of helicopters are, in general, close to those of compounds designed for the same cruise speed.

Wing Area & Span vs. Rotor Disc Area and Diameter. With respect to the configuration geometry of the compound, it may be of interest to examine whether any definite trends exist regarding the ratio of wing to disc areas as well as wing-span to rotor-diameter. Furthermore, both ratios will appear in the simplified expression for estimating relative download in hover. These latter aspects will be discussed later in this report.

Ratios of the wing areas (both total and exposed) to those of rotor disc(s) are shown in Fig. 3.32, which indicates that for single-rotor compounds, the total wing area usually amounts to about 5.5%, and the exposed portion to about 4.5% of the rotor disc area.

The Fairey Gyrodyne with its total wing area to disc area ratio of 3% (exposed area to rotor disc area of 1.8%), obviously represents an exception to the norm with its lower levels of these ratios, while the McDonnell XV-1 having the same ratios equal to 13% and 9.7%, respectively, represents another exception—this time, to the higher levels of the area ratios. For side-by-side compounds, one may expect that because of the basic geometry of the configuration, the designer would have less freedom in optimizing the wing geometry, with

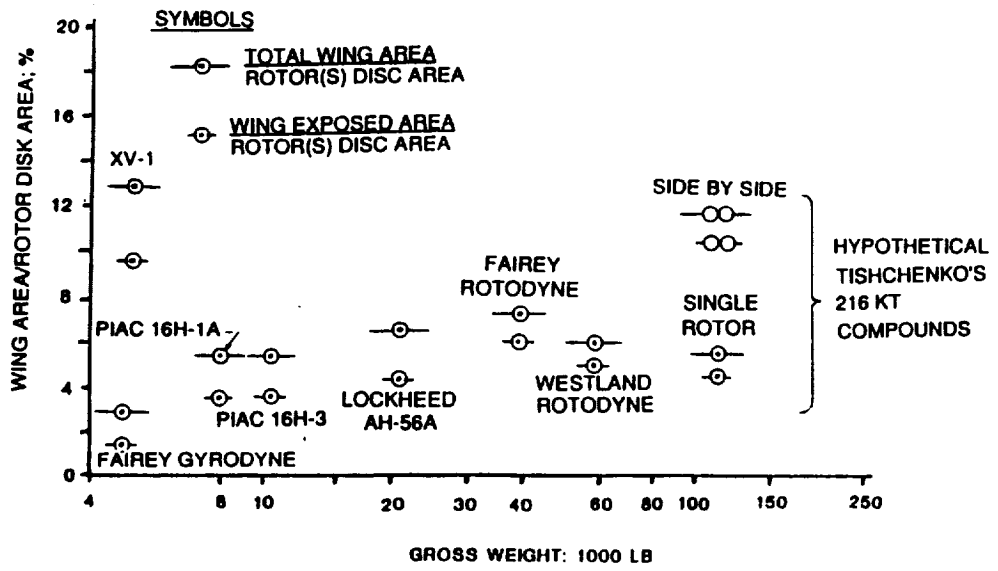

Figure 3.32 Ratios of wing areas (total and exposed) to rotor-disc area(s)

the result that the wing area would probably be larger than its optimal value. While not shown on the graph, this reasoning seems to be confirmed by the wing to the rotor disc area values for the Kamov Ka-22, where this area is equal to 21%, and approximately equal to 11.5% for the hypothetical side-by-side compounds.

Ratios of the wing span to rotor diameters are shown in Figure 3.33.

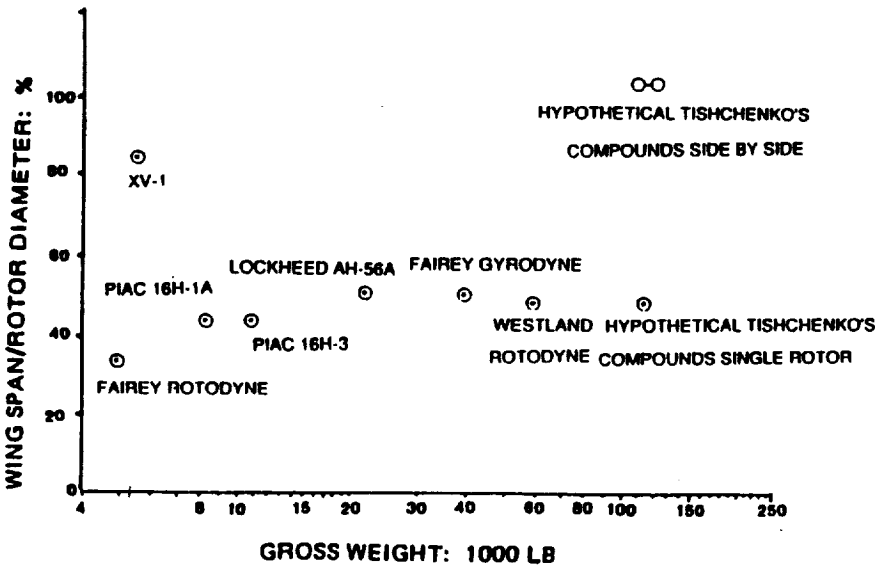

Figure 3.33 Wing span to rotor diameter ratios of compounds

As in the preceding case, one can see from this figure that there is no appreciable scatter of points for single-rotor configurations from the average value of the wing span/ diameter of approximately 45%. Again, the Fairey Gyrodyne represents an exception of the lower value level of 34%, and the XV-1 is well above other configurations at the higher value level of 84%. It is obvious that the ratio for side-by-side configurations is about 100%.

High-Speed Capabilities of Past and Hypothetical Compounds vs. Helicopters. Fig. 3.34 was drawn in order to give the reader some idea regarding a comparison of the high-speed capabilities of compounds vs. those of helicopters.

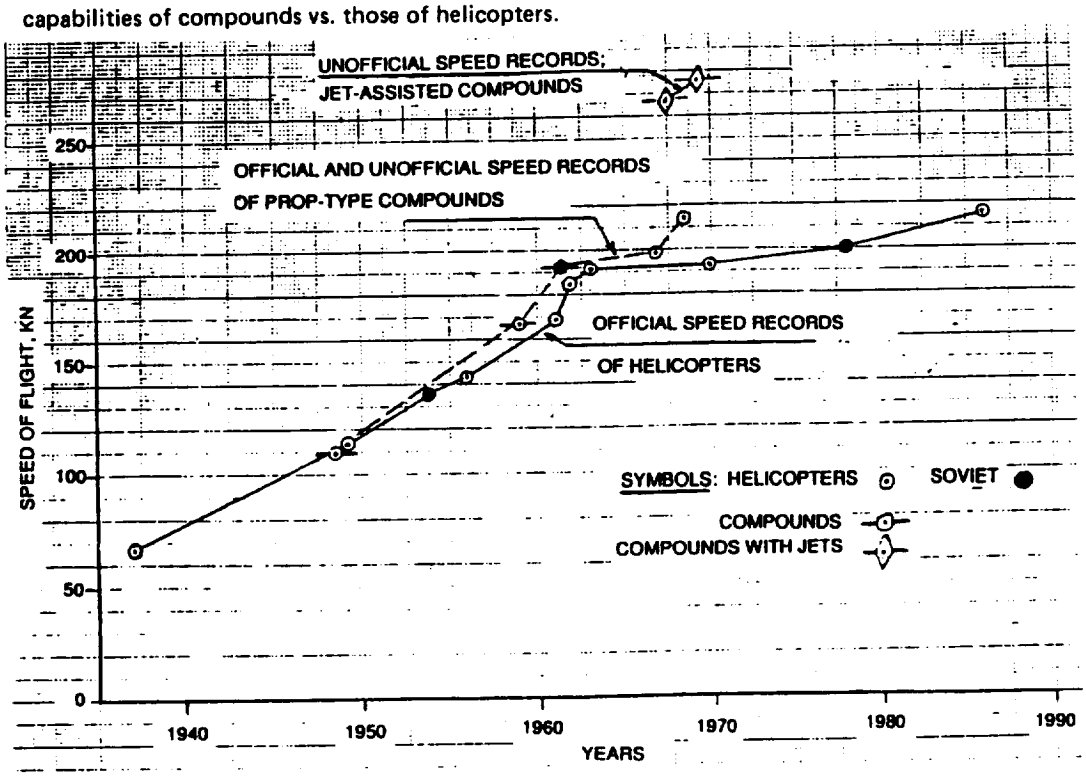

figure 3.34 Speed of flight records for helicopters and compounds

In this figure, official high-speed records and years of their establishment are shown for helicopters, while for compounds, both official and unofficial speed record points are marked. It can be seen from this figure that up to the late sixties, not much difference can be detected as far as the high-speed capabilities of both configurations are concerned. However, jet-assisted compounds seem to indicate that the compounds could, in principle, but not necessarily in operational aircraft, have an advantage of about 70 knots with respect to the high-speed capabilities of pure helicopters.

From a practical operational point of view, it may be interesting to see what advantage the compound may have as far as cruise-speed capability is concerned. The graph presented in Figure 3.35 was prepared to answer this question.

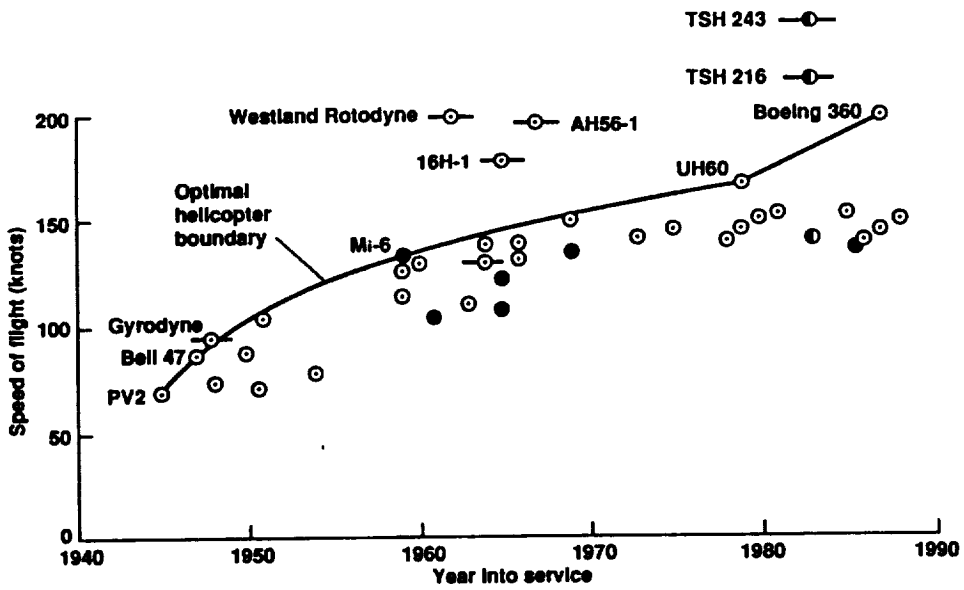

Figure 3.35 Temporal trend in fast cruise speed for helicopters and compounds

A glance at this figure would indicate that judging from the optimal boundary of helicopters extending up to 1980, the compounds may have an advantage up to about 50 knots as far as cruise speed is concerned. However, should helicopter cruise speeds be close to 200 knots as predicted for the Boeing helicopter Model 360, then the potential cruise speed advantage would decrease to some 20 to 30 knots.

Temporal Trends in Relative Weights Empty. To complete this review of actual past, as well as hypothetical, compounds of the Soviet Union, a temporal trend in relative weight empty values in comparison to those of helicopters is presented in Figure 3.36.

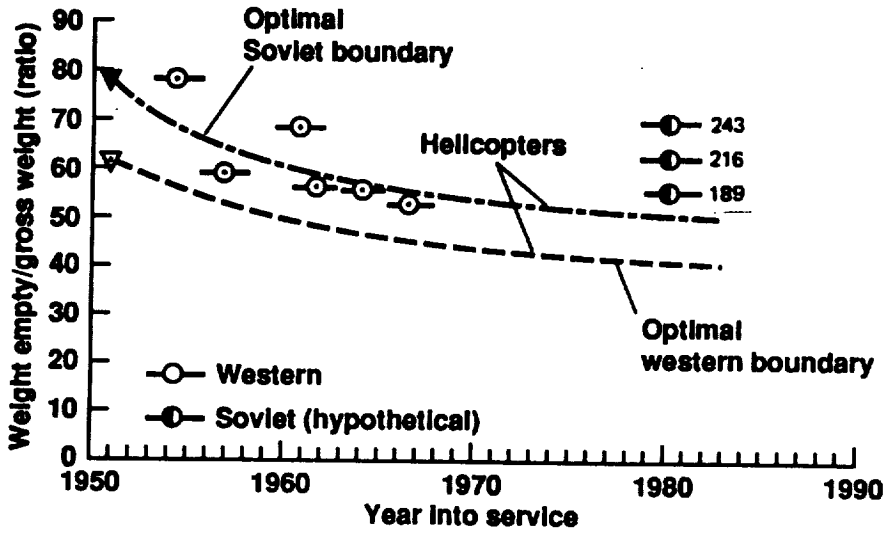

Figure 3.36 Temporal trend in relative empty weights of compounds in comparison with those of helicopters

This figure shows that, as might be expected, relative empty weights of compounds appear, in general, to be higher than empty weights of helicopters of the same time frame. The reader's attention should be called to the trend exhibited by the Soviet hypothetical single-rotor compounds. Here, one can see how the relative weight-empty values increase with the increasing design cruise speed requirements from 189 to 243 knots.

3.3 Advantages and Penalties of Compounding

3.3.1 Hover

General. With respect to hover, there are probably no advantages when one compares compounds with pure helicopters. As far as penalties resulting from compounding are concerned, the most significant will probably be as follows: (a) increase in download due to the wing and, possibly, larger horizontal control surfaces than those for helicopters, (b) greater loss of power required for main-rotor torque compensation for single-rotor configurations should the torque compensating devices be less efficient than the classic tail rotor, and (c) increase in relative weight empty of the compound because of the presence of a wing and the forward propulsion system.

Problems expressed by items (a) and (b) will be discussed in this section, while those related to weight-empty aspects (item (c)) will be discussed in the Concluding Remarks.

Increase in Download Due to Wing. In order to estimate the penalty resulting from the dowload OGE associated with the presence of the wing, the following approximate formula of Vil'dgrube (Ref. 29) will be used:

$$\Delta\overline{T}_w \equiv D_{v_w}/W = 0.375\overline{S}_w\bar{b}_w. \tag{3.1}$$

Where the relative rotor thrust increase ($\Delta\overline{T}_w$) required to overcome the wing download (D_{v_w}) represents the ratio of this download to the gross weight of the rotorcraft, $\overline{S}_w \equiv S_w/\pi R^2$ is the ratio of the total wing area to the lifting rotor disc area, and $\bar{b}_w \equiv b/R$ is the relative wing span.

The relationship given in Eq. (3.1) is graphically presented in Fig. 3.37. In addition, the estimated $\Delta\overline{T}_w$ values for various past Western and Tishchenko's hypothetical single-rotor are also marked. Again looking at this figure, one could come to the conclusion that on the average, the thrust of the lifting rotor in hover OGE would increase by about 2.5% of the gross weight, unless special devices such as highly deflected flaps and drooped leading edges are used.

Specific Power Required in Hover OGE. Specific shaft power (in ft.lb/sec) required per pound of gross weight in hover OGE at air density ρ for helicopters can be simply expressed as

$$\widetilde{SP}_{he} = \sqrt{w_{he}/2\rho}/FM_{ov_{he}} \tag{3.2}$$

and for compounds,

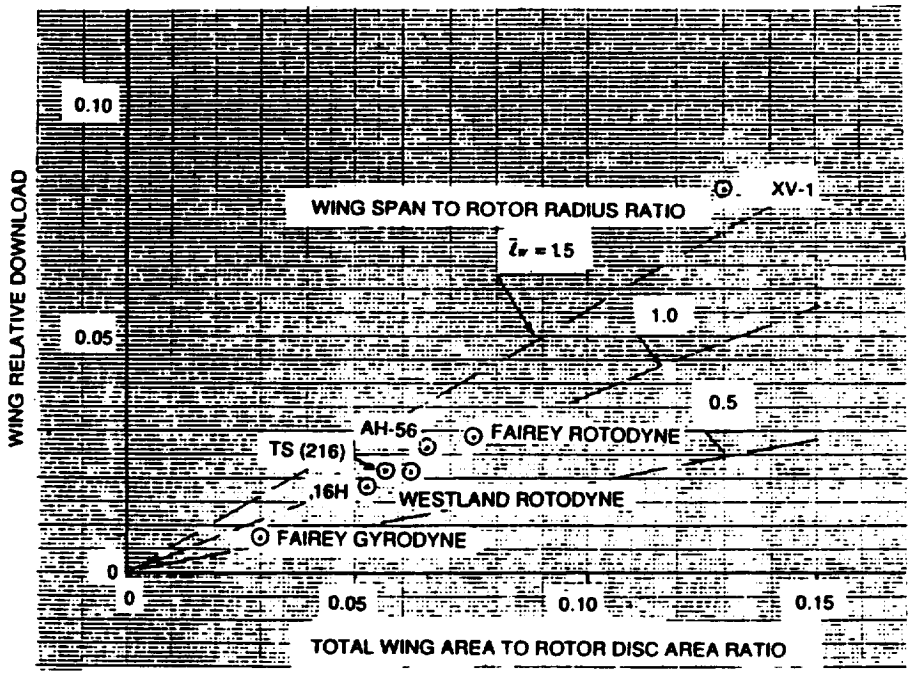

Figure 3.37 Relative wing download shown as a function of the relative wing area and span

$$\widetilde{SP}_{co} = \sqrt{w_{co}/2\rho}/FM_{ov_{co}}. \tag{3.3}$$

It can be seen that Eqs. (3.2) and (3.3) differ only in the subscripts identifying the type of aircraft; otherwise, the symbols have the same meaning: w is the disc loading, and FM_{ov} is the overall figure of merit—expressing the ratio of the ideal power to the shaft power required in hover OGE. The so-defined ratio can be written as follows:

$$FM_{ov} = \sqrt{w/2\rho}/(\bar{T}\sqrt{\bar{T}_0 w/2\rho}/FM\eta_{ov}) \tag{3.4}$$

which leads to

$$FM_{ov} = FM\eta_{ov}/(\bar{T}_0)^{3/2} \tag{3.5}$$

where $\bar{T}_0$ is the ratio of total thrust required to hover OGE to the gross weight ($\bar{T}_0 \equiv T_{req}/W$), FM is the figure of merit of the rotor, and η_{ov} is the power utilization coefficient, which also can be called the overall transmission efficiency, expressing the ratio of the rotor power to the shaft power.

Now, assuming that both conventional helicopters and compounds have the same disc loading and the figures of merit of their lifting rotors are identical and that the air density is identical, the ratio of $\overline{SP}_{co}/\overline{SP}_{he}$* can be expressed as follows:

---

*Because of forward-flight considerations, the assumption that $FM_{co} = FM_{he}$ may be unconservative since, in compounds, a smaller built-in blade twist may be favored; thus leading to less favorable figure-of-merit values in hover. However, the influence of FM values on the $\overline{SP}_{co}/\overline{SP}_{he}$ ratio would probably be less significant that those of $\bar{T}_0$ and η_{ov}.

$$\overline{SP}_{co}/\overline{SP}_{he} = (\overline{T}_{0co}/\overline{T}_{0he})^{3/2}(\eta_{ov_{he}}/\eta_{ov_{co}}). \tag{3.6}$$

$\overline{T}_0$ can, in turn, be written as

$$\overline{T}_0 = 1 + (\Delta\overline{T}_{fus} + \Delta\overline{T}_{h_{em}}) + \Delta\overline{T}_w \tag{3.7}$$

where $\Delta\overline{T}_{fus}$ is the relative download on the fuselage, $\Delta\overline{T}_{h_{em}}$ is the relative download on the horizontal empennage, and $\Delta\overline{T}_w$ is the relative download on the wing.

The two terms shown in parentheses in Eq. (3.7) are common to both compounds and helicopters. Again, making a somewhat nonconservative assumption that $\Delta\overline{T}_{h_{em_{co}}} = \Delta\overline{T}_{h_{em_{he}}}$ (download due to the horizontal control surfaces of the compound would probably be higher than for helicopters) and further assuming that $(\Delta\overline{T}_{fus} + \Delta\overline{T}_{h_{em}}) \approx 0.025$ (see Ch. 2, Part II of Ref. 30), and $\Delta\overline{T}_w \approx 0.025$, the ratio of the total download factor of compounds to those of helicopters would be

$$\overline{T}_{0co}/\overline{T}_{0he} \approx (1.05/1.025) = 1.024.$$

For a wing with a large flap (44% chord) deflected 80 degrees, the relative download could be reduced to about $\Delta\overline{T}_w \approx 0.016$ (Ch. 4, Part II of Ref. 30), thus decreasing the total download coefficient ratio from 1.024 to $\overline{T}_{0co}/\overline{T}_{0he} \approx 1.015$.

With respect to the overall power utilization coefficient (η_{ov}), it can be expressed as

$$\eta_{ov} = 1 - \Delta\overline{P}_{tx} - \Delta\overline{P}_{cool} - \Delta\overline{P}_{tr} \tag{3.8}$$

for both single-rotor mechanically-driven conventional helicopters and compounds, where $\Delta\overline{P}_{tx}$ is the relative power lost in the transmission(s) ($\Delta\overline{P}_{tx} = \Delta P_{tx}/SHP$); $\Delta\overline{P}_{cool}$ is the relative power expended in cooling ($\Delta\overline{P}_{cool} = \Delta P_{cool}/SHP$) and $\Delta\overline{P}_{tr}$ is the relative power required to balance the main rotor torque ($\Delta\overline{P}_{tr} = RHP_{tr}/SHP$) where RHP_{tr} is the tail-rotor horsepower needed for torque compensation.

Relative transmission and cooling losses should not be much different from those for pure helicopters, and will be assumed as follows: $\Delta\overline{P}_{tx_{co}} \approx \Delta\overline{P}_{tx_{he}} \approx 0.045$; $\Delta\overline{P}_{cool_{co}} \approx \Delta\overline{P}_{cool_{he}} = 0.015$. However, the $\Delta\overline{P}_{tr}$ values may be higher for compounds than for helicopters using the open-airscrew type tail rotors.

For the single-rotor helicopters examined in Ref. 5, the average ratio of tail-rotor to main-rotor power amounts to $RP_{tr}/RP_{mr} = 0.108$ or, assuming $\eta_{ov} \approx 0.85$, the relative shaft-power based tail-rotor losses become $\Delta\overline{P}_{tr} = \eta_{ov}(RP_{tr}/RP_{mr}) = 0.092$, and the second approximation of overall efficiency would amount to $\eta_{ov_{he}} = 0.85$.

Now, the $\eta_{ov_{co}}/\eta_{ov_{he}}$ can be expressed as

$$\eta_{ov_{co}}/\eta_{ov_{he}} = (0.94 - \Delta\overline{P}_{tr_{co}})/0.85. \tag{3.9}$$

Figure 3.38 will give the reader some idea regarding the influence of $\Delta\overline{P}_{tr_{co}}$ values on the $\eta_{ov_{co}}/\eta_{ov_{he}}$ ratio.

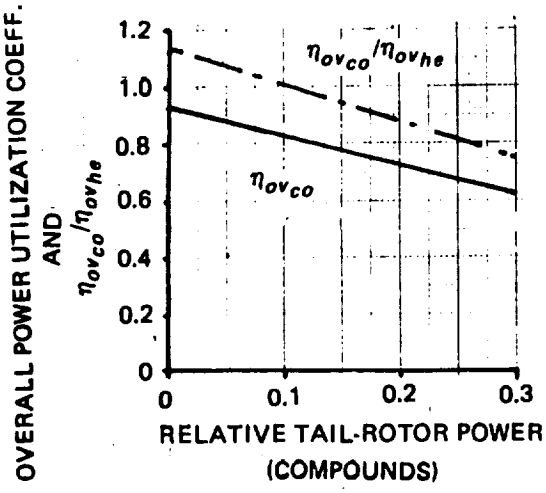

Figure 3.38 Influence of the relative tail-rotor power of compounds on the overall power utilization coefficient and $\eta_{ov_{co}}/\eta_{ov_{he}}$ ratio

Assuming that $\overline{T}_{0_{co}}/\overline{T}_{0_{he}}$ = 1.024 for wings without deflecting flaps, and that $\overline{T}_{0_{co}}/\overline{T}_{0_{he}}$ = 1.015 for those with large flaps, the ratio of the specific shaft-power in hover OGE of compounds to those of helicopters of the same disc loading was computed from Eq. (3.36) and graphically presented vs. the relative tail-rotor power of compounds in Figure 3.39.

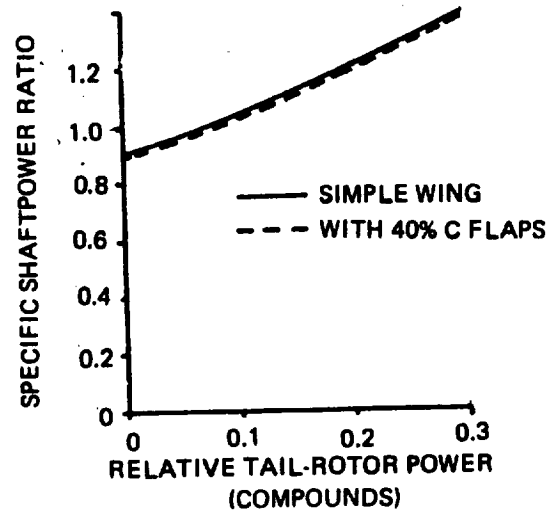

Figure 3.39 Ratio of specific power required of compounds to that of helicopters in hover OGE

A glance at this figure will indicate that the dominant factor in achieving specific shaft powers in hover for compounds comparable to those of single-rotor helicopters of the same disc loading would be to have the main-rotor torque compensating devices using fractions of the shaft power required similar to those of helicopters. However, obtaining this equality of $\Delta\overline{P}_{tr}$ values with respect to classic helicopters (with open tail rotors) is not very probable, since an open tail rotor (still widely used in conventional single-rotor helicopters) would probably be unacceptable because of the operational requirements. It appears, hence, that designers of compound configurations must accept the fact that specific shaft power required in hover OGE of their rotorcraft will be higher than that of conventional helicopters having the same disc loading.

In hover, the penalty in $\overline{SP}$ values may not prove to be too important for pure helicopter operations, as hover and near-hover flight modes would represent only a small fraction of the whole operation. But, for military applications where 'hiding' in hover may be a tactical necessity, reducing a gap in the $\overline{SP}$ values in hover between compounds and helicopters may become quite important.

Figure 3.39 clearly illustrates the significance of the $\Delta\overline{P}_{tr}$ levels in comparison to those of the reduction of the wing download. It appears, hence, that if one wants to contribute to the survival of the compound configuration, one should direct a considerable fraction of the total research effort devoted to compounds to the development of rotor power torque-compensating devices requiring main-rotor power fractions not excessively higher than those for contemporary helicopters, including the Fenestrone and NOTAR.

3.3.2 Horizontal Flight

Power Required. The following considerations are chiefly aimed at an understanding of the importance of the various components comprising the total power required by the compound in horizontal flight, and possible methods of reducing these components.

It should be assumed for simplicity that in high-speed horizontal flight all forward thrust needed to overcome aerodynamic drag is exclusively generated by the propulsor and also that the weight (W) of the aircraft is jointly supported by the rotor thrust (T_R) and wing lift (L_w). Consequently, along the vertical axis, the following force equations become valid:

$$T_R + L_w = W \tag{3.10}$$

which can be rewritten as

$$\overline{T}_R + \overline{L}_w = 1, \tag{3.11}$$

where $\overline{T}_R = T_R/W$ and $\overline{L}_w = L_w/W$.

Along the horizontal axis, the force balance equation is as follows:

$$T_h = D_{par} + D_{ind_R} + D_{ind_w} + D_{pr_R} + D_{pr_w}. \tag{3.12}$$

where D_{par} is the parasite drag of the whole airframe, excluding the blades and the wing, D_{ind_R} is the induced drag of the rotor resulting from developing thrust $T_R = W\overline{T}_R$ while the influence of the wing is neglected. D_{ind_w} is the induced drag resulting from developing a lift $L_w = W(1 - \overline{T}_R)$ and experiencing an additional drag ΔD_{ind_w} due to the influence of the rotor. D_{pr_R} is the drag resulting from the profile drag of the rotor blades, and D_{pr_w} is the profile drag of the wing.

The specific shaft horsepower required by a compound in horizontal flight can be written as follows:

$$\overline{SHP_f} = [(D_{par} + D_{ind_R} + D_{ind_w} + D_{pr_R} + D_{pr_w})V/325W\eta_{tr}\eta_{pr}] + \Delta\overline{SHP}_R \qquad (3.13)$$

where the speed of flight V is in knots, η_{tr} is the transmission efficiency (including cooling and accessory-drive losses), η_{pr} is the propulsive efficiency of the forward thruster, and $\Delta\overline{SHP}$ is specific shaftpower going directly to the rotor.

In order to show a practical way toward optimization of Eq. (3.13) all terms appearing on the right side will be discussed separately. Furthermore, since the importance of the propulsive and transmission efficiencies will be considered separately, all contributions enclosed in the parentheses in Eq. (3.13) will be examined, disregarding the influence of the η_{tr} and η_{pr} coefficients, and represented by the symbols $\overline{AHP}$ with suitable subscripts; thus symbolizing various components of the airframe specific horsepower.

Parasite Power. The specific airframe parasite horsepower can be written as follows:

$$\overline{AHP_{par}} = (1.69^3/1100)f\rho_0(\rho/\rho_0)V^3/W, \qquad (3.14)$$

which can be rewritten as

$$\overline{AHP_{par}} = 1.04 \times 10^{-5}(\rho/\rho_0)V^3/w_f, \qquad (3.15)$$

where the speed of flight V is in knots, the equivalent flat-plate area (f) loading $w_f = W/f$ in psf, and ρ/ρ_0 is the ambient air density ratio.

Assuming various values of the equivalent flat-plate area loading, Eq. (3.15) is plotted in Fig. 3.40. This figure clearly illustrates the importance of aerodynamic cleanness as expressed through high w_f values, especially at $V > 200$ knots. Consequently, in order to retain their competitive position with respect to modern high-speed helicopters where projections are made for $w_f \geq 1000$ psf (Refs. 5 and 31), designers of compounds should strive for 1500 psf. Practical possibilities of achieving that level of aerodynamic cleanness represent some of the most important challenges of the compound design.

Induced Power. Expressions for the specific airframe induced power of the compound as a whole was developed under the following assumptions: (1) thrust carried by the rotor ($T_R = W\overline{T}_R$) leads to generation of induced power ($\overline{AHP}_{ind_R}$), which can be computed in much the same way as for an isolated helicopter rotor; ie, neglecting the influence of the wing, (2) induced power associated with lift carried by the wing ($L_w = W(1 - \overline{T}_R)$) is computed as the

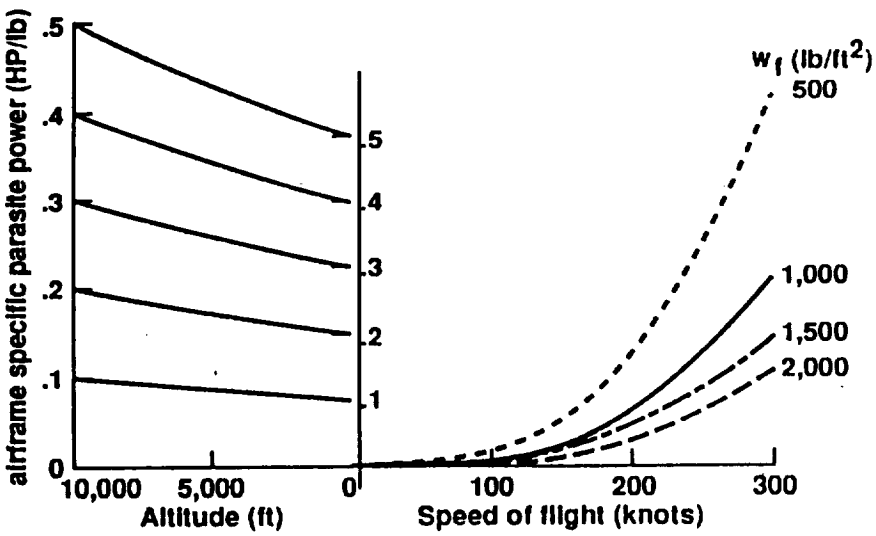

Figure 3.40 Specified airframe parasite power vs. speed of flight

sum of the induced power corresponding to the isolated wing, and power resulting from the presence of the rotor induced velocity—assumed to be equal to the ideal induced velocity of the rotor times the factor k_f.

Using common expressions for rotor induced power in forward flight (Ref. 30, Ch. 2), the specific airframe induced power due to rotor becomes

$$\overline{AHP}_{ind_R} = k_f(\bar{T}_R W)^2/1100\rho 1.69VW\pi R^2 \tag{3.16}$$

which, assuming $k_f = 1.1$, can be rewritten as follows:

$$\overline{AHP}_{ind_R} = 0.249\bar{T}_R{}^2 w/\bar{\rho}V \tag{3.17}$$

where w is the nominal disc loading ($W/\pi R^2$), $\bar{\rho}$ is the air density ratio ($\bar{\rho} = \rho/\rho_0$) and speed of flight V is in knots.

The average induced velocity (equal to ideal induced velocity times the k_{f_w} factor for the wing) for an isolated wing having span b_w can be expressed as

$$v_{ind_w} = 2k_{f_w}W(1 - \bar{T}_R)/\pi b^2 w\rho 1.69V \tag{3.18}$$

or, expressing wing span in terms of the rotor radius $b_w = \bar{b}_w R$, and assuming $k_{f_w} = 1.1$, Eq. (3.18) can be rewritten as follows:

$$v_{ind_w} = 547.0(1 - \bar{T}_R)w/\bar{\rho}V\bar{b}^2{}_w. \tag{3.19}$$

C-2

The induced velocity of the rotor will be

$$v_{ind_R} = k_f \bar{T}_R W/2\pi R^2 \rho 1.69V \tag{3.20}$$

or, assuming $k_f = 1.1$,

$$v_{ind_R} = 136.7\bar{T}_R w/\bar{\rho} V \tag{3.21}$$

and specific induced airframe power of the wing becomes

$$\overline{AHP}_{ind_w} = (1 - \bar{T}_R)(v_{ind_w} + v_{ind_R})/550. \tag{3.22}$$

The total specific induced airframe power of the compound will be obtained by substituting the right-hand sides of Eq. (3.19) and (3.21) for v_{ind_w} and v_{ind_R} into Eq. (3.22) and adding the so-modified Eq. (3.22) to Eq. (3.17) Thus, an expression for the total specific induced airframe power for the compound is obtained:

$$\overline{AHP}_{ind_{co}} = \{0.249\bar{T}_R^2 + (1 - \bar{T}_R)[(0.994(1 - \bar{T}_R)/\bar{b}_w^2) + 0.249\bar{T}_R]\} w/\bar{\rho} V. \tag{3.23}$$

Assuming $w = 7$ psf and $\bar{b}_w = 1$ as typical values for the compound (see Tables 3.1A and 3.1B), the $\overline{AHP}_{ind_{co}}$ values as given by Eq. (3.23) were plotted vs. speed of flight at SL STD for three $\bar{T}_R$ levels (Figure 3.41).

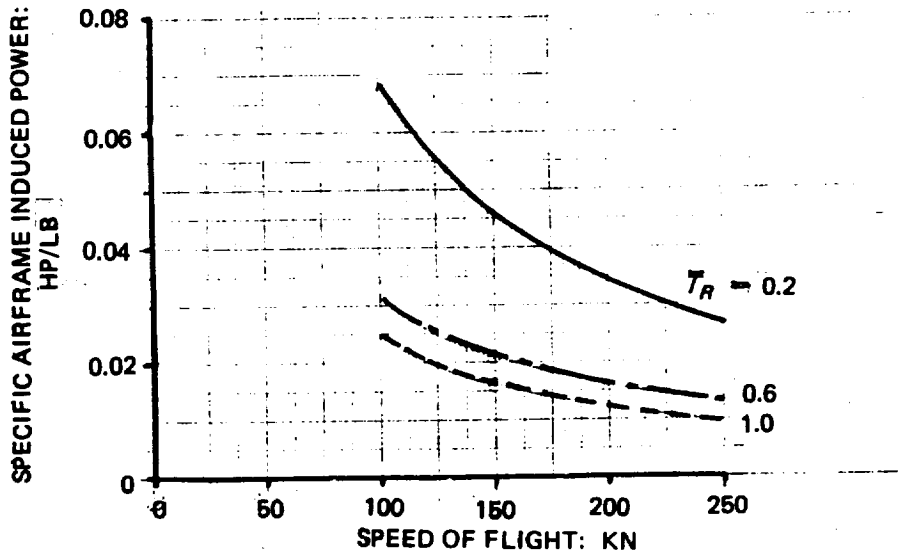

Figure 3.41 Specific airframe induced power for the compound as a whole, shown vs. speed of flight and various levels of the relative rotor loading

Fig. 3.41 and Eq. (3.23) clearly illustrate that for the practical relative wing span $\bar{b}_w < 2.0$, the transfer of lift from the rotor to the wing leads to an increase in the total specific induced power of the compound as a whole. However at say, 250 knots, even at almost complete rotor unloading ($\bar{T}_R = 0.2$) would result in $\overline{AHP}_{ind_{co}} \approx 0.025$ hp/lb, while for a relatively aerodynamically clean rotorcraft having $1000 \leq w_f \leq 1500$ psf, the corresponding specific airframe parasite power would be $0.115 \leq \overline{AHP}_{par} \leq 0.170$ hp/lb. Consequently, paying a penalty in a higher specific induced power resulting from low $\bar{T}_R$ values may be acceptable if this action would permit one to: (1) reduce the aircraft parasite drag, say, through a more favorable airframe attitude with respect to the flight path than for pure helicopters, and (2) decrease the specific profile power considerably below the level characteristic for helicopters.

Profile Power. According to Eq. (3.13), the portion of power resulting from the contribution of the blade profile power drag to the airframe drag (D_{pr_R} term in parentheses) should be considered separately from the portion of the rotor profile power directly affecting the power transmitted through the rotor shaft (the last term in Eq. (3.13)). However, for the sake of simplicity, the specific profile of the whole compound will be treated here as a single unit, as is usually done in the case of pure helicopters[30]. Consequently, it will be called the specific rotor profile horsepower ($\overline{RHP}_{pr}$) and expressed as follows:

$$\overline{RHP}_{pr} = \sigma\pi R^2 \rho_0 \bar{p}\bar{c}_{d_o} V_t^3 (1 + 4.7\mu^2)/4400W \tag{3.24}$$

where σ is the rotor solidity, $\bar{c}_{d_o}$ is the average blade profile drag coefficient, V_t is the tip speed in fps, and μ is the advance ratio.

Remembering that the nominal blade loading is $w_{bl} = W/\sigma\pi R^2$, Eq. (3.24) can be rewritten as follows:

$$\overline{RPH}_{pr} = 5.41 \times 10^{-7} \bar{p}\bar{c}_{d_o} V_t^3 (1 + 4.7\mu^2)/w_{bl}. \tag{3.25}$$

In order to get some idea regarding the importance of the contribution of the profile power to the total specific power required levels of the compound, Eq. (3;25) is plotted in Fig. 3.42 for SL STD, assuming $\bar{c}_{d_o} = 0.01$, and $w_{bl} = 90.0$ psf.

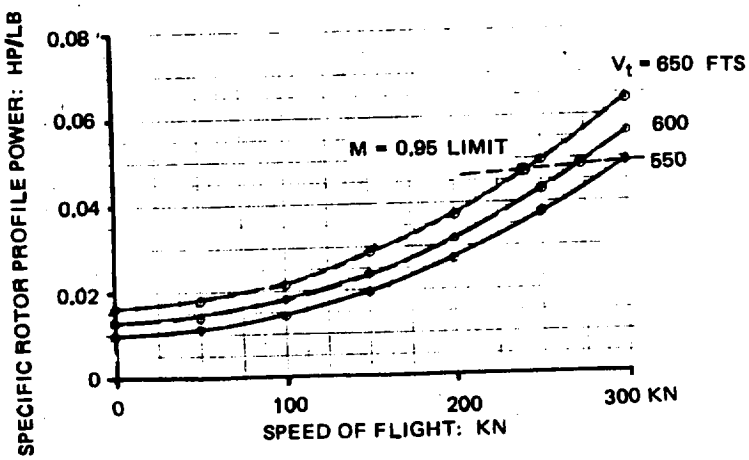

Figure 3.42 Specific rotor profile power vs. speed of flight

A glance at Fig. 3.42 will indicate that in the flight-speed region of about 250 knots, contributions of the profile power to total specific power would be of a similar level as those of the induced power. It can also be seen that a reduction in the tip speed is quite important, both as a means of reducing the specific power required by the compound and as a provision for extending the advancing blade compressibility limits to higher speeds of flight.

As to other possibilities of reducing rotor profile power in general, one should note that reduction of the average blade-lift coefficient (C_T/σ) through rotor unloading, and elimination of the rotor thrust inclination through a separate propulsor should prove beneficial. This point is illustrated in Fig. 3.43 (based on cross-plots from Figs. 4.6 and 4.7 of Ref. 29), where the effects of rotor tilt and average blade-lift coefficient values are quite visible.

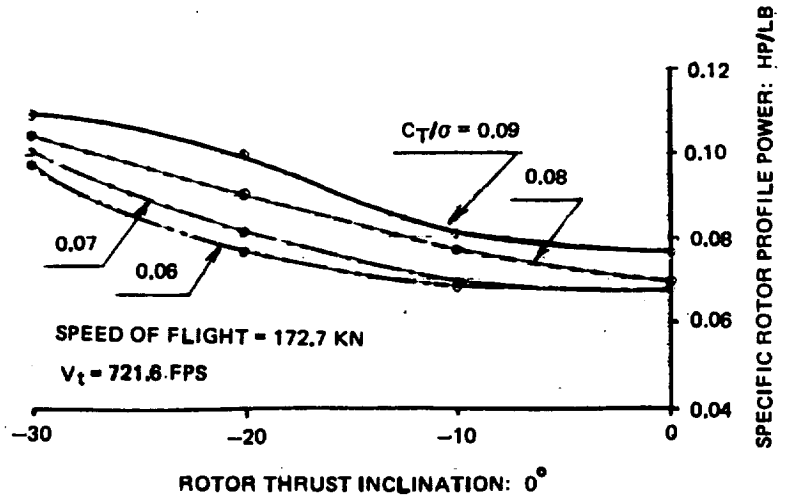

Figure 3.43 Example of the influence of rotor thrust inclination and C_T/σ values on specific rotor profile power at 172.7 knots

However, the most effective means of reducing the rotor profile power would be through the application of the variable diameter rotor concept; for instance, as outlined in Refs. 32 and 33.

Assuming a structurally simpler concept wherein the rotor rpm remains constant as its radius varies, the following expression for the ratio of rotor specific profile power at reduced radius to that of the fully extended position ($R = R_0$) can be developed from Eq. (3.25):

$$\overline{RP}_{pr}/\overline{RP}_{pr_0} = (R/R_0)^4 [1 + 4.7\mu_0^2 (R_0/R)^2]/(1 + 4.7\mu_0^2) \qquad (3.26)$$

where μ_0 symbolizes the advance ratio corresponding to the fully extended rotors.

Figure 3.44 was drawn in order to give the reader some idea as to how rapidly the profile power of the retracting rotor decreases at $\mu_0 = 0$ (at constant rpm) in comparison to that of the fully extended rotor.

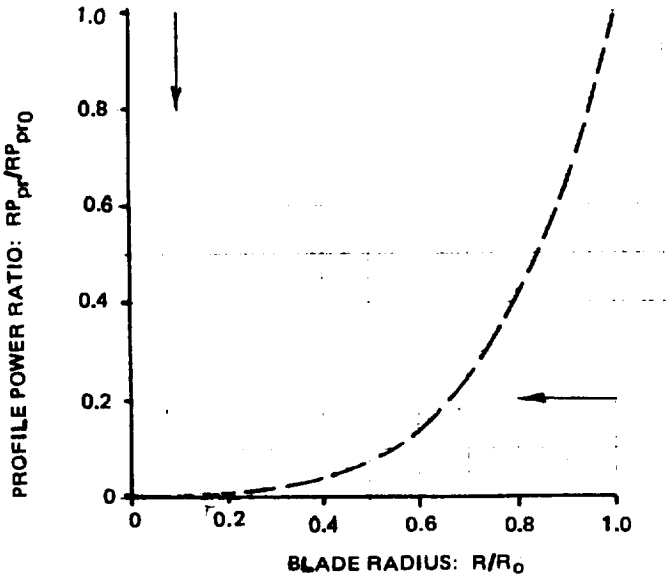

Figure 3.44 Relative reduction of specific rotor profile power due to the effect of telescoping blades at $\mu_0 = 0$ and constant rotor rpm

In spite of some detrimental effect of the $4.7\mu_0^2(R_0/R)$ term in Eq. (3.16), in forward flight the relative reduction in the profile power is quite dramatic, even when the retraction is as small as that corresponding to $R/R_0 = 0.8$ (See Figure 3.45).

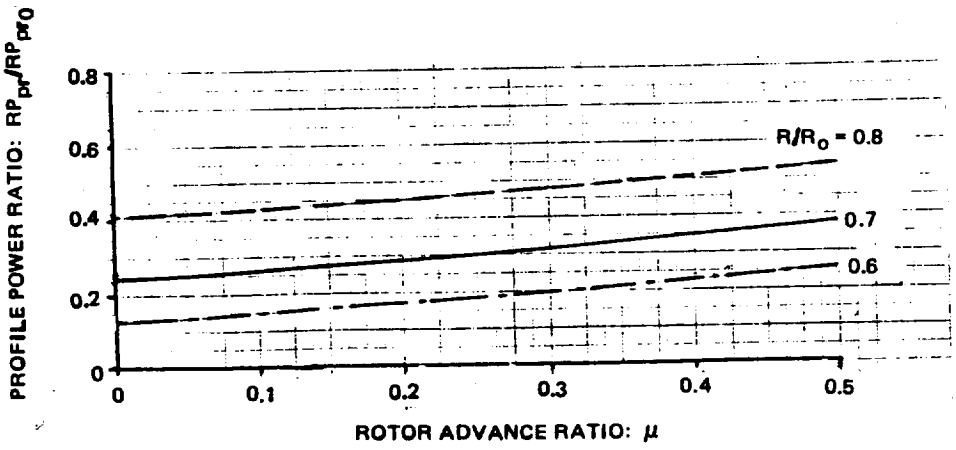

Figure 3.45 Relative reduction in specific rotor profile power in forward flight, caused by the effect of telescoping blades at constant rpm

Looking at this figure, one should conclude that as far as reducing the specific rotor profile power is concerned, it would, in principle, be best to use a variable diameter rotor.

This, of course, should be combined with unloading of the rotor by the wing. When determining the amount of rotor unloading, two aspects should be taken into consideration: (1) gains in the reduced specific profile power vs. losses resulting from higher aircraft induced power, and (2) dynamic consequences of decreased blade loading, leading to reduced damping in flapping (see, for instance, Fig. 1.9, Ref. 30). However, probably the most important aspect regarding possible application of the variable diameter rotors would be weighing potential performance gains vs. additional complexity, airframe weight increase, and cost.

Transmission and Propulsive Efficiencies. Looking at Eq. (3.13), one may note that transmission efficiency would influence the term appearing in the parentheses as well as the ΔSHP term although, in this latter case, η_{tr} does not appear as explicitly as in the other specific shaft horsepower components given in this equation. It is obvious that, similar to the case of pure helicopters, the η_{tr} level of compounds should be as high as possible. The η_{tr} values for the compounds could be expected to be slightly higher than for single-rotor helicopters of the same gross-weight class. This would be due to the fact that in cruise and high-speed regimes of flight, only a small fraction (if any) would be channeled to the main rotor, along the way requiring a considerable reduction in rpm. The main engine power would go to the forward propulsors through the transmission system, requiring much smaller rpm variations.

For the same reason that $\overline{\Delta SHP}_R$ values are much smaller than those appearing in the square brackets in Eq. (3.13), the main-rotor torque compensating losses, which are often 'charged' to transmission efficiency, would also be smaller for a compound than for a helicopter of the same gross-weight class.

Propulsive efficiency (η_{pr}) affects the main portion of the total specific shaft horsepower required in cruise and high-speed flight. Consequently, it is desirable to use propulsive devices capable of high η_{pr} values in the 200-275 knot speed range. In this respect, an open propeller would probably be the most efficient. However, for operational safety and overall design reasons, there may be a tendency to combine foward propulsion functions with torque compensation in hover by creating a single device based on the enclosed airscrew concept.

This approach would probably require some compromise between torque compensation effectiveness in hover and low-speed flight, and high propulsive efficiency in cruise and at high speeds.

In principle, the direction for this compromise would be dictated by the envisioned mission of the compound (time in hover vs. time in cruise). However, in practical applications, cruise and high-speed capabilities of the compound would probably take priority over hover and low-speed requirements. Consequently, designers of these universal units should probably lean toward assuring the highest possible η_{pr} values at high-speed forward flights, even if this would mean some lowering of the main-rotor torque compensating effectiveness in hover and near-hover conditions.

3.4 Concluding Remarks and Recommendations

3.4.1 Concluding Remarks

General. Helicopter compounding consists of providing a source of horizontal propulsion, independent of propulsive forces generated by the lifting rotor(s). This approach brings many operational advantages, which appear especially valuable in military applications (e.g., retention of a basically horizontal position of the fuselage at all flight speeds, as well as during forward accelerations or decelerations).

From a performance point of view, the presence of auxiliary horizontal propulsion also helps to move the rotor high-speed barrier (blade stall and compressibility effects) toward higher levels. Utilization of a wing(s), unloading the rotor in forward flight, further helps to improve high-speed capabilities of the compound, making it, in principle, some 40-50 knots higher than for pure helicopters. In addition, the use of wing ailerons could contribute to an improvement in roll controllability of the aircraft, especially in the case of unloaded articulated rotors with moderate flapping hinge offsets. Movable horizontal surfaces may contribute to a sensitive pitch control.

Unfortunately, compounding can not be achieved without some penalties.

Hover. In hover, the presence of wings and, usually, large horizontal empennages, leads to download factors higher than for conventional helicopters. Furthermore, if rotor geometry favoring high-speed performance is applied, the rotor figure of merit levels for compounds may be lower than for helicopters. Finally, the fraction of rotor power spent on torque compensation in single-rotor configurations may be higher than for conventional helicopters, especially those having open airscrews as tail rotors. This higher power expenditure of compounds would result from the probable use of main-rotor torque compensating devices (for example, Notar, Fenestrone, Piasecki ring-tail) or propellers requiring more power per pound of thrust developed in hover than conventional tail rotors.

Hence, in summary, it may be stated that the power required per pound of gross weight in hover for compounds may be some 10 to 15 percent higher than for conventional helicopters of the same disc loading.

From the structural weight point of view, compounding, in general, leads to higher relative weight-empty ratios (up to 10 percent higher) than those of conventional helicopters. This, obviously, means that the relative zero-time, and hence, zero range payload, of compounds would be some 5 to 10 percent lower than for conventional helicopters.

As a result of the higher fuel consumption per unit of gross weight and unit of time for compounds in hover, accompanied by the lower zero-time relative payload values, a comparative character of the relative payload vs. time relationship in hover would be as shown in Figure 3.46.

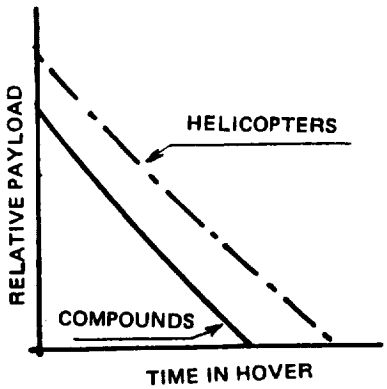

Figure 3.46 Relative payload vs. time relationship in hover for compounds and conventional helicopters.

Horizontal Flight. In forward flight, auxiliary propulsion as well as unloading of the lifting rotors by use of a wing(s) moves the blade tip Mach number/stall barrier of compounds to higher speed levels than for conventional helicopters.

From the performance point of view, the main design task would be to select the principal design parameters of the aircraft, including lift distribution between the lifting rotor(s) and the wing(s) in such a way that the resulting W/D_e vs. speed of flight relationship for compounds would be, in comparison to conventional advanced helicopters of the same gross-weight class, of the character depicted in Fig. 3.47.

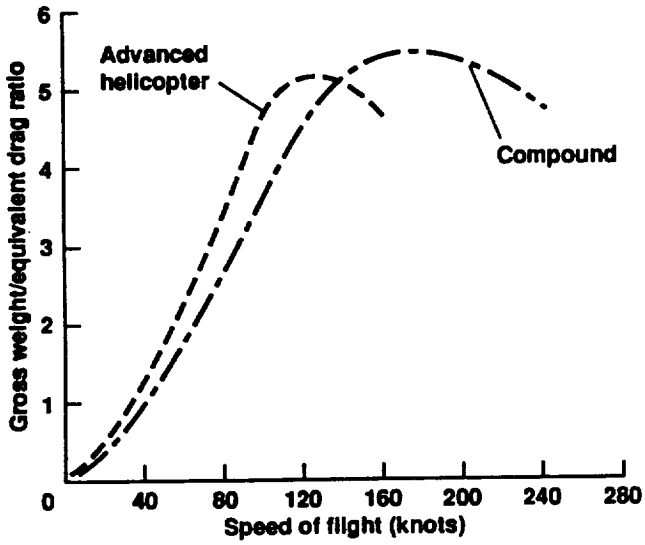

Figure 3.47 (W/D_e) vs. speed of flight relationship for advanced helicopters and compounds

Fig. 3.47 implies that at some high speeds of flight (about 130 kn in the figure), the SHP required per pound of gross weight should become lower for the compound than for helicopters of the same nominal disc loading and gross-weight class. This would not be an easy task for the reasons explained below.

At a given speed of flight, the induced SHP per pound of gross weight for the compound carrying some load on the wing will, in general, be higher than for helicopters of the same nominal disc loading. Fortunately, at high speeds of flight, the induced portion represents only a small fraction of the total power required.

At high speeds of flight, the parasite portion obviously constitutes the largest contribution to the total power required per pound of gross weight. In this respect, the general aerodynamic cleanness of compounds (as expressed by equivalent flat-plate area loading) can not be expected to be much better than for conventional helicopters of the same class. Nevertheless, because of a more favorable attitude of the body of the compound with respect to the airstream, some gains in the parasite drag to gross-weight ratio of compounds over those of helicopters can be expected. However, these gains will not be very significant.

The brightest hope for the designer to reduce the SHP per pound of gross weight values of the compounds during high speeds of flight to levels lower than for corresponding helicopters lies in controlling the profile power. Here, the designers have three factors which could be applied toward that goal: (1) reduction of the rotor tip speed, (2) lowering C_T/σ levels through unloading of the rotor by the wing, and (3) zero, or close to zero angle of attack of the rotor disc with respect to the flight path.

Telescoping blades could, in principle, represent a very powerful tool toward reduction of the profile power, but mechanical complexities and structural weight penalties make the practicality of that approach somewhat doubtful.

Finally, it should be emphasized that during high speeds of flight all, or at least, a large fraction of the SHP of the compound is channeled toward forward propelling devices. Consequently, a high propulsive efficiency of such devices becomes an important factor in reducing the SHP required per pound of gross-weight levels.

In closing, looking at the weight aspects, one should note that the higher the design cruise speed of the compound, the higher its relative weight empty.

This trend is depicted in Fig. 3.48, where $\overline{W_e}$ values for some actual, as well as three hypothetical compounds of Tishchenko (half-black points), are shown vs. high design cruise speeds.

Looking at this figure, it can be seen that increasing the design cruise speed from some 210 knots to 240+ knots would be associated with an increase in $\overline{W_e}$ values from about 0.6 to 0.7. The resulting losses in the zero-range relative payload may not be compensated by the higher cruise speed, with the result that relative ideal productivity of the fastest compounds would be considerably inferior to that of their slower, but structurally relatively lighter, counterparts.

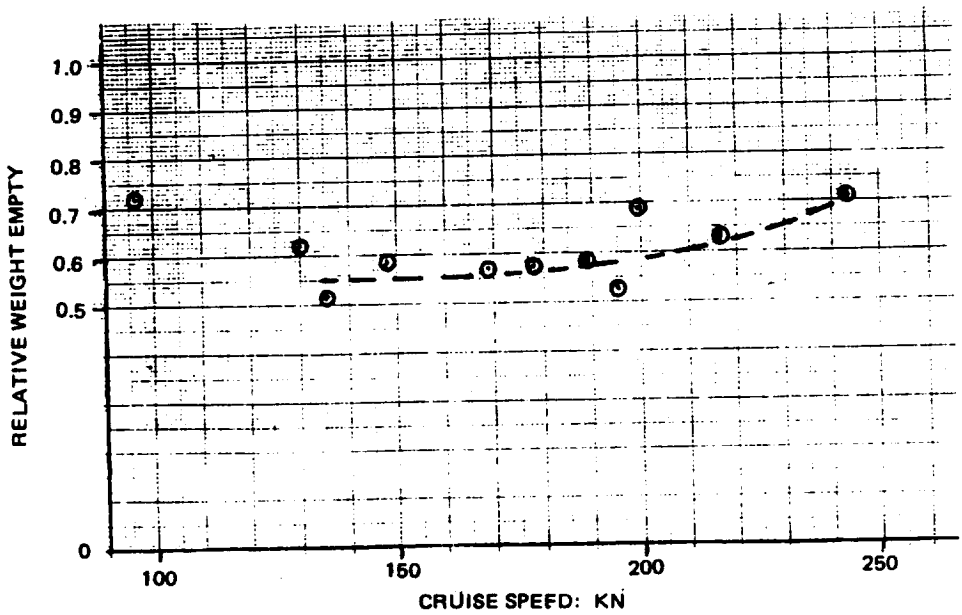

Figure 3.48 Trend in relative weight empty vs. high cruise speed of compounds

3.4.2 Recommendations

Because of the potential advantages of compounding, especially in military applications, the following programs appear desirable.

1. Gaining a better than the present understanding of the aerodynamic interaction between major components of the compound at high speeds of flight through analytical studies of the total flow field around the aircraft.

2. Indication of the way toward optimization of the W/D_e vs. speed of flight for shaft-driven configurations, or $(FC_w)_t$ vs. V as a more general criterion applicable to all types of propulsion using jet fuel. This would include study of the influence of such design parameters as (a) ratio of wing area to rotor(s) area, (b) ratio of wing span to rotor diameter, and (c) distribution of the total lift between the rotor and the wing.

3. In-flight check on the RSRA of analytical prediction re W/D_e vs. V or $(FC_w)_t$ vs. V for a selected set of (a), (b), and (c) parametric values.

4. Perform design studies of aerodynamically optimal or near-optimal configurations in order to obtain an insight into structural problems in general, and weight penalties associated with compounding in particular.

5. Conduct studies and support development of enclosed, or shrouded, forward propelling devices with good propulsive efficiency in the 200-250-kn speed range, and still capable of serving as acceptable main-rotor torque compensators in hover.

CHAPTER 4

HIGH SPEED CONFIGURATIONS USING OPEN AIRSCREWS FOR VTOL

4.1 Introduction

The tip-driven helicopters and compounds discussed in the preceding two chapters exhibited cruise speed capabilities well below those of propeller-driven and jet-propelled fixed-wing aircraft of similar gross-weight classes. The same, of course, is true with respect to shaft-driven helicopters. Consequently, it may be stated that some 180-knot limit may be seen as a rather optimistic limit set as a practical cruise speed for helicopters (either shaft or tip-driven), and 220 knots for compounds.

The main source of the high-speed limitations for these configurations in forward flight stem from the rotating rotor(s) or open airscrews in general with discs making a sharp angle with respect to the flight path. It becomes clear, hence, that the following options can be executed in order to overcome the high-speed barrier of aircraft relying on rotors or propellers for VTOL operations: (a) rotation of the lifting airscrew to the position where it can serve as a propelling device, (b) complete elimination of the rotor or propeller from an active participation in the process of flight by stopping and stowing it, and (c) converting rotor blades of the stopped rotor into fixed wings.

There are, of course, many possible design schemes and concepts aimed at reducing to practice the above outlined approaches (for instance, see Ref. 34). However, because of limitations placed on this study, only the following configurations will be discussed in some detail: (a) tilt-rotors, (b) tilt wings, and (c) retractoplanes.

It should be noted at this point that because of the large research effort already made in conjunction with the development of the tilt-rotor configuration, discussions here will be chiefly limited to the accumulation and interpretation of performance data presently available regarding the most important – actually flight tested – representatives of the tilt-rotor; namely, the Bell XV-15 and the Bell-Boeing V-22. Furthermore, generalized performance of these two aircraft will serve as a baseline for gauging transport capabilities of other configurations. There will also be a brief discussion of one possible way toward improvement of the inherently low wing aspect ratios of tilt-rotors.

In the tilt-wing study, emphasis will be placed on the possibility of extending high-speed capabilities of these aircraft up to M = 0.8 regions through the application of propellers incorporating technological advances resulting from the development of propfans (PF). Problems associated with this approach will be indicated and areas of required additional research efforts will be briefly outlined. A more detailed look at stowable rotor concepts will be limited to two configurations: one, representing stoppable and stowable helicopter rotors and two, the tilt-rotor with folding blades. These studies will be preceded by a general discussion of stowable-rotor concepts.

The above-outlined detail studies will be supplemented by a glance at the concepts of converting rotor blades into fixed wings. This will be done on the examples of the X-wing and the Rotafix. A large research and development effort has been devoted to the X-wing concept. Consequently, without trying to add to the wealth of already existing material, only the present status of this project will be briefly summarized. The Rotafix concept will be briefly described, since it appears to these investigators that at least, in principle, it represents one of the simpler, but still feasible, approaches to the idea of converting rotor blades into fixed wings.

4.2 Tilt-Rotor

4.2.1 General

The Bell XV-3 convertiplane (Figure 4.1), developed under the leadership of R. Lichten, was the first tilt-rotor aircraft that accomplished complete transition from the helicopter to airplane regimes of flight and vice versa in December of 1958. Subsequently, during the flight research program, this aircraft achieved 90 full conversions and, by June 1960, had attained 125 hours of actual time in flight, a speed of 157 knots, and an altitude of about 12,000 ft (Ref. 7).

Figure 4.1 The Bell XV-3 convertiplane (450 hp Pratt & Whitney R-985 engine)

The flight-test program conducted on the XV-3 proved the basic feasibility of the tilt-rotor concept, thus opening the way toward design and development of a more sophisticated flight-research aircraft; namely, the Bell XV-15 (Fig. 4.2).

The XV-15 went through a very successful flight-test and demonstration program from 1977 to the present. A strong research program, both analytical and experimental, including full-scale wind tunnel and stand tests of the whole aircraft and its major dynamic components, complemented the actual flight testing.

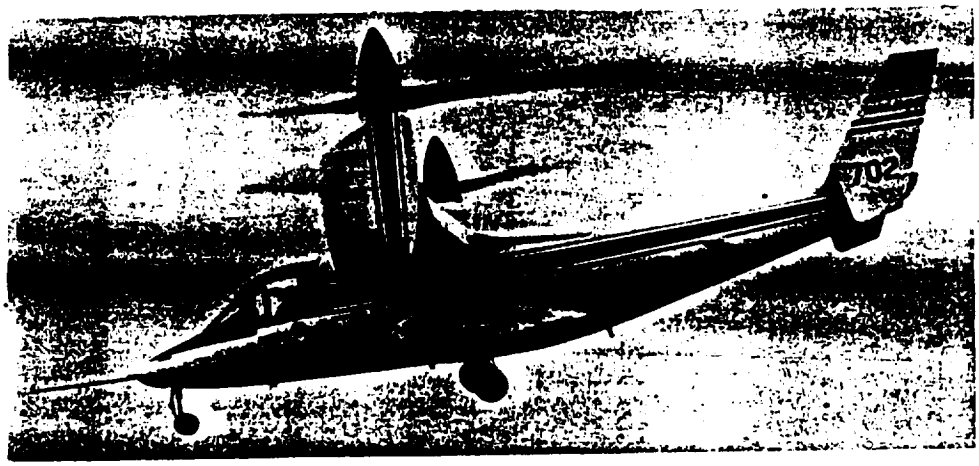

Figure 4.2 Bell XV-15 filt-rotor research aircraft in low-speed flight

These efforts led to a vast accumulation of technical data and a high confidence level, which resulted in a multi-billion dollar program for an operational tilt-rotor aircraft, the Bell-Boeing V-22 (Fig. 4.3).

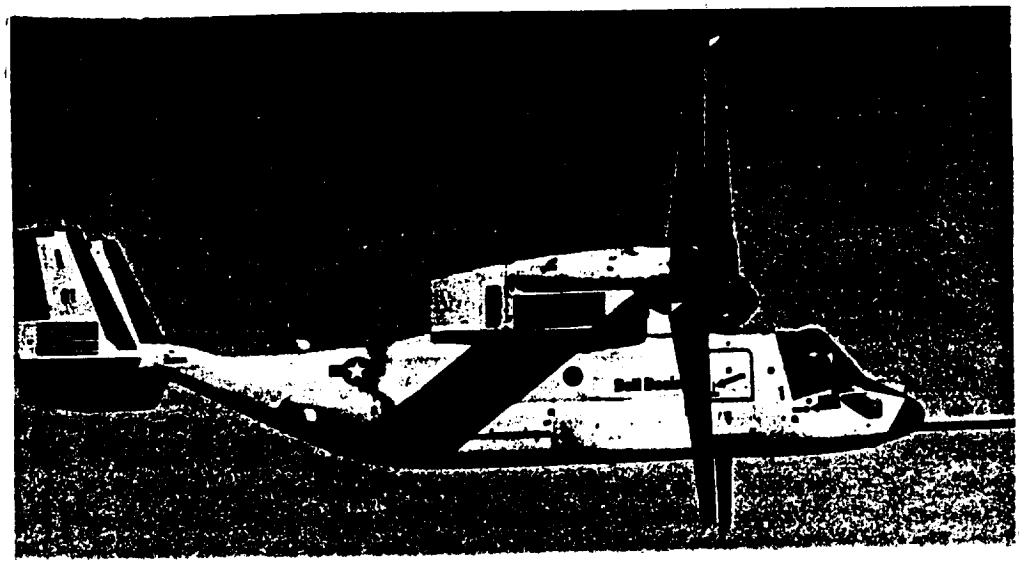

Figure 4.3 Bell-Boeing V-22 tilt-rotor

Several prototypes of this aircraft have been built and flight tested, and a full transition from the helicopter regime of flight to fixed-wing flight and vice versa, was accomplished in September 1989.

Development of short-haul civilian transport aircraft based on tilt-rotor principles became feasible, and several studies were made to investigate possibilities of this concept (Refs. 35, 36, and 37). Some of the studies were based on the concept of an evolutionary development of civilian versions starting with the XV-15 and V-22 as baseline designs (Fig. 4.4), and others looked at completely new approaches to the civilian transport tilt-rotor aircraft (Fig. 4.5).

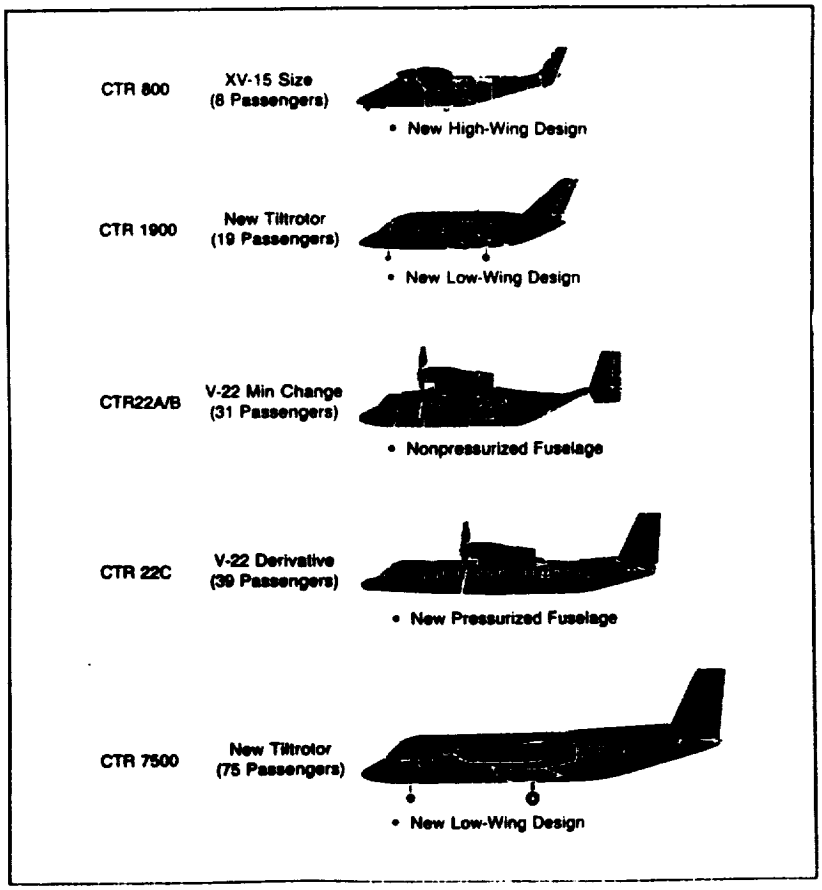

Figure 4.4 Civilian transport tilt-rotor configurations, evolved from the XV-15 and V-22 aorcraft

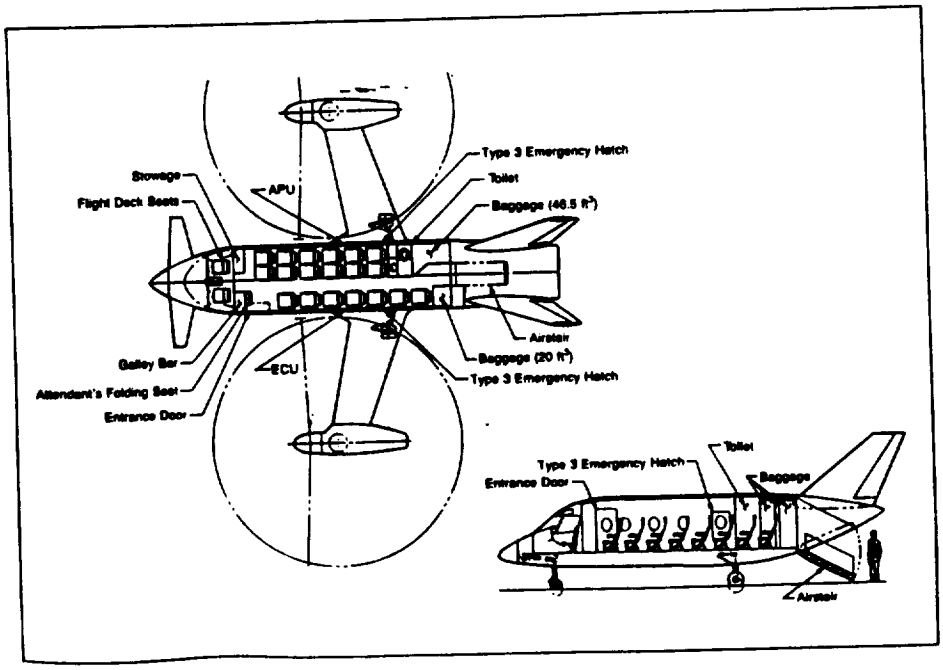

Figure 4.5 Example of an independent look at the civilian transport tilt-rotor configuration

European designers and manufacturers also became interested in the tilt-rotor concept and an international team composed of Aeritalia, Aerospatiale, Agusta, Casa, MBB and Westland was formed in 1987 in order to design and develop the so-called EUROFAR (Fig. 4.6) – a civilian commuter aircraft capable of carrying 30 passengers over 600 miles at a cruise speed of 300 knots and an altitude of 7500 m (Ref. 38).

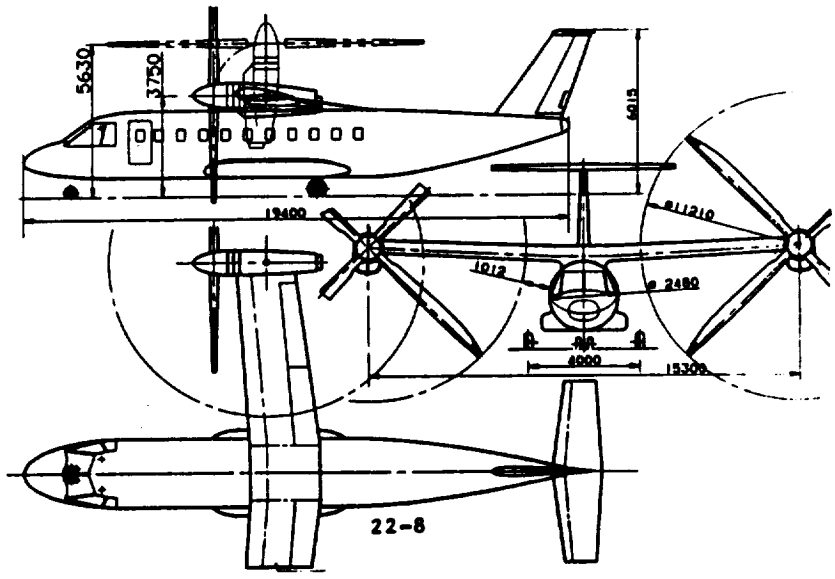

Figure 4.6 EUROFAR – 3-view drawing of the baseline configuration

Present, widely publicized, difficulties encountered by the V-22 program stem more from national fiscal policy and political interplay than from any technical problems. Consequently, regardless of the future of the V-22 program, one may assume that because of the amount of effort already spent on the development of this aircraft, many performance items and weight characteristics could be considered as representing, in general, the true state of the art of the tilt-rotor configuration. However, it should also be remembered that because of the special operational requirements associated with ship-board operation (folding of rotors, wing rotation, and rear cargo loading), aerodynamic cleanness and weight-empty values of civilian transports may be better than for the V-22. For this reason, when establishing a baseline figure for generalized performance and relative weights, data from the V-22 and XV-15 will be supplemented by inputs (where available) from studies of the civilian tilt-rotor.

At the conclusion of these general remarks regarding the tilt-rotor configuration, a few important characteristics of two existing and some hypothetical aircraft of that type are shown in Table 4.1.

4.2.2 Hovering

Shaft horsepower required per pound of aircraft gross weight in hover OGE ($\overline{SHP_h}$) for the tilt-rotor will be expressed by the same relationship as for any other shaft-driven VTOL aircraft. Consequently, Eq. (1.19) can be rewritten as follows:

$$\overline{SHP_h} = 0.0264 k_v^{3/2} \sqrt{w/\bar{\rho}}/FM\, \eta_{ov}. \tag{4.1}$$

In discussing the influence of various parameters appearing in the above equation, it should be noted that the disc loading (w) of the tilt-rotors shown in Table 4.1 range from about 14 to 24 psf. It appears, hence, that a disc loading of about 26 psf represents the upper limit for conventional tilt-rotor aircraft.

The overall ratio of rotor power to engine shaftpower of the tilt-rotor configuration will probably be close to that of the V-22 and XV-15 which, including accessory drive, amounts to $\eta_{ov} \approx 0.92$.

In the overall examination of hovering capabilities of the tilt-rotor, an investigation of the figure of merit (FM) and download factor(k_v) values is of particular interest.

Figure of merit levels for isolated rotors appears quite high, as can be seen from Fig. 4.7, which shows the FM vs. average blade-lift coefficient ($\overline{c_l}$) plots for the XV-15 and V-22 models (see Refs. 40 and 41).

Furthermore, one should take note from Figure 4.7 that the high FM values of about 0.8, or even slightly higher, extend through a considerable range of the average blade-lift coefficient levels from $\overline{c_l} \approx 0.5$ to 1.0 and possibly higher. This FM vs. $\overline{c_l}$ characteristic has definite operational advantages, as it permits one to have the rotor working efficiently through various combinations of disc loadings, tip speeds, and relative air densities ($\bar{\rho}$).

TABLE 4-1

PRINCIPAL CHARACTERISTICS AND PERFORMANCE
OF ACTUAL & HYPOTHETICAL TILT-ROTORS

ITEM	ACTUAL		HYPOTHETICAL		
	BELL XV-15	BELL-BOEING V-22	NASA CTR-22C	NASA CTR-7500	EUROFAR
APPLICATION	FLT. RES.	MILITARY	PASSENGER TRANSPORT		
POWERPLANT	LYCOMING LTC1K-4K	T406	T406	GROWTH T406	
Number of Engines	2	2	2	2	2
Output Shaft RPM		15,000			
Total TO or MIL SHP	3,100	12,300	13,610	25,766	(8046)
Total Max. Con't. SHP		11,780			6892
ROTOR, RADIUS, FT	12.5	19.0	19.0	23.0	18.37
Direction of Rotation	T_tFF^*	T_tFF^*	T_tFF^*	T_tFF^*	T_aFF^{**}
Number of Blades	3	3	3	3	4
Blade Chord, Ft	1.17, 0.7R	2.85 Root			
Blade Chord, Ft		1.83 Tip			
Articulation	Restrained Gimbal		Restrained Gimbal		
Tip Speed, FPS		779/662	779/662		722/677
Rotor Solidity	0.089	0.12^T			0.095^T
WING					
Span, Ft	35.0	46.0	45.83	63.0	
Area (Total), Sq.Ft.	169.0	382.0	382.0		
Area (External), Sq.Ft	127.0	302.0	302.0		
Aspect Ratio	6.1	5.5	5.5		
EXTERNAL DIMENSIONS					
Overall Length, Ft	41.0	57.3	68.8	83.7	
" Height to Rotor Disc	(12.8)	21.6	21.6		18.47

NOTES: * In hover, tips advance toward fuselage front
** In hover, tips move away from fuselage front
( ) Estimated
T Geometric Solidity

TABLE 4-1 (CONT'D)

ITEM	ACTUAL		HYPOTHETICAL		
	BELL XV-15	BELL-BOEING V-22	NASA CTR-22C	NASA CTR-7500	EUROFAR
WEIGHTS (ABSOLUTE)					
Max. GW, Lb	15,000	55,000			
Normal GW, VTO	13,000	47,500	46,230	79,821	30,100
Weight Empty, Lb	9,570	31,886	30,242	53,795	19,290
Zero Range Payload, VTO	(3,000)	(15,155)	(15,320)	(25,360)	(10,140)
RELATIVE WEIGHTS					
W_e/W_{max}	0.64	0.58			
W_e/W_{normal}	0.74	0.67	0.65	(0.67	0.64
W_{opl}/W_{normal}	(0.23)	(0.32)	(0.33)	0.32)	(0.34)
DISC LOADING					
Normal GW, PSF	13.2	20.95	20.4	24.03	14.20
Max. GW, PSF	15.2	24.24			
TOTAL WING LOADING					
Normal GW, PSF	76.92	124.34	121.0		(82.7)
Maximum GW, PSF	88.76	144.0			
INSTALLED POWER LOADING, VTOL					
Maximum GW, Lb/SHP		3.86	3.4	3.1	3.74
PERFORMANCE, KN					
Max. Flight Speed, N.E.	364				
Fast Cruise @ 17,000 Ft	303	300***			300
Economic Cr @ 20,000 Ft	200	275****	282	300	

NOTES: *** Optimum Altitude

**** Sea Level

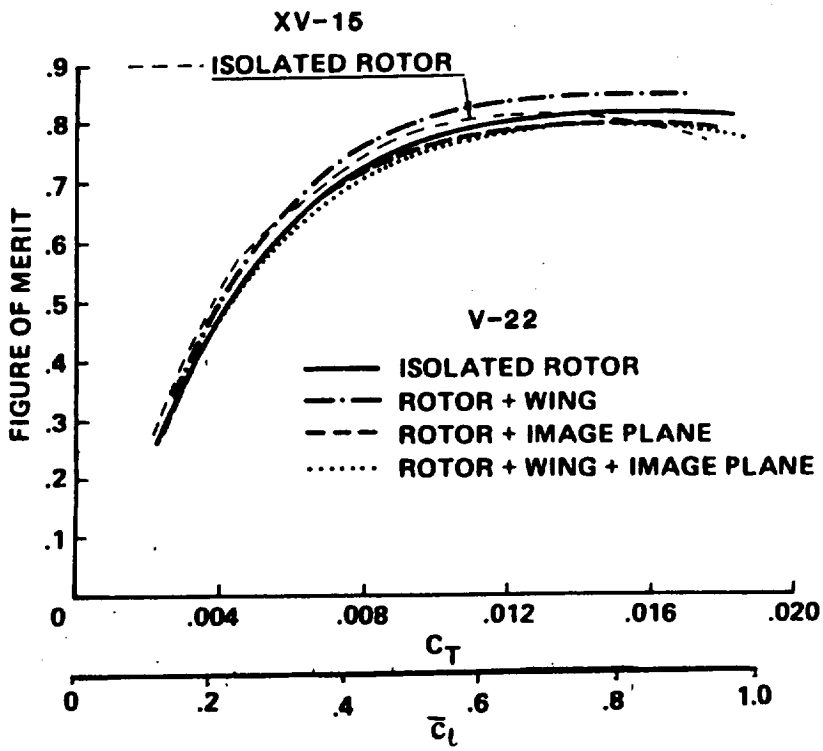

Figure 4.7 Figure of merit values vs. c_l for V-22 and XV-15 rotors

A closer investigation of Figure 4.7 would indicate that the wing has a beneficial 'ground' effect' on *FM* values. However, this beneficial wing effect disappears in the presence of the image plane, simulating the presence of a second rotor, which would cause some downstream flow to turn upward.

When one looks at the tilt-rotor configuration, one of the first questions that comes to mind is: How serious is the download problem or, in other words, what is the k_v value? It is indicated in Ref. 40 that the download (D) to the rotor thrust (T) ratio amounts to D_v/T = 0.10 for the V-22 and 0.11 for the XV-15. Consequently, D_v/T = 0.105 can be accepted as a representative value

Since the download factor

$$k_v = 1/[1 - (D_v/T)],$$

its corresponding representative value can be taken as k_v = 1.12.

Having established ranges of the values of parameters appearing in Eq. (4.1), trends in the $\overline{SHP}_h$ vs. w for the tilt-rotor configurations in hover OGE at SL, STD and 4000 ft, 90°F were calculated, assuming the following values: k_v = 1.12, FM = 0.75, and η_{ov} = 0.92. Calculation results are shown in Figure 4.8.

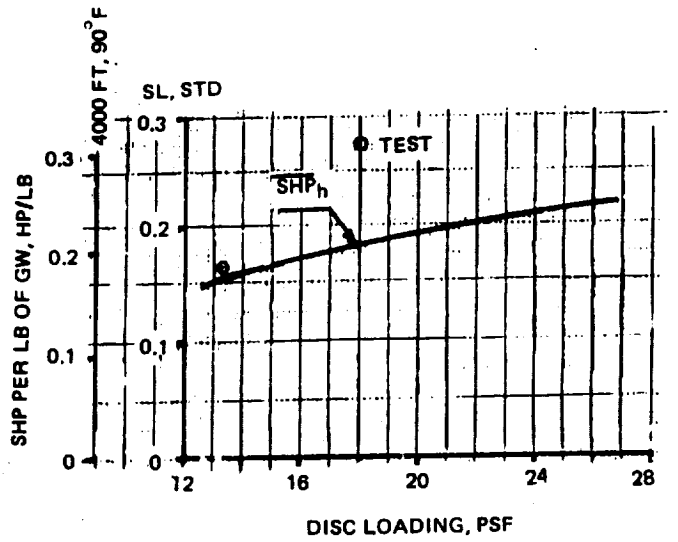

Figure 4.8 Trend in shaftpower required per pound of gross weight by tilt-rotors in hover OGE at SLS and 4000 ft, 90°F

Fuel consumption per pound of gross weight and one hour can be computed from Eq. (1.21), which is rewritten in a simpler form as

$$(FC_w)_{t_h} = \overline{SHP}_h sfc. \tag{4.2}$$

Taking the $\overline{SHP} = f(w)$ values shown in Fig. 4.8 and assuming two values of engine specific fuel consumption; namely, sfc = 0.4 and 0.5 lb/hr,hr, the anticipated trends in $(FC_w)_t$ values vs. w for tilt-rotor configurations in hover OGE at SLS were computed and are shown in Fig. 4.9. An area representing $(FC_w)_{t_h}$ vs. w for the existing shaft-driven helicopters examined in Ref. 5 is also marked on this figure.

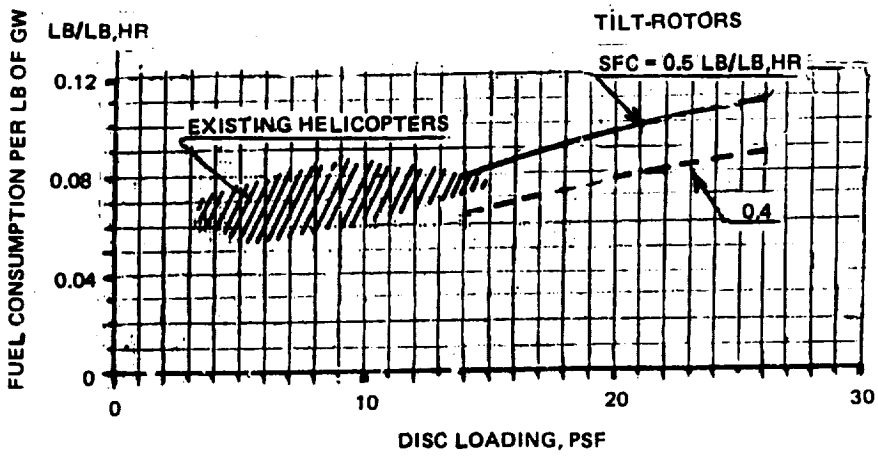

Figure 4.9 Trends in fuel consumption per lb of GW for tilt-rotors in hover OGE at SLS

One can see from Table 4.1 that relative weight-empty values for existing and hypothetical tilt-rotor aircraft amount to $0.64 \leq \overline{W}_e \leq 0.67$ for VTOL operations. Consequently, for tilt-rotors of the 50,000-lb gross weight class, assuming a crew of 2 (360 lb) and 80 lb of trapped liquids, the relative zero-time payload would amount to $0.32 \leq \overline{W}_{0_{pl}} \leq 0.35$.

Assuming lower relative zero-time payload values close to the lower figure, namely, $\overline{W}_{0_{pl}} = 0.32$ and the higher, somewhat better, $\overline{W}_{0_{pl}} = 0.38$, the relative payload vs. time in hover OGE at SLS was computed from Eq. (1.11) and is shown in Fig. 4.10. In these calculations, two values of fuel consumption per pound of gross weight and hour were assumed: $(FC_w)_t = 0.110$, corresponding to the upper right corner of the graph shown in Fig. 1.10, and $(FC_w)_t = 0.064$ lb/lb,hr shown in the lower left corner.

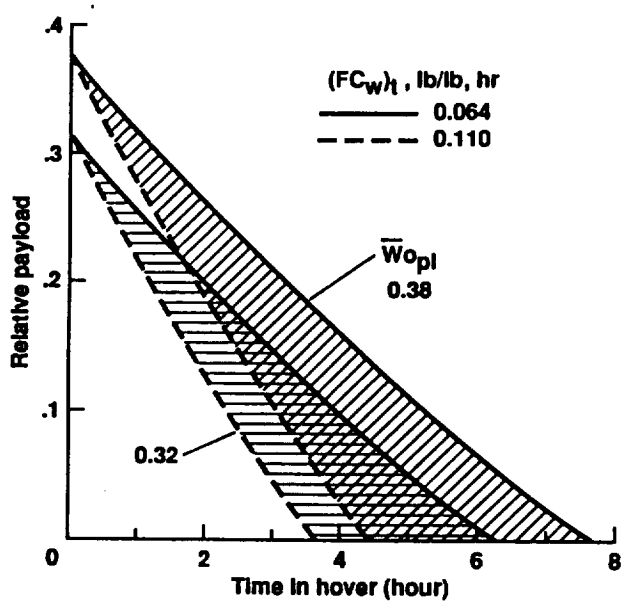

Figure 4.10 Possible domain of payload vs. time in hover (SLS, OGE) relationship for conventional tilt-rotors

A glance at this figure would indicate that the domain of the possible payload vs. time in hover (SLS, OGE) relationships is quite large. This, of course, stems from the fact that here, wide probable ranges of such parametric values as disc loading, relative weight empty and engine sfc were taken into consideration. It appears that, depending on the interplay between levels of the above-mentioned parameters, the conventional tilt-rotor can, in principle, be designed as an effective payload-carrying vehicle in hover and near-hover operations. A truism is also apparent from this figure: a low relative weight empty; i.e., high zero-time relative payload is a very important factor in achieving a high effectiveness regarding payload-carrying capabilities in hover.

Finally, it may be stated that with the exception of a few missions (such as rescue) for which applications of conventional tilt-rotors can be visualized, the whole payload vs. time relationship would probably be less important in determining the utilization appeal of these aircraft than horizontal flight aspects.

4.2.3 Horizontal Flight

Important Factors Affecting Aircraft Effectiveness in Horizontal Flight. Of the many factors affecting the effectiveness of the open airscrew propeller aircraft in horizontal flight, the following may be singled out as deserving specific consideration.

1. Shaft horsepower per pound of gross weight ($\overline{SHP}$), which also may be interpreted as gross weight (lift) to equivalent drag ratio (W/D_e) ≡ (L/De) vs. speed of flight at some representative attitudes. This, obviously, may be considered as a gauge of the aerodynamic excellence of the aircraft.

2. Fuel consumption per pound of aircraft gross weight and one hour of flight $(FC_w)_t$ vs. speed of flight. Fuel consumption per pound of GW and one nautical mile flown, $(FC_w)_R$ vs. speed of flight at selected altitudes. Both of these relationships should be interpreted as a measure of the aerothermodynamic excellence of the aircraft.

3. Relative weight empty and thus, relative zero-range payload. These quantities would reflect the structural effectiveness of the configuration.

4. Trends in relative payload vs. range and typical ideal relative productivity values vs. range at selected cruise speeds plus V_{max} levels would indicate operational capabilities of the aircraft.

The above-listed characteristics will be discussed and then summarized for conventional tilt-rotors—either existing or representing development of existing models. In this way, baseline information will be established for determining the competitive position of other VTOL transport concepts and configurations.

General Discussion of Factors Affecting $\overline{SHP}$ and L/D_e Levels. Conventional tilt-rotors operate in horizontal flight as any other open-airscrew driven aircraft. Consequently, their required SHP values can be deduced from Eq. (1.28) as follows:

$$\overline{SHP} = 0.00308V/(L/D)\eta_{pr}\eta_{ov} \tag{4.3}$$

where the speed of flight V is in knots, (L/D) is the lift to drag ratio corresponding to that speed and flight altitude, η_{pr} is the propulsive efficiency of the airscrew, and η_{ov} accounts for power losses resulting from the operation of the transmission system, including instrumentation.

The lift (gross weight) to equivalent drag ratio (L/D_e) can be expressed as

$$(L/D_e) = 0.00308V/\overline{SHP}. \tag{4.4}$$

Looking at Eq. (4.3), one will see that the $\overline{SHP}$ level corresponding to a given speed of flight and altitude depends on the value of the product appearing in the denominator. In order to get a clearer idea about the possibility of achieving favorable $\overline{SHP}$ and thus, (L/D_e) vs. speed of flight relationships, factors appearing in the $(L/D) \times \eta_{pr} \times \eta_{ov}$ product are briefly reviewed.

Starting with η_{ov}—the ratio of rotor power to engine power—one may expect that its value in horizontal flight would, in general, be not much different from that in hover. This means that $\eta_{ov} \approx 0.92$ to 0.94 may be assumed as representative levels for conventional tilt-rotors. With the increasing disc loading, η_{ov} values could become slightly higher because of the decreasing rpm ratios and fewer gear meshes between those of the engine shafts and those of the rotors.

Propulsive efficiency of the rotors acting as propellers in horizontal flight would depend on the possibility of retaining high levels of the two-dimensional ratios (c_l/c_d) of the blade elements, especially in the outboard regions.

Since, in horizontal flight, only a fraction, $(W/D)^{-1} \equiv (L/D)^{-1}$, of the hovering thrust is required, the sectional lift coefficient of the blade elements could become very low; e.g., $c_l < 0.1$. Even if quite low sectional c_d levels could be maintained (e.g., $c_d \approx 0.007$ to 0.009), the resulting c_l/c_d values would be quite small.

Consequently, in order to minimize the drop in the blade element c_l levels, the rotor-propeller rpm in forward flight should be reduced with respect to the rpm in hover.

A reduction in the rotor tip speed in forward flight of actually constructed tilt-rotors (XV-15 and V-22), as well as those presently in the design stage (EUROFAR), is achieved by lowering the engine rpm within its acceptable limits (85% of the takeoff values). Thus, for the V-22, the rotor tip speed in hover is 800 fps, while in cruise, it drops to 680 fps. In this way, the necessity of having a gearshift arrangement was avoided.

The problem of retaining low c_d levels at the blade elements, especially in the tip regions, is usually attained through the following means: (1) Incorporation of thin airfoil sections, retaining low c_d levels at low c_ls and elevated helical Mach numbers. (2) Adaptation of swept blade planforms. This could range from those simply having properly shaped blade-tip regions, while the blade itself remains basically unswept, to radically curved blade shapes as in propfans. (3) The previously mentioned rotor-propeller rpm reduction which, in addition to improving the sectional c_l values, also lowers the helical Mach number at given flight speeds and ambient conditions.

Depending on the degree of geometric sophistication of the blade, a wide spectrum of propulsive efficiency becomes possible, as illustrated in Fig. 4.11 (courtesy of J. Wilkerson, Boeing Helicopters Co.).

Looking at this figure, one will see that conventional rotors, when used as propellers, experience deterioration of their propulsive efficiencies at $M > 0.52$. This, of course, would present a strong constraint against achieving fast cruise and V_{max} dash capabilities by conventional tilt-rotors at $M \geq 0.52$; i.e., $V > 340$ kn at SLS, and 320 knots at, say, 20,000 ft. In order to penetrate this barrier, properly shaped blades must be used if one relies on open airscrews for forward propulsion. Otherwide, turbofan or turbojet (unlikely) thrusters must be used.

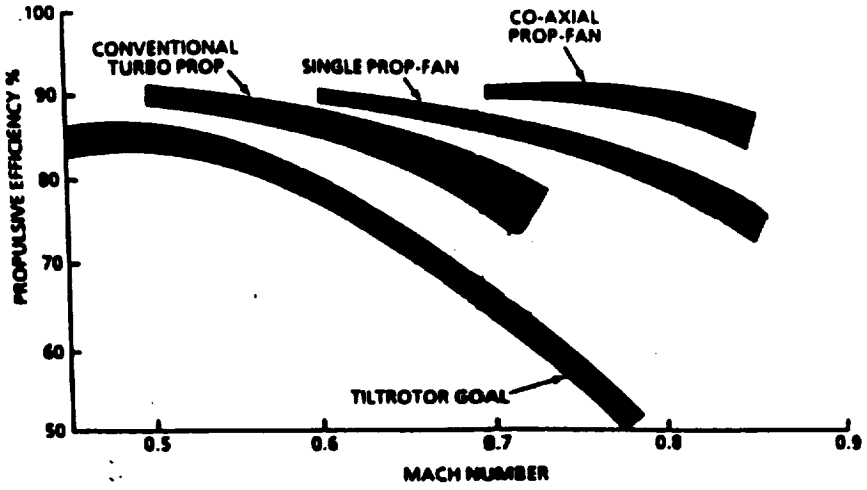

Figure 4.11 Trends in propulsive efficiency of open airscrew-type thrusters

Up to flight Mach numbers where serious deterioration of the propulsive efficiency is encountered, the L/D values corresponding to various flight speed levels and altitudes, in other words, dynamic pressure (q) of flight, remain the most important factor affecting $\overline{SHP}$ and thus, L/D_e vs. V relationships.

In order to see what L/D levels may be exprected in conventional first generation tilt-rotors, and how various design parameters should be modified in order to improve the lift to drag ratios of future tilt-rotor designs, the following expression will be used:

$$L/D = [(C_{D_{par}} + C_{D_o}\lambda_{compr})/C_L) + (C_L/\pi AR_e)]^{-1} \tag{4.5}$$

where $C_{D_{par}}$ is the parasite drag coefficient of the nonlifting aircraft components, C_{D_o} is the profile drag of the wing, and λ_{compr} is the drag-rise factor due to compressibility effects.

It should be noted that in the above equation, it was assumed that the compressibility correction (λ_{compr}) would apply to the wing alone, while other components of the aircraft are of such aerodynamic shape that their parasite drag coefficients ($C_{D_{par}}$) do not measurably increase up to, say, M = 0.8.

The expression for $(L/D)_{max}$ now becomes

$$(L/D)_{max} = \tfrac{1}{2}\sqrt{\pi AR_e/(C_{D_{par}} + C_{D_o}\lambda_{compr})}. \tag{4.6}$$

For a conventional first-generation tilt-rotor, as represented by the V-22, the equivalent flat plate area of the whole aircraft (including the wing) is f = 24 sq.ft'. Assuming that λ_{compr} = 1.0 and the reference wing area is 382 sq.ft, the total noninduced drag coefficient ($C_{D_{nind}} = C_{D_{par}} + C_{D_o}\lambda_{compr}$) would amount to 0.063. Consequently, $C_{D_{nind}}$ = 0.055 to 0.065 may be assumed as typical for conventional first-generation tilt-rotors.

The geometric aspect ratio of existing conventional tilt-rotors (as well as those still in the design stage) ranges from AR = 5.5 (V-22) to $AR \approx 6.4$ (EUROFAR). Assuming a span efficiency factor, $e = 0.85$, the effective aspect ratio would be $AR_e = 4.7$ to 5.4.

Using the above determined typical $C_{D_{nind}}$ and AR_e values, and combining the highest AR_e with the lowest $C_{D_{nind}}$, and then the lowest AR_e with the highest $C_{D_{nind}}$, the probable domain of L/D vs. C_L for conventional first-generation tilt-rotors is charted (Fig. 4.12).

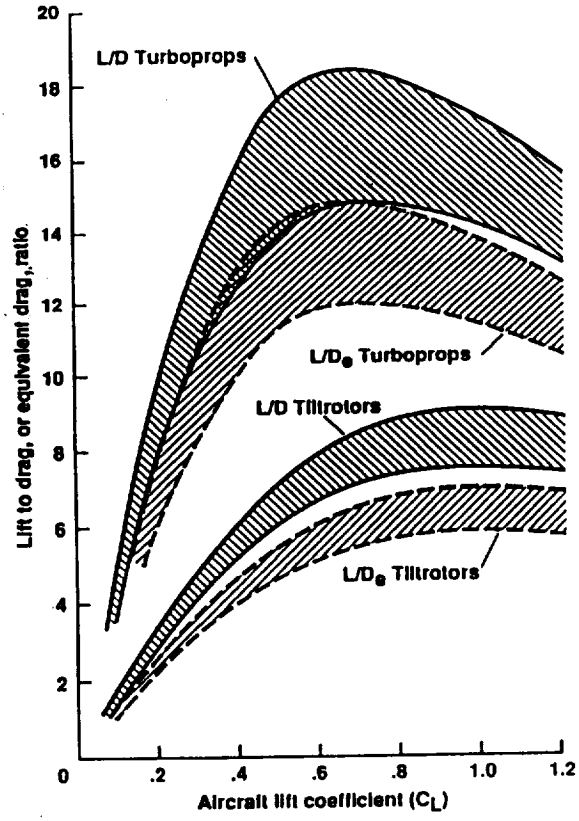

Figure 4.12 Probable domain of L/D and L/D_e vs. C_L relationships for first generation tilt-rotors and transport turboprops

The outline of the probable domain of L/D_e vs. C_L relationships is obtained by multiplying the L/D's by $\eta_{ov}\eta_{pr}$, assumed to be equal to 0.93 and 0.82, respectively. The so-obtained probable domain of the L/D_e vs. C_L relationships for first generation tilt-rotors is also shown in Fig. 4.12.

It would be of interest to see how the so-established L/D and L/D_e domains for conventional tilt-rotors would compare with similar relationships for turboprop transports.

In Ref. 42, $C_{D_{nind}}$ = 0.018 to 0.24 is given as typical noninduced drag coefficients for transport turboprops, while geometric aspect ratios would range from $AR \approx 8.0$ to 9.2. Again, assuming $AR_e = 0.85\,AR$ and, using the above $C_{D_{nind}}$ values, the probable domain of the L/D vs. C_L relationship for clean turboprop transports was established and added to Fig. 4.12.

The L/D_e vs. C_L domain for turboprops was established, assuming the same propulsive efficiency (0.83) as for tilt-rotors, but upping the η_{ov} values to 0.97 in view of the fact that, in turboprops, there is usually no transmission associated with the transfer of engine power to propellers, and only some power losses resulting from instrument usage may be encountered.

The so-established L/D_e vs. C_L domain for turboprops is also shown in Fig. 4.12.

Looking at the completed Fig. 4.12, one would see that as far as the general trend in L/D and L/D_e levels are concerned, the first generation tilt-rotors appear inferior to transport turboprops. It is also clear that in order to narrow the L/D gap, higher wing aspect ratios must be used, and a higher degree of aerodynamic cleanness (higher w_f; i.e., lower $C_{D_{nind}}$ levels) must be achieved. Furthermore, one may expect that along with the requirements for improvements in the lift to drag ratios, there may appear a demand for high-speed capabilities better than the some 300+ knots of the present tilt-rotor generation. Should the anticipated high-speed requirement approach the M = 0.7 to 0.8 range, then designers of future tilt-rotors would face an additional challenge of the drag rise of the unswept, relatively thick ($\bar{t} \geq 14\%$) airfoils (see Figure 4.13).

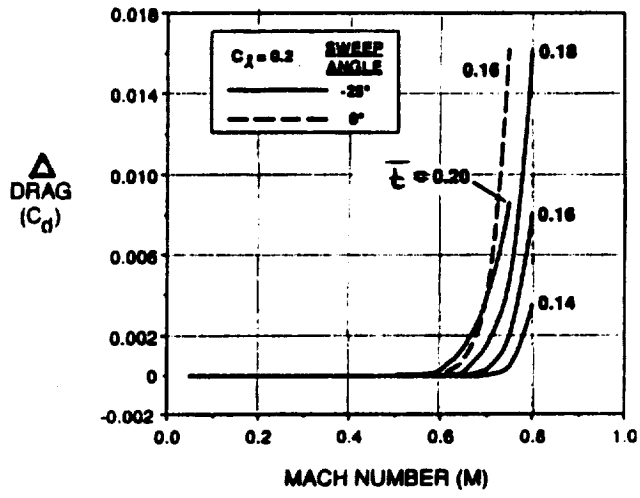

Figure 4.13 Compressibility drag increments

It appears, hence, that in order for the tilt-rotors in horizontal flight to have the lift to drag ratios and high-speed capabilities of their fixed-wing counterparts (turboprops, prop-fans, and turbofan types), the following design features should be incorporated.

(1) Higher aspect ratio ($AR > 5.5$), relatively thinner ($t < 14\%$) and either forward or back-swept wings.

(2) Degree of aerodynamic cleanness, as measured by an equivalent flat-plate area loading considerably higher than the present $w_f \approx 2000$ psf.

(3) Means of assuring that the lifting airscrews become efficient pulsors in horizontal flight, or incorporation of non-open airscrew devices (e.g., turbofan section of the convertible engines) as horizontal thrusters at high subsonic speeds.

Finally, as discussed in Chapter 1, in order to minimize fuel consumption per unit of gross weight and unit of distance flown, wing loading of the aircraft should be such that at the intended cruise speed and altitude; i.e, q of flight, the aircraft will be flown at, or close to, its $(L/D_e)_{max}$. Thus, taking data from Fig. 4.12, Fig. 4.14 was prepared to show what wing loadings of conventional tilt-rotors (aerodynamically similar to the so-called first generation) would be necessary to assure L/D_e levels enclosed between their maximum and about 10% lower values.

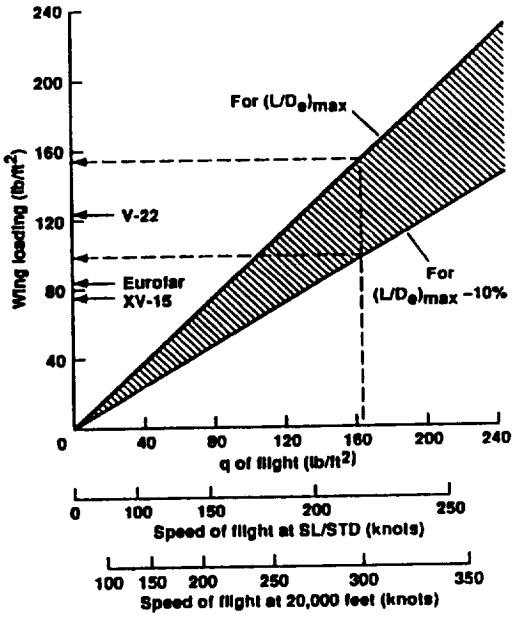

Figure 4.14 Indications of wing loadings desirable for tilt-rotors, geometrically similar to the V-22 for cruise speeds at SLS, or 20,000 ft

Looking at this figure, one will see that for an intended cruise speed of 300 kn at 20,000 ft, a wing loading of about 155 psf should lead to flight at $(L/D_e)_{max}$ and about 100 psf at L/D_e levels some 10% lower than its maximum value.

Wing loadings of the V-22, X-16, and EUROFAR are marked for reference in Fig. 4.14.

It should be emphasized that the relationships presented in Fig. 4.14 are applicable to aircraft having their noninduced drag coefficients within 0.056 to 0.065 and the effective aspect ratio within 4.7 to 5.4 ranges.

Factual Data re $\overline{SHP}$ and L/D_e for First Generation Tilt-Rotors. From flight-test established ralationships between the rotor horsepower and speed of flight at SLS for the XV-15 aircraft (courtesy of McVain, Boeing Helicopters Co), a graph was prepared giving the power required per pound of gross weight vs. speed of flight at SLS (Fig. 4.15).

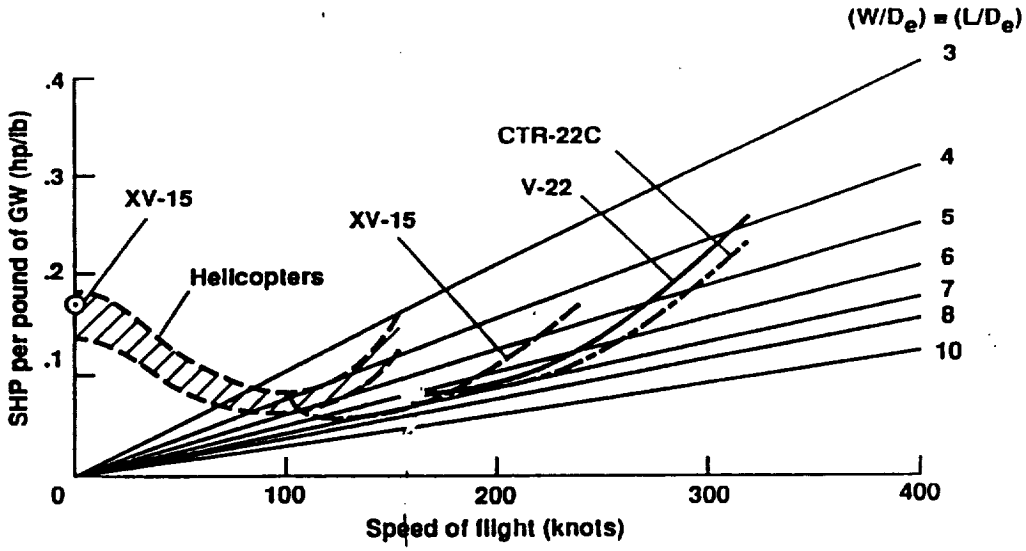

Figure 4.15 SHP required per pound of gross weight vs. speed of flight at SLS for XV-15, V-22, and CTR-22C tilt-rotor aircraft

For the V-22 aircraft, only the estimated SHP required was available (obtained from Boeing Helicopters, courtesy of H. Rosenstein). $\overline{SHP}$ values for SLS conditions were added to Fig. 4.15.

Estimated $\overline{SHP}$ required curves for the civilian transport version of an aircraft based on the V-22 dynamic system and wing (CTR-22C) were also obtained from Boeing Helicopters (courtesy of J. Wilkerson). $\overline{SHP}$ values for the SLS conditions for this aircraft are also plotted in Fig. 4.15. Typical values for the shaft-driven helicopters studied in Ref. 5 are shown (shaded area) for comparison.

The gross weight (lift) to equivalent drag ratios for the two above-mentioned actual and one hypothetical aircraft were computed using Eq. (4.4).

The results vs. speed of flight are shown in Figure 4.16.

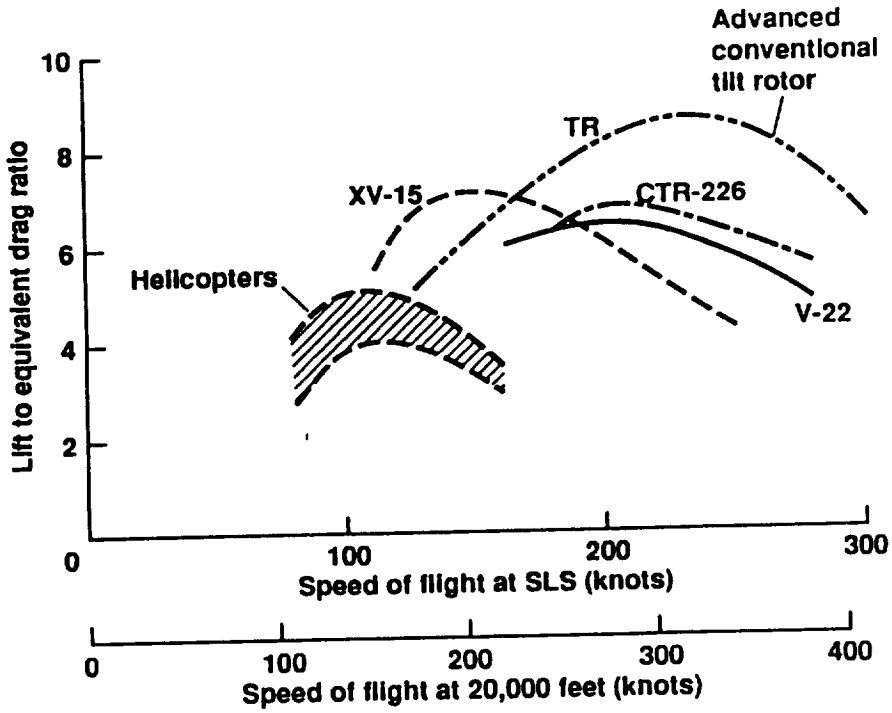

Figure 4.16 Lift to equivalent drag ratios vs. speed of flight for tilt-rotor aircraft

One can see from this figure that the lift to equivalent drag ratio of the two existing, as well as projected, conventional commercial transport tilt-rotor aircraft (CTR-22C) of the up to 50,000-lb gross weight class are quite low, although somewhat higher than for conventional shaft-driven helicopters.

It should be noted, however, that studies reported in Ref. 43 express some hope of improving L/D_e values for aircraft basically similar to the first-generation types, to the levels indicated in Fig. 4.16 by the curve marked 'Advanced Conventional Tilt-Rotors.' This curve (TR) represents the aircraft in Fig. 4.17, and its L/D vs. speed-of-flight relationship is shown in Fig. 4.18.

Future Tilt-Rotor Configurations. L/D values as high as 14 are projected in Ref. 43 for the canard-configured transport tilt-rotor aircraft (CTR) shown in Fig. 4.17.

One should note that in the CTR aircraft, several features previously indicated as possible methods of improving L/D and L/D_e levels are incorporated. A higher aspect ratio and improved aerodynamic cleanness contribute to generally higher L/D's. Considerably forward swept wings and properly configured rotor blade tips would delay aircraft drag divergence and somewhat improve the propulsive efficiency at higher subsonic speeds. But without adaptation of the propfan blade planforms, a low propulsive efficiency would still create an obstacle to flying speeds at about Mach 0.68 and higher (Fig. 4.11).

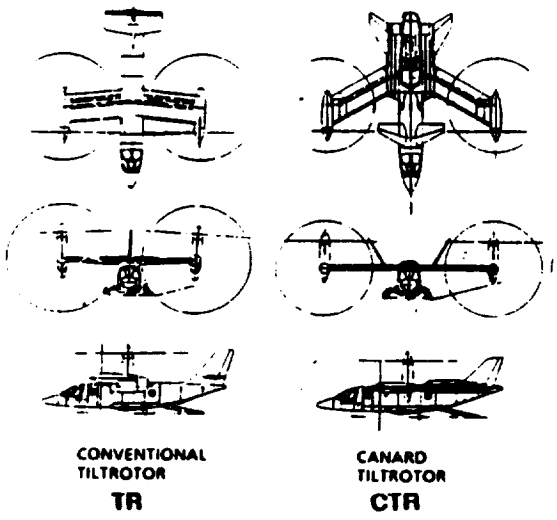

Figure 4.17 3-View drawing of advanced tilt-rotor configurations (Ref. 43)

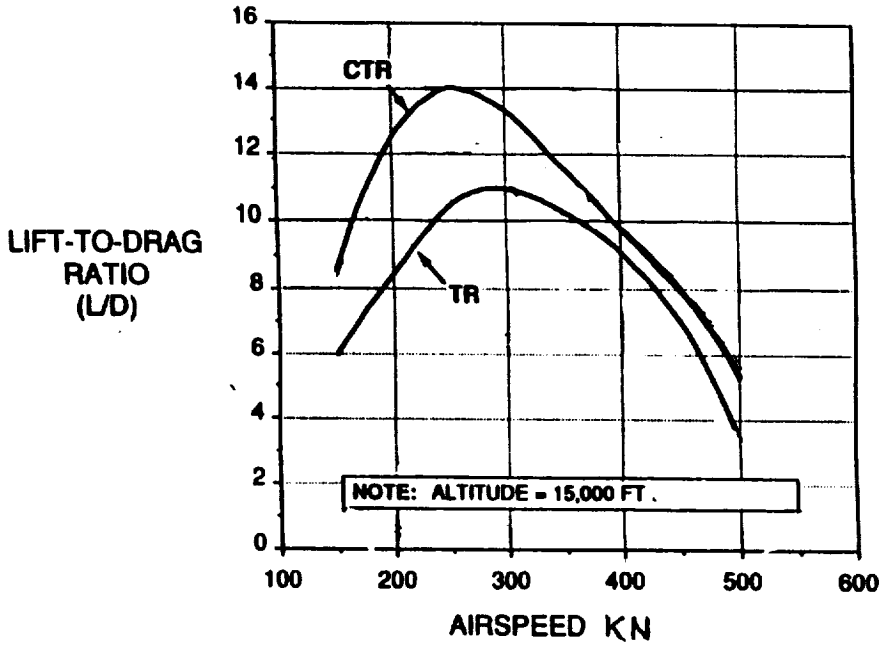

Figure 4.18 *L/D* values for configurations (TR) and (CTR) shown in Fig. 4.17

Tiltable Winglets—A Possible Method of Improving L/D Ratios of Conventional Tilt-Rotor Aircraft. It is evident that aerodynamically cleaner designs, as demonstrated by the (TR) configurations shown in Fig. 4.17, would be required in order to bring L/D and thus, L/D_e, values of conventional tilt-rotors closer to those of advanced turboprops.

However, in some tilt rotors, for example, the V-22, the relatively high parasite drag would stem from special military and, possibly, other operational requirements. The question hence, arises whether an increase in the geometric wing aspect ratio alone would be a practical means of improving the L/D levels of tilt-rotors basically similar to the first generation of these aircraft. Incorporation of winglets—tilting with the nacelles and, thus, contributing little to the download in hover—appears as a possible approach.

To get an initial, although very rough, answer to the question of possible gains from the above approach, tiltable winglets as shown in Fig. 4.19 were assumed, with no attempt to optimize their size.

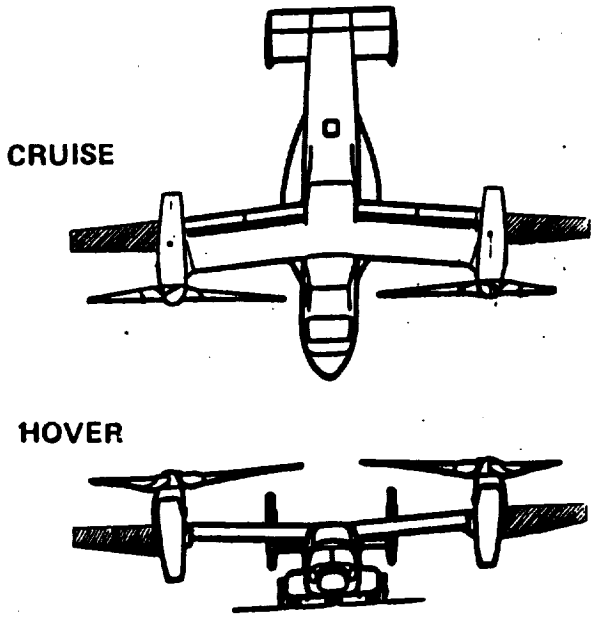

Figure 4.19 The V-22 configuration with assumed tiltable winglets

In order to create a gauge for measuring potential improvements resulting from the application of winglets, L/D's for the baseline aircraft and another, modified with winglets, were computed from the following relationship (see Chapter 1, Sect. 1.3.5):

$$L/D = [(C_{D_{nind}} w_w/q) + (q/\pi AR_e w_w)]^{-1}. \tag{4.7}$$

Data required for computations for the above equation are listed in Table 4.2.

TABLE 4.2

LIFT-TO-DRAG ESTIMATES

AIRCRAFT	CHARACTERISTICS						
	GROSS WT Lb	WING AREA Sq.Ft	WING AR	WING ARe	WING LOADING PSF	f_{nind} Sq.Ft.	$C_{D_{nind}}$
BASELINE	45,000	382	5.5	4.7	117.8	24.0	0.063
MODIFIED	45,000	489	10.7	9.1	92.0	24.86	0.051

Using inputs from Table 4.2, the L/D values were computed from Eq. (4.7) and plotted vs. q of flight as shown in Fig. 4.20, where speed of flight scales are also marked for SLS and 20,000-ft altitude.

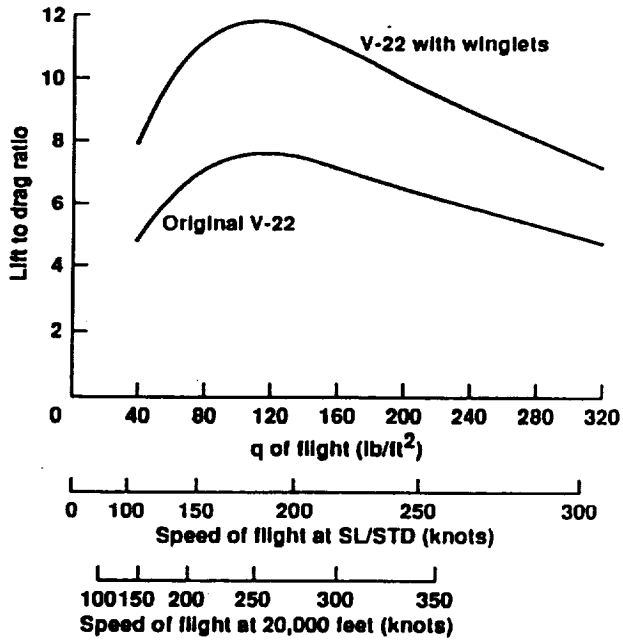

Figure 4.20 Estimated lift-to-drag ratios vs. q of flight for a tilt-rotor similar to the V-22 and the same aircraft with tiltable winglets

A glance at this figure will indicate that, indeed, there should be a potential for improving the L/D levels of conventional tilt-rotor aircraft (similar to the V-22 and XV-15) throughout the anticipated speed of flight range by the application of tiltable winglets. However, various penalties associated with this approach should be expected.

For example, separate programming of the angular movement of the winglets, when tilting with the engine nacelles, may be necessary in order to avoid airflow separation and reduction of the effectiveness of yaw control. This will create some mechanical complications. Furthermore, an increase in structural weight will be unavoidable. In this respect, very rough preliminary estimates indicated that in the case of a tilt-rotor similar to the V-22, the weight penalty would amount to some 370 lb; i.e., about 0.8% of the gross weight. However, it appears that in view of the potential gains in L/D levels, the whole idea of tiltable winglets deserves a more detailed investigation.

Possibilities of High Disc-Loading Tilt Open-Airscrew Aircraft. Schneider and Wilkerson indicated in Ref. 43 that for twin-rotor configurations, disc loading in hover should not be higher than 40 psf, when the presence of people may be required in the vicinity of hovering aircraft. However, one can imagine tasks where the presence of people close to the hovering aircraft would not be needed and, in addition, vertical takeoffs and landings would be performed from prepared areas. Commercial VTOL transport operations may be cited as an example of possible applications where limitation of the disc loading to some 40 - 50 psf may not be required.

Should this happen, then a possibility presents itself of developing configurations which, in the two-airscrew, side-by-side types, would be basically similar to the tilt-rotors. But instead of rotors, they would use highly loaded airscrews, basically similar to the propfans, as vertical lifters and forward thrusters.

Propfan-based configurations appear attractive as a design philosophy, since the same thrust generators can be used from VTOL maneuvers to high subsonic speeds up to $M \approx 0.8$.

Another advantage of this approach over conventional tilt-rotors would be more freedom in developing various configurations of aircraft—from monoplanes with variously shaped wings (sweep, taper, and thickness distribution) to tandems somewhat similar to those shown in Figs. 6 and 7, Ref. 43.

A rough sketch of the highly loaded tiltable airscrew, side-by-side configuration of a commercial transport aircraft of the 46,000-lb gross-weight class, where hovering disc loading is 100 psf, and wing loading is 127 psf, is shown in Fig. 4.21.

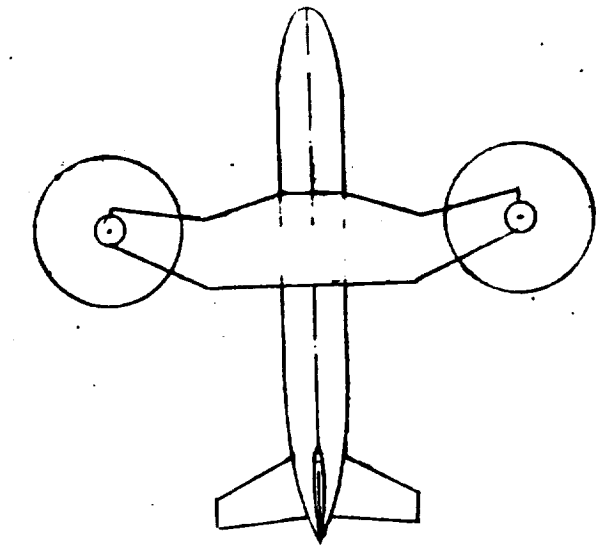

Figure 4.21 Rough sketch of a commercial high-disc-loading tiltable airscrew aircraft

An aircraft such as that shown in Fig. 4.21 can, in principle, be developed as an aerodynamically clean configuration where, in addition, a greater freedom of optimizing wing loading can be exercised. Consequently, various aspects of its forward flight performance might be quite good.

Unfortunately, the above-described type would also have many drawbacks—some immediately noticeable, and some that could probably be discovered during a more detailed study of the concept.

The so-called obvious objectionable characteristics can be listed as follows:

(1) Except for roll control, which can be achieved by differential thrust changes, pitch and yaw controllability in hover and transition poses a problem. In principle, pitch control may be achieved by the introduction of cyclic controls in propfan units, but this solution would complicate its design and increase its weight.

(2) A radical decrease in the diameter of the thrust unit (38 ft for the V-22 vs. 17.1 ft for a hypothetical aircraft with propfans) would also create problems in the case of CG travel, where possible limits are usually expressed as some fixed fraction of the airscrew radius.

(3) Cyclic control of the propfans may not solve the yaw problem. In this case, differential angular tilt of the nacelles could be provided but, obviously, at the price of increased complexity and weight.

(4) Pitch and yaw control of the tilt propfan aircraft could be achieved by installing tail or nose control thrusters of the open airscrew or shrouded type, but this solution carries its own drawbacks due to a more complex drive system, added structural weight, and generally negative effects on aircraft performance. A four-rotor tandem wing configuration (somewhat similar to the Curtiss-Wright X-14A) could be helpful in solving some of these problems.

(5) Download on the wing also appears, at first sight, as a potentially serious drawback.

Using a simplistic approach of determining download as vertical drag (D_v) experienced by the part of the wing immersed in the fully developed slipstream (radius equal to 0.707 of the rotor radius), one would write

$$D_v = \tfrac{1}{2}\rho(2\sqrt{w/2\rho})^2 S_{w_{dw}} C_{D_v} \tag{4.8}$$

where w, as always, is the airscrew disc loading, ρ is the air density, $S_{w_{dw}}$ is the wing area immersed in the downwash of both rotors, and C_{D_v} is the vertical drag coefficient of the wing.

$S_{w_{dw}}$ may be expressed as follows:

$$S_{w_{dw}} = (W/w_w)\sigma_{w_{dw}} C_{D_v} \tag{4.9}$$

where W is the aircraft gross weight, w_w is the wing loading, and $\sigma_{w_{dw}}$ is the fraction of the total wing area submerged in the fully developed slipstream.

Substituting Eq. (4.9) into Eq. (4.8), and simplifying, one obtains

$$(D_v/W) = (w/w_w)\sigma_{w_{dw}} C_{D_v}. \tag{4.10}$$

For example, for the aircraft shown in Fig. 4.21, w = 100 psf, w_w = 127 psf, and $\sigma_{w_{dw}}$ = 0.153. Assuming C_{D_v} = 1.3, the vertical drag to gross weight ratio of approximately 0.16 would be obtained. This, obviously, would lead to a higher download factor than the 1.12 for conventional tilt-rotors.

However, in reality, the whole phenomenon will be more complicated than that corresponding to the simple physico-mathematical model used in download estimates. First of all, the presence of the wing could generate a beneficial 'ground effect,' whose magnitude would depend on the relative elevation (height to airscrew radius ratio) of the disc plane above the wing.

Spanwise flow of the slipstream air along the wing toward the fuselage could also generate some lift on the wing. This benefit may be decreased should the flow from the left and right wings go upward at the fuselage. Some retractable vanes directing the flow horizontally or, still better, with some downward components, could prove beneficial.

It is obvious, hence, that a better understanding of all aspects of the interaction of both airscrews with the whole airframe is required before a final judgement regarding the download factor can be made.

This need of a better understanding applies equally well to the whole concept of the tilt propfan aircraft before one can decide whether application of highly loaded open airscrews would have any practical merit.

Fuel Consumption Aspects. It may be assumed that fuel consumption per pound of gross weight and hour of flight as well as fuel consumption per pound of gross weight and one nautical mile for the V-22 represent the present state of the art. Consequently, these characteristics vs. speed of flight can be considered as representative for the so-called first generation tilt-rotors basically similar to the V-22.

Taking a glance into the future, it becomes interesting to establish optimal boundaries, which would indicate possible improvements in fuel consumption aspects that may be made in coming generations of tilt-rotors, still using open airscrews as vertical thrust generators in VTOL maneuvers and forward thrusters in cruise.

It may be recalled that in horizontal flight, fuel consumption per pound of gross weight and one hour is

$$(FC_w)_{t_f} = 0.00307 V sfc/(L/D)\eta_{pr}\eta_{ov}. \tag{4.11}$$

Omitting, for simplicity, the subscript f and assuming that η_{ov} values for coming generations of tilt-rotors will be practically the same as for contemporary ones, fuel consumption per pound of gross weight and hour for the new generation aircraft (subscript n) with respect to those of the baseline (ie., V-22, subscript b) will be

$$(FC_w)_{t_n} = (FC_w)_{t_b}(sfc_n/sfc_b)(\eta_{pr_b}/\eta_{pr_n})[(L/D)_b/(L/D)_n]. \tag{4.12}$$

Looking at Eq. (4.12), one would see that in order to establish the optimal boundary of the $(FC_w)_t$ vs. speed of flight for future tilt-rotor generations, ratios appearing in parentheses and brackets should be determined.

The sfc vs. speed of flight at SLS for the V-22 was computed on the basis of total fuel flow and SHP data obtained from Boeing Helicopters. The results are shown in Fig. 4.22.

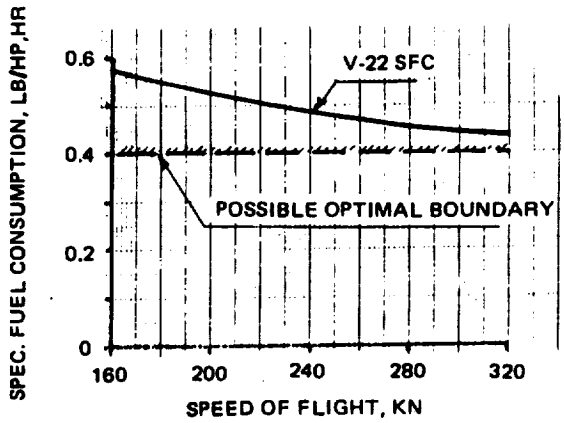

Figure 4.22 Possible optimal boundary, and sfc vs. speed of flight for the V-22

One can see from this figure that due to the engine partial-power setting—associated with lower power requirements at reduced flight speeds—the sfc goes up from about 0.43 to 0.58 lb/hp,hr. It is assumed, however, that in future designs, it would be possible, in principle, to achieve sfc = 0.4 lb/hr,hr throughout flight speeds from 160 to 320 knots. This assumption establishes the possible boundary for engine specific fuel consumption.

Variation of the propulsive efficiency vs. speed of flight and thus, Mach number, for the V-22 is assumed to be represented by the line marked 'tilt-rotor goal' in Fig. 4.11. It is also assumed that the line marked 'conventional' in the same figure would be representative for rotor-props of improved aerodynamics at Mach numbers higher than 0.5, but still not incorporating radical blade planforms as in the propfans. The required propulsive efficiency ratios needed in Eq. (4.12) will be obtained from these two trends.

L/D's will be established, assuming that the line marked 'Original V-22' in Fig. 4.20 represents the *L/D* vs. *q* of flight relationship, while the line marked 'CTR' in Fig. 4.18 is the best that can be expected in the coming generations of tilt-rotors.

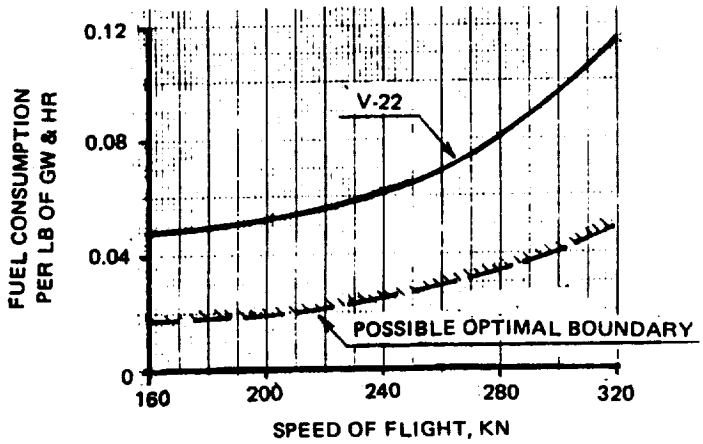

Figure 4.23 Possible domain of fuel consumption per lb of GW and hour for tilt-rotors in horizontal flight at SLS

Using the above-described approaches for determining various ratios in Eq. (4.12), the optimal boundary for $(FC_w)_t$ vs. speed of flight at SLS was established for (near) future tilt-rotors. Data from the predicted fuel flow vs. speed of flight at SLS for the V-22 (courtesy, Boeing Helicopters) were used to obtain the upper limit of the $(FC_w)_t$ vs. speed domain (Fig. 4.23).

Fuel consumption per pound of gross weight and nautical mile flown was computed (see Eq. (1.13)) from the relationship presented in Fig. 4.23 and shown in Fig. 4.24.

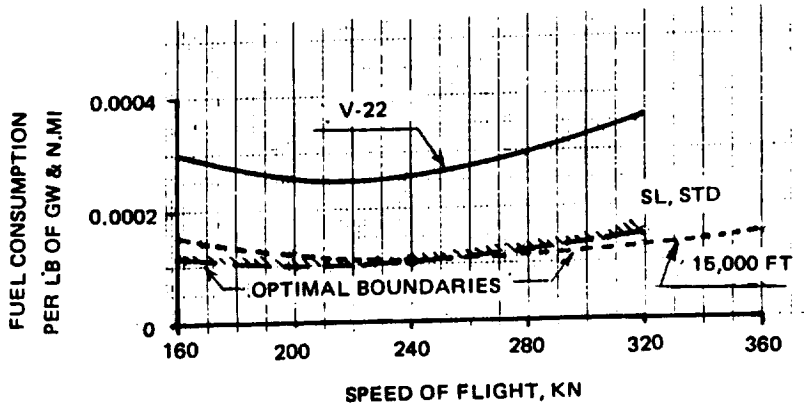

Figure 4.24 Possible domain of $(FC_w)_R$ vs. V value for tilt-rotors at SLS and optimal boundary at 15,000 ft

Here, again, the upper limit for the SLS case is represented by the line based on V-22 predictions, and the optimal boundary corresponds to the $(FC_w)_R$ vs. V relationship possible to achieve for a tilt-rotor having aerodynamic characteristics similar to those of the CTR aircraft depicted in Fig. 4.17, while sfc = 0.4 lb/hp,hr.

In Fig. 4.24, an additional optimal boundary for the 15,000-ft flight altitude is also indicated.

Looking at Figs. 4.23 and 4.24, one would realize that great improvements in fuel consumption aspects per pound of aircraft gross weight over those represented by the present state of the art (V-22) are potentially possible.

A degree of success in moving toward and, perhaps, reaching or even exceeding, the optimal boundaries of Figs. 4.23 and 4.24 would largely depend on the ability to achieve L/D vs. V levels as high as those shown in Fig. 4.18 for the CTR aircraft of Schneider and Wilkerson.

It should also be recalled that the optimal boundaries reflect assumptions that engine sfc = 0.4 lb/hp,hr can be maintained throughout the whole range of flight speeds shown in Figs. 4.23 and 4.24. Fulfilling, or approaching, this requirement does not appear impossible in future generations of turboshaft engines.

Finally, one should be reminded that in order to achieve the fuel consumption levels represented by the optimal boundaries, propulsive efficiencies should not be lower than some 82 percent. This looks like an achievable goal for the flying speeds up to 360 kn at 15,000 ft (M = 0.58) shown as the abscissa limit in Fig. 4.24.

Relative Weight Empty and Zero-Range Payload. Relative weight empty of the V-22 for VTOL operations is 0.67. It can be seen from Fig. 4.25 that similar $\overline{W}_e$ levels are forecasted, not only for the civilian version of the first generation tilt-rotors (CTR-22C) in Ref. 35, but also for future generations (CTR and TR, Ref. 43).

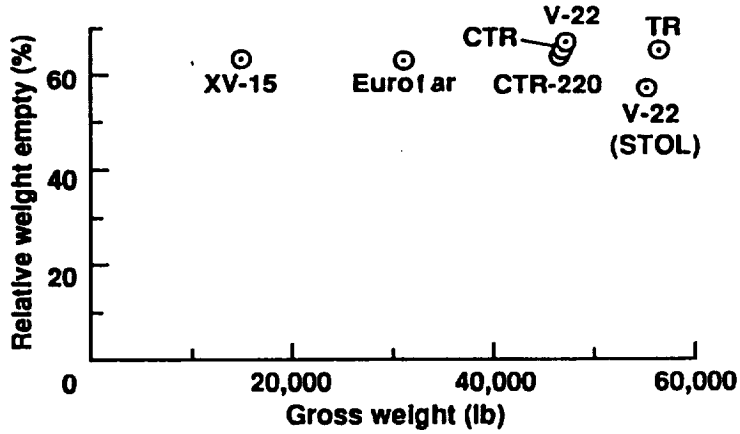

Figure 4.25 Trend in relative weight empty of tilt-rotors

It is hoped, however, that in future generations of tilt-rotors, further reductions in structural weight (say, about 6%) will be possible. Thus, $\overline{W}_e = 0.61$ is assumed as the optimal boundary for relative weight-empty trends.

The relative zero-range payload for current and next generation tilt-rotors will be 0.32, and the optimal value as foreseen for future generations could be 0.38.

Relative Payload vs. Range Trends. It would be of interest to have some idea of the progress in relative payload vs. range relationships that can be expected for future tilt-rotor generations in comparison with those representing the current state of the art (V-22). To achieve this goal, the relative payload vs. range relationship is computed from the following formula (see Sect. 1.2.3):

$$\overline{W}_{pl} = \overline{W}_{0_{pl}} - 1 + \exp[-(FC_w)R] \tag{4.13}$$

where, for current tilt-rotors, $\overline{W}_{0_{pl}} = 0.32$ and $(FC_w)_R = 0.00025$ lb/lb,n.mi, while for the optimal trend, $\overline{W}_{0_{pl}} = 0.38$ and $(FC_w)_R = 0.0001$ lb/lb,n.mi are assumed.

The $\overline{W}_{pl}$ vs. R relationships computed under the above-outlined assumptions (Fig. 4.26) would represent the best payload-carrying characteristics, as the aircraft are assumed to be flown at cruise speeds corresponding to the lowest fuel consumption per pound of gross weight and one nautical mile.

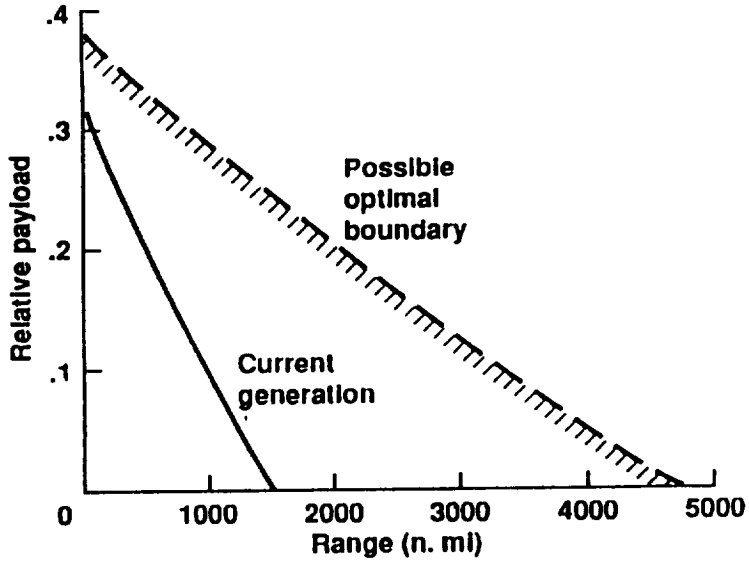

Figure 4.26 Relative payload vs. range trends for tilt-rotor aircraft

A glance at this figure will clearly indicate that dramatic improvements with respect to the current state of the art in payload-carrying capabilities are potentially possible to achieve for future generations of tilt-rotor aircraft. However, it is also clear that in order to attain, or at least approach, the payload-carrying characteristics indicated by the optimal boundary, substantial improvements should be made in the $(FC_w)_R$ levels, and relative weight empty reduced; i.e., relative zero-range payload increased.

Relative Ideal Productivity. It may be recalled that the relative ideal productivity associated with range (Section 1.25) can be expressed as follows:

$$PR_{id} = \overline{W}_{pl_R} V / \overline{W}_e \tag{4.14}$$

where $\overline{W}_{pl_R}$ is the relative payload that can be carried over range R, V is the cruise speed, usually in knots, and $\overline{W}_e$ is, as always, relative weight empty.

In order to determine the improvements that may be expected regarding the ideal relative productivity for future tilt-rotors when compared to the first generation aircraft as represented by the V-22 and similar configurations, the following computations were performed.

Assuming the $(FC_w)_R$ vs. V relationships as given for SLS in Fig. 4.24, relative payloads that can be carried over 200, 400, and 800 n.mi. were computed and, then taking $\overline{W}_e$ = 0.67 for the first generation, and 0.61 for future tilt-rotors, the relative productivities were determined from Eq. (4.14). The results were plotted vs. cruise speed for the three above-selected ranges (Fig. 4.27).

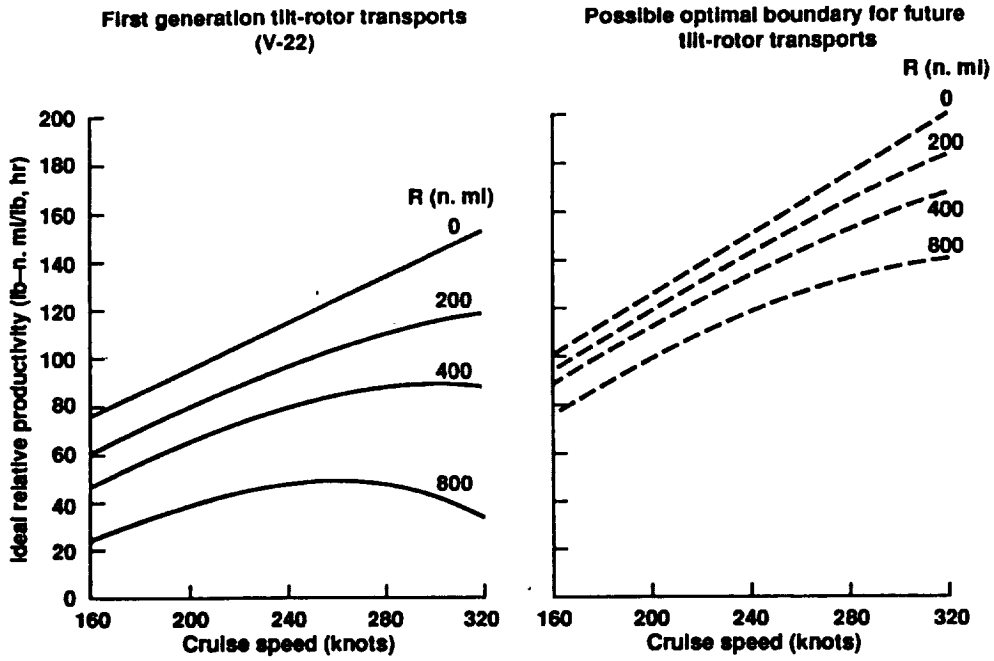

Figure 4.27 Relative ideal productivity

In order to give the reader some idea of how the PR_{id} vs. V character varies, $R = 0$ was added, although, per se, it obviously has no physical meaning.

Looking at Figure 4.27, one will note that for short ranges (e.g., 200 n.mi), the difference between the ideal relative productivity of the present generation of tilt-rotors and their optimal projections is not too great. Furthermore, it stems more from the assumed higher zero-range relative payload levels (0.38 vs. 0.32) than from the better values of $(FC_w)_R$ at the same speed. However, as the operational ranges become longer, the ideal relative productivity foreseen for future generations of tilt-rotors becomes much better than for the V-22 (for example, at R = 800 n.mi.).

It also appears from Figure 4.27 that over short ranges, the cruise speed value is one of the most important factors influencing the ideal relative productivity level. In real life, however, an a priori conclusion that faster aircraft will obviously be more productive may not be correct. It was shown in Ref. 1, for instance, that actual transport productivity depends on the block speed based on the time elapsed between consecutive transport operations. Consequently, a slower aircraft, as far as cruise speed is concerned, but using less time for ground operations, takeoff, and landing maneuvers, might show a higher block speed than the faster one.

4.2.4 Concluding Remarks

At present, the tilt-rotor, as represented by the Bell-Boeing V-22 configuration, is the only nonhelicopter open-airscrew type VTOL aircraft that has been developed to the stage of readiness for quantity production and incorporation into the Armed Forces. In addition, studies conducted jointly by Boeing Commercial Airplane Company, Bell Textron, Boeing Vertol, and NASA (Ref. 36) indicate that tilt-rotors having wings and dynamic systems basically the same, or generally similar, to those of the V-22 may find an application in the civilian transportation field. Efforts in Europe, as exemplified by the EUROFAR project—configurationally similar to the V-22—also indicate that even the so-called first generation of the tilt-rotor may represent aircraft which could find practical applications in the contemporary short-haul transportation system. Furthermore, smaller tilt-rotors similar to the V-15 can probably be applied as executive and commuter aircraft, as well as play a practical role in various specialized fields of applications (for example, medical evacuation and forestry).

However, one should realize that tilt-rotors representing the so-called first operational generation of these aircraft are characterizad by relatively low lift to effective drag ratios—although better than for compound and conventional shaft-driven helicopters, but worse than for fixed-wing turboprops of the same gross-weight class. As a result of this, the fuel consumption per pound of gross weight vs. speed of flight is, in general, inferior to that of fixed-wing transports of the same gross-weight class. This obviously means that fuel consumption per pound of gross weight and one nautical mile for tilt-rotors will be worse than for their conventional fixed-wing counterparts. This gap in the energy consumption aspect would widen still more, once unit of payload, instead of gross weight, is selected as a basis.

Finally, high-speed (dash capabilities) of the first-generation tilt-rotors are limited to some 320-340 knots, chiefly because of the deterioration of propulsive efficiency at $M > 0.65$ of rotors working as propellers.

It appears from very cursory studies that the lift to effective drag ratio of tilt-rotors representing first-generation configurations can be considerably improved through incorporation of winglets basically tilting in unison with the nacelles. But more study is required to evaluate the practical advantages of this concept.

For missions where high-velocity downwash in hover may be acceptable (for example, in urban transportation), application of the propfan or such similar type airscrews as lifting and propelling devices appears to open the possibility of pushing the high-speed barrier to $M \approx 0.8$. However, as in the case of winglets, more analytical and experimental studies are required before passing final judgement on the practical value of this concept.

In future generations of tilt-rotors using relatively lightly loaded ($w \leq 25$psf) rotors (which become propellers in the airplane mode of flight), considerable improvements in their lift to equivalent drag ratios can be achieved, as indicated by recent design studies. But potential improvements in high-speed capability would be minor. It appears that in order to achieve high-speed capabilities in tilt-rotors, it is necessary to abandon the idea of using geometrically unchanged, lightly loaded ($w \leq 25$ psf) rotors, which convert to propellers in the airplane mode of flight. Application of the variable diameter rotor (Ref. 44) appears as a half-measure toward

achieving this goal. But stopping and stowing the rotor, while forward propulsion is provided by the turbofan section of the convertible engine, seems to provide a more efficient solution to the high subsonic capability problem of tilt-rotors. This approach will be discussed in Section 4.4.

4.3 Tilt-Wing

4.3.1 Historic Perspective

It is difficult to establish the exact time when the idea was first proposed for a VTOL aircraft based on an open airscrew wing assembly tilting from the vertical prop axis position for vertical takeoff and landing operations, to the horizontal prop axis position for forward flight regimes. However, as far back as 1952, during the Convertible Aircraft Congress at Franklin Institute in Philadelphia, a rubber band powered model was demonstrated that performed transitions from hover to forward flight.

The first flight article of the tilt-wing type (U.S. Army VZ-2) was designed and built in the 1955-57 time period by Vertol (now Boeing Helicopters) under the direction of the author of this report who remained in charge of the program until the termination of the contract in 1964. P. Dancik served as chief design engineer from the beginning of the project through 1962. In that year, he was succeeded by J. Cline, who remained with the project until its completion. The coauthor of this report was also a member of the design team, responsible for the design of propellers and tail fans.

The VZ-2 (Boeing Vertol 76). This machine was conceived as an inexpensive flight-research aircraft with the single purpose of demonstrating the basic feasibility of the tilt-wing concept. This was intended to be done by proving that the aircraft could be flown with adequate control in hover, demonstrate transition to forward flight in the aircraft mode, and then go back through reversed transition, ending with a vertical landing.

Consequently, the original version of the VZ-2 incorporated a simple wing without flaps or any other lift increasing devices (Fig. 4.28). Pitch control in hover and transition consisted of a horizontal fan submerged in the horizontal stabilizer, while a vertical fan enclosed in a lift-augmenting ring provided yaw control. Rolling motions of the aircraft were generated through differential collective pitch control of the propellers. The powerplant consisted of a Lycoming T-53 turbine limited to 700 hp.

Continuous flight testing of the VZ-2 began in September 1957, and complete conversion was demonstrated on 15 July 1958.

Extensive modifications were performed to improve partial-power descent and to check the feasibility of eliminating vertical fan as a means of yaw control in hover and low-speed flight. A low-altitude ejection seat was also installed, and full-span flaps were incorporated (Fig. 4.29). The aircraft underwent an extensive flight-test program, chiefly at NASA Langley, that continued until 1964.

In addition to the flight-test program, full-scale wind-tunnel testing was performed at NASA Langley in 1961 to investigate the influence of various leading edge lift-increasing devices on potential improvements of partial-power descent characteristics.

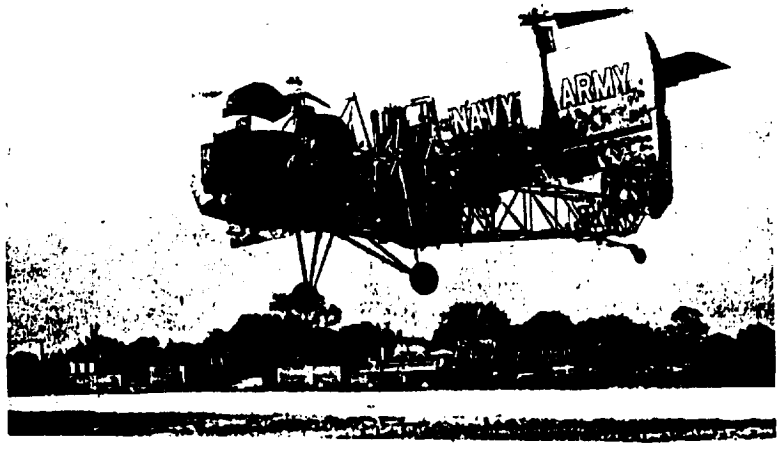

Figure 4.28 Original version of the Vz-2 aircraft

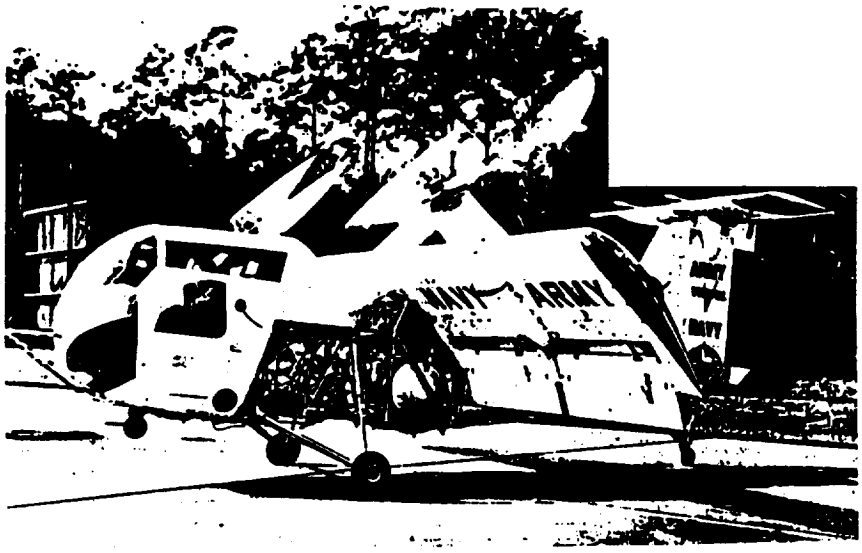

Figure 4.29 Final version of the VZ-2

A brief summary of the VZ-2 development and testing program can be found in Ref. 45, where a list of publications related to this program is also included.

The whole program of the development and testing of the VZ-2 was, in general, quite successful; thus encouraging the design and construction of tilt-wing aircraft in the U.S. and Canada, as well as design studies in England and other countries.

Chance Vought-Hiller-Ryan VHR-447 (Military Designation, the XC-142A). The design of the XC-142A aircraft won a competition in September 1961 for a VTOL transport for the U.S. Armed Forces, and five prototypes were ordered.

The XC-142A was a large four-engine, four-propeller military transport aircraft with a maximum STOL takeoff weight of 44,500 lb (Fig. 4.30).

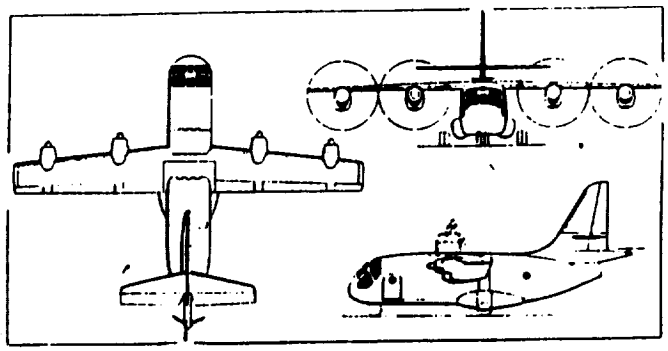

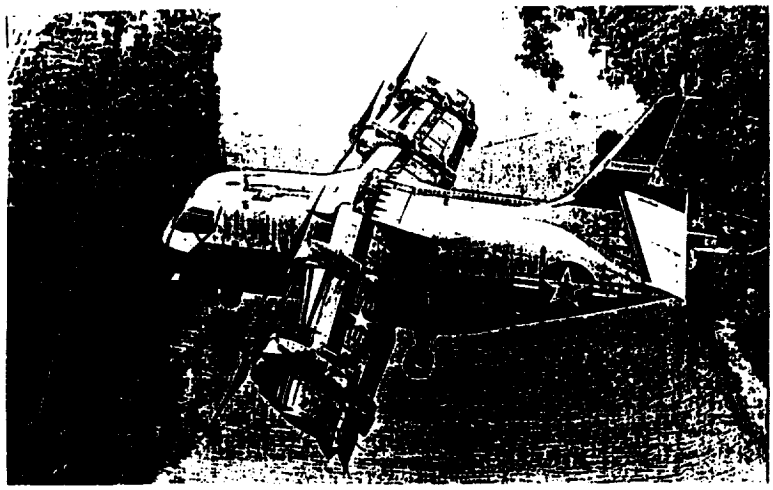

Figure 4.30 XC-142A large military transport VTOL aircraft

The four T64 turboprop engines propelled conventional airscrews and a horizontally-mounted three-blade variable-pitch tail rotor through a system of cross-shafting and gear trains, making it possible to maintain flight on any two engines in an emergency. The wing was able to rotate through an angle of 100 degrees, giving the XC-142A the ability to hover in a tail wind.

During VTOL flight, roll control was achieved by means of differential collective propeller pitch, yaw control by means of ailerons working in the propeller slipstream, and pitch control by means of the variable-pitch tail rotor. During transition, a mechanical mixing linkage integrated the VTOL control system with conventional ailerons and tail control surfaces in correct proportions as a function of the wing tilt angle. In normal cruising flight, control was achieved by conventional control surfaces, with the tail rotor locked.

A dual four-function stabilizer system ensured stability during IFR flight, hovering, and transition.

The flight of the XC-142A was successfully completed on 29 September 1964 and, after the ensuing flight test program, it appeared that production orders would follow, but due to changes in requirements, and political and fiscal aspects, the program never materialized[7].

Canadair CL-84. After preliminary studies, which began in 1956, Canadair and the Canadian Government announced in February 1963 that a decision had been made to go ahead with further engineering work, [redacted] development and construction of the Canadair CL-84 prototype. Construction was started in November 1963, and the prototype was rolled out in December 1964. The first flight on 7 May 1965 was in the hover mode. In December 1965, a series of flights in the conventional mode were made, showing that there were no significant problems at either end of the transition regime. On 17 January 1966, the first complete transition was accomplished[7].

The aircraft can be defined as a medium size (VTOL, 12,200 lb GW, and STOL, 14,700 lb GW) tilt wing (Fig. 4.31) capable of performing the following tasks: reconnaissance and surveillance, tactical-support, transport, helicopter escort, attack, casualty evacuation, search and rescue, antisubmarine warfare, liaison and communications, and city-center to city-center transport.

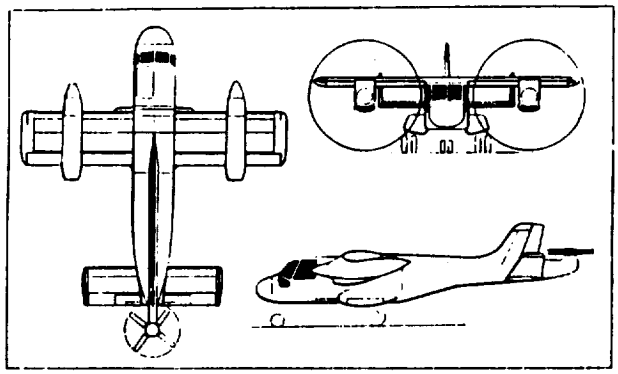

Figure 4.31 CL-84 tilt-wing aircraft

In conventional flight, the CL-84 achieved a speed of 265 kn in level flight at 8000 ft (2440 m) and carried out acrobatic 360-degree rolls in less than five seconds.

During 1966, the CL-84 performed three live demonstrations of various hoisting in simulated air rescue from land and water.

In spite of quite successful flight demonstrations for the U.S. Navy, the aircraft was never ordered into serial production, although attempts to regenerate the government's interest have been undertaken; some quite recently.

Hiller X-18 (Fig. 4.32). The Hiller X-18 had two contrarotating propellers of 16.08-ft diameter, and was powered by two Allison YT40-A-14 turboprop engines rated at 5850 shp each. Exhaust from a single Westinghouse J34WE-36 turbojet engine was used for pitch control It was first flown in November 1959. On its 20th flight, propeller control malfunctions resulted in an unintentional roll and spin. The pilot managed to recover the aircraft and land it safely, but the contract was terminated. Nevertheless, experience gained from the development of the X-18 contributed to the award of the CX-142A contract to the Chance Vought-Hiller-Ryan Team.

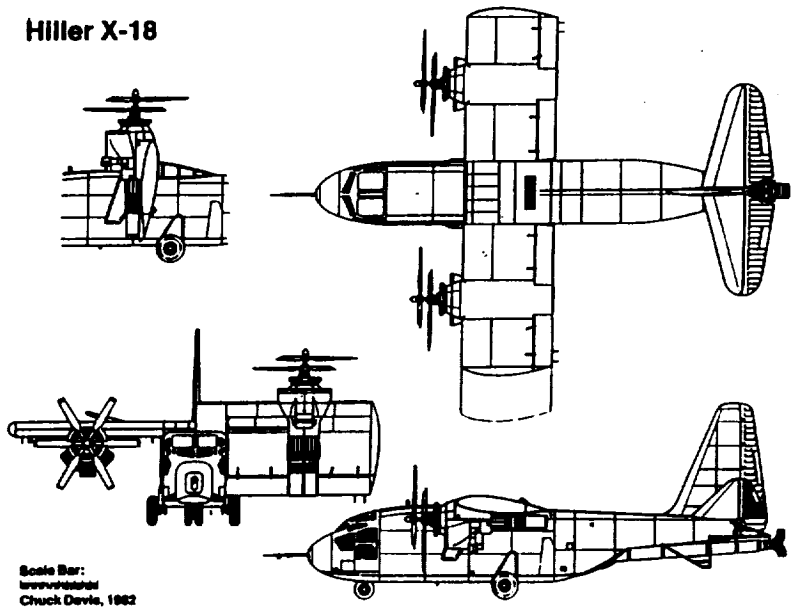

Figure 4.32 The Hiller X-18

At Boeing Vertol, serious design efforts were made to create tilt-wing aircraft in response to Armed Forces competitions for a large military transport[46] (eventually won by The Chance Vought-Hiller-Ryan team with the CX-142A design) and for the AAFSS mission. An artist's sketch of the aircraft proposed for the AAFSS mission is shown in Fig. 4.33[47].

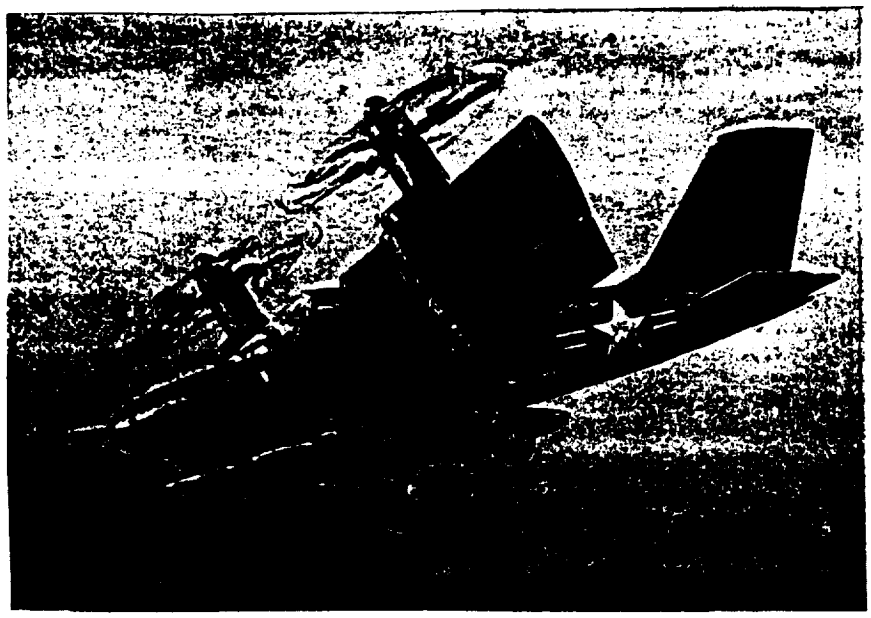

Figure 4.33 Artist's Concept of Boeing Vertol entry into AAFSS competition

Ishida/DMAC TW-68. According to Ref. 48, the Ishida Group of Nagoya, Japan, plans to build a new tilt-wing transport aircraft in the U.S. if development work, now under way, is completed successfully.

The aircraft, undergoing extensive design and wind-tunnel studies (Figs. 4.34 and 4.35), will be a 14-passenger transport powered by two 2200 shp turboprop engines capable of 300-350-kn cruise speed and a range of about 600 n.mi.

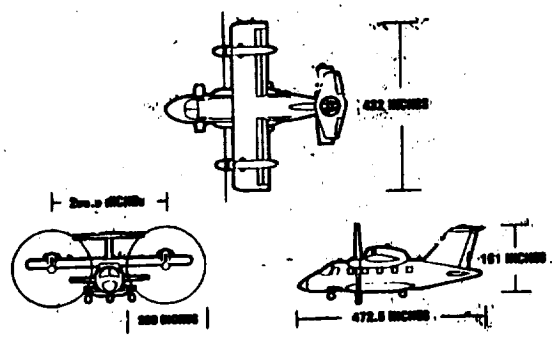

Figure 4.34 Three-view drawing of Ishida DMAC TW-68 tilt-wing transport

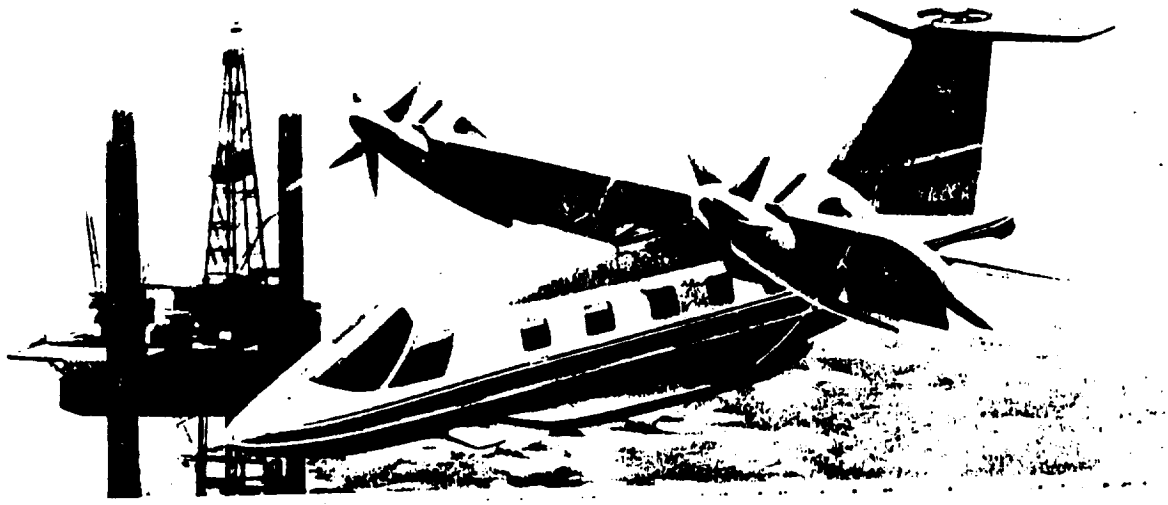

Figure 4.35 Artist's concept of the TW-68 with wings in a partially tilted position

The basic design philosophy of the DMAC TW-68 was summarized as follows[48]:

"Tiltrotor aircraft are essentially helicopters, with all of the advantages and disadvantages of a helicopter. They have helicopter rotors, helicopter controls, and helicopter vibrations."

"The TW-68 is a turboprop aircraft with beta controls on the propellers and a wing-tilt system. It can hover like a helicopter, although it is not as efficient in hover as a helicopter, and it can fly like a turboprop, and in that regime it is much more efficient than a tiltrotor in forward flight."

Tip speed in hover will be about 750 fps and in cruise, will come down to 650 fps.

Summary of Data. The most important characteristics of actual tilt-wing aircraft are summarized in Table 4.3, which also contains data related to hypothetical tilt-wings which will be discussed later.

TABLE 4-3

PRINCIPAL CHARACTERISTICS AND PERFORMANCE OF ACTUAL AND HYPOTHETICAL TILT-WING AIRCRAFT

	ACTUAL				HYPOTHETICAL
ITEM	BOEING VZ-2	HILLER X-18	LTV XC 142A	CANADAIR CL-84	CTW-22C-100
APPLICATION	FLIGHT RESEARCH	TRANSPORT TEST BED	MILITARY TRANSPORT	MILITARY TRANSPORT	PASSENGER TRANSPORT
POWER PLANT	LYCOMING T-53 (700 HP LIMIT)	ALLISON* YT-40-A-14	GE T-64	LYCOMING T-53	
NO. OF ENGINES	1	2	4	2	4
TOTAL T.O. SHP	700	11,700	11,400	2,800	20,000
PROPELLER					
RADIUS, FT	4.75	8.04	7.75	7.00	6.05
NO. OF BLADES	3	2X4†	4	4	8
ARTICULATION	FLAPPING	RIGID	RIGID	RIGID	RIGID
TIP SPEED, FPS	700				800/680
PROPELLER RPM	410				1263/1074
DISC LOADING, PSF	23.84	81.2	52.69		100
IND. VELOCITY, FT/SEC	70.77	130.6	105.21	85.06	149.9
WING					
SPAN, FT	24.88	48	67.5	33.33	58
AREA (TOTAL) SQ. FT	118.18	528	524.8	233.3	389
ASPECT RATIO	5.24	4.36	8.68	4.16	8.6
EXTERNAL DIMENS.					
OVERALL LENGTH, FT	26.12	6.3	58.33	45.54	72
OVERALL HEIGHT, FT	9	24.6	26.1	14.58	21.5
WEIGHTS					
MAX. GW, LB	3,723	33,000	37,474	12,200	46,000
WEIGHT EMPTY, LB	3,329	27,052	22,545	7,300	30,210
RELATIVE WEIGHT	0.89	0.85	0.60	0.60	0.656
WING LOADING, PSF	29.6	62.2	71.4	52.3	118
INST. POWER LOADING LB/SHP	5.32	2.82	3.29	4.36	2.3
PERFORMANCE					
FLT. SPEED AT S.L., KN		220	355	287	470
FLT. SPEED AT 20,000 FT					488

*PLUS SINGLE WESTINGHOUSE J-34-WE-36 TURBOJET FOR PITCH CONTROL
†CONTRAROTATING

Fig. 4.36 is shown in order to get a better idea regarding trends in the disc and wing loadings of tilt-wings.

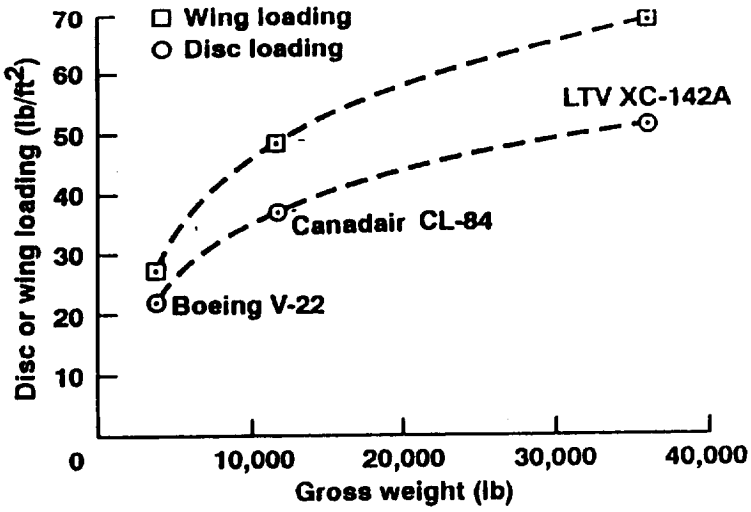

Figure 4.36 Trends in disc and wing loadings of actually built tilt-wing aircraft

4.3.2 Remarks re Basic Design Philosophy of Tilt-Wings.

New Opportunities. Relatively recent efforts directed toward development of prop-fans (PF) and open airscrews in general, capable of efficiently operating at elevated subsonic Mach numbers, have opened new opportunities for tilt-wing configurations. There appears a possibility of using the same thrust generators for vertical takeoffs and landings to cruise speeds up to $M \approx 0.8$, or even slightly higher.

However, in order to take advantage of this new situation, designers and concept formulators of tilt-wing aircraft should free themselves from "the helicopter complex," and not try to visualize the tilt-wing performing tasks that can be much better accomplished by helicopters or tilt-rotors. Instead, they should direct their efforts toward the creation of the most efficient transport machine with true vertical takeoff and landing capabilities. In other words, the aircraft should have flight characteristics enabling them to safely perform operationally required approaches, initial climb (up to conversion in the airplane configuration) under all weather conditions, and execute actual VTOL maneuvers under specified surface wind conditions.

Controls in Hover. The last requirement translates into the need of effective aircraft controls in hover and near hover. It appears that differential collective pitch control of the airscrews should provide, as in the past, the most effective means of roll control.

As demonstrated on the VZ-2 and then later used on all actually built tilt-wing aircraft, the differential deflection of ailerons submerged in the airscrew slipstream should provide adequate yaw control.

Finding a relatively simple and, at the same time, effective pitch and c.g. travel control appears to be the most challenging task in the whole domain of hovering and near hovering controls of the tilt-wing. Three methods of pitch control of tilt-wing aircraft in hover and transition may be taken into consideration: (1) the use of tail propellers or fans, (2) introduction of cyclic pitch change in propellers or propfans, (3) Churchill geared-flap concept.

The first method of pitch control was used in VZ-2, XC-142, and CL-84 tilt-wing aircraft, and is also anticipated for the TW-68. The second, under the name of monocyclic pitch control was proposed by Boeing Vertol Corporation in competition for the Advanced Aerial Fire Support System (AAFSS), and triservice VTOL transports[4,6] (Fig. 4.37). Nevertheless, this concept was not brought to the hardware stage. In addition, the level of moment available for pitching motions and/or c.g. travel control is usually related to the airscrew radius. Consequently, this type of pitch and/or c.g. travel control will be less effective for the high disc loading configuration than for helicopters and conventional tilt-rotors.

Therefore, the most conservative method of a tail propeller unit driven either by an interconnecting shaft system or by hydraulic motor, appears at present as the only practical approach for single-wing tilt-wings. In the aircraft mode, the tail unit will be covered by folding doors.

The problem of pitch and c.g. travel control for the tandem-wing configuration can easily be solved through differential collective pitch variation of the front and rear airscrews. However, this solution will entail the even more difficult problem of mechanical interconnection of airscrews on both wings.

Since the basic justification for the development of a tilt-wing aircraft would be its potential capability of high-speed cruise, the whole configuration should be oriented toward this goal. Wings should be adapted to high-speed regimes of flight. Consequently, in external appearance, modern tilt-wings should, in principle, be similar to modern subsonic turbofans and propfans as far as their fuselage and wings (planform and airfoils) are concerned. Unfortunately, it appears that direct adaptation of the swept-back, moderately tapered, wings of contemporary subsonic transport configurations to four-propeller, tilt-wings having a disc loading of about 50 psf or lower is impractical, as can be seen from the following considerations.

In order to submerge the whole wing in the propeller slipstream (which is essential in tilt-wing concepts) and, at the same time, assure a wing aspect ratio suitable for aircraft performance, the installation of multiple propfan units per half-span is preferable. A single propfan unit (i.e., two per aircraft) seems to be impractical, considering the fact that the diameter of the propfan is, at the present time, limited to the already tested or, at least, designed high-speed props.

To gain a further insight into the sweep-wing problem and, later, performance aspects, a commercial version of the Bell/Boeing tilt-rotor V22, designated the CTR-22C, was used as the aircraft with which the tilt-wing configuration will be compared.

Whereas the disc loading of the CTR-22C is 20.3 psf, the tilt-wing baseline configuration, designated as CTW-22-50 will feature a disc loading of 50 psf. This figure is the maximum disc loading which, as per wording of the contract, is to be used in this study. However,

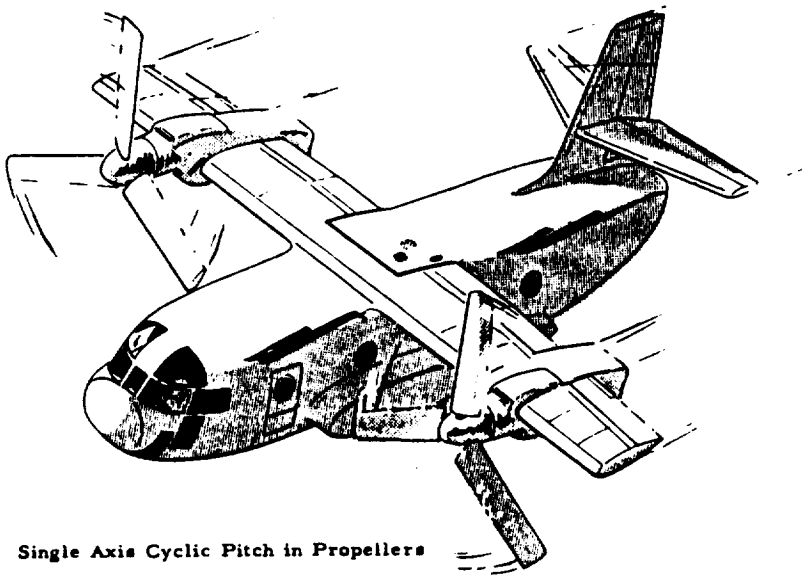

Single Axis Cyclic Pitch in Propellers

The pitching moment on the aircraft due to cyclic pitch in a flapping propeller is made up of two components:

1. The hinge offset component.
2. The thrust vector tilt component.

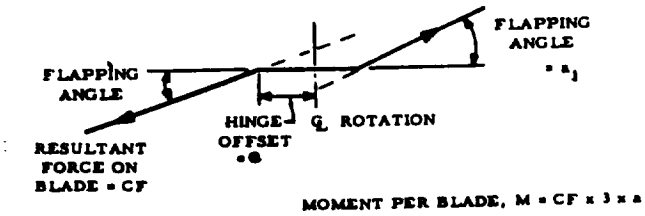

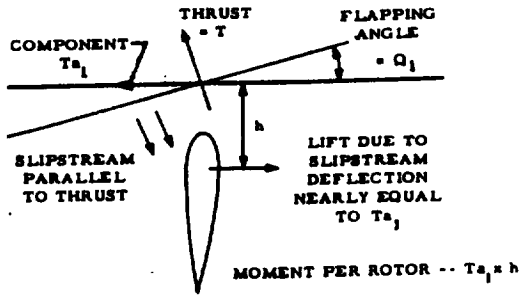

Figure 4.37 Artist's sketch of Boeing Vertol Model 137 tilt-wing aircraft and explanation of the monocyclic control principle

for the sake of an evaluation of the effect of disc loading on performance of tilt-rotor aircraft, higher disc loadings (75 psf and 100 psf) were used, leading to three versions of hypothetical tilt-wing aircraft differing in propfan size and wing geometry (see Table 4.4).

TABLE 4.4

TILT-WING CTW-22 CHARACTERISTICS
(Disc Loading 50, 75, and 100 psf, and GW = 46,000 Lb)

AIRCRAFT	WING AREA FT^2	WING SPAN FT	WING AR	WING LOADING PSF	P.F. DIA. FT	DISC AREA FT^2	DISC LOADING PSF	ESTIMATED WE TREND LB	TOTAL WET AREA* FT^2
CTW-22-50	697	76	8.3	66	17.1	920	50	33,000	5300
CTW-22-75	494	64.5	8.4	93	14.0	613	75	31,500	4900
CTW-22-100	389	58.0	8.6	118	12.1	460	100	30,000	4700

*Approximate

All three aircraft will be of the same gross weight (46,000 lb), and will use the same fuselage as the CTR-22C (except for modifications in the tail portion). However, they will differ in the disc loading of lift/propulsion units as well as in the wing loading.

Assuming a LE sweepback of 17°, the location of the tilt axis at 33 percent, and a wing taper ratio of 2.6 for the 50 psf disc-loading version, we arrived at the configuration shown in Fig. 4.38 which, for the same landing-gear height and width as in the CTR-22C, becomes impractical since, in the wing-up position, the wing tips will dig into the ground under conditions of ground rocking or slope landings.

Attempts to solve the wing-tip clearance problem by making the landing gear taller would require an unacceptable lengthening of the landing gear (Fig. 4.39).

With a sweepback as shown in Fig. 4.38 ruled out in tilt-wing aircraft featuring the above-described geometry and disc loading of 50 psf, the forward swept-wing configuration was investigated with negative results. Looking at the wing planform shown in Fig. 4.40, one will note that the wing tilt axis would be moved well outside of the wing planform, rendering this approach impractical.

Kuchemann, In Ref. 49, Ch. 5 indicated that good high subsonic performance can be obtained with backward-forward swept wings. Consequently, cursory attempts were made to adopt this approach for tilt-wing aircraft (Fig. 4.41).

Once the idea of a forward-backward swept wing plan is accepted, there appear many possibilities for developing shapes best suited for the tilt-wing configuration (Fig. 4.42).

CTW-22-50

Hypothetical tilt wing A/C with four props and tail prop control. Counterpart of tilt rotor CTR-22C

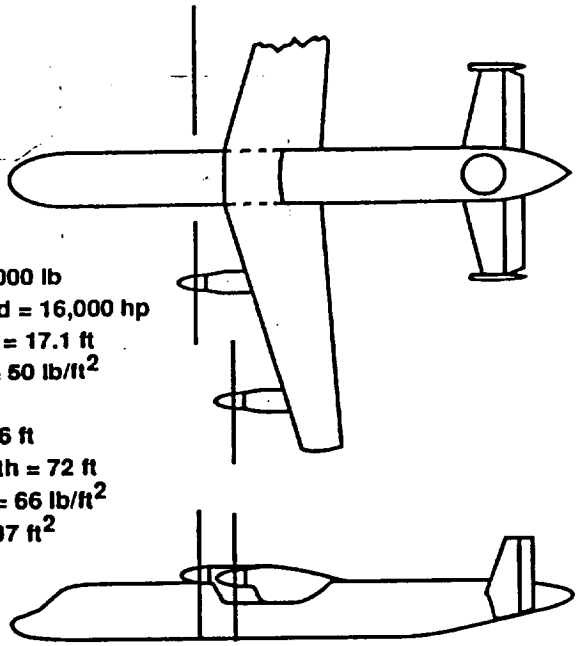

VTO GW = 46,000 lb
Power installed = 16,000 hp
Prop diameter = 17.1 ft
Disc loading ≅ 50 lb/ft^2
Wing AR = 8.3
Wing span = 76 ft
Fuselage length = 72 ft
Wing loading = 66 lb/ft^2
Wing area = 697 ft^2

Figure 4.38 Hypothetical tilt-wing aircraft with 50 psf disc loading

Front view of CTW-22-50 with wing up

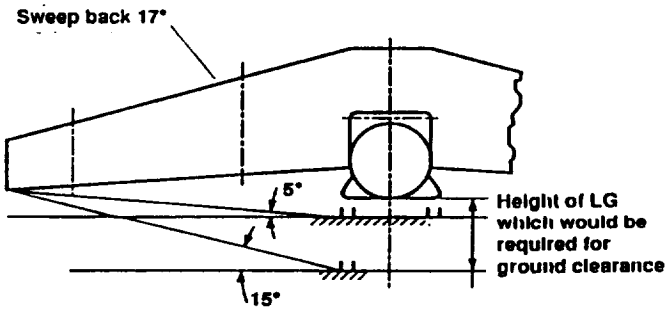

Figure 4.39 Proximity of wing tips to the ground when wing is in the vertical position

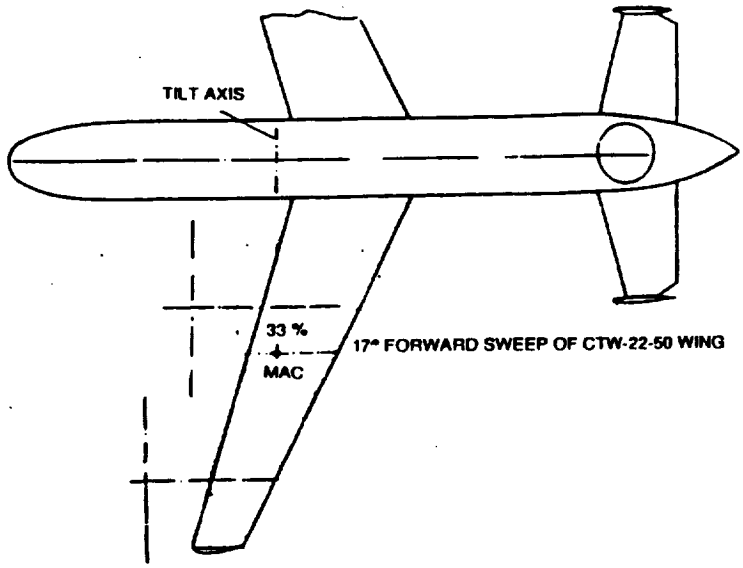

Figure 4.40 Sketch showing impracticality of tilt-wing forward-sweep concept

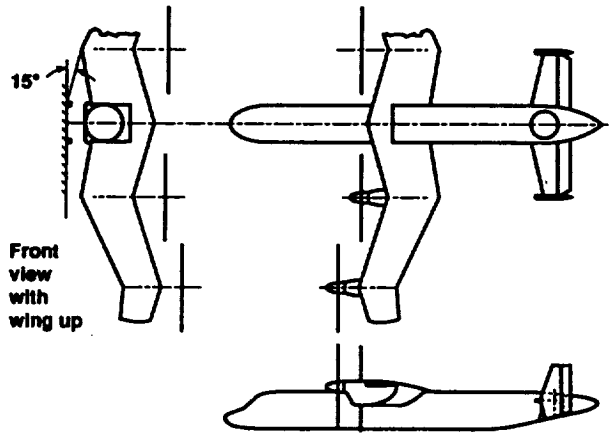

Hypothetical tilt wing A/C	Prop diameter = 17.1 ft
CTW-22-50 with "W" wing	Disc loading = 50 lb/ft^2
with four UDF units and	Wing area = 697 ft^2
tail prop control.	Wing AR = 8.3
Counterpart of tiltrotor CTR-22C	Wing loading = 66 lb/ft^2
VTO gross weight = 46,000 lb	Wing span = 76 ft
Power installed = 16,000 hp	Fuselage length = 72 ft

Figure 4.41 Four-prop, multiple-sweep, tilt-wing configuration

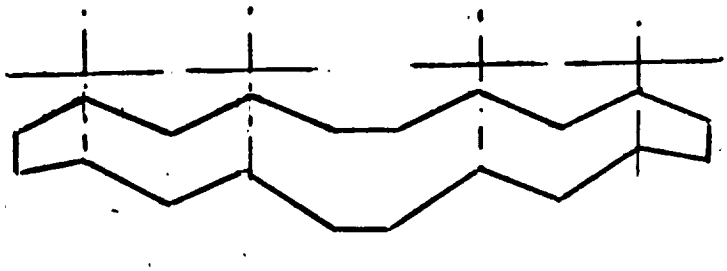

Figure 4.42 Possible wing planform for tilt-wing aircraft with high subsonic speed capabilities

It should be realized, however, that at present there is little, if any, experimental material on such shapes, especially on the problems of propeller slipstream/wing interaction in situations reflecting transitions between hover and horizontal flight and vice versa, as well as partial-power descent. In conjunction with this latter point, special studies would be needed regarding the behavior of the leading and trailing edge lift-increasing devices on multi-sweep wings. Structural aspects of such wings should also be examined.

One may note that the previously-discussed wing-tip clearance problems pertain to tilt-wing aircraft with a disc loading of 50 psf. Once high disc loadings of, say, 100 psf is featured as in the CTR-22-100 tilt-wing shown in Fig. 4.43, the wing sweepback becomes practical and even attractive, considerably simplifying the wing structure and interconnecting shaft systems.

Keeping the same LE sweep (i.e., 17°), it became possible to obtain a reasonable wing tip to ground clearance of 15°, while still conserving the LG feature of the CTR-22C. A slight increase (measured in inches) of height and width of the LG would considerably increase the tilt angle.

Thus, the smaller wing span of this aircraft provides acceptable lateral tilt angles with the wing in the up position. Furthermore, the weight empty of the aircraft is considerably smaller (about 3000 lb less than for the 50 psf disc-loading version). This weight difference results from a substantial wing weight saving (wing area of 389 sq.ft vs. 694 sq.ft) and lighter propfan units (diameter, 12.1 vs. 17.1 ft), in spite of a higher weight of the powerplant (20,000 hp vs. 16,000 hp).

A question may be asked concerning the practical use of tilt-wing aircraft having such a high disc loading. One possibility which is open is intercity high-speed transport. A hard surface heliport landing pad would not be affected by high downwash velocity (149.9 ft/sec for the 100 psf disc loading vs. 102.5 ft/sec for 50 psf), while the lower weight-empty of 100 psf disc-loading aircraft will contribute to a higher payload or range.

As a result, it was decided to examine only the 100 psf disc-loading version in some detail.

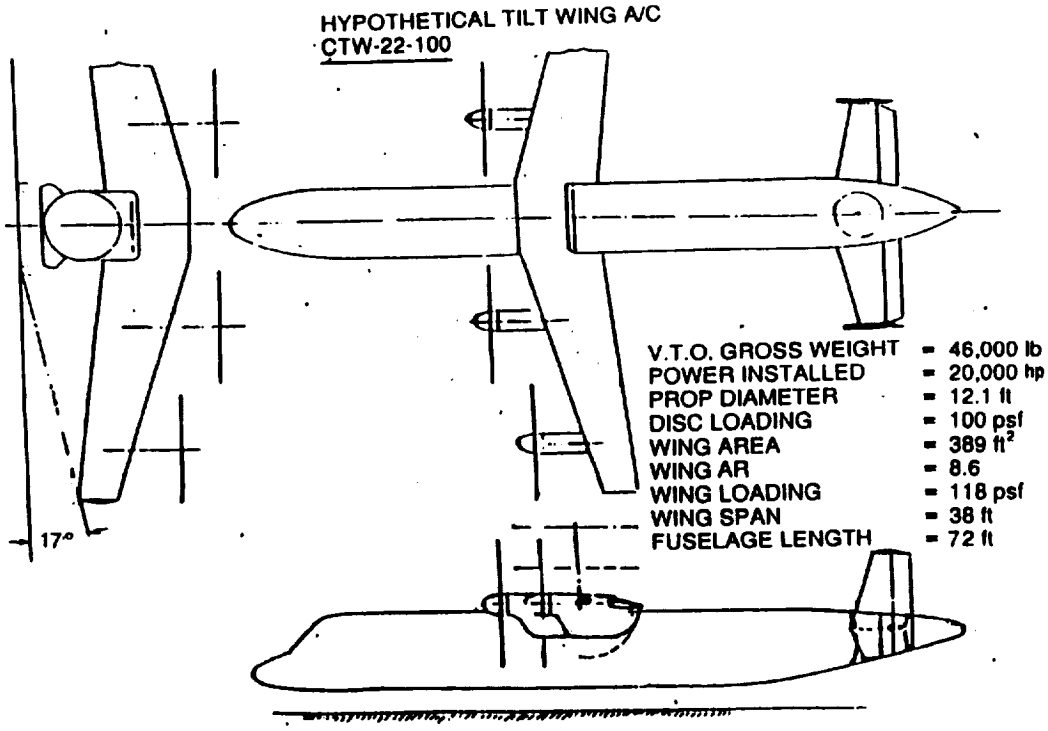

Various performance aspects of tilt-wing aircraft will be discussed in the following sections.

4.3.3 Hover

As for all other open-airscrew VTOL concepts, the shaft horsepower required per pound of aircraft gross weight in hover OGE will be

$$\overline{SHP_h} = 0.0264 k_v^{3/2} \sqrt{w/\bar{\rho}}/FM\eta_{ov}. \tag{4.15}$$

It would be of interest to examine the values of k_v, FM, and η_{ov} that can be expected for tilt-wing configurations.

Download Factor, k_v. Assuming that the whole exposed wing area ($S_{w_{exp}}$) is submerged in the fully developed airscrew slipstream, the resulting vertical drag can be expressed as follows:

$$D_v = wS_{w_{exp}}C_{D_0} \tag{4.16}$$

where w is the airscrew disc loading, and C_{D_0} is the wing drag coefficient at $C_L \approx 0$.

Dividing both sides of Eq. (4.16) by the gross weight W, one obtains

$$D_v/W = (w/w_{w_{exp}})C_{D_0} \tag{4.17}$$

where $w_{w_{exp}}$ is the exposed wing area loading.

The old 'rule of thumb' resulting from conversion and partial power descent requirements in the tilt-wing design was that the wing chord should be approximately equal to the propeller radius. Although with more effective lift-increasing devices, this ratio could probably be reduced to lower values. It will be conservatively assumed here that the wing chord $c_w = R$. Further assuming that the wing is rectangular, its exposed area can be expressed in terms of the propeller radius as follows:

$$S_{w_{exp}} = 2nR^2. \tag{4.18}$$

where n is the number of propellers.

The corresponding total disc area will be

$$S_{disc} = n\pi R^2. \tag{4.19}$$

In Eq. (4.17), one can see that

$$w/w_{exp} = S_{w_{exp}}/S_{disc} = 2/\pi \tag{4.20}$$

and thus, Eq. (4.17) becomes

$$(D_v/W) = 0.64C_{D_0}. \tag{4.21}$$

Since C_{D_0} would probably be <0.01, one can see from Eq. (4.21) that the relative download value in the tilt-wing will probably not exceed 0.6 percent. Consequently, it may be assumed that the download factor $k_v < 1.006$ and, thus, the download problem is negligible.

Figure of Merit. It should be emphasized that the following discussion of figure-of-merit aspects should be considered as only a rough guide regarding the possibilities of adapting current propfan technology to tilt-wing configurations. More analytical and experimental studies would be required to obtain a better insight into the possibilities and problems of designing a propfan that would be efficient in hover, and exhibit high propulsive efficiency in forward flight.

As far as future tilt-wings are concerned, the most attractive feature of the propfan concept is its high propulsive efficiency up to a flight speed of $M \approx 0.8$. Thus, the necessity of maintaining high η_{pr} values would shape the design philosophy of tilt-wing airscrews.

However, for the new generation of tilt-wings, as well as for conventional tilt-rotors, the problem is to design an open airscrew which would work efficiently both in hover (high figure of merit) when the total thrust of the airscrews is about equal to the aircraft gross

weight, and in the airplane mode of flight (high propulsive efficiencies) when the total required airscrew thrust represents only a small fraction of the gross weight (Fig. 4.44).

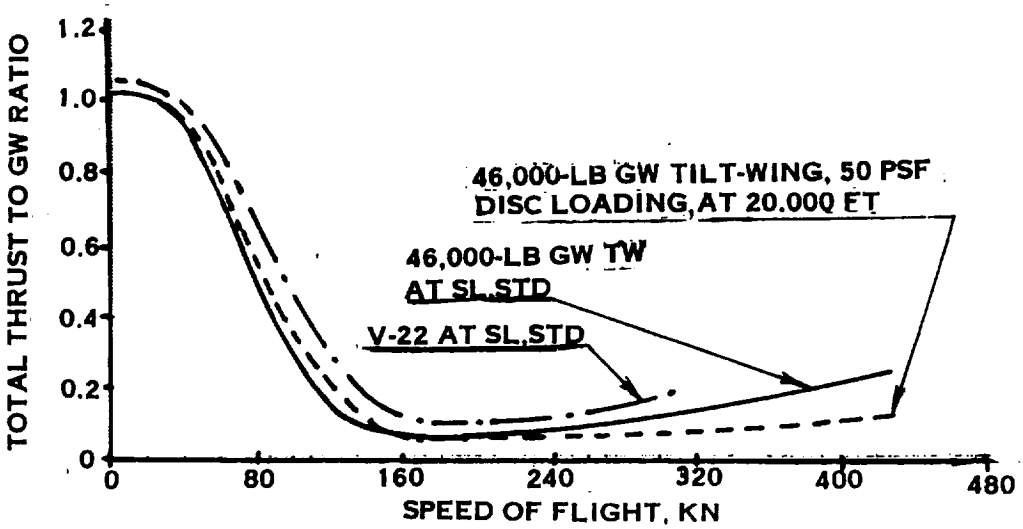

Figure 4.44 Example of total airscrew thrust to GW ratio vs speed of flight for tilt-wing

This, obviously, means that sectional lift coefficients along the blades would considerably vary between the vertical and airplane regimes of flight. Reduction in the airscrew tip speed could partially alleviate that problem. But, if one wants to avoid the complexity and weight of a gearshift arrangement, the possible tip-speed reductions would not go much above the 15 percent variation presently available in the V-22.

With this in mind, tilt-wing airscrews must be designed with the constraint of limited operational tip-speed variation.

Achieving high propulsive efficiency at elevated subsonic flight Mach numbers favors rather low ($c_l \approx 0.2$) sectional lift coefficients in order to avoid drag rise due to compressibility effects. However, the sectional lift coefficients cannot be too low, as the c_l/c_d ratio becomes very low, even in the absence of compressibility.

Should the blade sectional lift coefficients be about 0.2 when the thrust of the airscrews is equal to, say, one-tenth of the gross weight, and tip speed amounts to 85 percent of that in hover, then they would have to grow to $c_l \approx 0.2 \times 10 \times 0.85^2 = 1.44$ or even higher in hover and vertical flight maneuvers. The $c_l \geq 1.44$ coefficient is, unfortunately, impossible for the thin airfoil sections required for propfans capable of operating efficiently in the high Mach number environment.

PAGE 151 INTENTIONALLY BLANK

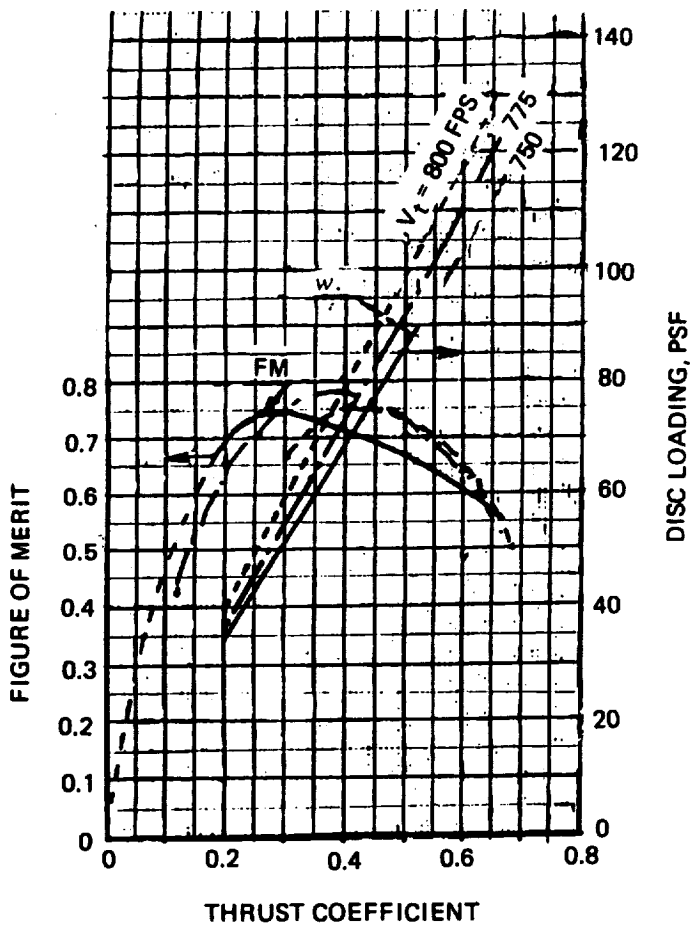

Figure 4.46 Examples of Figure of Merit and SLS disc-loading levels vs. thrust coefficient values for propfans

Because, unlike tilt-rotors, for tilt-wings there is little influence of the wing on the airscrew, data for the isolated propfans can be considered as being directly applicable to the aircraft installation. Thus, looking at Fig. 4.46, one may expect that for propfans having disc loadings optimized for hovering, maximum figure-of-merit levels between 0.75 and 0.78 may be expected. Therefore, FM = 0.73 may be assumed as the operational average value. One can also see from Fig. 4.46 that, assuming a hover tip speed of 800 fps, the optimal disc loading for SLS operations would be between 50 and 90 psf.

Propfan Power to Shaft Power Ratio. In the tilt-wing as well as tilt-rotor, the overall transmission efficiency level (η_{ov}) would reflect (a) mechanical losses in the transmission system, and (b) power needed for running instruments and accessories. However, in the tilt-wing case, power required to operate the pitch fan would represent an additional source of lost power.

Power lost in the transmission system between engine powerplant shafts and airscrew(s) is reflected in the transmission efficiency (η_{tx}) values. Assuming the same tip speed for the two configurations, rpm for the four-prop tilt-wing vs. rpm of the two-rotor tilt-rotor of the same gross weight will be

$$\text{rpm}_{tw} = \text{rpm}_{tr}\sqrt{2w_{tw}/w_{tr}} \tag{4.26}$$

where the subscripts *tr* and *tw* mean tilt-rotor and tilt-wing, respectively. It can be seen from Eq. (4.26) that for the tilt-wing having a disc loading in hover of about 50 psf, the propellers or propfan rpm will be more than two times, and for the 100 psf configuration, about three times, higher than for the V-22 tilt-rotor. Consequently, transmission losses for the tilt-wing should be lower, and the transmission efficiency higher, than for the tilt-rotor of the same gross-weight class.

Power losses associated with running instruments and accessories should be practically the same for the tilt-wing as for the tilt-rotor.

Further assuming that about five percent of the engine power would be used for pitch control, it may be expected that for the tilt-wing, $\eta_{ov} \approx 0.9$ vs. 0.92 assumed for the tilt-rotor.

In view of the above considerations for the k_v, FM, and η_{ov} factors, the shaft horsepower required per pound of gross weight in hover at SLS for the tilt-wing equipped with propfans will be

$$SHP_{req_0} = 0.04\sqrt{w} \tag{4.27}$$

and at 4000 ft, 95°F,

$$SHP'_{req} = 0.045\sqrt{w}. \tag{4.28}$$

Using Eqs. (4.27) and (4.28), specific power required in hover for propfan type tilt-wings was computed and is shown vs. disc loading in Fig. 4.47.

4.3.4 Horizontal Flight

Propulsive Efficiency. It has been indicated many times that the most attractive aspect of using propfans as lifting and propelling airscrews in the tilt-wing is the potential of high propulsive efficiency at high subsonic speeds. Consequently, it would be of interest to determine the levels of propulsive efficiencies that may be expected from propfans when they are used as vertical lifters in VTOL operations and as forward thrusters in horizontal flight.

Propulsive efficiency (η_{pr}) expressed in terms of power coefficient (C_P), thrust coefficient (C_T), and advance ratio (J) becomes

$$\eta_{pr} = C_T J/C_P \tag{4.29}$$

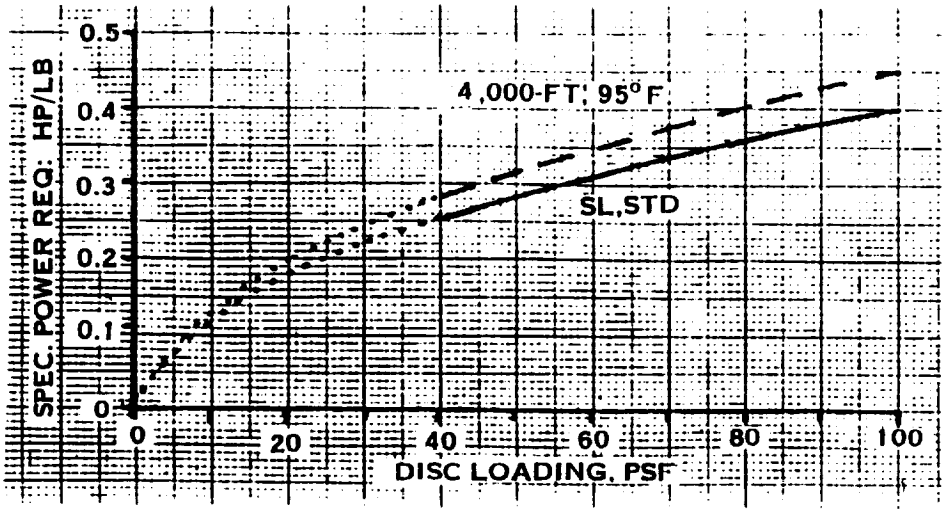

Figure 4.47 Anticipated trends in specific power required for propfan tilt wings in hover

where, using notations from Ref. 50, the symbols appearing on the right side of Eq. (4.29) are defined as follows:

$$C_T = J/66.1(ND/10{,}000)^2 D^2 \bar{\rho} \tag{4.30}$$

$$C_P = PSHP/20(ND/10{,}000)^3 D^2 \bar{\rho} \tag{4.31}$$

$$J = 101.4\,V/ND \tag{4.32}$$

where D is the propfan diameter in ft, N is the propfan rpm, V is speed of flight in knots, $\bar{\rho}$ is the relative air density, and $PSHP$ represents propeller-shaft horsepower.

In terms of the disc loading (w), disc area power loading ($4PSHP/\pi D^2$), and tip speed (V_t), the above equations can be rewritten as follows:

$$C_T = 3257.1\,w/V_t^2 \bar{\rho} \tag{4.33}$$

$$C_P = 1{,}175{,}793(4PSHP)/\pi D^2)/V_t^2 \bar{\rho} \tag{4.34}$$

$$J = 5.31V/V_t \tag{4.35}$$

where, in the above three equations, the disc loading is in psf, disc area power loading is in hp/sq.ft, tip speed is in fps, and the speed of flight is in knots.

In order to get some feeling regarding propulsive efficiency possibilities of propfans used in tilt-wing configurations, η_{pr} levels were computed at various speeds of flight at 20,000

ft for a propfan of the Hamilton SR-7L type, assuming that its disc loading in hover was, in one case, equal to 50 psf, and 100 psf in the other. It was then assumed that the disc loading in horizontal flight would vary vs. speed in a manner corresponding to the 20,000-ft line in Fig. 4.44, while the propfan rpm and thus, the tip speed as well, would amount to 85 percent of that in hover.

Some important inputs are given in Table 4.5, and the results of calculations are shown graphically in Fig. 4.48.

TABLE 4.5

PROPULSIVE EFFICIENCY OF THE SR-7L-TYPE PROPFAN AT 20,000 FT

SPEED OF FLIGHT V, Kn	MACH NUMBER M	TIP SPEED V_t, fps	ADVANCE RATIO J	DISC LOADING w, psf	THRUST COEFF. C_T	POWER COEFF. C_P*	PROPULSIVE EFFICIENCY η_{pr}
0	0	800.0	0	50.0	0.255	0.142	FM = 0.73
300	0.488	680.0	2.34	4.00	0.0529	0.205	0.604
350	0.569	↓	2.73	4.51	0.0595	0.260	0.624
400	0.651		3.12	6.01	0.0793	0.370	0.669
450	0.732		3.51	7.51	0.0992	0.510	0.682
0	0	800.0	0	100.0	0.510	0.432* 0.410**	FM = 0.68 FM = 0.71
300	0.488	680.0	2.34	8.00	0.1058	0.330	0.75
350	0.569	↓	2.73	9.02	0.1190	0.435	0.76
400	0.651		3.12	12.02	0.1586	0.620	0.80
450	0.732		3.51	15.02	0.1984	0.870	0.80
491	0.800		3.83	19.00	0.2510	1.200	0.80

NOTES:

* Interpolated from appropriate tables in Ref. 50

** From Figure 6.4, Ref. 51

FM values for SLS conditions

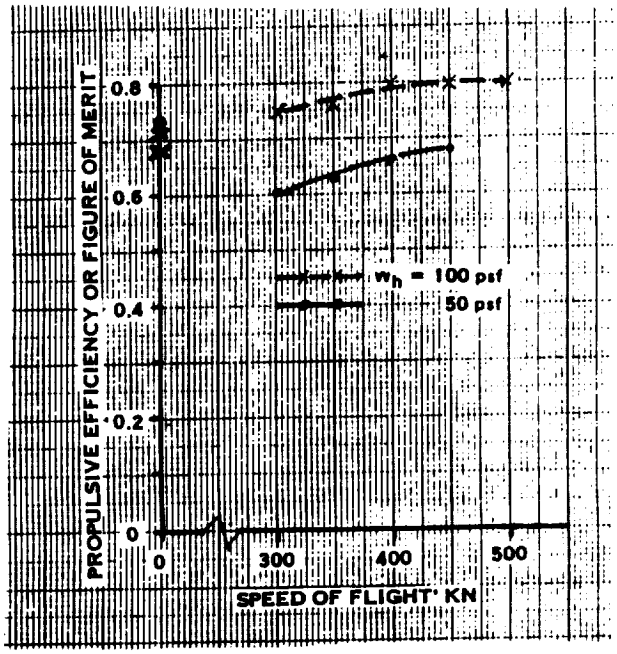

Figure 4.48 Trends in propfan propulsive efficiency vs. speed of flight at 20,000-ft and FM values of SLS

Looking at Table 4.5 and Fig. 4.48, one can see that even for an 'off the shelf' propfan, not specially designed for tilt-wing applications, a high propulsive efficiency of 0.8+ could be obtained when the disc loading in hover amounts to 100 psf. The Figure of Merit in hover OGE at SLS would be above 0.7.

For the case of disc loading in hover equal to 50 psf, the propulsive efficiency in high-speed flight would be considerably lower (below 0.7), but the Figure of Merit would be slightly higher.

These authors believe that for propfans designed exclusively for the tilt-wing, higher propulsive efficiencies and Figures of Merit than those shown in Table 4.4 and Fig. 4.48 can be achieved for airscrews having disc loadings in hover as low as 50 psf. It also appears that Figures of Merit at least 5 percent higher would be possible for the 100 psf hovering disc loading class of propfans, which would still be accompanied by some further gains in propulsive efficiency. However, even now in the light of the off the shelf technology of the eighties, the tilt-wing concept having a disc loading of 100 psf in hover looks quite attractive from an aerodynamic point of view. Furthermore, straight leading-edge wings, which appear possible in the w_h = 100 psf concept, represent definite structural simplification (both the wing itself and interconnecting shafting) over the zig-zag leading-edge designs, which may be needed for high cruise-speed machines having $w_h \approx 50$ psf.

In view of the above and the limited scope of this investigation, a somewhat more detailed look at performance capabilities of the tilt-wing concept will be limited to a glance at structural weights and some horizontal flight performance aspects of the w_h = 100 psf concept only. In analogy to the studies reported in Ref. 35, this aircraft will be designated as CTW-22-100.

4.3.5 Structural Weight Aspects

Basis for Comparison. It is of prime interest to see how structural weight as reflected in relative weight empty of the tilt-wing CTW-22-100 concept compares with other configurations of the same gross-weight class. In order to determine weight empty of the aircraft, a direct comparison is made between weights of its major components and those of the CTR-22C, whose gross weight is 46,230 lb (W_e = 30,024) vs. 46,000 for the tilt-wing. The actual weight estimate was performed as follows:

The weight of the total tilting system and weight of the wing assembly was subtracted from the weight empty of the CTR-22C, and the estimated weight of the tail rotor, its drive system, and additional weight of the aft portion of the fuselage was added, giving the weight of the whole nontilting portion of the weight empty of the aircraft. Then, the estimated weight of the tilting portion was added: wing assembly (including integral fuel tanks, flaps, slats, etc.), four engines (including nacelles), four gearboxes, four propfan units, interconnecting shafting, tilt-wing gearbox, and tilt-wing actuators.

It should once more be emphasized that because of the limited scope of this investigation, the predicted weight empty of the CTW-22-100 aircraft should be considered as only a rough indication of the possible trend in the relative weight empty values of the tilt-wing vs. tilt-rotors of the same gross-weight class.

Power Installed and Engine Weight. In design studies of the adaptation of the tilt-rotor to civilian transportation (Refs. 35 and 36), the design requirements stipulated that the vehicle be capable of hovering OGE at SLS conditions with one engine inoperative. It was also assumed in these studies that a 30-second OEI emergency rating could be achieved, providing about 125 percent of the takeoff rating.

Consequently, should the four-engined tilt-wing be designed to the same ground rules as accepted in Refs. 35 and 36, the installed power required for a 46,000-lb gross weight, 100 psf disc loading aircraft would amount to 46,000 X 0.4 = 18,400 hp.

However, taking a more conservative approach, it will be assumed that the total installed power will amount to 20,000 hp; i.e., 5000-hp per engine. Assuming an engine specific weight of 0.139 lb/hp, the dry weight of each engine would amount to 695 lb. Output rpm will be taken as equal to 15,570 — same as given in Ref. 35.

Weight of the Propfan Assembly. It is assumed that the propfan designed for 100 psf disc loading in hover will have the following characteristics needed for the weight estimate outlined in Ref. 50: diameter, 12.1 ft; tip speed, 800 fps; number of blades, 8; blade activity factor, 180; and maximum horsepower per foot of the disc area at a tip speed of 800 fps, 40.0 hp/sq.ft.

The weight of the propfan assembly at the above-indicated diameter, tip speed, and disc power loading of 70 hp/sq.ft would, according to Fig. 24, Ref. 50, be equal to 940 lb. This, corrected to the anticipated disc power loading of 40.0, would amount to

$$940 \times (40/70)^{0.3} \approx 795.0 \text{ lb.}$$

It should be emphasized at this point that the above weight is based on 1987 technology and, thus, may be considered as conservative for future designs.

Weight Empty. Weight empty of the CTW-22-100 model was computed using the CTR-22, depicted in Ref. 36 as a baseline aircraft. According to this reference, the weight empty of the CTR-22 is 30,242 lb. The weight of the wing, rotors, nacelles, transmission, etc., which will be called nonfuselage components and symbolized by the subscript *'nf'* amounts to $W_{nf_{tr}}$ = 15,548 lb. Consequently, the weight of the total fuselage group (subscript *'fu'*) of the CTR-22 would amount to

$$W_{fu_{tr}} = 30{,}242 - 15{,}548 = 14{,}694 \text{ lb.}$$

In the tilt-wing model, the basic fuselage group remains the same as for the CTR-22 aircraft, but the following items are added:

Tilt Gearbox	300 lb
Tail-Rotor Drive	60 lb
Tail-Rotor Gearbox	80 lb
Tail Rotor	180 lb
Delta Weight of Rear Portion of Fuselage	200 lb
Tilt-Wing Actuators and Support Structure	200 lb
$\Delta W_{fu_{tr}}$ =	1,010 lb

The weight of nonfuselage components of the CTW-22-100 are as follows:

Complete Wing (389 ft^2 X 4.9 lb/ft^2)	1,906 lb
Propfan Units (795 X 4)	3,180 lb
Dry Engines (700 X 4)	2,800 lb
Main Gearboxes (886 X 4)	3,544 lb
Center Gearbox	200 lb
Engine Installation (250 X 4)	1,000 lb
Nacelles (300 X 4)	1,200 lb
Wing Shafting	250 lb
Air Induction	150 lb
$W_{nf_{tw}}$ =	14,230 lb

Consequently, the total weight-empty of the CTW-22-100 would be

$$W_{e_{tw}} = W_{fu_{tr}} + \Delta W_{fu_{tw}} + W_{nf_{tw}}$$

or

$$W_{e_{tw}} = 14{,}694 + 1010 + 14{,}230 = 29{,}934 \text{ lb}$$

It can be seen from the above approximate estimate that the weight empty of the CTW-22-100 model should be slightly lower (by about 300 lb) than for the CTR-22 tilt-rotor, and the relative weight empty of the tilt-wing aircraft would amount to 0.65.

4.3.6 Performance in Horizontal Flight

L/D and L/D_e vs. Speed of Flight. Lift-to-drag ratio was computed from the following formula-

$$L/D = [(q/w_{f_{tot}}) + (w_w/\pi AR_e q)]^{-1} \tag{4.36}$$

where q is the dynamic pressure of flight, $w_{f_{tot}} \equiv W/f_{tot}$ is the total equivalent flat-plate area loading based on the f values for the whole aircraft, w_w is the wing loading, and AR_e is the effective aircraft aspect ratio.

The lift-to-equivalent-drag ratio will be

$$L/D_e = (L/D)\eta_{pr} \times \eta_{ov} \tag{4.37}$$

where η_{pr} is the propfan propulsive efficiency, and η_{ov} is the ratio of propfan shaft power to engine shaft power in forward flight; i.e., reflecting transmission and accessory running losses in that particular regime of flight.

The total equivalent flat-plate area was determined to be 14.1 sq.ft by estimating the total wet area as being equal to 4710 sq.ft and assuming that the skin friction drag coefficient C_f = 0.003, which may be even slightly conservative for a tilt-wing transport that has been made aerodynamically clean. The total flat-plate area of 14.1 sq.ft resulted in a $w_{f_{tot}}$ of 3,262 psf at the assumed gross weight of 46,000 lb.

The wing geometric aspect ratio is 8.6; thus assuming a span effectiveness factor of 0.85. The effective aspect ratio would then be 7.31.

When calculating the lift-to-equivalent-drag ratio from Eq. 4.37, it was assumed for the sake of simplicity that η_{pr} = 0.82 and η_{ov} = 0.96 remain constant throughout the speed range.

The lift-to-drag and lift-to-equivalent-drag ratios, computed under the above outlined assumptions are shown vs. speed of flight at SLS and 20,000 ft in Fig. 4.49.

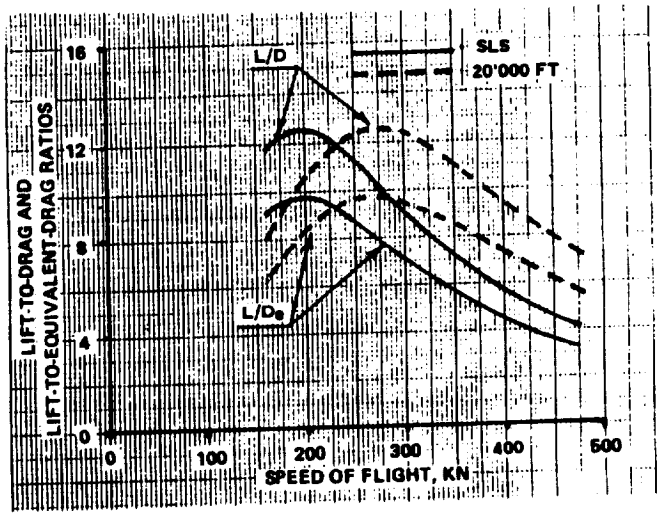

Figure 4.49 Lift-to-drag and lift-to-equivalent drag ratios for the CTW-22-100 tilt-wing aircraft

Power required per pound of gross weight vs. speed of flight at SLS and 20,000 ft is shown in Fig. 4.50.

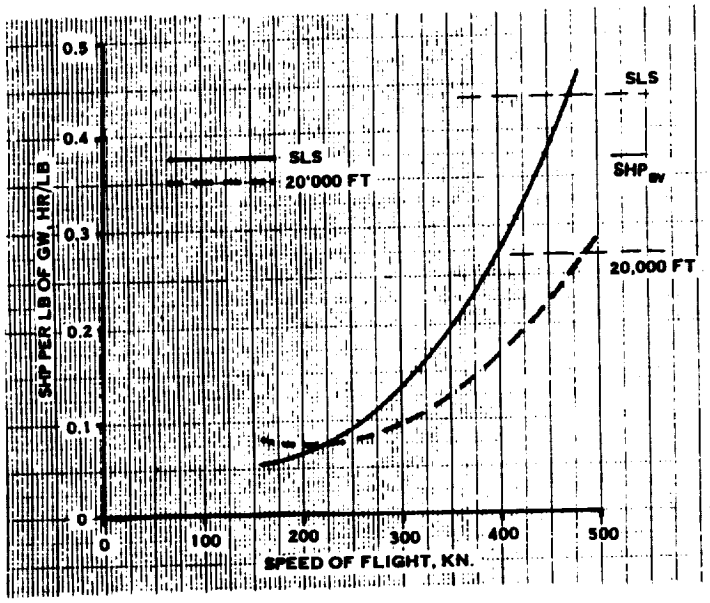

Figure 4.50 SHP required per pound of gross weight at SLS and 20,000 lb

SHP available per pound of gross weight at SLS is $\overline{SHP}_{av}$ = 20,000/46,000 = 0.435 hp/lb. Assuming a lapse rate of 0.62 at 20,000-ft altitude, one would obtain a $\overline{SHP}$ available amounting to 0.27 hp/lb. Marking the so-obtained powers on Fig. 4.50, one would find that the maximum flying speed would amount to about 470 kn at SLS, and 485 kn at 20,000 ft.

Fuel consumption per pound of gross weight and one n.mi flown was computed from the following:

$$(FC_w)_R = \overline{SHP}sfc/V \tag{4.38}$$

where the speed of flight is in knots.

The $(FC_w)_R$ vs. speed of flight at SLS and 20,000 ft was determined, assuming *sfc* = 0.4 and 0.5 lb/hp,hr as shown in Fig. 4.51.

The 0.4 sfc lines in Fig. 4.51 appear as optimal boundaries of $(FC_w)_R$ values at SLS and 20,000 ft. However, looking further into the future, the *sfc* of 0.4 lb/hp,hr may be considered as conservative. This can be seen from Fig. 4.52, where trends in future *sfc* values as envisioned by General Electric Company are shown.

One can see from this figure that a *sfc* as low as 0.33 is projected for the 1990–2005 time period. Furthermore, a representative from G.E. indicated to these authors that low specific fuel consumption at reduced power settings will also become available for future turboshafts.

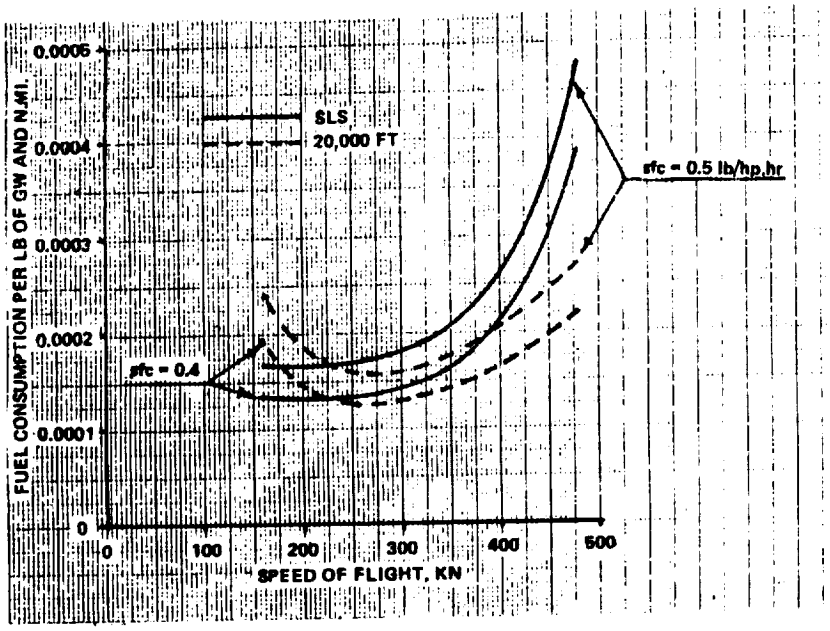

Figure 4.51 Fuel consumption per lb of GW and n.mi. for CTW-22-100 at SLS and 20,000 ft

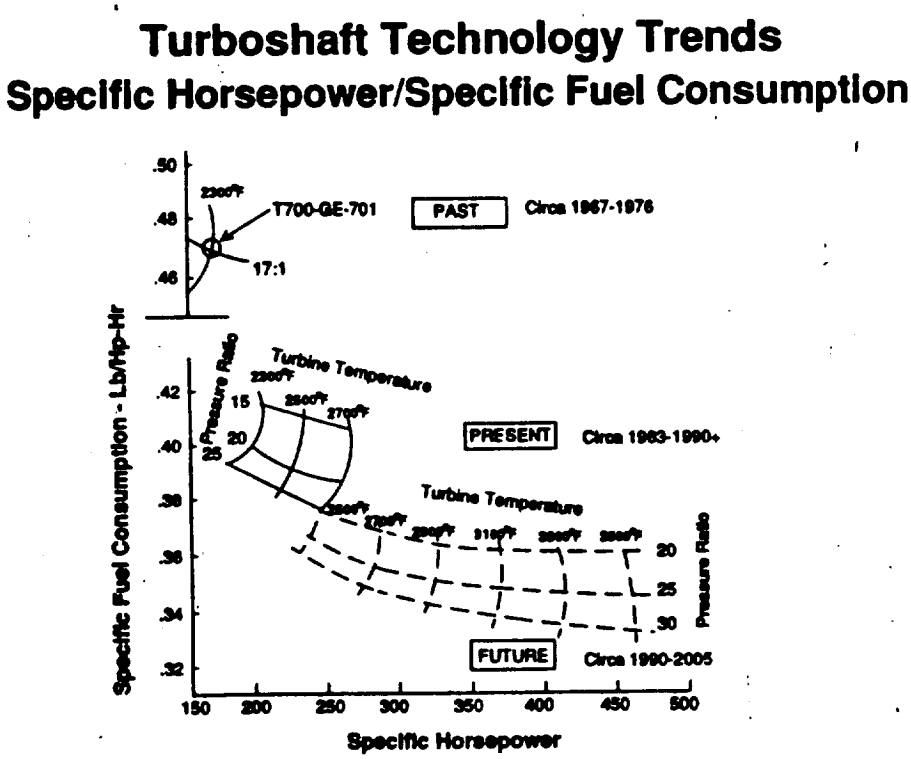

Figure 4.52 GE projections of future *sfc* turboshaft trends

Relative Payload vs. Range Trends. In order to have some idea regarding the relative payload vs. range trends which may be expected in the coming generation of tilt-wing aircraft, $\overline{W}_{pl}$ vs. R relationships were determined under the following assumptions.

Optimal Boundary: $\overline{W}_{0_{pl}} = 0.38$; i.e., 5 percent better than the 0.33 corresponding to $\overline{W}_e = 0.656$ for the CTW-22-100, and $(FC_w)_R = 0.000125$ lb/lb,n.mi—optimal values from Fig. 4.51.

Conservative Boundary: $\overline{W}_{0_{pl}} = 0.33$; $(FC_w)_R = 0.000170$ lb/lb,n.mi.

The relative payload vs. range relationships were computed from Eq. (1.10) under the above assumptions, and are shown in Fig. 4.53.

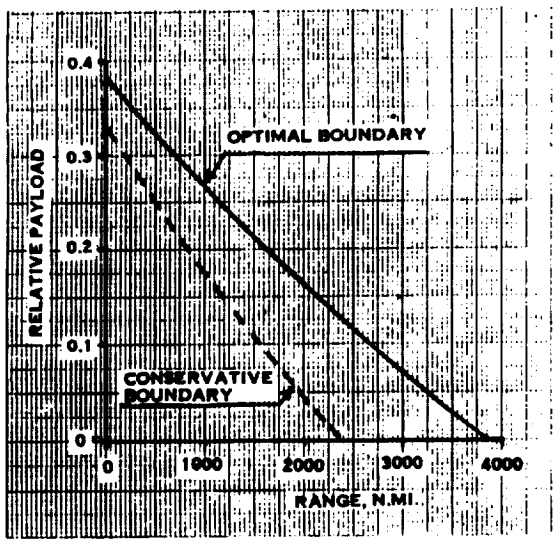

Figure 4.53 Trends in relative payload vs. range for the CTW-22-100 tilt-wing

It should be noted that the so-called optimal boundary shown in this figure probably contains some degree of conservatism. This is due to the fact that future tilt-wings of the CTW-22-100 configurations could probably achieve a higher degree of aerodynamic cleanness than that assumed in these calculations. Furthermore, propulsive efficiency will probably be higher than the 82 percent assumed here. Higher structural weight efficiency in future designs might lead to higher zero-range relative payloads than the assumed 38 percent and, finally, the sfc of future turboshafts will probably be better (as indicated in Fig. 4.52) than the assumed 0.4 lb/hp,hr. However, assessment of possible improvements in the optimal boundary in Fig. 4.53 would require detailed studies, which are out of the scope of the present contract.

Relative Ideal Productivity. Relative ideal productivity was computed for a 20,000-ft altitude, assuming optimal fuel consumption per pound of gross weight and n.mi values as given by the broken line in Fig. 4.51. Furthermore, the relative zero-range payload was assumed as 0.38 and the corresponding relative weight empty as 0.61.

Relative ideal productivity was computed from Eq. (1.17) for the following four ranges: 0, 200, 400, and 800 n.mi, and plotted vs. speed of flight (Fig. 4.54).

In view of the assumptions made in preparation for the graph shown Fig. 4.54, one may consider this figure as representative of a close to optimal trend as far as ideal relative productivity of the first generation of tilt-wings based on highly loaded (close to 100 psf) propfans are concerned. It is obvious that better values than those shown could be expected for more advanced future generations.

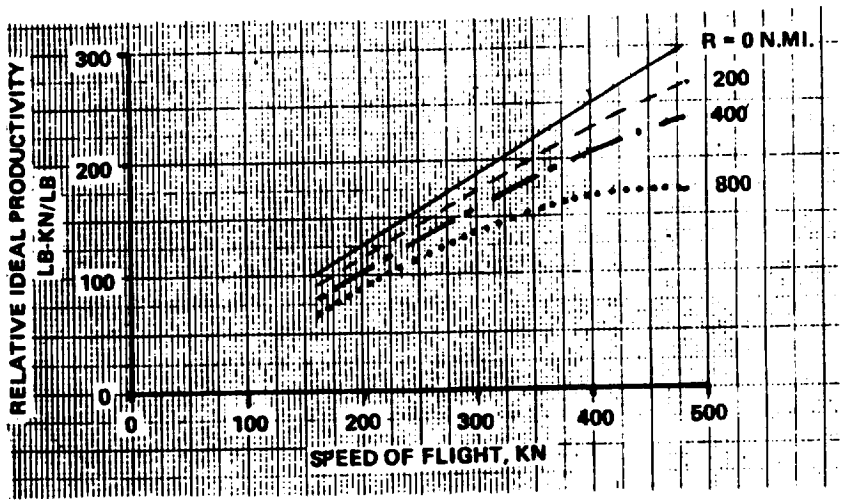

Figure 4.54 Optimal trends in ideal relative productivity for CTW-22-100-type tilt-wing aircraft

Partial Power Descent. Retention of an unseparated airscrew slipstream flow over the wing surface in all regimes of flight has always presented a difficult problem regarding the tilt-wing concept, especially during the conversion process, where the wing must generate lift required to compensate for the decrease of the vertical thrust component of the partially tilted airscrews. The situation becomes worse in partial power descent maneuvers when, due to the reduced slipstream velocity and elevated angles of the incoming flow, additional wing lift must be generated at high two-dimensional angles of attack at the wing elements.

Application of classical mechanical leading edge (Kruger flaps and slats) and trailing edge (various flaps, but especially, the Fowler type) lift-increasing devices combined with the proper wing chord to airscrew diameter ratio (usually about 0.5) allows one to develop designs which retain acceptable flight characteristics, not only during the conversion process, but also in partial-power descent. However, more freedom in selecting lower wing chord to airscrew diameter ratios (favorable for high aspect ratio wings) may be obtained while still

maintaining good partial power descent flight characteristics, if more effective lift-increasing devices that the present mechanical ones were used in tilt-wings. Circulation control in general, and super-circulation through strong leading-edge vortices come to one's mind in this respect.

Finally, it should be emphasized that fulfillment of the no wing-flow separation requirement through transition maneuvers greatly contributes to very good STO characteristics of the tilt-wing configuration. This was originally demonstrated on the VZ-2 (Ref. 45) and then reconfirmed by flight tests of the XC-142A and CL-84 aircraft.

4.3.7 Concluding Remarks re Tilt-Wings

It appears that in departing from the constraint of 50 psf airscrew disc loading in hover, new possibilities of creating an attractive tilt-wing VTOL/STOL transport aircraft open up.

Cursory studies presented in this report seem to indicate that through application of single-rotation propfans having disc loadings in hover as high as 100 psf, aerodynamically clean tilt-wing aircraft can be designed.

Furthermore, the tilt-wing exhibits a very important conceptual feature; namely, that the same open airscrew-turboshaft assemblies can be used from hovering to dash speeds in excess of 480 knots. This is, of course, well beyond the capability of conventional tilt-rotor concepts of present and even future generations. Relative payload vs. range and ideal relative productivity relationships of high disc-loading tilt-wing aircraft is also superior to their tilt-rotor counterparts.

The only drawback of this configurationally attractive picture of the basic simplicity of the tilt-wing is the apparent need for a horizontal tail fan, or rotor, as a means of pitch and c.g. travel control in hover and transition. This device obviously represents an unnecessary burden in the airplane mode of flight.

It should be emphasized that inputs regarding aerodynamic characteristics and weight trends of propfans used in the present study represent 'off the shelf' data related to technology levels of the eighties.

Consequently, since application of the propfan is essential to the high-speed tilt-wing concept, it would be desirable to perform indepth studies—both analytical and experimental—of propfan airscrews specifically designed for tilt-wing operations. Such a study should investigate the influence of the following parameters on figure of merit values in hover and propulsive efficiency in forward flight.

1. Disc loading in hover and its deviation at various stages of forward flight.
2. Tip speed in hover, and its possible reduction in forward flight within limits of engine rpm range, and through gearshift arrangements.

Investigation of the influence of the above outlined paramettric variations should also include noise considerations.

Structural weight aspects of propfans designed for tilt-wing configurations should complete this study. Once the basic knowledge regarding aerodynamic characteristics and structural weight trends of propfans specially designed for tilt-wing applications is assembled, then realistic design studies of transport aircraft based on this concept can be performed.

Possibilities of the propfan tilt-wing configuration as indicated by these cursory investigations appear to justify an indepth study of the concept.

4.4 Stowable Rotors

4.4.1 General

A constant requirement for higher performance of rotary-wing aircraft forces the industry to look for new concepts, allowing for increased maximum speeds. The question is how may the maximum speed of rotary-wing aircraft be increased beyond the present practical limit of tilt-rotors. This question was discussed with respect to classically configured tilt-rotors in Section 4.2, and tilt-wings in Section 4.3. Here, the concept of the stowable rotor is considered as still another possible way leading to high-speed rotary-wing aircraft.

The goal of stowable rotors can be achieved by either (a) elimination of the rotor by reducing its diameter and stowing it in the fuselage, or (b) folding the blades along the fuselage (in the single-rotor configuration) or nacelles (in the side-by-system). The use of one of these methods is a must, if the industry is to face the problem of designing a rotary-wing aircraft of low disc loading, which is essential in some military and commercial operations and, at the same time, have the capability of attaining high subsonic speeds.

4.4.2 Reduced Diameter Rotors

One method would be to reduce the diameter of the rotating rotor, stop its operation, and then to lower it into the cavity of the fuselage, leaving the cleanest possible configuration of the aircraft, which could be propelled by airscrews or, as an ultimate goal, by jet engines. In the latter case, the use of convertible engines should be necessary.

The concept of a reduced diameter rotor in the form of telescoping, three-segmented blades is shown in Fig. 4.55 (Ref. 32, Fig. 4.A).

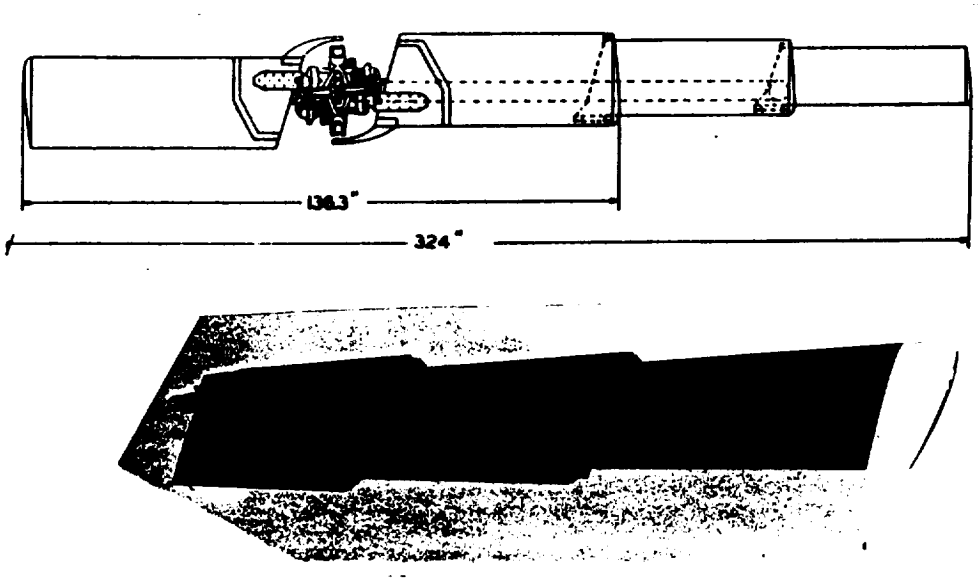

Figure 4.55 Piasecki/Vertol retractable rotor assembly and blade components

Kinetic energy of the rotor was used to retract two outboard segments of the blade as shown in Fig. 4.55, by means of cables, drums brakes, etc. (Fig. 4.56).

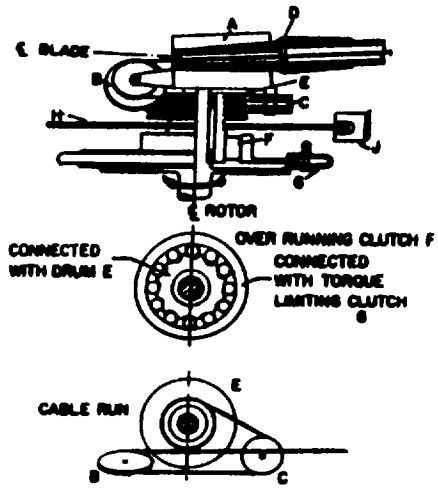

Figure 4.56 Schematic view of a blade retraction mechanism

The main objective was the application of this solution to high-speed aircraft with a low disc loading rotor which, after stopping, would be housed in the fuselage (Fig. 4.57).

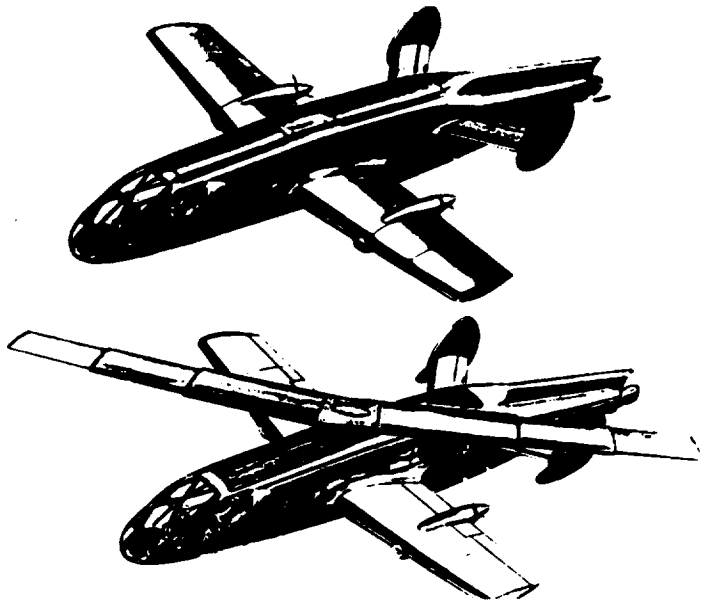

Figure 4.57 Artist's concept of a flight research aircraft with stowable rotor

This type of telescoping rotor was brought to the hardware stage in the form of a three-segmented blade applicable to a 27-ft diameter rotor. Further development was halted by lack of funds.

High-speed convertible aircraft using the telescoping and stowable rotor is depicted in in Fig. 4.58.

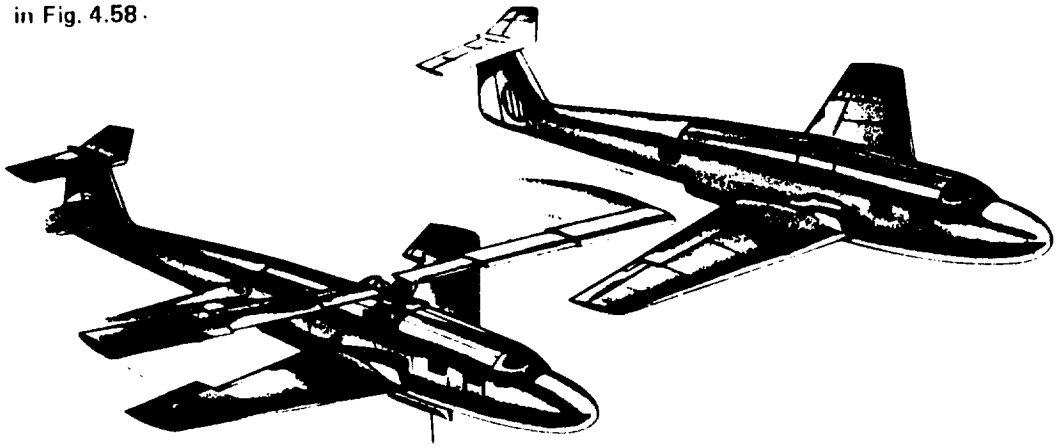

Figure 4.58 Retractoplane using rotor blades with reverse taper

It should be noted that the aircraft shown in this figure features a reverse configuration of the blade where, aerodynamically, the most important outboard segment telescopes, not inside, but outside two inboard segments, reducing the weight of the rotor and lowering its drag. The three-segmented blade allowed for reduction of the rotor diameter up to 42 percent of the original size. A further reduction could be achieved by increasing the number of blade segments, but weight and complexity may not justify this approach.

The telescoping blade idea was also studied by Sikorsky[33]. In their case, a two-segmented blade was telescoped by means of a jackscrew (see Fig. 4.59). In the Piasecki and Sikorsky concepts, the kinetic energy of the rotor was used as the source of power required to reduce the diameter. The difference was in mechanical solutions. Sikorsky applied the concept of differential drive to achieve this goal (Fig. 4.60).

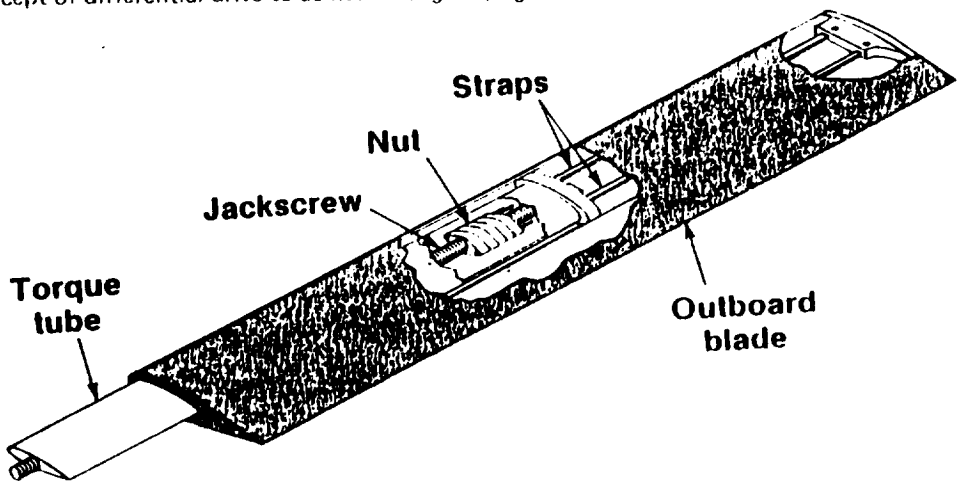

Figure 4.59 Two-segmented Sikorsky blade

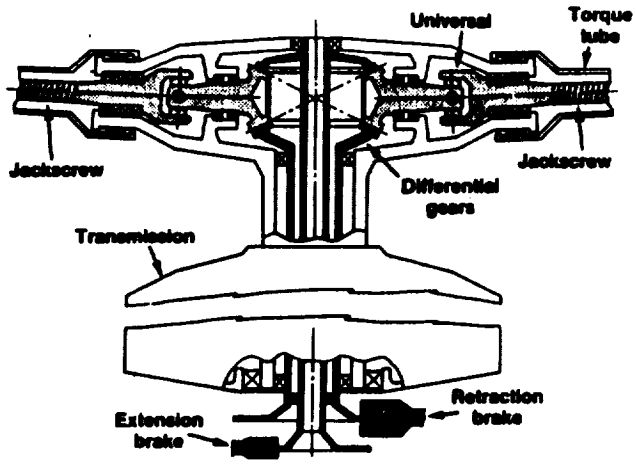

Figure 4.60 Sikorsky blade radius reduction mechanism

The two-segmented Sikorsky blade rotor system was successfully bench tested, but its application to the stowable rotor concept appears less attractive than the segmented blade of Piasecki, since Sikorsky's rotor diameter could be reduced to only 60 percent of the fully extended diameter compared with the 42 percent of Piasecki.

A high performance aircraft featuring a two-segmented rotor blade stowed in the fuselage, as studied by Sikorsky (Ref. 33), is shown in Fig. 4.61.

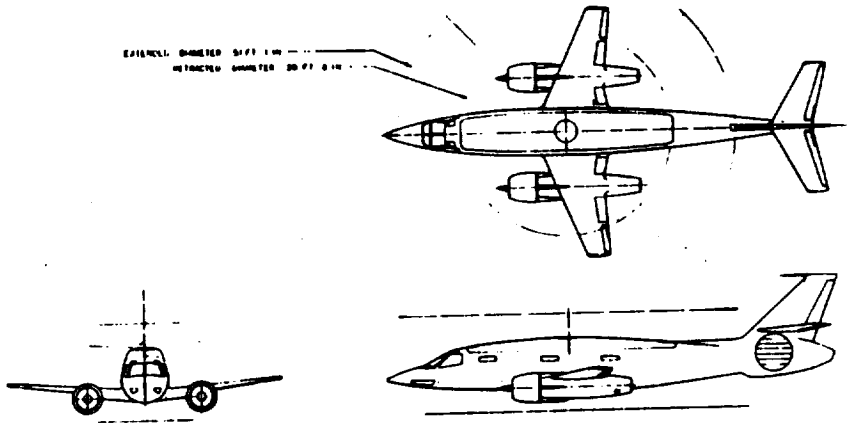

Figure 4.61 Sikorsky's stowed-rotor aircraft, designed for 400-knot cruise.

A radical reduction of the rotor diameter could be achieved by a 'winding' method that was considered for space application. In this case, cables and sheets of fabric were contemplated in blade structure.

4.4.3 Blade Folding

Various schemes of blade folding were, and are, being studied, although none have been brought to flight status. Among them are: (1) blade folding rearward, (2) tilt-fold method, and (3) zig-zag blade folding. Unlike the case of telescoping, where the initial stowing process is performed while the blades are rotating, all of the three above methods require bringing the rotor to a complete stop prior to folding. Methods (1) and (3) are suitable for incorporation on single-rotor aircraft, whereas method (2) is applicable to side-by-side configurations.

The first method, which seems to be the simplest from a mechanical point of view, was thoroughly studied by Lockheed under U.S. Army Contract. (Ref. 52 contains a wealth of information on this subject.) An artist's concept of this configuration is shown in Fig. 4.62, and schematic details are depicted in Figure 4.63 (Ref. 52).

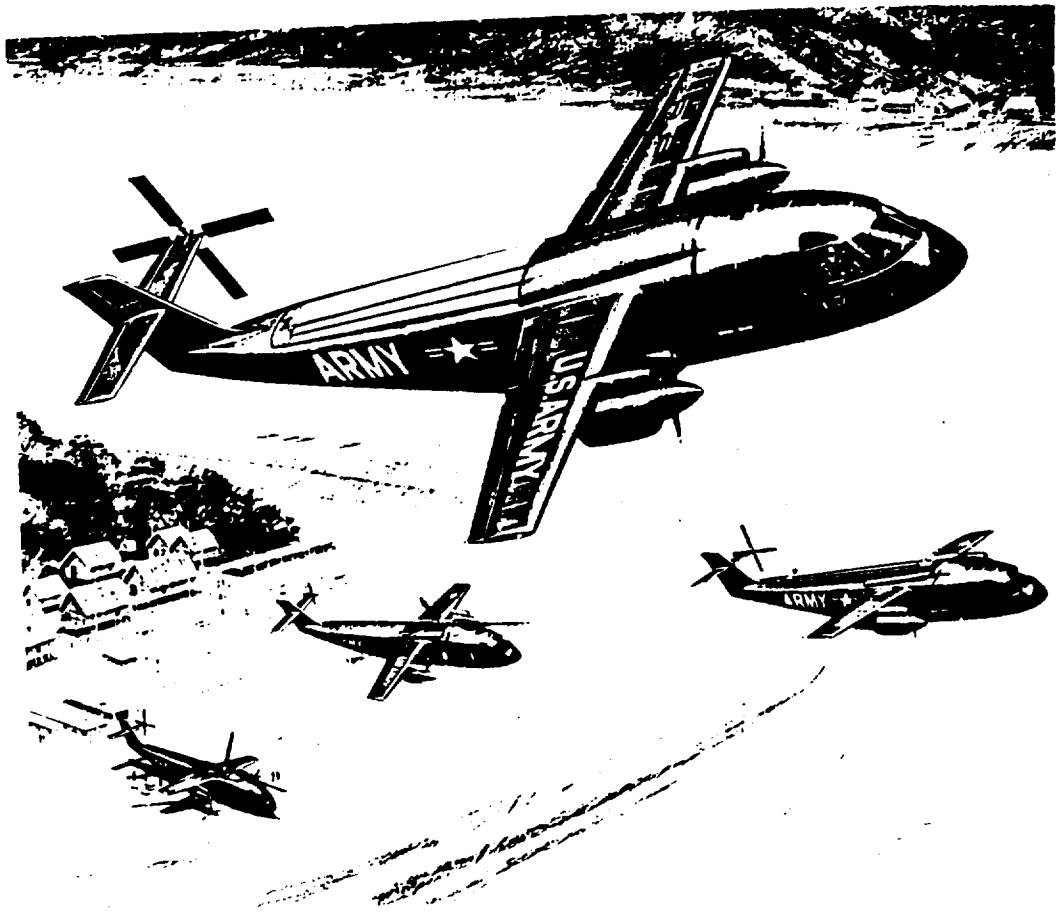

Figure 4.62 Lockheed's proposed 'composite' aircraft with stopped, folded, and stowed rotor

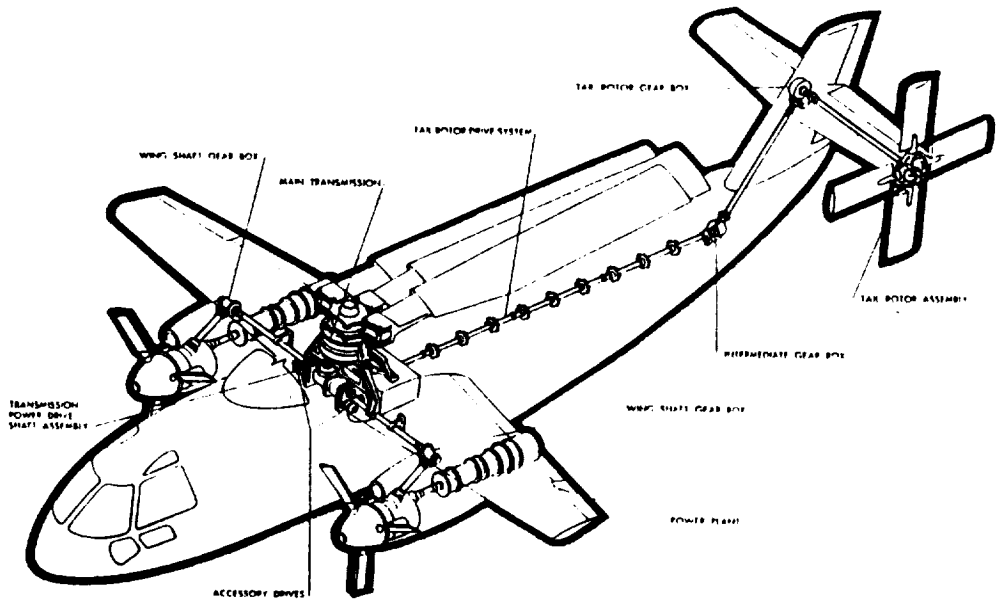

Figure 4.63 Scheme of mechanical system of Lockheed's 'composite' aircraft

A full-scale model of this aircraft was tested in the NASA-Ames wind tunnel (see Fig. 4.64).

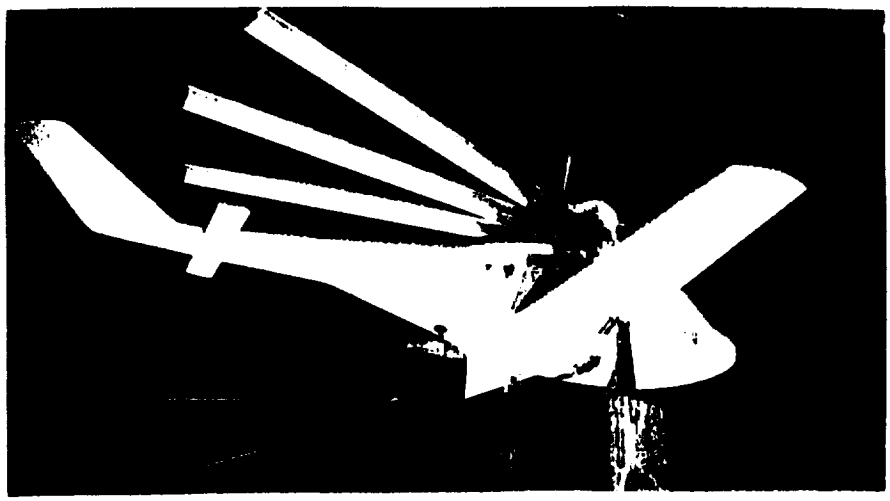

Figure 4.64 Lockheed full-scale model of three-bladed stopped/folded rotor mounted in the NASA-Ames wind tunnel

The second method was studied by various companies and individuals as a means of developing aircraft faster than the current high-speed helicopters. A technical report (Ref. 54) by Boeing Company, Vertol Division, deals with a side-by-side rotor system capable of attaining speeds of 350 to 400 knots (Fig. 4.65).

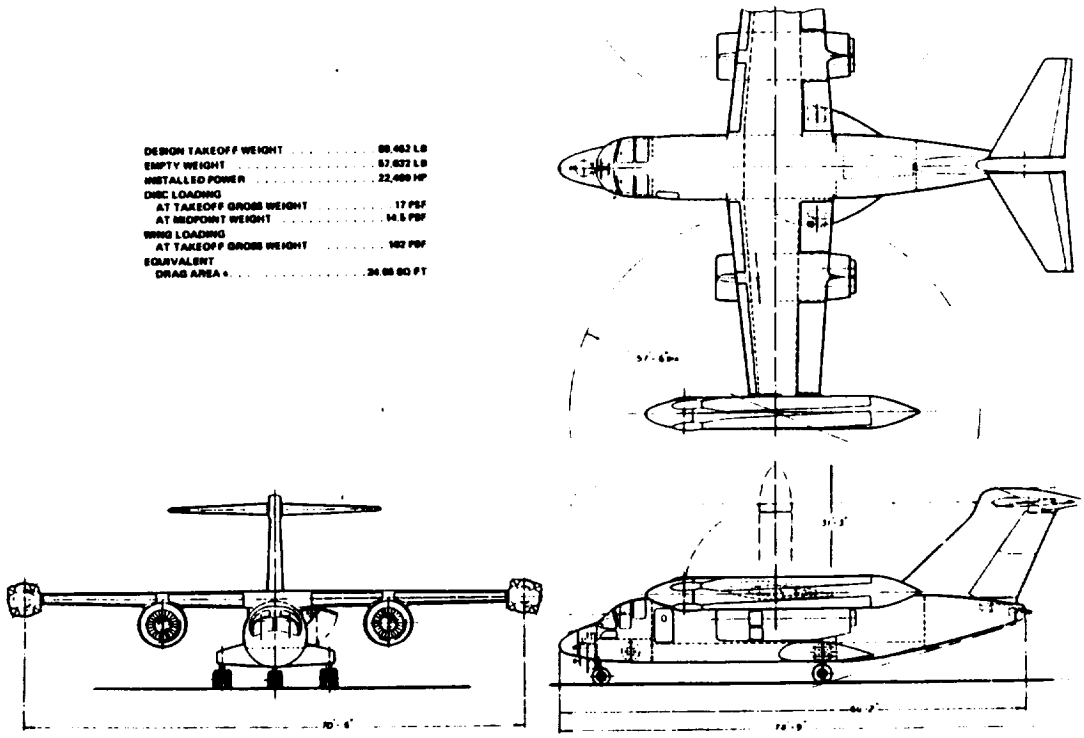

Figure 4.65 Boeing stowed tilt-rotor concept (1971)

In the field of tilt-fold rotor blades, more ambitious as far as speed is concerned, were the studies by Bell Helicopter Textron, Inc., reported by Drees in Ref. 37 (Fig. 4.66).

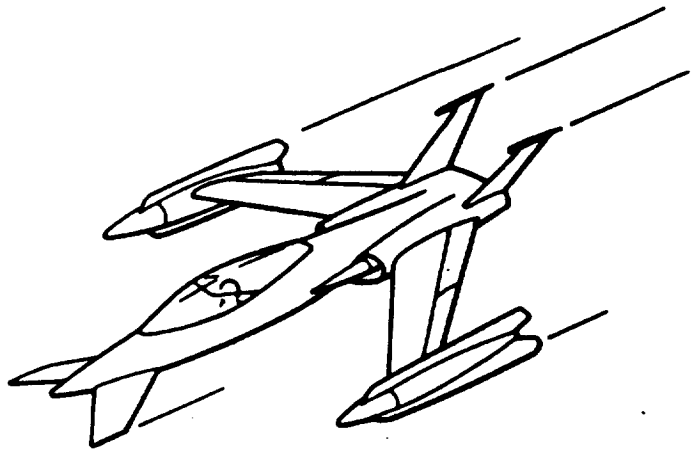

Figure 4.66 High-speed tilt-rotor concept

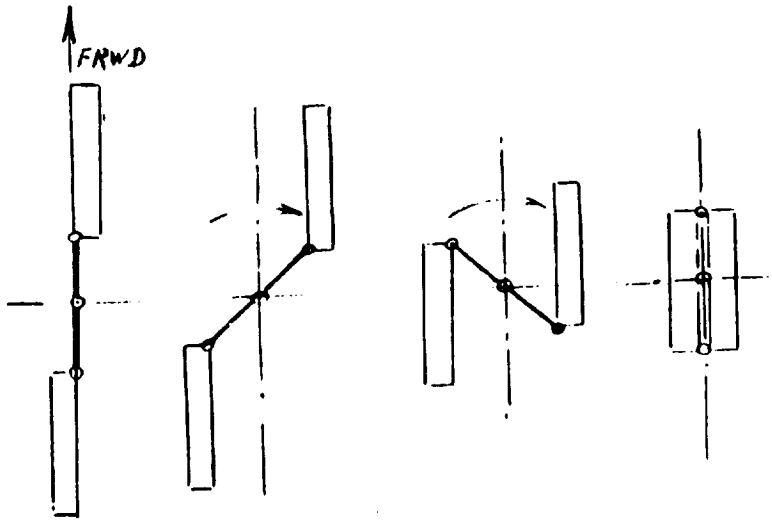

Figure 4.68 Zig-zag method of blade folding

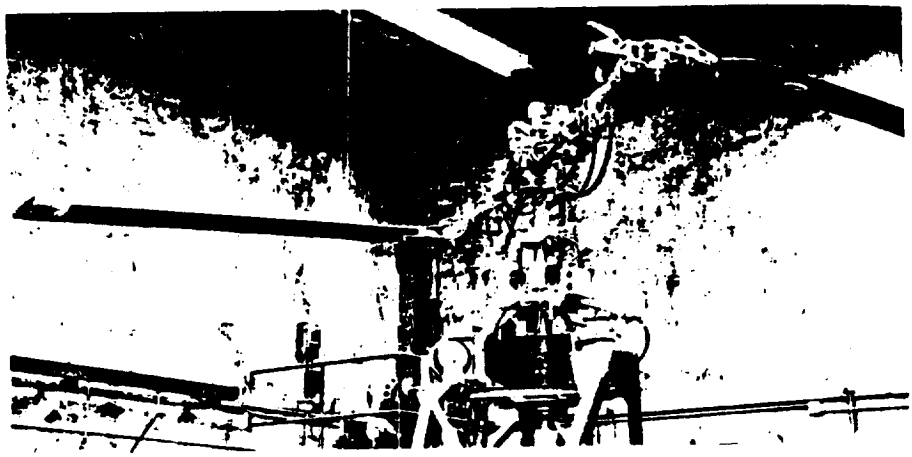

Figure 4.69 Hiller's stowable blades

An unusual scheme of stoppable rotor blades is shown in Fig. 4.70. It features a circular wing in which the blades are retracted. A low aspect ratio and poor wing airfoil characteristics are the main drawbacks of this scheme.

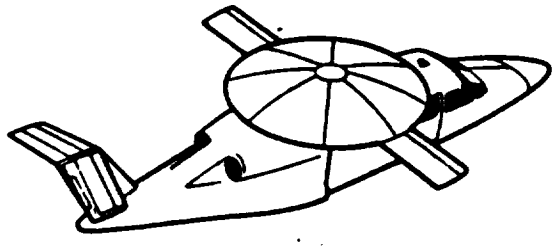

Figure 4.70 Stoppable rotor concept

It appears, hence, that the nacelle folding and fuselage stowable main rotor schemes represent the two most likely ways toward the retractoplane concept. A short list of the important characteristics of both types of aircraft considered here is shown in Table 4.5, and a brief review of their performance in hover and horizontal flight is examined in the following sections.

TABLE 4.5

ABBREVIATED LIST OF PRINCIPAL CHARACTERISTICS OF THE CONSIDERED RETRACTOPLANES

MODEL	GROSS WEIGHT LB	DISC AREA FT^2	DISC LOADING PSF	WING AREA FT^2	WING LOADING PSF	WING SPAN FT	BLADE RADIUS FT	WEIGHT EMPTY LB	WE/GW
PIASECKI PH55	3,451	572.26	9.52				13.5	2,591	0.75
LOCKHEED CL-946-400	31,000	3,210	9.64	280.0	110.7	40.0	32.0	20,600	0.66
SIKORSKY TRAC	26,643 (Approx)	2,048.2	13.0	288.5	99.23	37.84 (Approx)	25.54	8,000 (Approx)	0.67
BOEING 71 * (2 ROTORS) BASELINE AC	67,000	3,800.4	17.62	744.0	90.0	61.0	24.6	44,220	0.66
BOEING 90 ** (2 ROTORS)	53,600	2,144.0	25.0	595.0	90.0	59.3 (Approx)	18.48		

* Figure 4.65
** Figure 4.67

4.4.4 Hover

One of the frequently stressed advantages of retractoplanes is their ability to perform missions where either hovering with relatively low downwash velocities (as in rescues) or vertical takeoffs and landings from, or on, either unprepared or otherwise downwash-restricted areas, is an important requirement. Consequently, one may expect that the disc loading of retractoplanes would be close, or slightly higher, than for helicopters, and would not much exceed the values acceptable for tilt-rotors. This trend seems to be substantiated by Fig. 4.71, where disc loadings for a few hypothetical retractoplanes are plotted vs. gross weight.

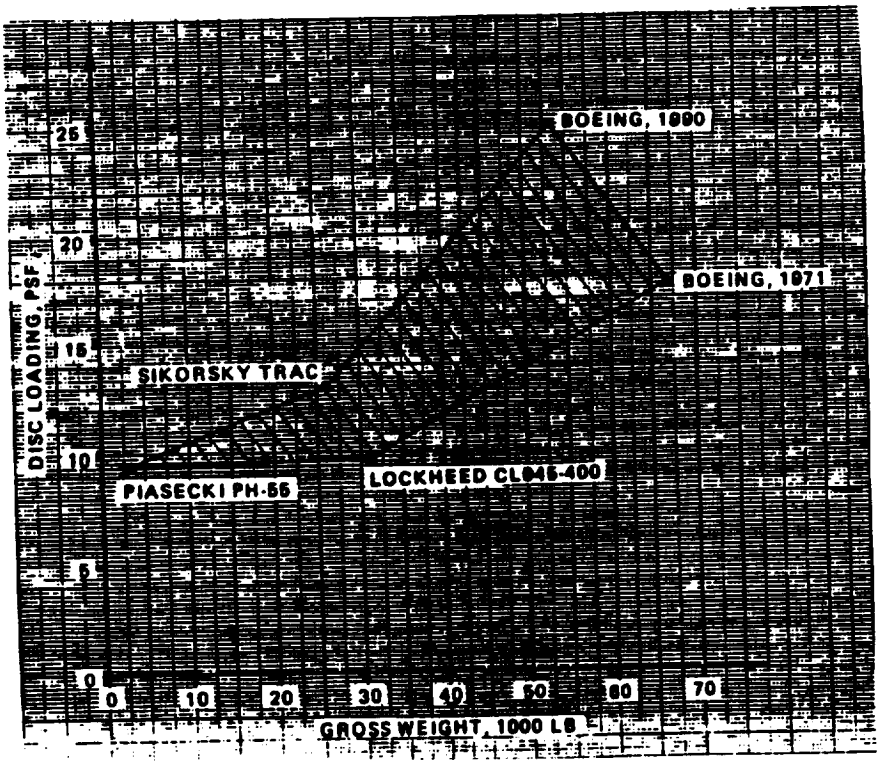

Figure 4.71 Indications of trends in disc loading levels in retractoplanes

Long hovering periods would probably never enter the mission requirements for retractoplanes. Thus, relative payload vs. time relationship will be of little interest. But shaft horsepower requirements per pound of gross weight in hover OGE is of interest, since this characteristic may play a role in the determination of the installed power level.

As in preceding cases, the shaft horsepower required in hover values would be determined by Eq. 4.1, and the role of various parameters appearing in that equation will be examined.

Retractoplanes of the two-nacelle configuration are, in hover, no different from conventional tilt-rotors. Consequently, their shaft horsepower per pound of gross weight required in hover at given ambient conditions should be the same as for tilt-rotors of the same disc loading. Then, Eq. 4.1 will also apply to retractoplanes of the side-by-side configurations with folding blades (as in the Boeing case). However, should variable diameter features be incorporated in the main rotor design, then the $\overline{SHP}_{req_h}$ values would be somewhat higher than for the classic tilt-rotor at the same disc loading. This increase in power required would be caused by somewhat lower figures of merit for variable diameter rotors where, because of mechanical constraints, it may be impossible to achieve blade twist and airfoil thickness distribution as advantageous as in the classical tilt-rotors.

With regard to single-rotor retractoplanes, it would be of interest to determine to what extent the power required per pound of gross weight of this configuration would be different from that of the side-by-side type, using the same disc loading and under the same ambient conditions. This can be done by examining the differences between the two types in the expected values of the parameters appearing in Eq. (4.1).

The figure of merit for the Lockheed type stowed rotor configuration may be close to that of the conventional tilt-rotor. But for the variable diameter types, the figure of merit will be lower—for reasons already explained. Consequently, for the Lockheed type retractoplane, FM = 0.75 and for the Sikorsky, FM = 0.65 will be assumed.

Download factor levels are estimated using the modified approximate formula of Vil'dgrube (Eq. (20), Ref. 55). Since the wing area to the disc area ratio ($\overline{S}_w$) can be expressed as the wing loading (w_w) to disc loading (w) ratio, the expression for the required thrust increment due to wing download ($\Delta\overline{T}_w$) can be written as follows:

$$\Delta\overline{T}_w = 0.375(w_w/w)\bar{b}_w \tag{4.39}$$

where the relative wing span $\bar{b}_w = b_w/R$.

The formula for the thrust increment due to download on the fuselage and nacelles ($\Delta\overline{T}_{f\&n}$) can be expressed as

$$\Delta\overline{T}_{f\&n} = 0.238(S_f + S_n)/\pi R^2 \tag{4.40}$$

where S_f is the horizontally projected area of the fuselage enclosed between the wing and the rotor-tip circle, and S_n is the horizontally projected area of the nacelles exposed to downwash.

Trends in disc loading of stowable rotor aircraft were given in Fig. 4.71, while those in wing loading are shown in Fig. 4.72.

Values of the relative wing span ($\bar{b}_w$) as well as of other parameters appearing in Eqs. (4.39) and (4.40) are shown in Table 4.6, where total $\Delta\overline{T}$ values are also indicated.

Looking at the results shown in Table 4.6, one can see that for the Sikorsky type, the download factor would be $k_v \approx 1.1$, which is quite similar to those of tilt-rotors and side-by-side retractoplanes. However, for the case of Lockheed, the download factor would be approximately 1.065, which is somewhat lower.

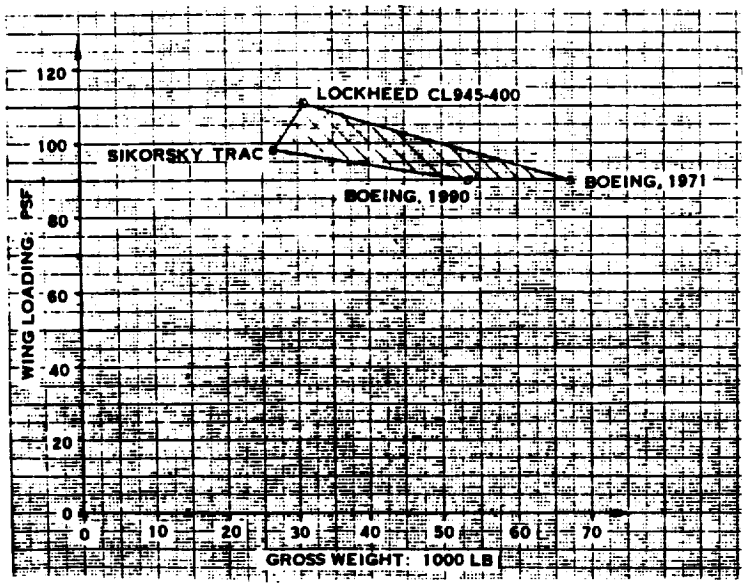

Figure 4.72 Trends in wing loadings of retractoplanes

TABLE 4.6

INPUTS FOR DETERMINATION OF DOWNLOAD FACTOR VALUES

AIRCRAFT	w_{psf}	$w_{w_{psf}}$	$\bar{b}_w$	$\Delta\bar{T}_w$	$(S_f+S_n)/\pi R^2$	$\Delta\bar{T}_{f\&H}$	$\Delta\bar{T}$
Lockheed CL-945-400	9.64	110.7	1.25	0.0408	0.097	0.023	0.0638
Sikorsky TRAC	13.0	99.23	1.52	0.0746	0.156	0.037	0.1116

With respect to the rotor power to shaft power ratio, one may expect that the overall transmission efficiency level values for the single rotor configuration will be considerably lower than the 0.92 which is accepted as typical for conventional tilt-rotors and thus, for the side-by-side retractoplanes as well.This decrease in the η_{ov} level will be chiefly caused by the power losses associated with the main rotor torque compensation requirements. In order to achieve aerodynamically clean configurations, main rotor torque compensating devices such as the Fenestrone or NOTAR type will probably be used. Power losses higher than those for conventional helicopters would reduce the η_{ov} levels to 0.8 or 0.75. Consequently, 0.77 may be assumed as a representative value.

Taking into account the probable figure of merit, overall transmission efficiency, and download factor values, the trends in shaft horsepower requirements per pound of gross weight in hover OGE for retractoplanes can be summarized as follows:

For the side-by-side retractoplane configurations, the $\overline{SHP}_{req_h}$ values should be the same as for classical tilt-rotors at the same disc loading and ambient conditions. In other words, trends in the quantities shown in Fig. 4.8 should also apply in this case.

For single-rotor retractoplanes incorporating variable diameter rotors (e.g., Sikorsky), the $\overline{SHP}_{req_h}$ values may be as much as 36 percent higher than for conventional tilt-rotors.

Single-rotor retractoplanes incorporating constant geometry main rotor blades (e.g., Lockheed) would require, in hover OGE, shaft horsepower per pound of gross weight lower than for their variable-geometry blade counterparts, but still about 18 percent higher than for conventional tilt-rotors (at the same disc loading and ambient conditions).

The percentages established above will also apply to the trends in fuel consumption per pound of gross weight and one hour of hover OGE when compared to those of conventional tilt-rotors as shown in Fig. 4.9.

4.4.5 Horizontal Flight

Optimization of Wing Geometry and Wing Loading. One of the most important factors in creating a fixed-wing type aircraft operating most efficiently under the envisioned cruise conditions of flight speed and altitude is freedom to optimize the combination of parameters representing wing geometry (planform, aspect ratio, twist, and airfoil distribution) with its loading.

In conventional side-by-side configurations, freedom in selecting these parameters is strongly constrained by such factors as relationship of wing span to rotor radius, positioning of the rotor axis in hover, and wing bending frequencies requirements.

Hence, it might appear that single-rotors would be more advantageous as far as selection of optimal wing geometry is concerned. However, selection of the optimal wing loading may run into a strong constraint, resulting from the necessity of maintaining the aircraft in controlled horizontal flight in the fixed-wing configuration at speeds and altitudes (i.e., air density) acceptable for the stopping and stowing process.

By contrast, nacelle-stowed rotors operating in the propeller configuration can be feathered and stopped at much higher flight speeds. Thus, this particular constraint regarding upper limits of the desirable wing loading will probably not exist in this case.

Going back to the problem of establishing the uppermost wing loading acceptable for the process of stopping and stowing the rotor at given flight speeds and ambient conditions, as reflected in the relative air density $\bar{\rho}$, one should remember that the relationship between wing loading (w_w) and aircraft lift coefficient (C_L) can be expressed as follows:

$$w_w = 0.00340\bar{\rho}V^2C_L \tag{4.41}$$

where the speed of flight V is in knots.

Assuming that the stopping and stowing process can be performed at $110 \leqslant V \leqslant 130$ knots and relative density is 0.8—roughly corresponding to 4000 ft, 90°F conditions—the relationships expressed by Eq. (4.41) were computed and shown in Fig. 4.73.

Looking at this figure, one would see, for instance, that at $C_L = 3.0$, which can be achieved through sophisticated lift-increasing mechanical devices, the uppermost acceptable wing loading would amount to about 140 psf at the speed of conversion of 130 knots, and only 100 psf at 110 knots.

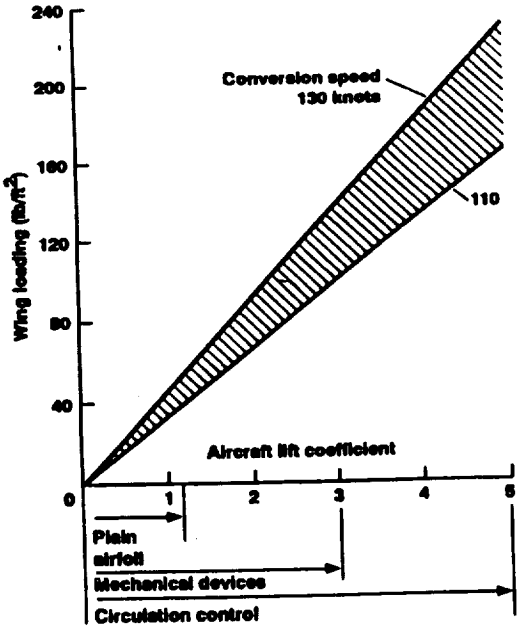

Figure 4.73 Uppermost wing loading vs. aircraft lift coefficient for two speeds of flight at a relative air density of 0.8

For an aerodynamically clean aircraft characterized by a typical non-induced drag coefficient of 0.03 and an effective aspect ratio of 8, the optimal lift coefficient (see Fig. 1.8 or Eq. (1.35)) would amount to 0.87. This means that in order to operate at the highest L/D ratio when cruising at M = 0.8 and an altitude of 30,000 ft, the wing loading would amount to 245 psf. Should the envisioned operation be such that the desirable cruise altitude be equal to 20,000 ft, then the optimal wing loading would be 372 psf.

The above example seems to indicate that wing loadings as high as 250 psf would be desirable for aircraft intended to operate most efficiently at M ≈ 0.8 and altitudes of about 30,000 ft, and exceed the 350 psf level should the operational altitudes be lowered to, say, 20,000 ft.

To achieve these high wing loadings, two ways, or a combination of both, appear possible: (1) increase the permissible flying speed of conversion, and/or (2) go beyond mechanical lift-increasing devices through such means as circulation control.

As to the designer's decision regarding the selection of the most suitable approach, the following factors should be taken into consideration. Through the application of variable diameter rotors, the speed of flight at which rotors of reduced diameters can be stopped and stowed should be higher than for those of constant diameter. Furthermore, reduced diameter rotors can be stowed within the fuselage with a lesser deformation of the fuselage aerodynamic shape than in the case of constant radius blades. The clean aerodynamic lines of the retractoplane shown in Fig. 4.61 illustrates this point.

Application of variable diameter blades obviously represents serious mechanical complexity and enters into completely virgin territory as far as any operational experience regarding this system is concerned.

Another approach based on achieving aircraft C_L values in excess of those obtainable through mechanical lift-increasing devices would require application of circulation control. Here, mechanical complexities would be unavoidable and there is also a lack of any substantial operational experience.

It is obvious, hence, that the designer must weigh all of the difficulties and complexities, as well as the structural weight increases that may be encountered on the road to obtaining the desirable low controllable flying speeds vs. using wing loadings below their optimal values. This, obviously, would lead in turn to operating the aircraft at lift to drag ratios below their potentially optimal levels.

Drag Penalties Resulting from Stowing. Both nacelle and fuselage stowing schemes lead to some parasite drag increases in comparison to aircraft having no requirement for accommodating the rotors.

In the case of tilt nacelle-folded blades, the drag penalty would depend on the design solution. In the simplest case, as illustrated by Bell's tilt-fold rotor tested in the NASA Ames Wind Tunnel (Fig. 4.74), the increment of parasite drag—expressed as an increment of the flat plate area—will be as follows:

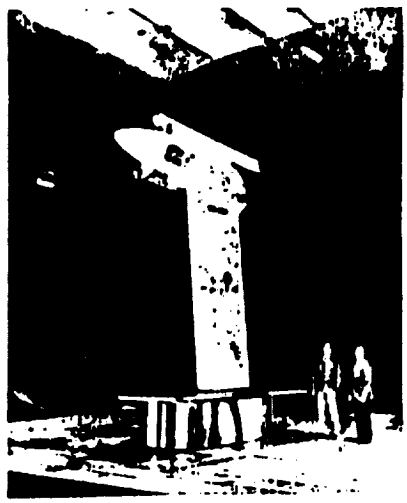

Figure 4.74 Bell's tilt-fold rotor test in NASA's 40 by 80-foot wind tunnel

$$\Delta f_{nf} = 4\sigma\pi R^2 C_f \tag{4.42}$$

where $4\sigma\pi R^2$ is approximately the wetted blade area for the whole aircraft, and C_f is the friction drag coefficient.

The expression for relative drag increment per pound of gross weight ($\bar{\Delta} f_{nf}$) is obtained by dividing Eq. (4.42) by W:

$$\bar{\Delta} f_{nf} = 4\sigma C_f / w \tag{4.43}$$

where w is the disc loading.

Assuming that the solidity ratio of the side-by-side retractoplane is about $\sigma = 0.10$, $C_f = 0.0035$, and $w = 20$ psf, one would see that for a 45,000-lb gross-weight class, the order of magnitude of the drag penalty would be 3.15 sq.ft. Through ingenious design solutions, the drag penalty can be reduced, but probably not lower than 50 percent of the value given by Eq. (4.43).

Rotor blades folded rearwards (Lockheed's composite aircraft, CL-945) will increase the fuselage wetted area by approximately 8 percent.

The wetted area of a transport aircraft of the 45,000-lb gross-weight class would be approximately 2900 sq.ft. Assuming the above-indicated area increment and a friction coefficient value as in the blade case; i.e, $C_f = 0.0035$, one would see that

$$\Delta f_{nf} \approx 2900 \times 0.08 \times 0.035 \approx 0.8 \text{ sq.ft.}$$

It appears that in the case of fuselage stowed variable radius rotors, the increase of the fuselage cross-section will be approximately 10 percent. Assuming a circular cross-section of the fuselage, the corresponding increment in the wetted area would be approximately 5 percent, and the corresponding increase of the equivalent plate area for an aircraft of the 45,000-lb gross-weight class would be $\Delta f \approx 0.5$ sq.ft.

However, there may be additional 'hidden' increases in the wetted fuselage area, resulting from the fact that both Piasecki and Sikorsky concepts require the installation of a blade telescoping system which is bulky and occupies a sizable portion of the fuselage volume just under the rotor shaft. This, in turn, might require an increase in the fuselage size in order to provide the necessary cargo or passenger space. This problem would be eliminated by raising the telescoping unit, and locating it above the ceiling of the cabin. However, this would result in increased fuselage drag.

The only system of stowing the retracted rotor in the fuselage that will not result in the above-mentioned drawbacks is the zig-zag method shown on Fig. 4.68. In this case, the whole blade folding system is located in the plane of the rotor, leaving an unobstructed fuselage.

Cruise Fuel Consumption per Pound of GW and N.Mi. In the retractoplanes, cruise is performed on the turbofan section of the convertible engines. Consequently, fuel consumption per pound of gross weight and one nautical mile flown will be expressed by Eq. (1.31), which is repeated as follows.

$$(FC_w)_R = (\text{tsfc}/V)/(L/D)_v \tag{4.44}$$

where speed of flight V is in knots.

In this equation, the (tsfc/V) ratio can be considered as a gauge of excellence (the lower, the better) of the powerplant, as it represents fuel consumption in pounds per pound of engine thrust and nautical mile flown. The $(L/D)_v$ values at the corresponding speed of flight expresses the aerodynamic excellence of the airframe.

Trends in tsfc vs. flight Mach number for convertible engines are shown in Figure 4.75 (courtesy of H. Semple, Boeing Helicopter Company).

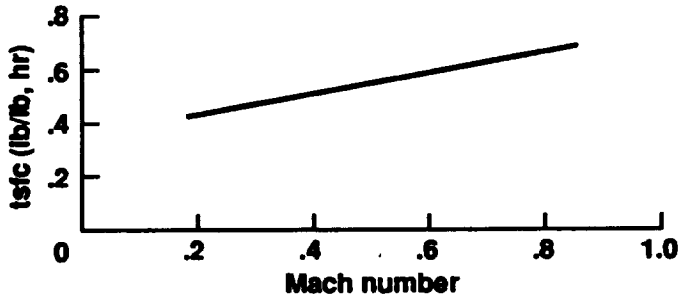

Figure 4.75 Trend in tsfc vs. flight Mach number for convertible engines

Based on inputs from Eq. (4.44), trends in the (tsfc/V) levels vs. speed of flight at SL and 30,000 ft are shown in Fig. 4.76.

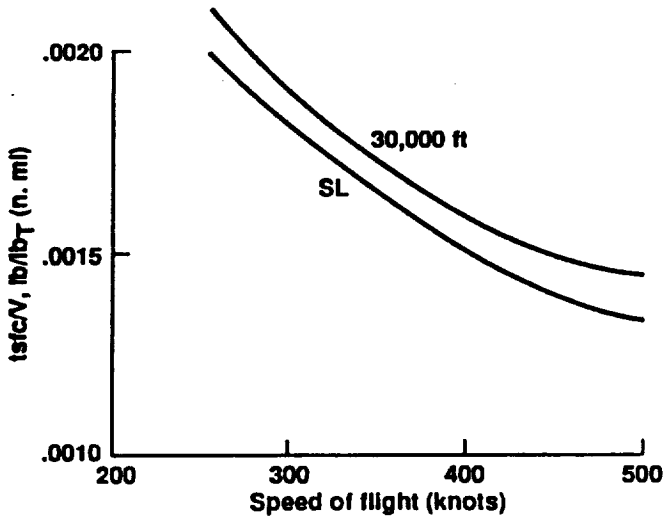

Figure 4.76 Trends in (tsfc/V) vs. speed of flight at SL and 30,000 ft

A glance at Fig. 4.76 would indicate that the (tsfc/V) factor decreases with speed of flight—at first, rapidly, and then at a somewhat slower rate.

Looking at Eq. (4.44), one would note that in order to minimize fuel expenditure per unit of gross weight and unit of distance flown, the designer must try to configure the aircraft in such a way that its maximum L/D values coincide with the low (tsfc/V) regions.

In the case of retractoplanes, this would mean that it would be desirable to select wing geometry and its loading so that, say, $(L/D)_{max}$ would appear in the 350 to 450-kn speed range when flying at 20,000 to 30,000-ft altitudes.

Assuming, in the above-indicated cruise speed range, that it would be possible to achieve (L/D) values from 10 to 14, the $(FC_w)_R$ values for retractoplanes may be expected to be included within the shaded area shown in Fig. 4.77.

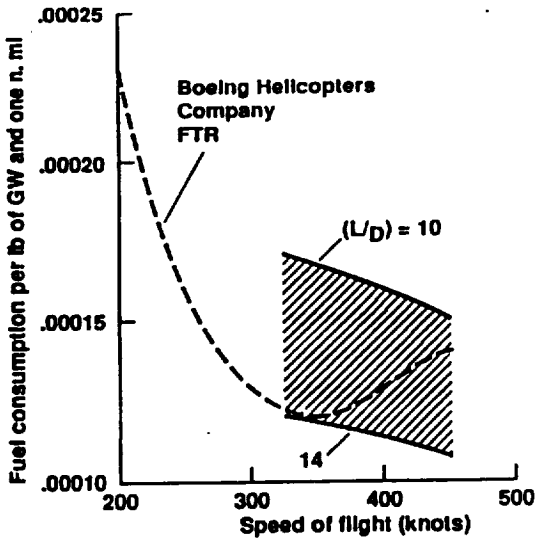

Figure 4.77 Trends in $(FC_w)_R$ values vs. speed of flight at 30,000 ft
(FTR folding tilt-rotor curve based on Ref. 43)

In actual design studies of the tilt-rotor type retractoplane (Ref. 43), the computed L/D vs. speed of flight at 25,000 ft (which may be considered close to the 30,000-ft case) is shown in Fig. 4.78.

Using inputs from Figs. 4.78 and 4.75, the $(FC_w)_R = f(V)$ relationship was computed and added to Fig. 4.77.

The '14-marked' line in Fig. 4.77 represents the potential possibilities of the stowed tilt-rotor concepts regarding optimal fuel consumption per pound of gross weight and one nautical mile flown in cruise at 30,000 ft. The above remarks should also apply to the single-rotor type retractoplanes.

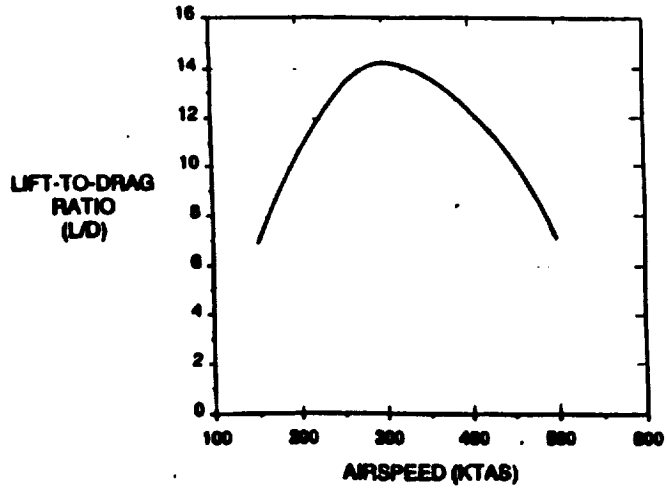

Figure 4.78 L/D vs. speed of flight at 25,000 ft for the FTR aircraft (Ref. 43)

It would be of interest to see how $(FC_w)_R$ values for stowable rotors compare with those of the open-airscrew type (propellers and propfans) shaft-driven aircraft. This will be done with the help of Eqs. 1.27 and 1.31, while assuming for simplicity that the flight (L/D) values for the stowable rotor types would be the same as for their shaft-driven propfan counterparts.

It should be noted at this point that this assumption may be somewhat unfair when applied to the propfan types, as their (L/D) levels should be higher than for stowable-rotor types, where some parasite drag increments would be encountered as a consequence of stowing the rotor(s). However, retaining the equality of the (L/D) value assumptions, the $(FC_w)_R$ ratios for the two types of aircraft can be expressed as follows:

$$(FC_w)_{R_{sr}}/(FC_w)_{R_{sh}} = 325\eta_{pr}\eta_{ov}\text{tsfc/sfc}\,V. \tag{4.45}$$

Assuming that a propulsive efficiency of 0.85 due to the use of propfans can be maintained up to some $V \approx 500$ kn, and that in forward flight, the overall transmission efficiency will be 0.95, Eq. (4.45) can be rewritten as follows:

$$(FC_w)_{R_{sr}}/(FW_w)_{R_{sh}} = 262.4(\text{tsfc}/V)/\text{sfc}. \tag{4.46}$$

Taking (tsfc/V) trends at SL and 30,000 ft as shown in Fig. 4.76 and, assuming that the specific fuel consumption of shaft turbines will be 0.4 and 0.5 lb/hp.hr, the trends expressed by Eq. (4.46) are shown graphically in Fig. 4.79.

One can see from this figure that should the tsfc of composite engines be as good as predicted by Fig. 4.75, then retractoplanes operating with such powerplants at cruise speeds higher than 400 to 425 knots would have better fuel consumption per pound of gross weight and one nautical mile flown than their propfan counterparts at the same L/D values. This would be true, even if the sfc of the shaft turbine were as low as 0.4 lb/hp,hr. However, should the sfc be in the 0.5 lb/hp,hr range, then the crossover region of propeller and propfan superiority would drop to some 275 to 300 kn cruise speeds.

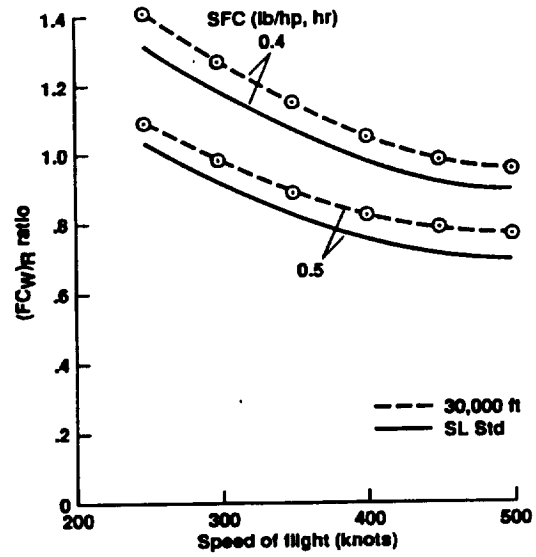

Figure 4.79 Ratios of fuel consumption per pound of gross weight and n.mi. for stowable-rotor aircraft with convertible engines to those of propfan types

It appears, hence, that in the high cruise-speed domain, retractoplanes can be competitive to propeller and propfan type aircraft, at least, as far as one factor in the overall transport effectiveness picture is concerned; namely, the $(FC_w)_R$ levels. Another important factor is the relative weight-empty levels.

Structural Weight Aspects. The establishment of trends in structural weight penalties – the price that must be paid for improved aerodynamic cleanness of retractoplanes–is obviously a very important factor in the overall evaluation of these concepts. Unfortunately, there is very little factual data to help in the development of such trends, as no stowable-rotor aircraft ever attained flight status. Consequently, one must use data obtained from paper studies only, supported by one's own intuitive judgement.

Telescoping blades may be used in both single-rotor and side-by-side stowed-rotor configurations. Thus, weight penalties (expressed as percentages of gross weight) resulting from a reduction in the original rotor diameter through this operation would be of interest. Fig. 4.80, based on Refs. 33 and 54, shows such a trend. It should be indicated at this point that the Piasecki/Vertol telescoping rotor blade was actually built, but the weight penalty–computed on the basis of a comparison with conventional rotor blades of the same geometric dimensions – was much higher than that shown in Fig. 4.80. For the 58 percent diameter reduction of the rotor only, the weight penalty would amount to about 6.2 percent of the gross weight of the aircraft. However, as indicated in Section 4.41, considerable weight savings can be accomplished by using the reverse taper concept. Thus, it may be assumed, at least at present, that this figure represents an approximately correct trend regarding relative structural weight increases of the rotor alone vs. the amount of the original rotor diameter reduction.

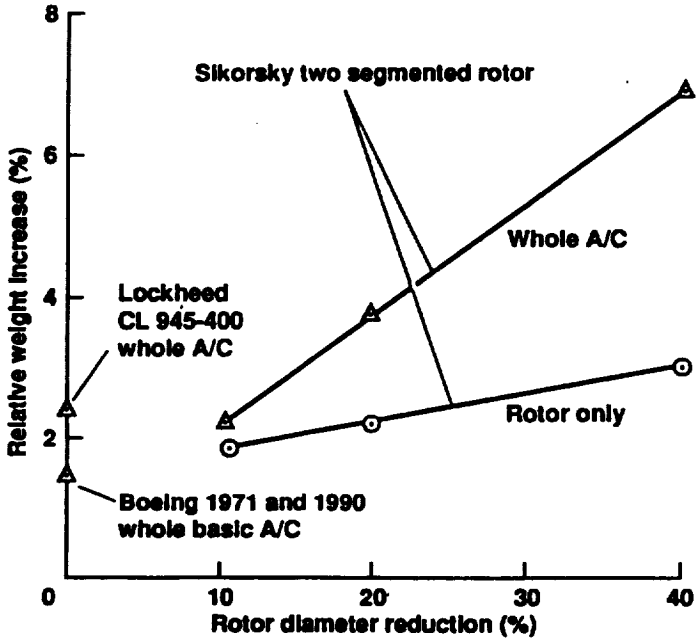

Figure 4.80 Relative weight penalties (percentage of GW) associated with rotor diameter reduction and complete stowing

It is obvious that in addition to the relative weight increases of the rotor per se, other structural weight increases will be encountered due to the retracting mechanism, stowing arrangements, etc. This trend is depicted in Fig. 4.80, where Sikorsky, as well as the Lockheed and Boeing (side-by-side) configurations are shown.

A glance at the lines and points in this figure seems to indicate that the overall weight penalty for the single-rotor, reduced diameter stowable configuration could be several times higher than for the schemes suitable for side-by-side configurations, as illustrated by the 1971 and 1990 point. It is interesting to note that the overall relative weight penalty for the Lockheed system, although higher than for the side-by-side case, would still be lower than for single-rotor schemes incorporating both reduction in the rotor-blade radius and stowing of the so 'shrunken' rotor in the fuselage.

Trends in the relative weight empty of stowable rotor aircraft can be deduced from Fig. 4.81.

From presently available data, it appears that the relative weight-empty values of stowable rotors are close to 65 percent, regardless of the configuration and gross-weight class. Although one would expect that for the Sikorsky TRAC configuration, the relative weight empty would be somewhat higher than for the side-by-side or Lockheed configurations.

Trends in Relative Payload vs. Range and Ideal Productivity. In order to get some idea about trends in relative payload vs. range relationships, the relative payload weight for the 50,000-lb gross-weight class retractoplane was estimated assuming a relative weight empty

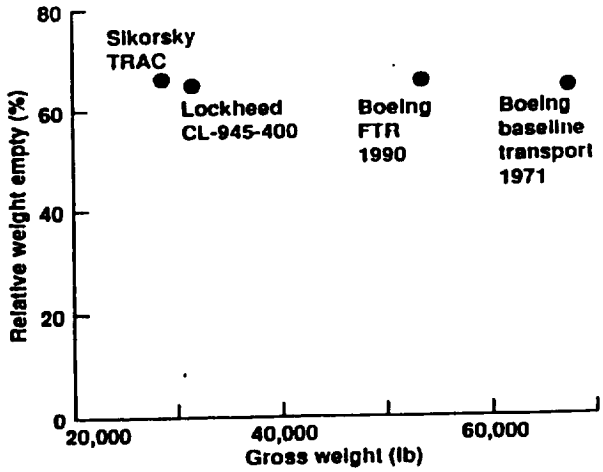

Figure 4.81 Trends in relative weights empty of stowable rotor aircraft

of 0.65 and the weight of crew and trapped fluids at 480 lb. This resulted in $\overline{W}_{opl} = 0.34$. Taking advantage of advanced technology, one may expect to improve this value to 0.4.

As to probable $(FC_w)_R$ values, a look at Fig. 4.77 would indicate that at, say, 400-knot cruise speed, the optimal $(FC_w)_R$ level could be about 0.000115 lb/lb,n.mi, but would probably be closer to 0.000138. Using the above-established values for relative zero-range payload and fuel consumption per pound of gross weight and nautical mile flown, the representative trends in relative payload vs. range were computed from Eq. (1.10), and are shown in Fig. 4.82.

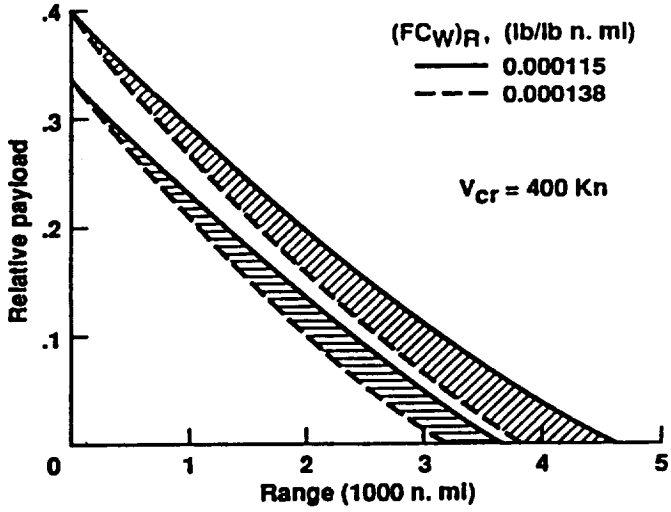

Figure 4.82 Anticipated trends in relative payload vs. range relationship for stowed-rotor concepts

One can see from this figure that in comparison with the relative payload vs. range relationship for conventional tilt rotors (Fig. 4.26), stowable rotor concepts would represent definite advantages.

In order to get some idea about the relative ideal productivity vs. range of stowable-rotor aircraft in general, the $\overline{W}_{pl} \times V_{cr}/\overline{W}_e$ values were computed for a 50,000-lb gross-weight aircraft, using the $\overline{W}_{pl}$ values shown in Fig. 4.82, where W_e = 32,500 and 29,500 lb, and assuming that V_{cr} = 400 kn. The resulting relationship is shown in Fig. 4.83.

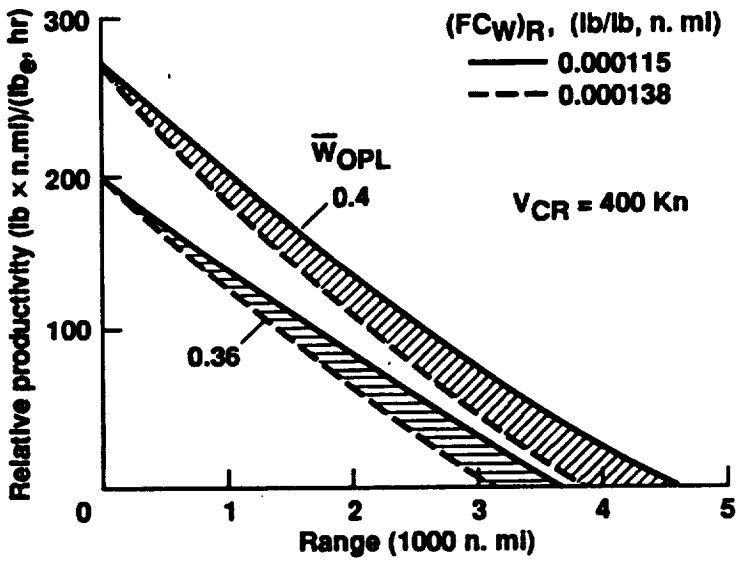

Figure 4.83 Ideal relative productivity vs. range trend of stowable-rotor aircraft

A glance at this figure will indicate that for short and medium ranges (say, up to 1000 n.mi) and an assumed constant cruise speed, obtaining the lowest possible relative weight-empty levels (i.e., the highest zero-range relative payloads) would represent the most important factor as far as achieving high ideal relative productivity values for the stowable-rotor concepts is concerned.

4.4.6 Concluding Remarks re the Stowable Rotor Aircraft Investigation

One design requirement, which is quite apparent in the stowable rotor concepts (retractoplanes), is the need for separate lifting and propelling systems in the VTOL and low-speed operation vs. high-speed regimes of flight. This, in turn, leads to mechanical complexities associated with stopping and stowing the rotors, and unavoidable higher equivalent flat plate area values than for fixed-wing counterparts of the same gross-weight class. Mechanical complexities involve higher structural weights (higher relative weight-empty values) and, of course, cost. Also, mechanical complexities usually represent an invitation for decreased operational reliability and safety.

It appears, hence, that practical applications for the stowable-rotor concept can be found for only those missions where low disc loading in hover (similar to that of helicopters) is an absolute necessity, while a high subsonic, or even supersonic, flight speed capability is also a strong requirement.

As far as comparing side-by-side retractoplanes with their single-rotor counterparts is concerned, it appears to these authors that stopping and stowing the rotors can be accomplished somewhat easier in the SBS configurations.

As for the single-rotor class, the Lockheed approach to stopping and stowing the rotor should, in the overall picture, be somewhat simpler than for other concepts. This, in spite of the fact that other problems, such as prevention of an excessive c.g. shift when the blades are folded backward, could be encountered.

In order to see what modern technology may contribute to possible improvements in the Lockheed concept, a very rough study on this subject was performed, with the following tentative general conclusions.

The original Lockheed stowable-rotor aircraft, the CL-945-400 combines a low disc loading of 9.64 psf and a maximum flight speed exceeding 350 kn—high for propeller driven machines. However, speed performance may be substantially increased by replacement of the wing-mounted conventional propellers and turboshaft engines (rated at 3435 hp, sfc of 0.483, and weighing 700 lb) with propfans and modern turboshafts. Thus, the CL-945-400 would become a high performance aircraft, retaining all basic hovering capabilities of the original, but with substantially better high-speed capabilities due to the high propulsive efficiency of propfans at elevated subsonic Mach numbers (see Fig. 4.11). The main modification, outside of the powerplant, would be a new wing gearbox adapted to the new rpm's and shp (5000 hp) of the engine. Preliminary investigation shows that replacing the old propulsive system (1967 vintage) by one representing the current technology in propfan and turboshaft engines should result in little change in the overall weight of the main dynamic system.

Aerodynamic refinement of the body, as well as of the wing (sweepback and new airfoil) should result in a decrease in drag. In addition, replacement of conventional tail rotors with the Fenestron type covered with doors in forward flight would further reduce the fuselage drag. The use of Fenestron will not have a detrimental effect on hovering capabilities of this aircraft because large additional excess power – 2 X 5000 hp vs. the 2 X 3435 hp installed—would be available for main rotor torque compensation.

However, more detailed studies of various parameters such as the diameter of the propfans, tip speed, rotor disc loading, and wing loading would be necessary in order to confirm the attractiveness of using modern propulsive means to substantially boost the performance of the Lockheed-type stowable rotor.

With respect to recommendations regarding stowable rotors in general (both single and side-by-side), it appears that coordinated experimental efforts regarding the actual process of stopping and stowing is needed. Because of cost aspects, at least the first phase of this effort should be carried out on scale models.

A meaningful reliable aerodynamic wind-tunnel test program should be established to provide data for realistic assessment of the parasite drag penalties associated with stowing of the rotors. Indepth design studies of retractoplanes should parallel experimental efforts.

4.5 Convertible Rotor Concepts

4.5.1 General

The idea of developing aircraft using open airscrews for VTOL operations as well as for performing fixed-wing type flights has also been approached through the concept of converting stopped blades into fixed wings. As in the preceding cases, there have been many proposed solutions. However, very few of them have ever advanced to serious wind-tunnel and flight studies. In most cases, development of the idea was carried out as private ventures by individuals having little or no support from either the government or large aeronautical companies. The X-wing represents an exception, as considerable analytical experimental and design efforts have been spent on this project.

As to pioneering efforts regarding convertible rotor concepts, the works of Herrick during the thirties come to one's mind. In his concept the upper wing of the biplane could operate as both a fixed wing and an autorotating rotor (Figure 4.84).

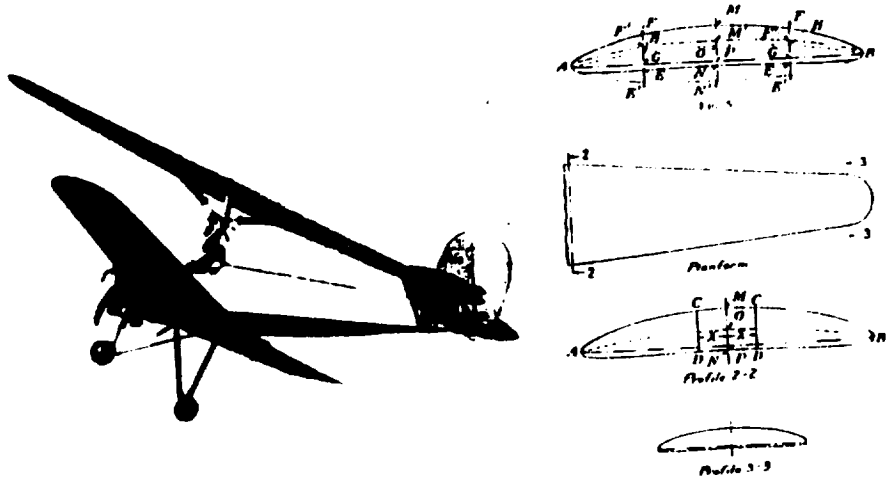

Figure 4.84 HV-2A "Vertiplane" which achieved first successful transition in 1937 (left) and airfoil section of upper wing (right)

As shown in this figure, the upper wing had a symmetrical airfoil. Numerous conversions from the fixed-wing to the autogiro stage were flight demonstrated in 1937. However, since this aircraft had no VTOL and hover capability, its practical appeal was minimal, and no further development of the concept was undertaken.

As to contemporary activities in the convertible rotor field, it appears that, at present, only the Rotafix (strictly private venture) and the X-wing (government supported efforts) represent active projects.

4.5.2 Rotafix

This concept, developed by A. Kisovec, is based on a side-by-side configuration, where either two-bladed, or single-bladed rotors are located at the tips of wings with dihedrals. When the rotor is stopped in flight, the advancing blades form a spanwise extension of the wing, while the retreating blades in the two-bladed, or counterweight in the single-bladed configurations are retracted into the fixed-wing structure. In this way, the rotorcraft is converted into a high aspect ratio aeroplane.

Although, in principle, this concept can be used for transport aircraft, the present efforts of Kisovec are chiefly directed toward RPV applications (Figure 4.85).

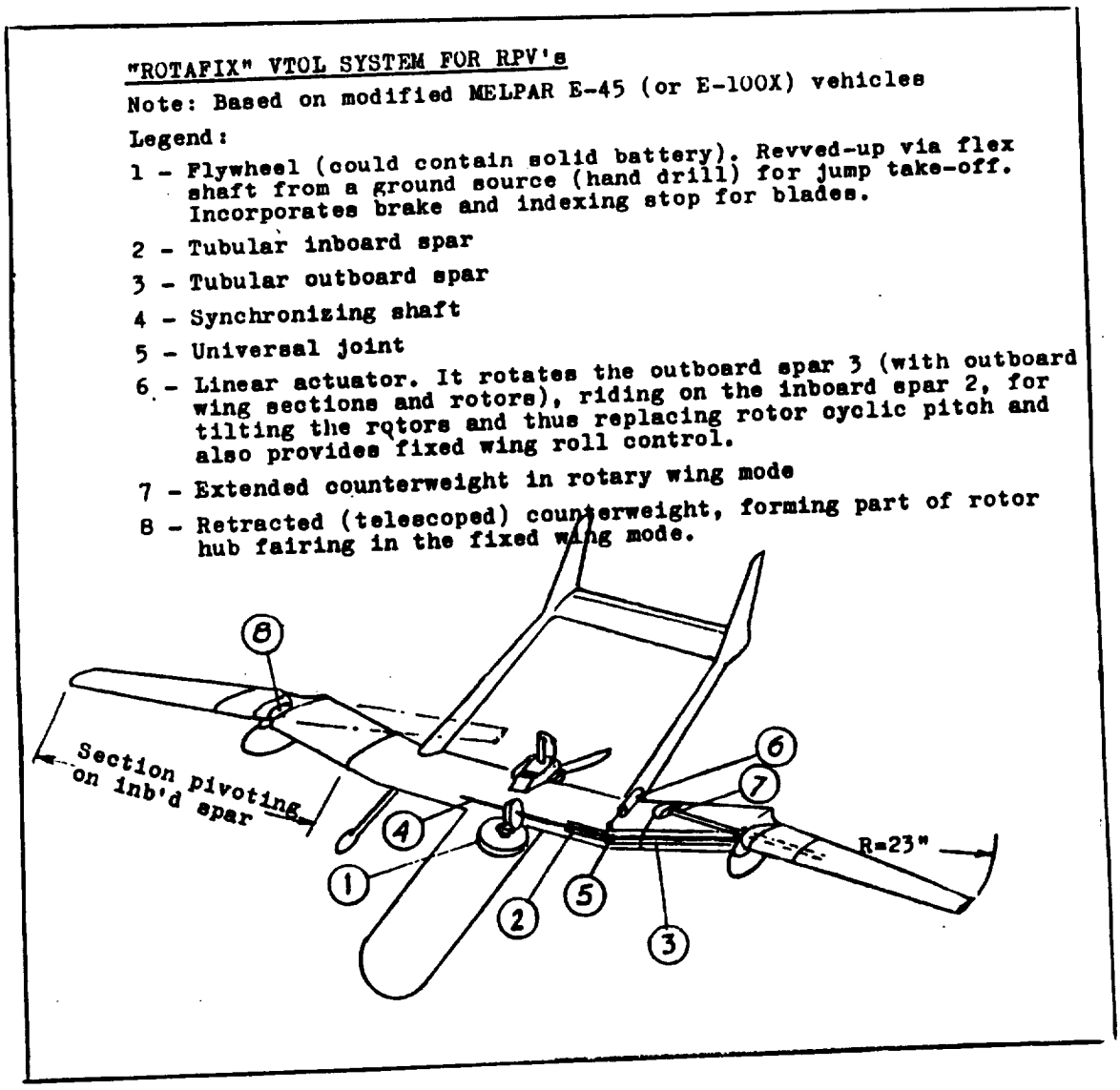

Figure 4.85 Example of the Rotafix concept application to RPVs

4.5.3 X-Wing

The original concept of the X-wing, developed under the guidance of R. Williams, is based on the idea of stopping a four-bladed rotor in the X position, and then converting it into a fixed wing with two half-spans at -45° and the other two at 45° sweeps. As the rotor is transformed into the X-wing, the incoming airflow on the previously advancing side comes toward the leading edge of the blades. However, on the previously retreating side, the blade trailing edges are now facing forward. Consequently, the blades must be symmetrical with respect to the vertical plane passing through their half-chord.

Considerable analytical, experimental, and design efforts have been spent in an effort to reduce to practice the idea of a rotor that, after stopping, could serve as a wing capable of high subsonic speeds.

The rotor-wing scheme evolved as a means of solving aerodynamic problems. This scheme was employed in the X-wing concept demonstrator, built by Sikorsky for NASA/DARPA under a $77 million dollar contract awarded in 1984. The X-wing was intended to be flight tested on the Sikorsky RSRA (Figure 4.86).

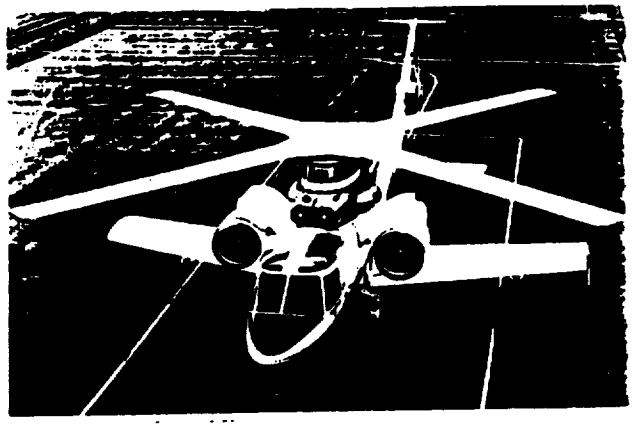

Figure 4.86 Sikorsky S-72X1 X-Wing rotor system research aircraft

In this system, compressed air is blown through slots along either edge of the symmetrical aerofoil section of each blade. Separate plenums in the leading and trailing edges carry the compressed air to circulation control slots. Rotating-wing flight is made possible by adjusting the flow of air from valves in the pneumodynamic system to the control slots. This provides control of cyclic and collective pitch.

In the helicopter mode, the rotor is shaft-driven. Thus, rotor torque-compensating devices are required.

Conversion to the fixed-wing mode is accomplished as follows: By means of a clutch, the X-wing can be made to stop turning and be locked into its correct fixed-wing position. All airflow from the blades is then ejected from the rearward-facing slots and can be modulated to provide roll control.

C-3

Initially, the X-wing concept attracted the interest of several aerospace companies as well as government agencies. Design studies (Boeing Vertol, Lockheed, and Sikorsky, among others) were made of aircraft ranging from transports to fighters. A Lockheed project of a flight demonstrator from the late seventies is shown in Fig. 4.87 while an artist's impression of a military X-wing is given in Fig. 4.88.

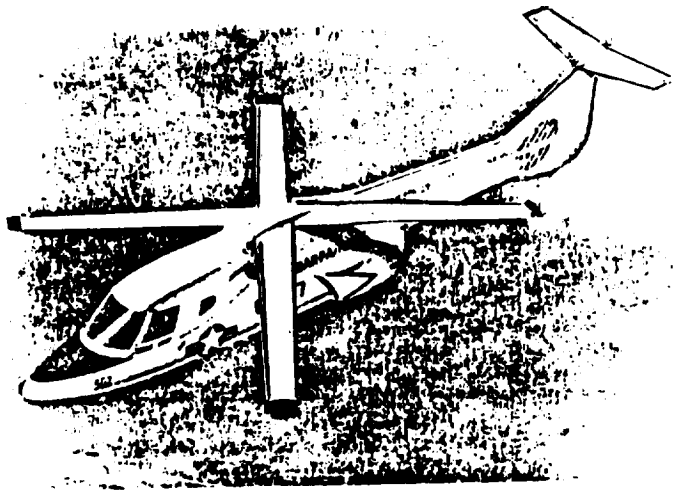

Figure 4.87 Example of a design study of the X-wing aircraft by Lockheed

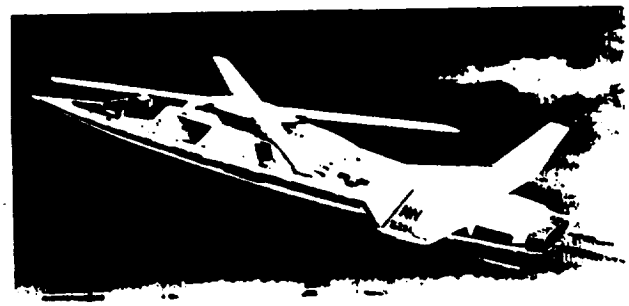

Figure 4.88 Artist's impression of a military X-wing aircraft capable of speeds in the Mach 0.8 range

At present, it appears that interest in the X-wing is decreasing because of technical and financial difficulties, as well as the political climate – lacking a strong champion of this concept.

Concluding Remarks

Basis of Comparison. The tilt-rotor, as represented by the first generation; namely, the V-22 and, to some extent, the XV-15 is, at present, the only VTOL aircraft based on an open airscrew type vertical lifter that has attained the state of operational acceptability as a military system. Indepth studies tend to indicate that configurations conceptually close to the V-22 and XV-15 scheme could find a niche in the civilian field as short-haul transporters and business aircraft because of their economic and environmental aspects. Consequently, generalized performance as well as environmental characteristics and cost aspects of the V-22 may be accepted as a basis for comparison for future generations of conventionally configured tilt-rotors and other systems relying on open airscrews for VTOL maneuvers. In this report, a comparison of the investigated configurations with the V-22 will be limited to generalized performance only. Thus, attention will be focused on the following items:

Hover OGE:

1. Power required per pound of gross weight.
2. Fuel consumption per pound of gross weight and hour.
3. Zero-time relative payload, and payload variation vs. time in hover.
4. Downwash velocity.

Horizontal Flight:

1. Power required per pound of gross weight vs. speed of flight, or $(W/D_e) \equiv (L/D_e)$ vs. speed of flight.
2. Fuel required per pound of gross weight and n.mi. vs. speed of flight.
3. Zero-range relative payload, and payload variation vs. range.
4. High-speed capabilities.
5. Ideal relative productivity.

The SHP required per pound of GW in hover at SLS and 4000 ft,95° vs. disc loading for the V-22 and other configurations is shown in Fig. 4.89.

A glance at this figure will indicate that the relative shaft horsepower required in hover values for the advanced tilt-rotor and side-by-side retractoplanes are quite similar to those of the V-22. For the single-rotor retractoplane, the relative shaft horsepower required in hover values could also be close to those of the V-22 as, in both cases, the rotor disc-loadings would be much the same. By contrast, the specific power required for the high disc-loading tilt-wing would be approximately twice as high as for the V-22.

The fuel required in hover OGE per lb of gross weight and hour for the compared aircraft is shown in Fig. 4.90. Here, optimal projections of fuel required per pound of gross weight and hour in hover OGE at SLS for studied configurations is shown vs. actual value for the V-22.

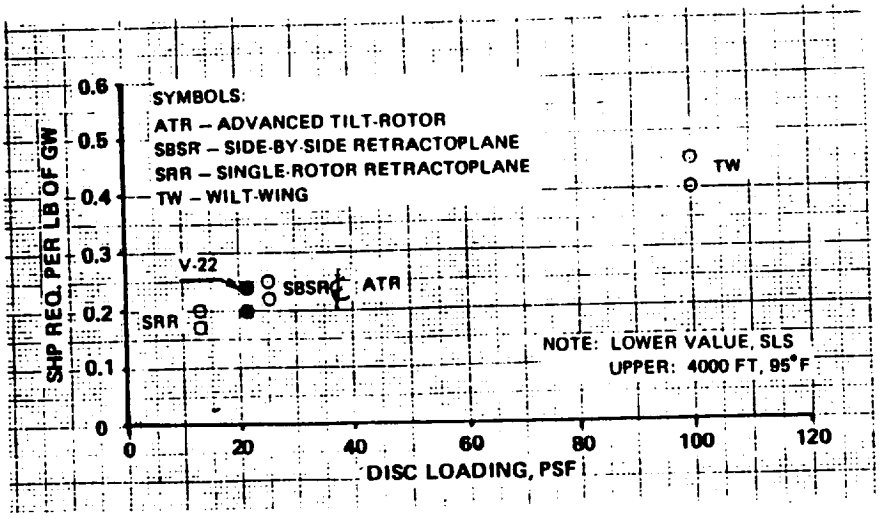

Figure 4.89 SHP required per lb of GW in hover OGE at SLS and 4000 ft, 95°F

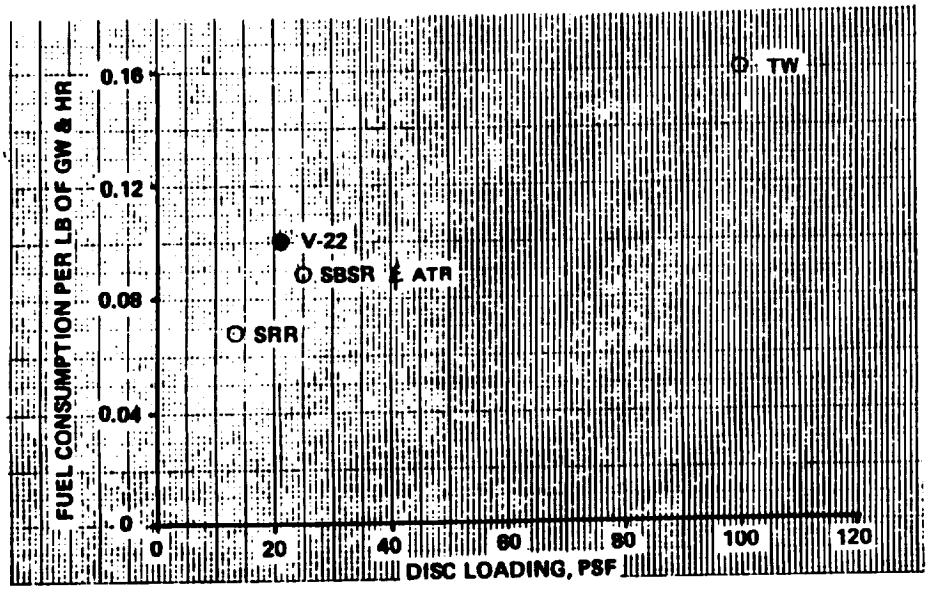

Figure 4.90 Fuel consumption per lb of GW and hour vs. disc loading

The optimal values of specific gross-weight-related fuel consumption in hover OGE for rotor-type aircraft could be lower than for the V-22. It should be remembered, however, that the projected gains in $(FC_w)_t$ levels stem from anticipated improvements in the sfc levels of future turboshafts and convertible engines. The projected optimal gross-weight-related specific fuel consumption of the high disc-loading tilt-wing will still be considerably higher than for the V-22 (approximately 60 percent), while the specific power excess amounted to about 100 percent.

Payload vs. Time in Hover OGE and SLS. The actual relative weight-empty and zero-time (zero range) relative payload of the V-22, plus estimated values and optimal projections for the compared configurations are shown in Fig. 4.91.

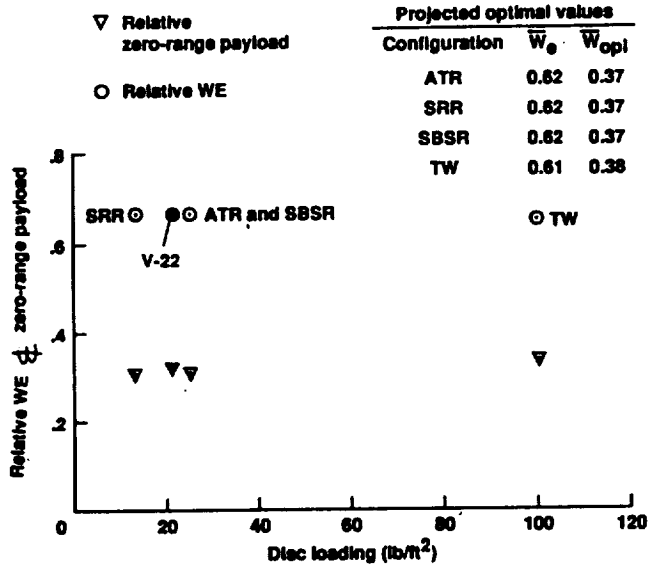

Figure 4.91 Relative *WE* and zero-time *PL* vs. disc loading for V-22 and compared configurations

Looking at this figure, one notes that the estimated values for relative weight-empty and thus, for the relative zero-time (range) payloads of the investigated configurations are quite close to the actual ones of the V-22. However, assuming that, in the future, some gains in reduction of structural weights are possible, projected optimal values of $\overline{W}_e$ and $\overline{W}_{0_{pl}}$ are also indicated.

The actual relative payload vs. time in hover at SLS for the V-22, and optimal projections for the compared configurations are shown in Fig. 4.92

It should be emphasized at this point that in establishing the so-called projected optimal relationships for payload vs. time in hover in Fig. 4.92, the $\overline{W}_{0_{pl}}$ values were taken from the table in Fig. 4.91, while the $(FC_w)_t$ values were assumed to be as shown in Fig. 4.90.

Looking at Fig. 4.92, one will note that for the advanced tilt-rotor and side-by-side retractoplane, considerable improvements in that relationship appear possible with respect to the V-22 characteristics. In the single-rotor retractoplane, even better payload vs. time in hover characteristics than those of the side-by-side types can be expected. It should be recalled that in the design philosophy of the high disc-loading tilt-wing, hovering is considered as transient maneuvers only, and not as an operational stage.

Downwash Velocities. To complete the picture of hovering aspects, ideal induced velocities at the disc in fps, as well as ideal fully developed downwash values in mph for the V-22 and other examined configurations are shown in Fig. 4.93.

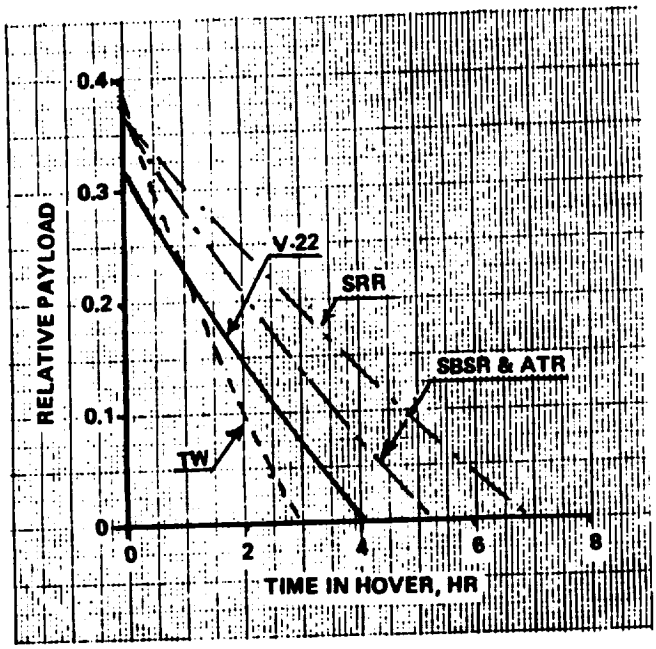

Figure 4.92 Relative payload vs. time in hover for V-22 and compared configurations

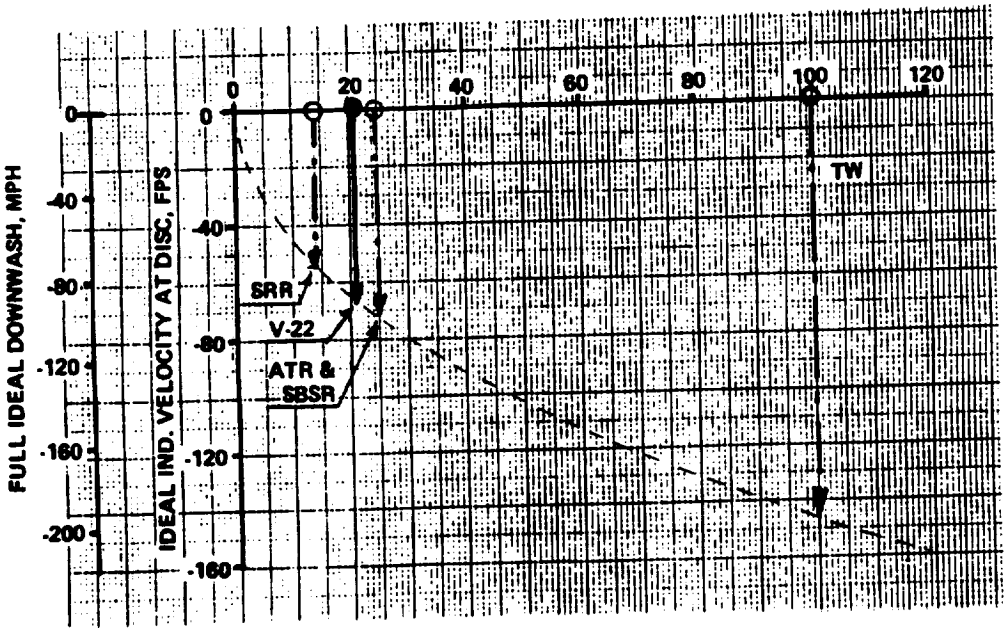

Figure 4.93 Ideal induced velocities and downwash of the V-22 and compared configurations

Looking at this figure, one will note that the downwash velocities for the ATR and SBSR would be quite similar to those of the V-22, but somewhat lower for the SRR. This means that all of the above-mentioned configurations will be similar to the V-22 with respect to environmental aspects resulting from the lifter downwash. By contrast, the high disc-loading tilt-wing will probably require prepared surfaces for VTOL operations.

SHP Required per Lb of GW vs. Speed of Flight. In this summary, emphasis is placed on a relative comparison of various characteristics of the examined configuration. Thus, $\overline{SHP}_f$ values vs. speed of flight are shown for the SLS case only (Fig. 4.94). This presentation should give the reader some idea of the ranking of the overall aerodynamic effectiveness of various designs having shaft-powered horizontal thrusters as a means of aircraft propulsion in forward flight.

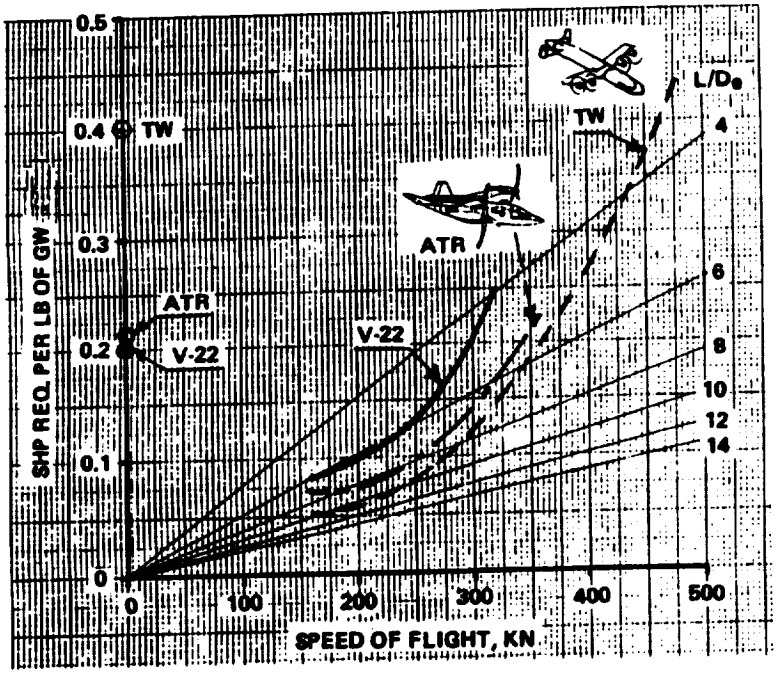

Figure 4.94 Power required per pound of GW vs. speed of flight at SLS

When comparing shaft-driven with jet propelled configurations, fuel consumption per pound of gross weight and one hour could serve as a means for establishing how various concepts and configurations may be ranked regarding their aerothermodynamic effectiveness (Fig. 4.95).

It should be noted that the auxiliary scales are marked in these figures. In the specific power required case, this auxiliary scale of the L/D_e values would permit the reader to see at a glance the maximal lift to equivalent drag ratio levels that can be expected for the examined aircraft.

In Fig. 4.95, the auxiliary scale should permit one to judge how good the various concepts and configurations are with respect to fuel consumption per pound of aircraft gross weight and one nautical mile.

In Figs. 4.94 and 4.95, the V-22 curves and points are based on the manufacturer's data. However, other points and curves represent estimates by these authors. Thus, deviations from more accurate calculations may be expected. But, nevertheless, it is believed that the general trend shown by these figures is correct.

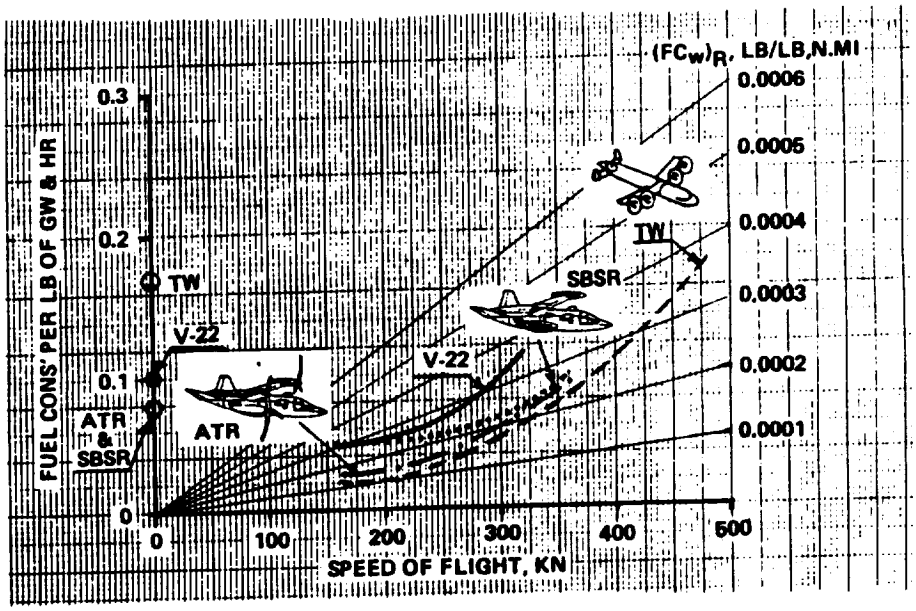

Figure 4.95 Fuel consumption per pound of GW and hour vs. speed of flight at SLS

It appears, hence, that in the new generation of tilt-rotors, as represented by the Canard configuration discussed by Schneider and Wilkerson in Ref. 43, considerable advances in aerodynamic effectiveness in comparison with the V-22 may be expected.

The tilt-wing, based on high disc-loading propfans, appears to have even better relative shaft horsepower required vs. speed of flight characteristics than the advanced tilt-rotor.

Fig. 4.95 offers a general picture of the potential progress in the thermo-aerodynamic effectiveness of new VTOL designs in comparison with the V-22. It should be noted that under SLS conditions, the appearance of the $(FC_w)_t$ vs. speed of flight relationship for such turbofan-driven configurations as the side-by-side retractoplane (SBSR), would be worse with respect to its shaft-driven counterparts than at higher altitudes of flight. For shaft-driven types, Fig. 4.95 should correctly reflect the relative standing of various configurations regarding their thermo-aerodynamic effectiveness.

With the above remarks in mind, one would see that in the investigated configurations, large improvements regarding energy requirements per units of gross weight and time at various speeds of flight can be expected with respect to the V-22 characteristics, Here, again, it appears that the tilt-wing could have a slight edge over other configurations.

Using fuel consumption per pound of gross weight and nautical mile as read from Fig. 4.95 relative payload vs. range was computed for the V-22 and compared configurations. In this process, the zero-range relative payload value of 0.32 was used for the V-22, and optimal projected values of 0.37 were assumed for the ATR and SBSR configurations (see Fig. 4.91,. while a value of 0.38 was accepted for the tilt-wing. Relative payloads vs. range computed under the above assumptions for SLS conditions are shown in Fig. 4.97.

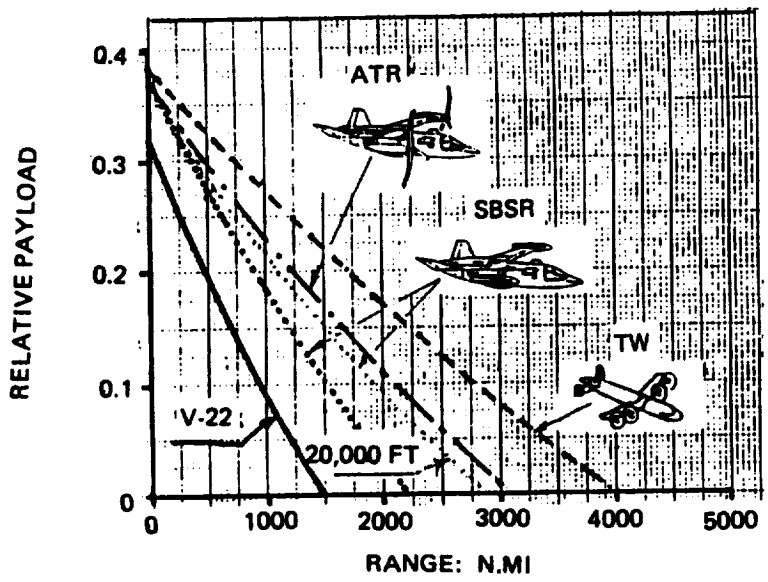

Figure 4.96 Relative payload vs. range, SLS

A glance at this figure will indicate that considerable progress in load-carrying characteristics may be expected for new generation tilt-rotors, side-by-side retractoplanes, and high disc-loading propfan tilt-wings. Turbofan-type aircraft would inherently be at a greater disadvantage than their shaft-driven counterparts regarding load-carrying capabilities at low altitudes of flight. Thus, for the side-by-side retractoplane, the relative payload vs. range relationship is also shown for a 20,000-ft altitude.

Ideal Relative Productivity. Using fuel consumption as shown in Fig. 4.95 and relative weight data from Fig. 4.91, the ideal relative productivity for the V-22 and the other three compared aircraft was computed for 200 and 400-n.mi distances. The results are shown in Fig. 4.97.

Looking at this figure, one will see that the ideal relative productivity of all the examined configurations should be considerably better than for the V-22. Furthermore, one would note that for short ranges as represented by 200 n.mi, the trend lines of all three examined aircraft are close to each other in spite of considerable differences in the fuel consumption per pound of gross weight and n.mi values. This indicates, as stressed before, that for short-haul operations, the zero-range payload levels (which were assumed at 0.37 and 0.38) are more important than the $(FC_w)_R$ values. However, for a 400-n.mi distance, relative fuel consumption aspects regain their significance, showing the increasing advantage of the thermo-aerodynamically effective (low $(FC_w)_R$) aircraft.

As to the ranking of the examined aircraft regarding their ideal relative productivity levels, it appears that the high disc-loading tilt-wing configuration could have a slight advantage over the advanced classic and folding tilt-rotors.

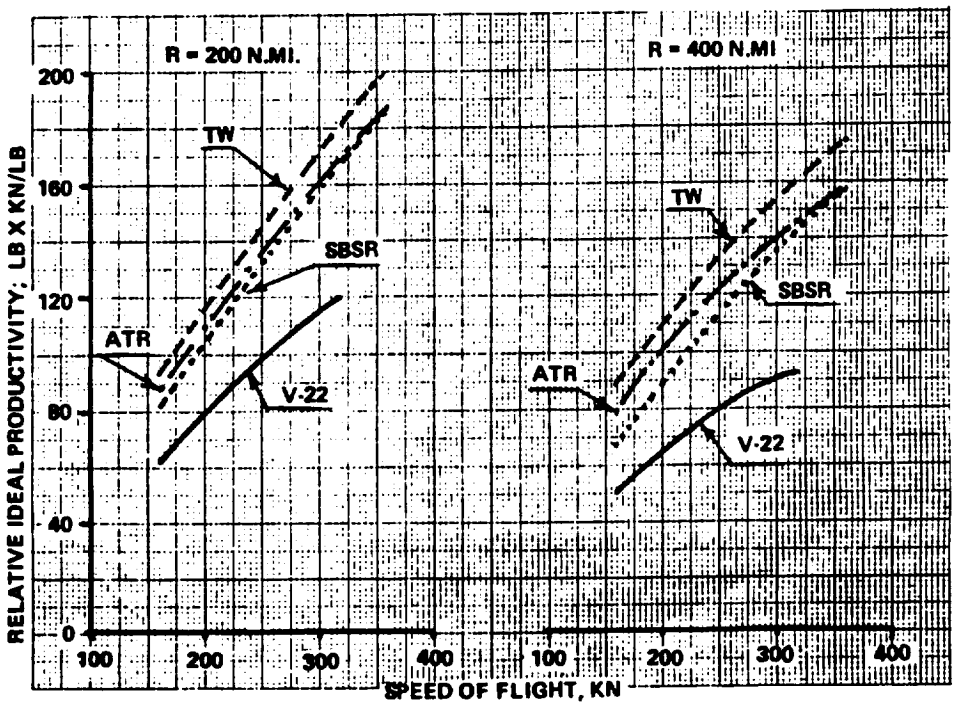

Figure 4.97 Ideal relative productivity vs. speed of flight at SLS

High-Speed Capabilities. Chiefly due to the deterioration of propulsive efficiency of straight-bladed, conventional rotor propellers (as in the V-22 or EUROFAR), the maximum dash capabilities of such aircraft would be limited to about $M < 0.55$; i.e., some 350 knots.

Boeing studies as reported by Schneider and Wilkerson in Ref. 43 suggest that by using advanced geometry high-speed rotor blades (Fig. 4.98), cruise speeds of 450 kn at 25,000 ft, -30°F could be achieved.

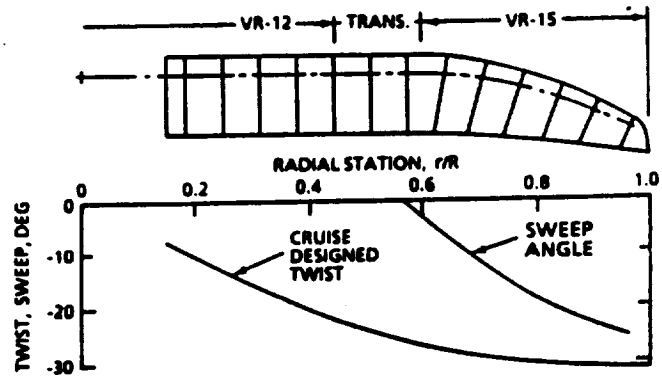

Figure 4.98 Advanced-geometry high-speed rotor blade[43]

For retractable-rotor configurations such as the folding tilt-rotor, high-speed capabilities could, in principle be the same as for turbofan transports of a similar gross-weight class. This means that $V_{max} > 0.8 \times V_{sound}$ are possible.

The propfan type tilt-wing configurations should also, in principle, have the same high-speed capabilities as those anticipated for unducted fan-driven transports. In other words, here, also, $V_{max} > 0.8 \times V_{sound}$ may be expected. This expectation is further supported by trends in estimated propulsive efficiency of the high disc-loading propfans adapted to the tilt-wing configuration. For instance, it can be seen from Fig. 4.48 that at 500 knots at 20,000 feet ($M \approx 0.814$), propulsive efficiently higher than 0.8 can be maintained.

Concluding Remarks. In the new generation of VTOL aircraft – based on open airscrews for vertical takeoff and landing operations – great progress in overall performance can be expected in comparison to that of the first generation operationally acceptable aircraft of the type represented by the V-22. If the presence of people near the hovering aircraft and/or extensive time in that regime of flight are necessary requirements, then configurations based on the application of the rotor-type vertical lifters appear as one of the most feasible in light of present technology approaches.

However, should it become possible to operate VTOL aircraft from prepared surfaces without people being in the immediate vicinity of the hovering machine, then tilt-wing configurations based on highly loaded propfans could become quite competitive with the advanced and stowable tilt-rotors.

It should be remembered, however, that aviation history teaches us that creation and development of the most successful and significant aircraft was not usually the product of the best possible analysis alone. Many factors, such as individual or collective talent, or even genius, of the designer or design group, perservence, willingness to accept new ideas, and aesthetic appeal enter the picture. All of the above factors contribute to acceptance of the truth that design and development of a flight vehicle is not only a science, but also art.

In the realm of aerial transportation, a masterpiece created by that art would be an operationally safe, economically viable, and environmentally acceptable VTOL aircraft.

APPENDIX

CURSORY DESIGN STUDY OF 400,000 AND 200,000-LB GW PROP-FAN DRIVEN HELICOPTERS

A.1 General

Design studies were performed in this country (Refs. 10, 15, 18, 56, and 57) and abroad (Refs. 8 and 11) to assess the competitive position of large and very large blade-driven helicopters with respect to shaft-driven concepts. For the up to 200,000-lb gross-weight range, there was no clear-cut agreement as to the precise weight level at which the blade driven types should become superior to their shaft-driven counterparts. However, it appeared that for helicopters exceeding 200,000-lb gross-weight, designs based on cold, warm, and hot jet propulsion, as well as those having turbofans directly mounted on the blades, should prove superior to shaft-driven types.This superiority of the blade-driven concepts would be the strongest for crane-type and other short-range missions.

In order to give the reader some idea about the possible configurations of large and very large blade-driven helicopters, Figures A.1 through A.4 are shown in addition to the Fitzwilliams Giant, Boelkow Bo-X, Hughes XV-9A, Hughes/David Taylor, Voljet, and the ITA propfan concepts already shown in Chapter 2.

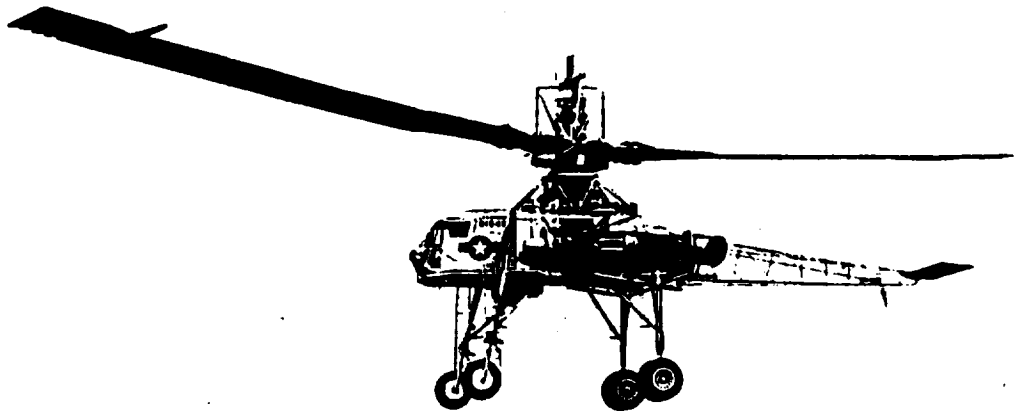

Figure A.1 Hughes XH-17 experimental heavy-lift jet-driven helicopter

Figure A.2 Artist's impression of Hiller's tip turbojet-powered very heavy-lift aerial vehicle

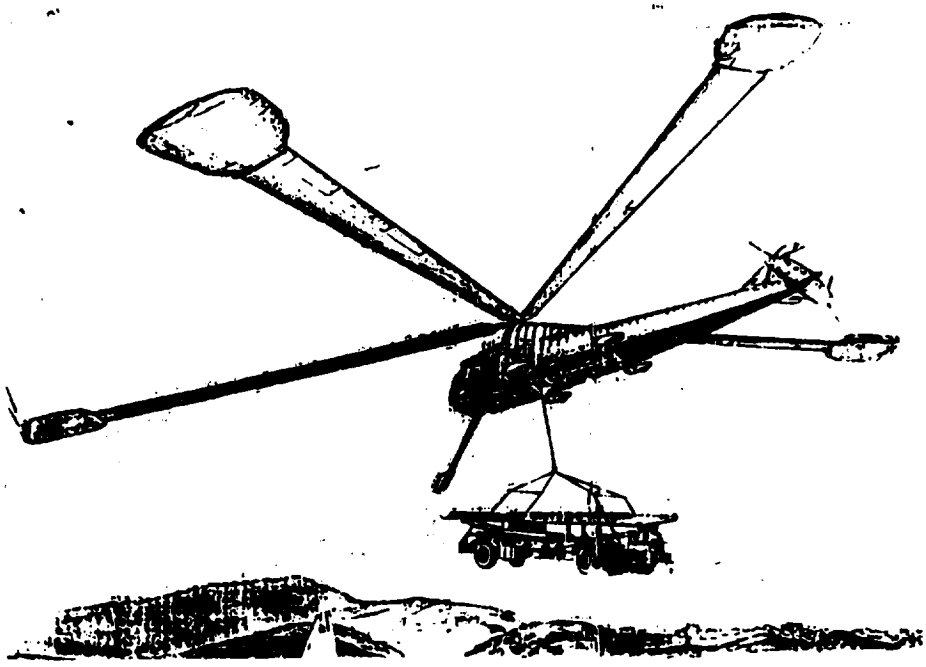

Figure A.3 Artist's conception of the Piasecki PA-1 very heavy helicopter with blade-tip mounted turbojets

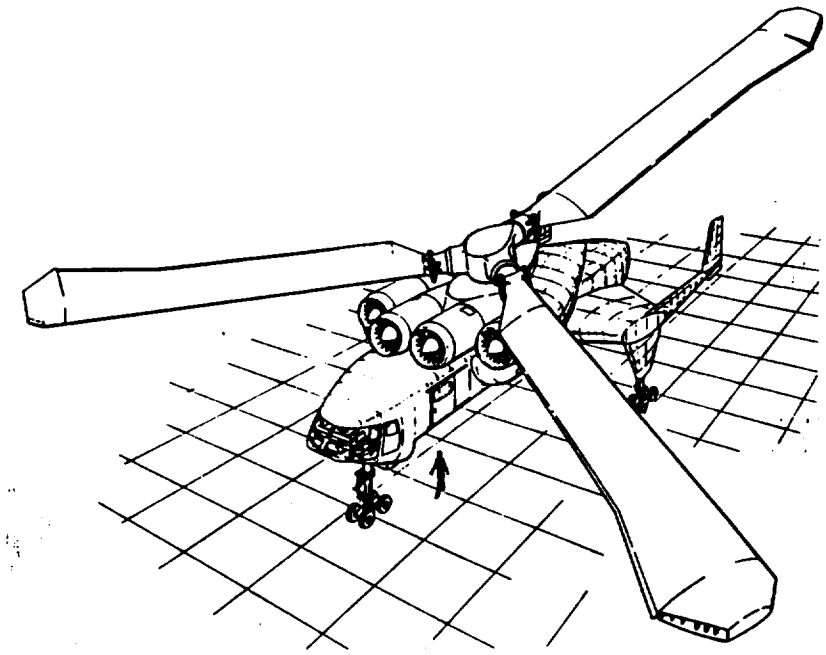

A.4 Sketch of the four-engine version of the Boeing 166-006, VHL warm-cycle helicopter

The principal characteristics of the above-mentioned helicopters are given in Table A.1, where most of the presented data were taken from available literature. However, data for the Hiller aerial vehicle and the Piasecki PA-1 were obtained through the courtesy of Messrs. Stanley Hiller, Frank and Fred Piasecki, and Dr. Richard M. Carlson.

With respect to the competitive position of the propfan concept, a glance at Table A.1 would indicate that as far as structural weight is concerned, the relative weight-empty levels of the propfan type should be at least as good as those for other blade-driven types. But with respect to fuel consumption in hover per pound of gross weight and hour, the propfan concept would be greatly superior to all other blade-driven types. In addition, investigations performed in Chapter 2 clearly indicated that helicopters with prop fan-driven (also called unducted) rotors may be on the same level as, or even superior to, their shaft-driven counterparts, as far as fuel consumption aspects in hover are concerned. On the other hand, one would expect that many problems—including those resulting from the high centrifugal acceleration at the blade tips—would be encountered on the road toward practical realization of the concept.

In view of the positive, as well as negative, aspects related to the propfan (PF) concept, it appeared advisable to perform a cursory design study in order to (1) verify the overall feasibility of the concept, and (2) single out potential areas of difficulties.

TABLE A.1
LARGE AND VERY LARGE BLADE-DRIVEN HELICOPTERS

	HELICOPTER										
	KELLETT-HUGHES XH-17	FITZWILLIAMS GIANT	PIASECKI PA-1	HILLER, BOOSTER RECOVERY CRANE	B'ØLKOW BO-X	HUGHES XV-9A	HILLER-1108 DA-44-177-AM	BOEING 166-006	HUGHES DAVID TAYLOR	VOLJET 281	I.T.A VHLH
TYPE	TIP BURNING	TIP TURBOJETS	TIP TURBOJETS	TIP TURBOJETS	WARM CYCLE	HOT CYCLE	TIP TURBOJETS	WARM CYCLE	WARM CYCLE	COLD JET	TIP PROP FAN
APPROX. DESIGN YEAR	1948-52	1950	1955	~1958	1960	1960	1964	1972	1980	1988	1990
GROSS WEIGHT, LB	52,000	60,000	103,000	≈ 1,000,000*	147,735	25,500	72,104	200,000	268,000	291,000	400,000
WEIGHT EMPTY, LB	35,900	20,700	43,970		44,100	8,670	34,700	89,077	91,100	109,750	167,000
RELATIVE WEIGHT EMPTY %	0.69	0.345	0.427		0.3	0.34	0.48	0.44	0.34	0.38	0.42
ROTOR RADIUS, FT	65	52	80	200	58.55	27.5	55.9	80	92.5	103.5	100
ROTOR ACTUATION	FLAPPING		FULLY ARTICULATED		FULLY ARTICULATED	FLAPPING*	UNIVERSAL + SPRING REST.	FULLY ARTICULATED	FLAPPING	GIMBAL	GIMBAL
NUMBER OF BLADES	2	3	5	2	3		4	3	2	6	6
ROTOR SOLIDITY		~.105			0.139		0.148	0.11	0.067	0.106	0.103
BLADE t/c %					≈20-10		15	24-12	≈18		24-12
DISC LOADING PSF.	3.9	7.1	5.1	≈8.0	13.7	10.5	7.34	9.95	10	8.7	12.5
TIP SPEED, FPS		550	570				650/592	700-715		5500	700
JET VELOCITY, FPS	≈1,500	≈1,500	≈1500	≈1500			≈1500	1250		~1180	760
POWER PLANT(S) TMAX LB		6x1,000	10x1810*								
POWER PLANT(S) HP								3x20,400*		8x8,079	6x13,840
POWER PLANT LOCATION	FUSELAGE	BLADE	BLADE	BLADE	FUSELAGE	FUSELAGE	BLADE	FUSELAGE	FUSELAGE	FUSELAGE	BLADE
FUEL CONSUMPTION PER LB OF GW & HR		≈0.11			≈0.125	≈0-.15	≈0.10	≈0.11	≈0.217		≈0.07
NOISE LEVEL	VERY HIGH	HIGH	HIGH	HIGH	MEDIUM	MED/HIGH	HIGH	MEDIUM	MEDIUM	LOW	POSSIBLY LOW
REMARKS			ROLLS ROYCE* SOAR TURBOJET	PL 400,000 LB	EXHAUST t ≈ 230°C	EXHAUST t ~1,000°F	DESIGN STUDY U.S. ARMY CONTRACT	ρ*GHP,SLS	GHP, SLS		

NOTES:

2 PER BLADE RADIALLY MOUNTED WESTINGHOUSE MODIFIED TO OPERATE IN 120g FIELD.

*WITH GIMBAL STRAP RETENTION

As to the gross-weight class for which the propfan-driven rotors would be suitable, these investigators believe that they should be applied to very heavy (> 200,000 lb) and heavy lift (> 100,000-lb) helicopters. Consequently, a 400,000-lb crane helicopter, capable of transporting the M-1 battle tank, was selected for a rough design study, which was supplemented by an even less detailed look at the 200,000-lb GW crane. Both 400,000-lb and 200,000-lb GW helicopters may be used in many civilian applications such as cargo unloading, construction, installation of power lines, and logging.

It should be emphasized that in both studies, no attempt was made to optimize the design according to any a priori established criteria. Consequently, such design parameters as disc loading and tip speed similar to those of modern heavy-lift helicopters (Sikorsky 53-E, Boeing Vertol XCH-62, and Mil Mi-26) were selected. Determination of other parameters; for instance, blade geometry and number, will be discussed later in this Appendix.

A.2 The 400,000-Lb GW Helicopter

Selection of Disc Loading and Tip-Speed Values. Disc loading and tip-speed values for three actual heavy-lift helicopters are shown in Table A.2. It can be seen from this table that the average disc loading amounts to 12.16 psf when the tandem configuration is included,

TABLE A.2

DISC LOADING & TIP SPEED OF THREE LARGE TRANSPORT HELICOPTERS

CHARACTERISTICS	HELICOPTERS			
	Mi-26	XCH-62A	CH53E	AVERAGE
GROSS WT, LB	123,480	148,000	73,500	114,493
DISC LOADING, PSF	12.61	8.88	15.0	12.16
TIP SPEED, FPS	690	750	740	726.66

Tip speed, on the average, is equal to 726.76 fps. It appears, hence, that the disc loading and tip-speed values for 400,000-lb GW helicopters should be close to the above values. However, a glance at Fig. A.5 showing the influence (at a given GW) of the disc loading and tip speed on the centrifugal acceleration at the blade tip would indicate that when w and V_t values are lower, the tip acceleration is correspondingly lower. In order to retain acceleration at a level no higher than 150 g, it was decided to select a disc loading of 12.5 psf which, at an assumed tip speed of 700 fps, resulted in a rotor radius of 100.0 ft. The corresponding blade tip Mach number will be 0.63.

Power Installed and Number of Blades. The total installed power level was determined by the requirement of hovering OGE at 4000 ft, 95°F ambient conditions. The ideal power required per pound of thrust at SL,STD and under 4000 ft, 95°F ambient conditions is shown in Fig. A.6.

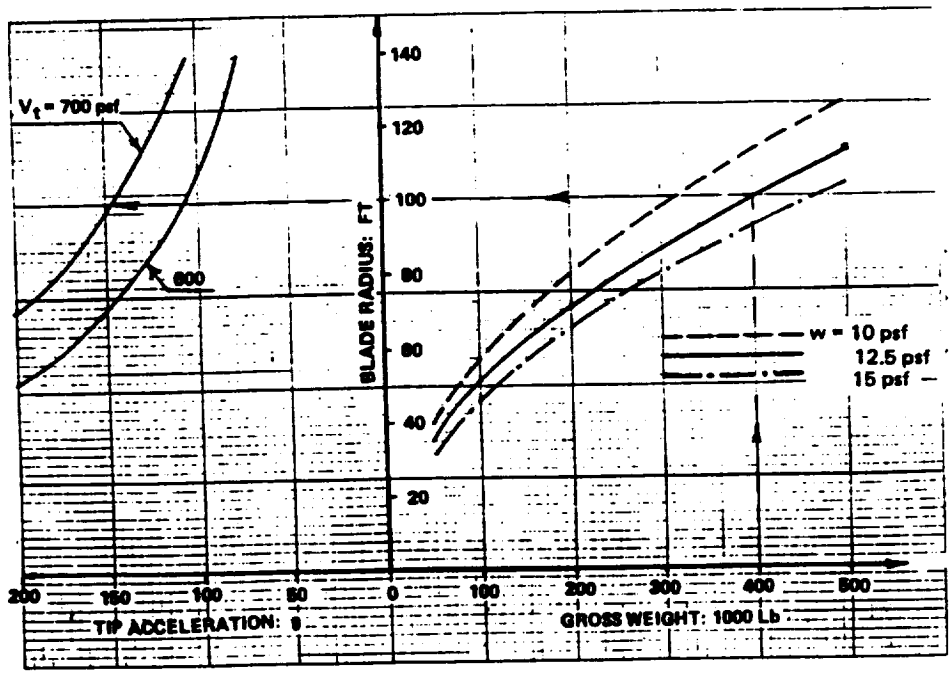

Figure A.5 Influence of GW, disc loading, and tip speed on the centrifugal acceleration at the blade tip

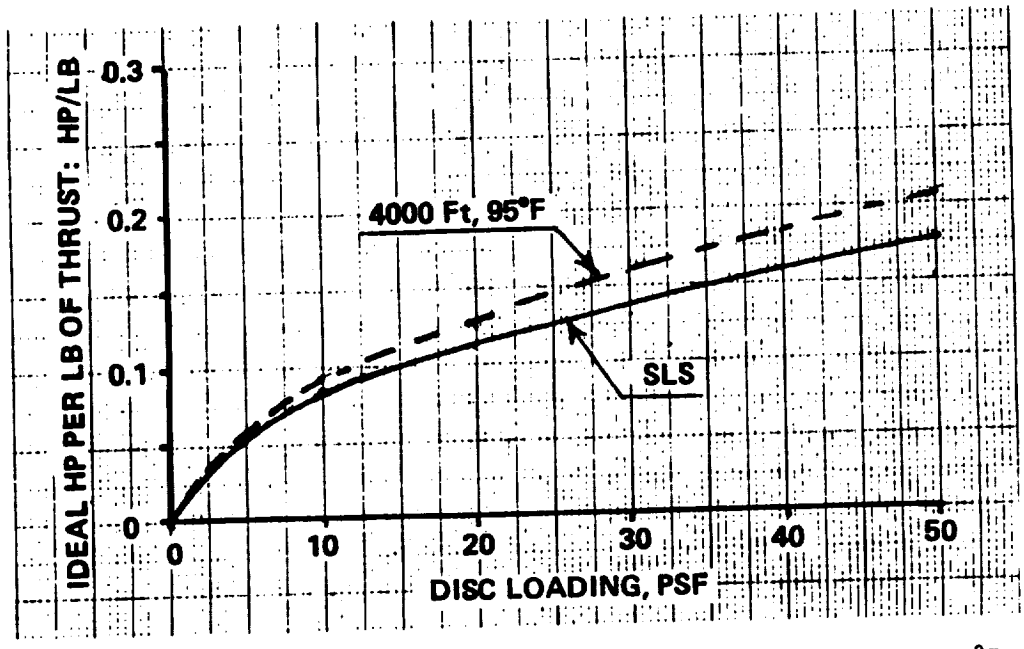

Figure A.6 Ideal hp required per lb of thrust in hover OGE at SL,STD and 4000-ft, 95°F ambient conditions

Assuming that the total rotor thrust $T = W$, one would find from Fig. A.6 that for a disc loading of 12.5 psf at 4000 ft, 95°F, $(RHP/W)_{id} \approx 0.10$ hp/lb. Thus, $(RHP)_{id} = 40{,}000$ hp. Assuming a figure of merit of 0.7, the rotor power required in hover becomes 57,143 hp.

Next, assuming a 5-percent power margin and a lapse rate of 0.85, and the propulsive efficiency of contra-rotating props at $M = 0.63$ as $\eta_{pr} = 0.85$ (see Fig. 2.17), the total installed power becomes 83,045 hp.

The number of blades (b) would be determined by the amount of power that can be installed at the blade tip. It was decided that a single power unit would be mounted at the blade tip. Consequently, the lowest b value possible under this assumption would be dictated by the highest installed power level available from a single unit. At the present time, the largest production turboshaft units are of the 13,000-hp class (Lotarev D-138). Thus, the number of blades becomes 6, and the power installed per blade is 13,840 hp.

Again, at this point, it should be emphasized that the installation of more powerful units, or pairing them, could lead to a reduction in the number of blades.

Rotor Solidity (0.7) and Blade Chord (0.7) at $\bar{r} = 0.7$. These values were determined assuming an average blade-lift coefficient in hover (at 4000 ft, 95°F) of $\bar{c}_{l_h} = 0.7$, which resulted in a rotor solidity of 0.103 and blade chord of 5.42 ft (65.0 in.).

Propfan Radius. The value of the propfan radius was established as follows: Thrust per blade tip, resulting from the known $RHP = 57{,}143$, rotor tip speed equal to 700 fps and 6 blades, amounts to 7483 lb.

Assuming that the disc loading of the propfan is 110 psf, leads to a propfan radius of 4.65 ft.

Overall Helicopter Configuration. The overall helicopter configuration (Fig. A.7) can now be determined, since all of the important design parameter values have been fixed. A glance at this figure will indicate that the hypothetical 400,000-lb GW helicopter was conceived as a crane, while the most important aspects of the layout are outlined below.

Rotor System. The rotor system of the hypothetical very heavy tip-driven helicopter is of a nonarticulated type with a gimbal articulated hub. Blade pitch-change controls are of the fly-by-wire type. Kaman-type elevons provide the required blade pitch control moments. Consideration may be given to the Canard version of elevons which could also be used as blade chord balancing means. The chordwise location of the propulsive unit at the blade tip can also be used as a means of shifting the CG of the blade forward, if needed. However, the most powerful means of shifting the blade CG forward would be through the use of the tractor-type propfan. This forward shift of the CG of the outer portion of the blade could eliminate the necessity of dead-weight balancing and, thus, reduce the blade weight.

It should be noted at this time that in the original studies reported in Ch. 2, Sect. 2.26, contrarotating pushers were assumed (see Fig. 2.23). This was done because at the time of the study, the only contrarotating propfan data available to these investigators was that of the GE-87, which was flight tested on the McDonnell Douglas MD-87. This information included weight, dimensional characteristics, sfc, and static thrust, as well as thrust at $M = 0.6$. However, at the time of revising this Appendix, contrarotating thrusting propfan units were already in flight status, as the Russians, in the meantime, had flown the Ilyushin Il-76 testbed (Aviation Week, May 21, 1990).

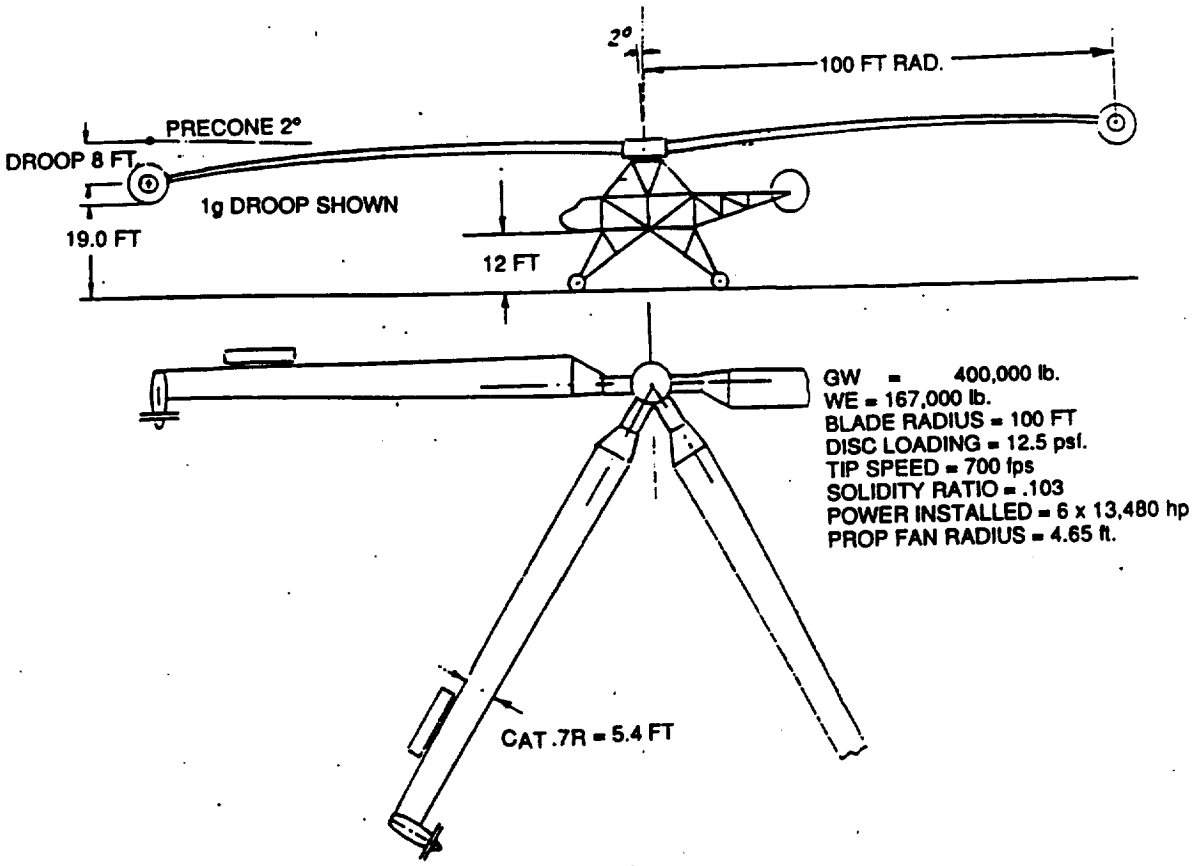

Figure A.7 Hypothetical 400,000-lb GW propfan helicopter

It should be strongly emphasized that for both cases of tractor and pusher-type powerplants, polar moments of inertia of the contrarotating components must be approximately equal to each other. This is necessary in order to eliminate variation of the gyroscopic moments of the powerplant units acting on the blade, especially under the one-engine-out condition, which would result in a change of the blade twist and, thus, its aerodynamic characteristics. The ability to feather the propfan blades in case of engine failure is another important requirement.

Proper blade design was strongly influenced by blade-deflection requirements. To cope with this problem, a spar box was assumed to be molded with unidirectional high modulus elastic carbon fibers. The wrap-around skin, as well as the TE element, is of glass-fiber structure.. Low density NOMEX is used in the aft portion of the blade—high density in the LE portion. The blade is balanced around 25-percent chord (Fig. A.8).

Should the conditions of blade natural frequency in the plane of flapping or magnitude of static droop require increased flapping stiffness, this may be achieved either by increasing the thickness of the airfoils or by use of higher E than presently contemplated, which is 21 X 10^6 psi in molded condition with Epoxy resin.

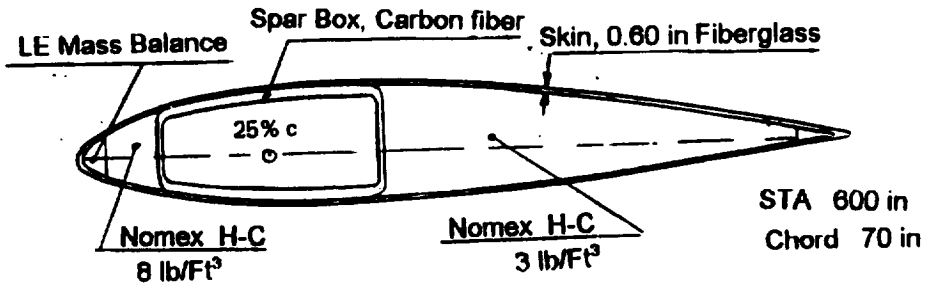

Figure A.8 Typical blade cross-section

The estimated blade weight at STA 1200 is 3.2 lb/in and at STA 600, is 6.0 lb/in (both balanced at 24% chord), and the estimated blade weight at STA 180 is 3.7 (unbalanced).

Concentrated weights at the blade tip were estimated as follows:

Engine (13,840 hp X 0.15 lb/hp)	2076.0 lb
Propfan (see Fig. 24, Ref. 50)	450.0 lb
Gearbox (Estimated)	900.0 lb
Nacelle (Estimated)	460.0 lb
Elevon plus Attachment (Assumed)	100.0 lb
Approximate Weight:	4000.0 lb

The rotor hub is in the form of a six-arm spider. It features a moderate precone of 2°, and is machined of steel or titanium alloy forging.

The blade retention system is of the tension-torsion type. The geometry of the blade used for this study is simple: (1) Straight taper in both chord size and blade thickness, and (2) linear distribution of EI in the flapping plane from the tip to half-span, and from half-span to STA 180.

The above was done for the sake of simplifying preliminary calculations. More elaborate geometry will result in a reduction of blade weight and its static deflection.

Other characteristics are:

Root STA 0	c = 95 in.	t/c = 24%
Root STA 1200	c = 45 in.	t/c = 12%

The blade structure follows the trend established in the helicopter industry; i.e., based on use of fiber filaments (carbon and glass) molded with epoxy resin. Nomex honeycomb is used to stabilize thin portions of the structure. A typical cross-section of the blade at 50% radius is shown in Fig. A.8.

Overall Characteristics. As there is no requirement for high-speed performance, the fuselage consists of a simple truss structure.

A high and wide landing gear is featured in order to accommodate an M-1 battle tank below the fuselage. A winch is provided in order to bring the payload to the required position under the fuselage, which houses a crew of three (two pilots plus winch operator).

A small diameter yaw control rotor is driven from the rotor shaft. Weight estimates of the main components were chiefly based on the weight trends indicated in Ref. 2. Exceptions were made for blade and hub weights. In the blade case, the relative weight was increased because of power units located at the blade tips. By contrast, the relative hub weight was decreased as a result of its simplicity in comparison with those indicated in Ref. 2.

Results of the weight estimates are summarized in Table A.3.

TABLE A.3

WEIGHT STATEMENT OF HYPOTHETICAL 400,000-LB GW VERY HEAVY-LIFT PROPFAN HELICOPTER

	REL WT, %	EST WT, LB
Main Rotor Blades	9.0	36,000
Hub and Hinges	4.0	16,000
Tail-Rotor Group	0.5	2,000
Fuselage	6.0	24,000
Landing Gear	6.0	24,000
Drive System (to Tail Rotor)	0.5	2,000
Engines Installed	6.0	24,000
Fuel System	2.5	10,000
Propulsion Subsystems	1.0	4,000
Flight Controls	1.0	4,000
Fixed Equipment	4.0	16,000
Contingency	1.25	5,000
Weight Empty	41.75	167,000

Blade Droop Problem. Blade droop may pose a potential problem for the propfan-driven rotors, especially those with a large number of blades, because of the high masses of the propulsion system concentrated at the blade tips. In order to get some feeling regarding the seriousness of the problem, static droop (1 g) was computed for the 400,000-lb GW helicopter with 6 blades, which probably represents one of the most severe blade-droop cases that may be encountered in the considered type of helicopters.

The basic differential equation for a beam in bending is

$$d^2y/dx^2 = M/EI \tag{A.1}$$

where x is the coordinate along the beam axis ($x \equiv \bar{r}$), y is the coordinate in the direction perpendicular to the beam axis (i.e., in this case, deflected), M is the bending moment at section x, I is the section moment of inertia at x, and E is the linear modulus of elasticity of the beam material.

Knowing the (M/EI) distribution along the blade span, the desired deflection at the tip can be obtained by integrating Eq. (A.1) twice within the limits of $x = 0$ to $x = R$.

In order to establsih the $M/EI = f(x)$ relationship, bending moments resulting from the powerplant installation at the tip, as well as the weight of the blade itself, is computed as shown in Fig. A.9, where blade weight per inch of its span is also drawn as a function of span.

The moment of inertia of the blade sections at several stations (20, 50, 180, 600, and 1200 in.) was computed, and then marked in the lower portion of the figure. For simplicity, the linear variation of I was assumed.

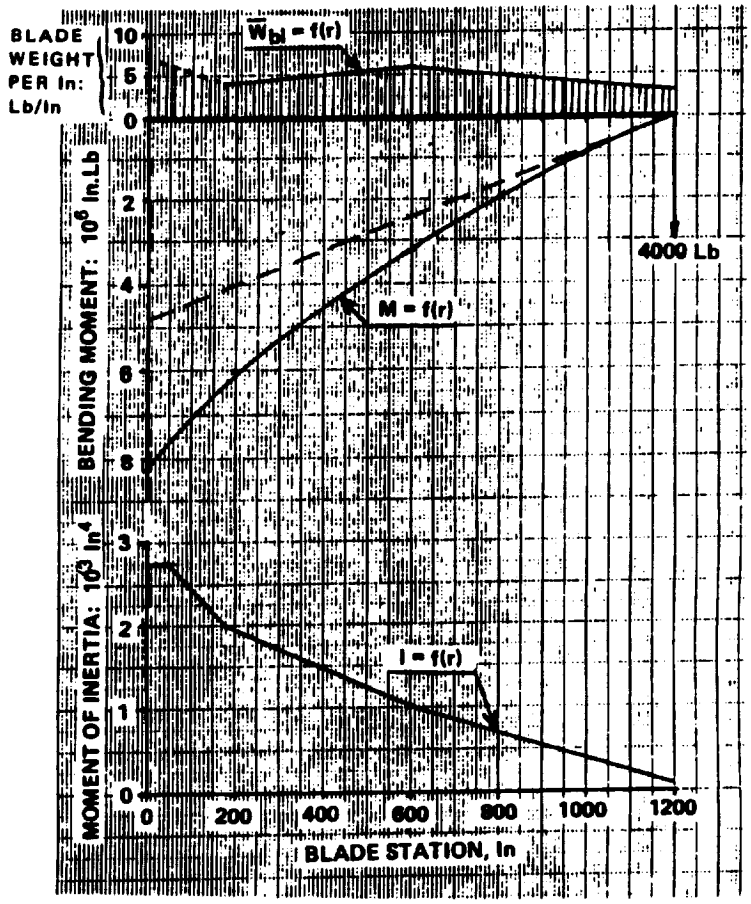

Figure A.9 Blade bending moment and sectional moment of inertia distribution

Next, assuming that the modulus of elasticity is constant along the blade and E = 21 X 10^6 psi, the $M/EI = f(x)$ relationship was established and plotted as shown in Fig. A.10 (continuous line, scale on the left side of the figure).

The dy/dx values at various blade stations were then computed by graphically integrating the area under the (M/EI) curve. The results of this procedure are also shown in Fig. A.10 with ordinates given on the right side of the graph.

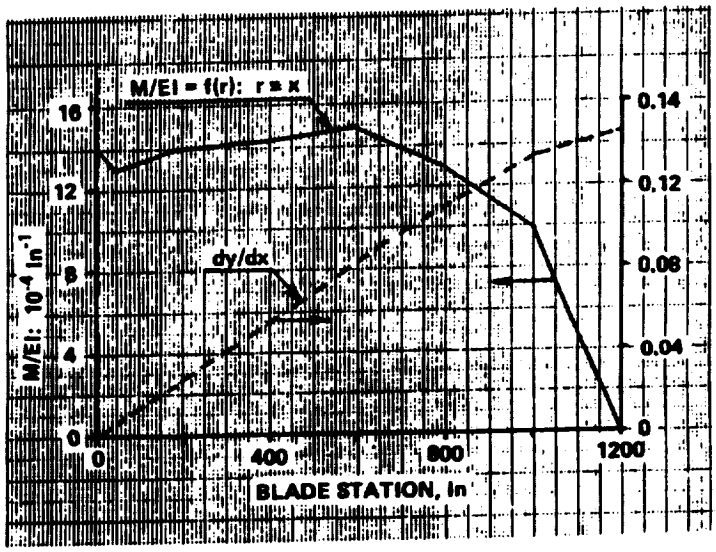

Figure A.10 Auxiliary graphs for determination of blade-tip deflection

Graphical integration of the $(dy/dx) = f(x)$ relationship yielded a deflection of the blade tip (y) of 96 in. This appears to be acceptable within a 2° precone angle of the blades. However, should more clearance with respect to the ground be required, then two steps may be taken, either separately or simultaneously: (1) raising the plane of the rotor, and (2) increasing the EI values, probably through the use of a higher modulus fiber.

The above-mentioned example probably represents one of the worst combinations of design parameters (e.g., number of blades and blade radius) with respect to the droop level that may be encountered in the propfan helicopter concept. Furthermore, the E value of 21 X 10^6 psi used in the above calculations should be considered as rather conservative, even in light of the present state of the art. One may conclude, hence, that blade droop should not present a serious problem as far as future designs of propfan-type helicopters are concerned.

Fuel Consumption in Hover. Because of budget and time limitations, fuel consumption aspects in hover are the only performance items examined in this cursory study.

The $(FC_w)_t$ value at SL,STD was computed from Eq. (2.20), using the following inputs: $(RHP/W)_{id}$ = 0.093 hp/lb, FM = 0.7, transmission efficiency (i.e., coefficient accounting for power losses due to bearing friction and directional control) = 0.98, propulsive efficiency of the propfans is 0.86, and specific fuel consumption of the turbine is 0.42 lb/shp,hr. This resulted in

$$(FC_w)_t = 0.066 \text{ lb/lb,hr.}$$

The relative zero-time payload was computed for W_e = 167,000 lb, assuming a crew of 3 (600 lb) and trapped fluids of 200 lb. This resulted in $\overline{W}_{o_{pl}} = 0.58$.

Using a slightly higher, but probably still conservative, value of $\overline{W}_{o_{pl}} = 0.59$ (see Table 2.2), the payload vs. time in hover relationship was established as shown in comparison with other helicopter concepts in Fig. 2.26

A glance at that figure would indicate that the 400,000-lb GW, propfan-based, very heavy-lift helicopters could become a fuel efficient vehicle as far as hovering and near hovering operations are concerned.

A.3 200,000-LB GW Tip-Driven Heavy-Lift Helicopter

In the study of helicopters having a GW of less than 400,000 lb, a 200,000-lb GW helicopter was arbitrarily chosen. But the basic design criteria; i.e., disc loading, power loading, tip speed, and the same design philosophy were retained. This study yielded the helicopter shown in Fig. A.11. Results of the weight estinates are shown in Table A.4.

Overview of the Propfan Helicopter Concept. The idea of rotors driven by blade-tip mounted jet engines is not new. Fitzwilliams proposed this solution in the study of his 'GIANT' helicopter in the 1950s (see Fig. 2.15 and Ref. 11). However, the concept of using propellers to drive the blades is even older, as demonstrated by Isacco in the late 1920s (see Fig. 2.16). But, at that time, technology was not far enough advanced to make either of these projects practical.

The introduction of high strength and high modulus materials and contrarotating propfans makes the whole approach of using blade-mounted powerplants much more feasible than in the past. In addition, high fuel consumption and noise levels encountered in early turbojet concepts could be reduced by the use of propfan engines. However, contrarotating propfans, a must in the case of tip-driven helicopters, still pose the problem of higher noise levels than their single-rotation counterparts. Consequently, more studies addressing this problem are required.

Static blade droop of large-diameter blades with heavily concentrated loads at the tip appeared as a potential problem. However, cursory investigations of those aspects in this Appendix seem to indicate that propfan-type helicopters, even with a large number of blades (6) should exhibit an acceptable static blade-tip droop.

Serious problems that would require additional studies are (a) effects of the high g fields on the powerplants, and (b) one-engine out conditions.

In the case of tip-mounted jet engines, a high g field created two-fold problems: (1) working conditions of engine bearings, and (2) blade twist resulting from engine gyroscopic moments. For contrarotating propfan powerplants, the second of these problems would practically disappear. But the first problem will still face propfan helicopters. However, the fact that the Williams jet engine was whirl tested at about 200 g's whereas, in the case of the hypothetical 400,000-lb GW helicopter, only 150 g's would be encountered. This appears to make this problem less critical. Also tremendous progress in engine technology made during the last few decades enhances the optimism regarding overcoming the high g bearing problems.

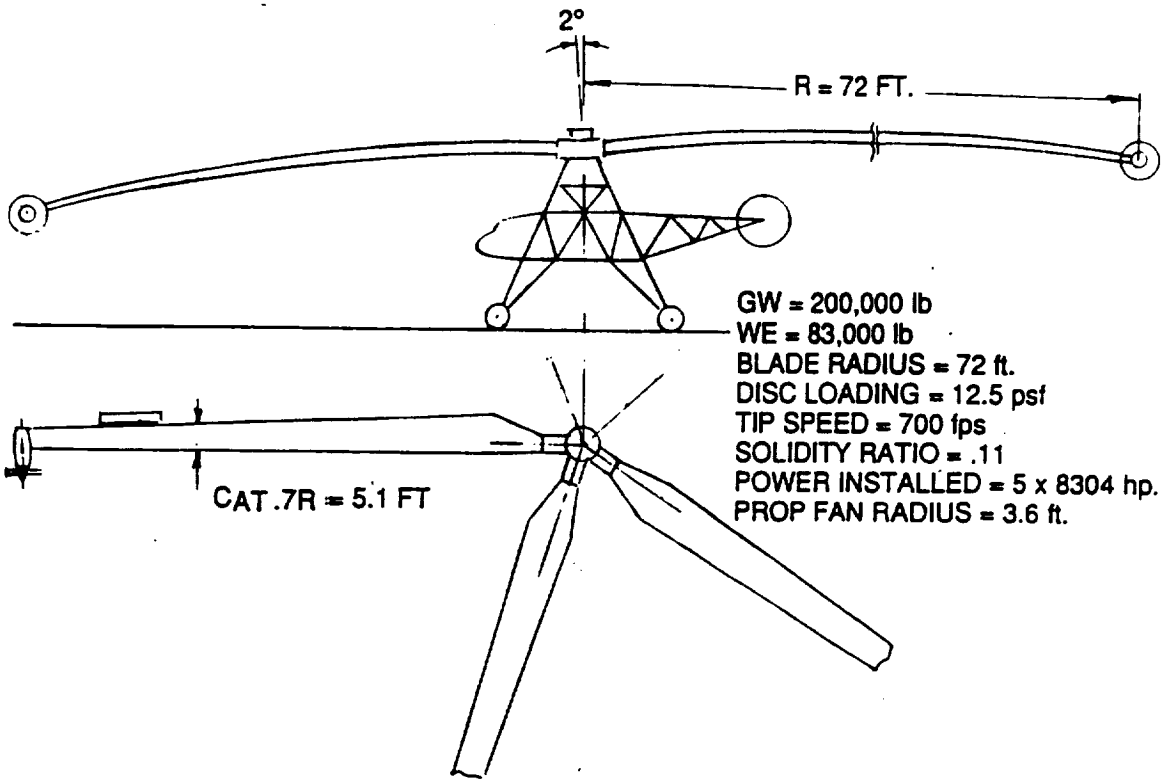

Figure A.11 200,000-lb GW heavy-lift propfan helicopter

TABLE A.4.

WEIGHT STATEMENTOF 200,000-LB GW HELICOPTER

	REL. WT, %	EST. WT, LB
Main Rotor Blades	9.0	18,000
Main Rotor Hub & Hinges	5.5	11,000
Tail Rotor Group	0.5	1,000
Fuselage	6.0	12,000
Landing Gear	6.0	12,000
Drive System (to Tail Rotor)	0.3	600
Engines Installed	5.0	10,000
Fuel System	2.5	5,000
Propulsion Subsystems	1.0	2,000
Flight Controls	2.0	4,000
Fixed Equipment	4.0	8,000
Weight Empty	41.8	83,600

A one engine inoperative condition creates the necessity of quick feathering of the propfan blades. But this requirement for the blade-tip mounted units should be no different than for those installed on fixed-wing aircraft. Consequently, solutions worked out for this latter case should be readily available for heavy and very heavy helicopters.

It should also be mentioned that in some regimes of flight, especially at high-speed translation of the aircraft as a whole, air flow components in the disc plane of the propfan may be encountered. Aerodynamic, dynamic, and, perhaps, acoustic effects of those in-plane velocity components should be investigated.

In summary, it appears that in spite of many serious problems facing propfans as a means of driving rotors of very heavy (GW $>$ 200,000 lb) and heavy (GW $>$ 100,000 lb) helicopters, this concept deserves more study. This is chiefly due to the fact that fuel consumption per pound of gross weight and unit of time in hover, as well as a unit of distance flown, can be as low or, in some cases, lower, than for the best shaft-driven helicopters. Lower relative weights empty, than of the shaft-driven counterparts, makes energy expenditure aspects with respect to payload even more attractive than for other concepts.

Finally, elimination of mechanical power transmission systems should certainly add to the operational appeal of propfan helicopters.

LIST OF SYMBOLS

AR	wing aspect ratio
BPR	bypass ratio
b	number of blades, or span; ft
$\overline{b}_w$	relative wing span; $\overline{b}_w \equiv b_w/R$
C_D	drag coefficient
C_L	lift coefficient
C_P	power coefficient
C_T	thrust coefficient
c	chord, blade or wing; ft
D	diameter; ft
	drag; lb
D_e	equivalent drag; lb $D_e \equiv 325\,SHP/V$
FC	fuel consumption
$FC_{o_{pl}}$	fuel consumption related to zero-time payload and hour ; lb/lb,hr
FC_w	fuel consumption per lb of aircraft GW; n.mi
GW	gross weight; lb
J	propeller advance ratio; $J \equiv 101V/ND$
M	Mach number
N	airscrew rpm
OGE	out-of-ground effect
$\overline{PR}$	relative productivity; (lb X n.mi/hr)/lb
R	range; n.mi
	airscrew radius; ft
RP	rotor power; hp or ft-lb/sec
RHP	rotor horsepower; hp
S	area; sq.ft
SHP	shaft horsepower
SP	shaftpower; ft-lb/sec, or hp
sfc	specific fuel consumption; lb/hr-hp
T	rotor thrust; lb
	absolute temperature
t	time; sec, min, or hr
$tsfc$	thrust specific fuel consumption; lb/hr-lb
V	speed of flight; kn
V_t	tip speed; ft/sec
v	induced velocity; fps
W	weight; lb or kg
W_e	weight empty; lb
$\overline{W}_e$	relative weight empty; $\overline{W}_e \equiv W_e/W$
w	disc, and area, loading; psf

List of Symbols (Cont'd)

Δ	increment
η	efficiency in general
η_{ov}	overall rotor-power transmission efficiency; $\eta_{ov} \equiv RP/SP$
λ_{compr}	compressibility drag increase factor
μ	rotor advance ratio; $\mu \equiv 1.69V/V_t$
ρ	air density; slugs/cu.ft
σ	airscrew solidity; $\sigma \equiv bc/\pi R$

Subscripts

comp	compressor
compr	compressibility
CJ	cold jet
duct	duct
e	effective or empty
f	equivalent flat plate
h	hover
id	ideal
j	jet
n	new
nf	new equivalent drag
nind	noninduced
noz	nozzle
o	sea level
ov	overall
pl	payload
pr	profile, or propulsive
R	range
req	required
sh	shaft
sr	stowable rotor
t	tip, or time
tf	trapped fluid
tot	total
uf	unducted fan
ul	useful load
v	vertical
w	wing, or gross weight
wc	warm cycle

Superscript

–	relative with respect to empty weight, reference gross weight, airscrew radius, or air density at SLS

PAGE 221 INTENTIONALLY BLANK

REFERENCES

1. Stepniewski, W. Z. and L. H. Sloan. *Some Thoughts on Design Optimization of Transport Helicopters.* Vertica, Vol. 6, No. 1, Jan. 1982.

2. Stepniewski, W. Z. *Rotorcraft Weight-Trends in Light of Structural Material Characteristics.* U.S. Army Aviation Systems Command, Technical Report TR-87-A-10, April 1987.

3. Raymer, Daniel P. *Aircraft Design: A Conceptual Approach.* AIAA Education Series, 1989.

4. Payne, P. R. Remarks re discussion of paper by John Brown. *Some Applications of Gas Turbines to Helicopter Propulsion.* The Journal of the Helicopter Association of Great Britain, Vol. 8, No. 3, Jan. 1955.

5. Stepniewski, W. Z. *A Comparative Study of Soviet vs. Western Helicopters.* NASA CR 3579, March 1983.

6. Torenbeck, Egbert. *Synthesis of Subsonic Airplane Design.* Delft University Press, 1982.

7. Jane's Yearbooks. *Jane's All the World's Aircraft.*

8. Boelkow Company. *Schwerer Lastenhubschrauber BO-X* (Heavy Cargo Transport Helicopter BO-X). Boelkow Report KIM 77D-2/66-01, Feb. 1966.

9. Nichols, J. B. *The Pressure-Jet Helicopter Propulsion System.* The Aeronautical Journal of RAeS, Sept. 1972, pp. 553-565.

10. Head, R. E. *Preliminary Design of a Tip-Jet-Driven Heavy-Lift Helicopter Incorporating Circulation Control.* David W. Taylor Naval Ship Research and Development Center Report DTNSRDC/ASED-81/07, March 1981.

11. Fitzwilliams, O. L. L. *The Giant Helicopter.* The Journal of the Helicopter Association of Great Britain, Vol. 5, No. 4, 1952.

12. Hughes, C. E. and J. A. Gazzaniga. *Summary of Low-Speed Wind Tunnel Results of Several High-Speed Counterrotating Propeller Configuration.* AIAA Report AIAA-88-3149, July 1988.

13. Hayden, J. S. and W. R. Lake. *Performance Evaluation of the Djinn Helicopter.* AFFTC-TN-60-8, Feb. 1960.

14. Hislop, G. W. *The Fairey Rotodyne.* The Journal of the Helicopter Association of Great Britain, Vol. 13, No. 1, Feb. 1959.

15. The E. K. Liberatore Co. *Voljet Model 280.* Voljet Report 280TA-4, Aug. 1987.

16. The E. K. Liberatore Co. *Cold-Cycle Pressure Jet Helicopters and Research.* Voljet Report 280TA-4, Aug. 1987.

17. Putman, V. K. and W. W. Eggert. *XV-1 Phase II Flight Evaluation.* AFFTC-TR-56-35, Feb. 1957.

18. Schrage, D. P., M. F. Costello, and D. N. Mittleider. *Design Concepts for an Advanced Cargo Rotorcraft.* Report AIAA-88-4496, Sept. 1988.

19. Asmus, F. G. *Parametric and Preliminary Studies of High & Low Speed Cruise-Fan Propulsion System.* Army AVLAB Report TR-65-57, Aug. 1965.

20. Carlson, R. M. and R. E. Donham. *Extending Helicopter Speed Performance.* Lockheed Horizons, Issue 6, July 1967.

21. Hislop. G. S. *The Fairey Rotodyne.* Journal of the Helicopter Assn. of Great Britain, Vol. 13, No. 6, Dec. 1959.

22. McKenzie, K. T. *Aerodynamic Aspects of the Rotodyne.* Journal of the Helicopter Assn. of Great Britain, Vol. 13, No. 6, Dec. 1959.

23. Marks, M. D. *Flight Test Development of XV-1 Convertiplane.* Paper presented at the AHS Third Annual Western Forum, Dallas, TX, Oct. 8, 1956.

24. Hohenemser, F. H. *Aerodynamic Aspects of the Unloaded Rotor Convertible Helicopter.* Journal of the AHS, Jan. 1957.

25. Tishchenko, M. N., A. V. Nekrasov, and A. S. Radin. *Viertolety vybor parametrov pri proektIrofaniy* (Helicopters, Selection of Design Parameters). Mashinostroyeniye Press, Moscow, 1976.

26. Anon. *The Piasecki Story of Vertical Lift.* Piasecki Aircraft Corp. Brochure.

27. de Simone, G., R. S. Blanch and R. A. Fisher. *The Impact of Mission on the Preliminary Design of an ABC Rotor.* AHS Mideast Region National Specialists Meeting "Rotor System Design", Philadelphia, Oct. 1980.

28. Acree, C. W. and R. M. Kufeld. *In-Flight Measurement of Rotor Hub Drag Using the RSRA–A Feasibility Demonstration.* Eleventh European Rotorcraft Forum, London, Paper no. 95, Sept. 1985.

29. Vil'dgrube, L. S. *Vertolety Raschet Integral'nykh Aerodynamicheskikh Kharakteristick i Letno-Mekhanicheskikh Danykh* (Helicopters—Calculations of Integral Aerodynamic Characteristics and Flight Mechanics Data). Moscow, Mashinostroyeniye, 1977.

30. Stepniewski, W. Z. and C. N. Keys. *Rotary-Wing Aerodynamics* (Two Volumes—bound as one). Dover Publications, Inc., New York, N.Y., 1984.

31. Torres, M. and A. Cler. *Improving Helicopter Aerodynamics.* 14th European Rotorcraft Forum, Milano, Italy, Paper No. 27, Sept. 1988.

32 Tarczynski, T. *The Development of a Retractable Rotor.* AHS Journal, Vol. 3, 1958.

33. Frandenburg. E. A. *Application of Variable Diameter Rotor System to Advanced VTOL Aircraft.* Paper presented at AHS Forum, May 1975.

34. Schneider, J. J. *The History of V/STOL Aircraft.* Vertiflight, Vol. 29, Nos. 3 & 4, 1983.

35. Wilkerson, J. B. *A Look at Tomorrow's Civil Tiltrotor.* The 8th Annual Northeast Regional Meeting of the Society of Allied Weight Engineers, Philadelphia, Pa. Paper No. 806, 1987.

36. Boeing Commercial Airplane Co., Bell Textron, Boeing Vertol, and NASA ARC. *Civil Tiltrotor, Mission and Applications.* NASA CR 177452, July 1987.

37. Drees, J. M. *Expanding Tilt Rotor Capabilities.* Vertica, Vol. 12, N 1/2, pp. 55-67, 1988.

38. Andres, J. and G. Monti. *EUROFAR – Status of the European Tilt-Rotor Project.* 14th European Rotorcraft Forum, Milano, Italy, 22-23 Sept. 1988, Paper no. 22.

39. Felker, F. F., M. D. Maisel, and M. D. Betzina. *Full-Scale Tilt-Rotor Hover Performance.* Journal of the AHS, Vol. 31, No. 2, Apr. 1986.

40. Felker, F. F. and J. W. Light. *Rotor/Wing Aerodynamic Interactions in Hover.* 42nd AHS Forum, Washington, D.C. June 1986.

41. McVeigh, M. A., W. K. Grauer, and D. J. Poisley. *Rotor/Airframe Interactions on Tiltrotor Aircraft.* Journal of the AHS, Vol. 35, No. 3, July 1990.

42. Torenbeek, Egbert. *Synthesis of Subsonic Airplane Design.* Delft University Press, 1982.

43. Schneider, J. J. and J. B. Wilkerson. *High-Speed Rotorcraft V/STOL – An Initial Assessment.* Paper presented at NASA Vertical Lift Aircraft Design Cong. San Francisco, CA. Jan. 1990.

44. Fradenburgh, E. A. *Improving Tilt-Rotor Aircraft Performance with Variable-Diameter Rotors.* Paper No. 30, 14th European Rotorcraft Forum, Milano, Italy, Sept. 1988.

45. Vertol Division of the Boeing Co. *Development of the U.S. Army VZ-2 (Boeing Vertol-76) Research Aircraft.* Tech. Report R-219, Aug. 1963.

46. Anon. Vertol Division of Boeing. *Boeing-Vertol Model 137.* Summary Report PR-378-1, 1961.

47. Fay, C. B. *Recent Developments in Simplifying and Improving the Tilt Wing Design.* Paper presented at the 20th AHS Forum, May 1964.

48. Brown, D. A. *Japan's Ishida Group May Build Tilt-Wing Transport in U.S.* Aviation Week & Space Technology, Jan. 1, 1990.

49. Kuchemann, D. *The Aerodynamic Design of Aircraft.* Pergamon Press, 1978.

50. Parzych, D., Cohen, S., and Shenkman, A. *Large-Scale Advanced Propfan (LAP) Performance, Acoustic and Weight Estimation.* (SP-06A83, Hamilton Standard, NASA Contract NASA3-23051) NASA CR-174782, 1985.

51. Jeracki, R. J., Mikkelson, D. C. and Blaha, B. J. *Wind Tunnel Performance of Four Energy Efficient Propellers Designed for Mach 0.8 Cruise*, NASA TM 79124 and SAE Paper 790573, April 1979.

52. Lockheed California Co. *Composite Aircraft Program.* Lockheed Report 20312, 1967.

53. Wheatley, J. B. and D. T. Sasaki. *Propulsion for Composite Aircraft.* Paper presented at 31st PEP Meeting on Helicopter Propulsion Systems, Advisory Group for Aerospace Research and Development, Ottawa, Canada, June 1968.

54. Fry, B. L. *Design Studies and Model Tests of Stowable Tilt-Rotor Concept.* The Boeing Co. Vertol Div. Tech Report AFFDL-TR-71-62, 1971.

55. Stepniewski, W. Z. and W. R. Burrowbridge. *Some Soviet and Western Simplified Performance Prediction Methods In Comparison with Tests.* Paper No. 47, Twelfth European Rotorcraft Forum, Garmisch-Partenkirchen, FRG, Sept. 1986.

56. Wagner, F. B., and R. R. Pruyn. *Design Studies of Large Reaction Driven Crane Helicopters.* The Boeing Company, D210-10485-1, 1972.

57. Sullivan, R. J. *Hot Cycle Rotor Propulsion.* Paper given at the 31st Meeting of the Propulsion and Energetics Panel, AGARD-NATO, Ottawa, Ont. Canada, 10-14 June 1968.

REPORT DOCUMENTATION PAGE

Form Approved
OMB No. 0704-0188

1. AGENCY USE ONLY *(Leave blank)*	2. REPORT DATE	3. REPORT TYPE AND DATES COVERED
	September 1992	Contractor Report

4. TITLE AND SUBTITLE

Open Airscrew VTOL Concepts

5. FUNDING NUMBERS

NAS2-12819

6. AUTHOR(S)

W. Z. Stepniewski and T. Tarczynski

7. PERFORMING ORGANIZATION NAME(S) AND ADDRESS(ES)

International Technical Associates, LTD.
1064 Pontiac Road
Second Floor
Drexel Hill, PA 19026-4817

8. PERFORMING ORGANIZATION REPORT NUMBER

A-93020

9. SPONSORING/MONITORING AGENCY NAME(S) AND ADDRESS(ES)

Ames Research Center
Moffett Field, CA 94035-1000

10. SPONSORING/MONITORING AGENCY REPORT NUMBER

NASA CR-177603

11. SUPPLEMENTARY NOTES

Point of Contact: Dr. Fredric H. Schmitz, Ames Research Center, MS 247-3, Moffett Field, CA 94035-1000; (415) 604-4166

12a. DISTRIBUTION/AVAILABILITY STATEMENT

Unclassified — Unlimited
Subject Category 01

12b. DISTRIBUTION CODE

13. ABSTRACT ***(Maximum 200 words)***

The following concepts, based on using open airscrew(s) for VTOL maneuvers, are re-examined in light of current technology: (a) Tip-driven helicopters, (b) compound helicopters, and (c) high-speed VTOL aircraft, represented by tiltrotors, tiltwings, retractoplanes and stoppable rotors. Criteria, permitting one to compare performance of aircraft using diverse lifting and propelling methods are established. Determination of currently possible performance, indication of near-future potentials, and comparison of those items with the baseline levels—as represented by contemporary shaft-driven helicopters, first generation tiltrotors, and commercial turbo-prop fixed-wing aircraft—constitutes bulk of this report.

14. SUBJECT TERMS	15. NUMBER OF PAGES
VTOL – open airscrew, Helicopters, Comparison – performance, Weight	224
	16. PRICE CODE: A10

17. SECURITY CLASSIFICATION OF REPORT	18. SECURITY CLASSIFICATION OF THIS PAGE	19. SECURITY CLASSIFICATION OF ABSTRACT	20. LIMITATION OF ABSTRACT
Unclassified	Unclassified		